

# NASA Technical Memorandum 4517

(NASA-TM-4517) SPACELAB J  
EXPERIMENT DESCRIPTIONS (NASA)  
246 p

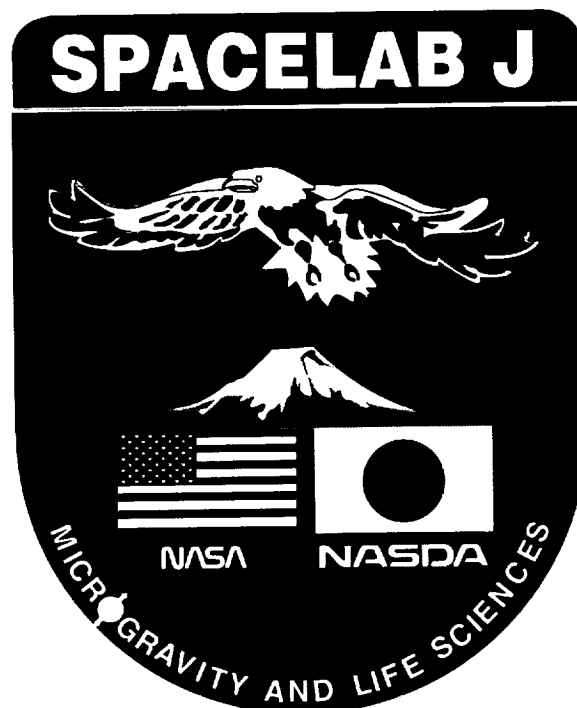
N94-13732  
--THRU--  
N94-13775  
Unclass

H1/29 0181115

## Spacelab J Experiments Descriptions

*First Edition*

August 1993



**NASA**



NASA Technical Memorandum 4517

# Spacelab J

## Experiments Descriptions

*First Edition*

*Edited by*  
Teresa Y. Miller  
*George C. Marshall Space Flight Center*  
*Marshall Space Flight Center, Alabama*



National Aeronautics and  
Space Administration  
Office of Management  
Scientific and Technical  
Information Program  
1993





## FOREWORD

The Spacelab J mission was a cooperative effort between the National Aeronautics and Space Administration (NASA) and the Japanese National Development Agency (NASDA), with a payload dedicated to life sciences and materials science research. The primary objective of the SL-J Mission was to conduct a variety of material and life sciences experiments utilizing the weightless and radiation environments of an orbiting spacelab.

The management of the SL-J program was directed by NASA Headquarter's Office of Space Science and Applications with Gary W. McCollum serving as Program Manager and Robert S. Sokolowski as Program Scientist. The SL-J Mission was managed by the Marshall Space Flight Center, Huntsville, Alabama. J. Aubrey King and Fred W. Leslie were designated as Mission Manager and Mission Scientist, respectively.

Spacelab-J, STS-47, was launched in September 1992, from the Kennedy Space Center aboard the Orbiter Endeavour. The mission duration was 8 days at an orbital altitude of 163 n.mi. and an inclination of 57 degrees. Science operations for the mission were directed from the Payload Operations and Control Center at Marshall Space Flight Center.

The crew for SL-J consisted of seven members; a flight crew composed of the commander, pilot, and a mission specialist, and a payload crew consisting of two mission specialists, one Japanese Payload Specialist, and one Science Mission Specialist. Science operations were conducted on a 24-hour, two-shift basis.

The payload complement of 44 elements included the NASDA developed First Material Processing Test (FMPT), a set of 35 investigations (13 in Life Sciences and 22 in Materials Science), and 9 U.S. experiments (7 Life Sciences and 2 Microgravity Science). Most of the experiments were maintained within the Spacelab module as shown in Figures 1 and 2, however, the Protein Crystal Growth Experiments were contained in thermally-stabilized refrigerator/incubator modules housed in the shuttle middeck. The Magnetic Resonance Imaging Experiment was conducted on the ground pre- and post-mission and required no on-orbit resources. Table 1 provides a list of the payload elements categorized by discipline and contains other pertinent information such as experiment number and experiment title, experiment acronym, principal investigator, and sponsoring country.

The life science experiments encompass a diverse group of biological investigations such as physiology, cell growth and development, separation processes for purification of biological materials, enzyme crystal growth, and radiation biology. Several of these experiments were designed to evaluate the specific effects of the space environment, such as radiation and microgravity, on biological systems and may have direct applications for improving the health and well being of astronauts. Other life science investigations utilized the microgravity environments to study methods to improve purification of biological materials and to grow protein crystals of interest to the biotechnology and pharmaceutical industries.

The materials science investigations are designed to utilize the unique microgravity environment of space for processing materials and for studying physical phenomena impacted by such gravity-related effects as buoyancy, sedimentation, and convection. The SL-J materials science experiments included crystal growth studies, material processing experiments, fluid physics investigations, and the characterization and monitoring of the acceleration environment of the Spacelab. These experiments have a wide range of applications in areas such as the pharmaceutical and biotechnology industries, metallurgy, infrared detector technology, superconductivity, semiconductor technology, and in providing basic information necessary to understanding specific physical phenomena occurring both on Earth and in space.

**LEGEND:**

Material Sciences

Life Sciences

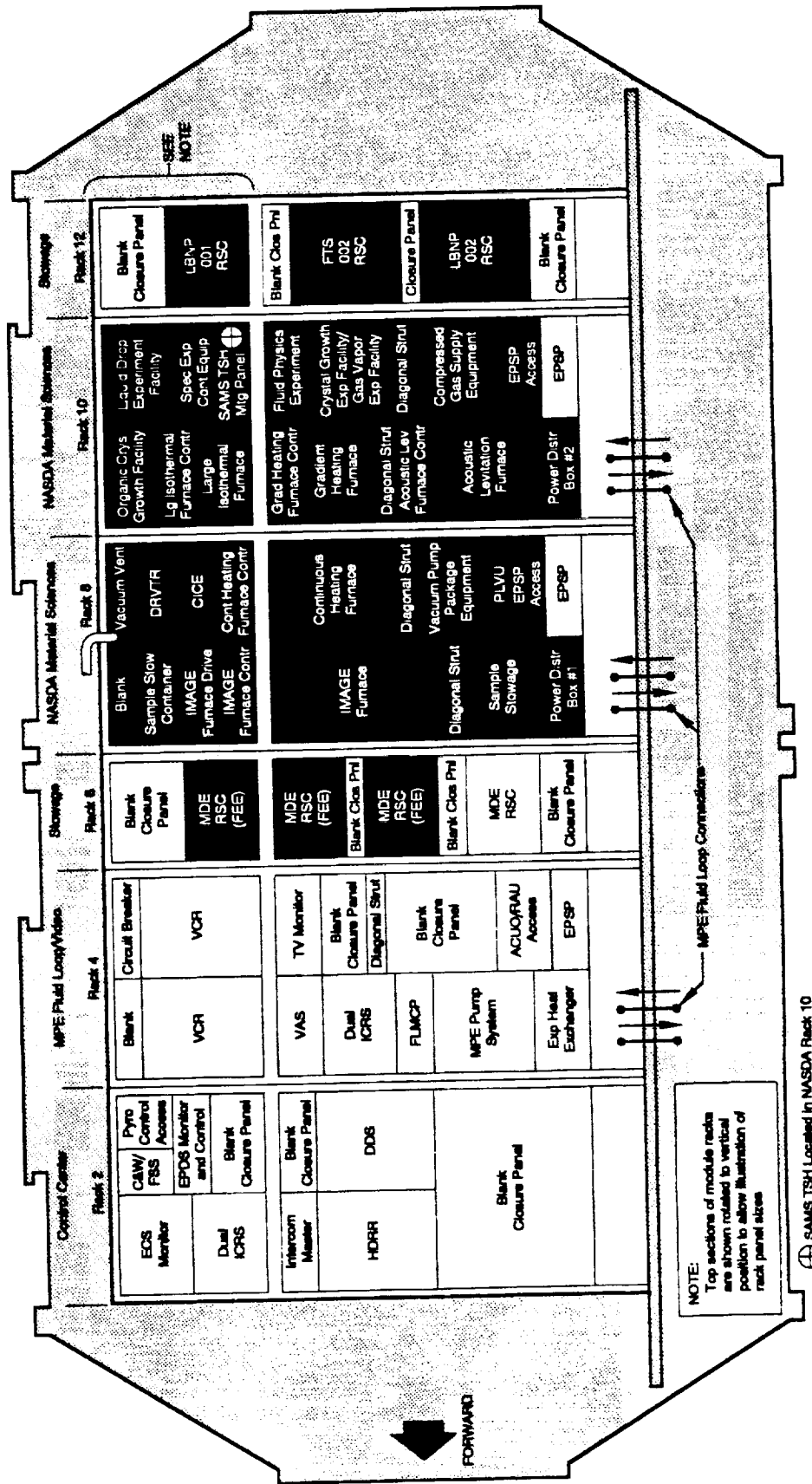


Figure 1. SL-J module configuration (starboard side).



TABLE 1. SL-J Payload Elements

Discipline	Experiment Number/ Acronym	Title	PI Name/Country
Life Science	AFTE	Autogenic Feedback Training	Cowings/USA
	FEE	Frog Embryology Experiment	Souza/USA
	LBNP	Lower Body Negative Pressure	Charles/USA
	MRI	Magnetic Resonance Imaging	LeBlanc/USA
	FTS	Fluid Therapy System	Lloyd/USA
	*BCR	Bone Cell Research	Partridge/USA
	*PCR	Plant Culture Research	Krikorian/USA
	L-0	Health Monitoring of Japanese Payload Specialist	Sekiguchi/Japan
	L-1	Endocrine and Metabolic Changes in Payload Specialist	Matsui/Japan
	L-2/(VFEU)	Neurophysiological Study on Visuo- Vestibular Control of Posture and Movement of Fish During Adaptation to Weightlessness	Mori/Japan
	L-3/(FFEU)	Separation of Biogenic Materials by Electrophoresis Under Zero Gravity	Kuroda/Japan
	L-4	Comparative Measurement of Visual Stability in Earth and Cosmic Space	Koga/Japan
	L-5	Crystal Growth of Enzymes in Low Gravity	Morita/Japan
	L-6	Studies on the Effects of Microgravity on the Structure and Function of Cultured Mammalian Cells	Sato/Japan
	L-7	Effect of Low Gravity on Calcium Metabolism and Bone Formation	Suda/Japan
	L-8	Separation of the Animal Cellular Organelle by Means of Free-Flow Electrophoresis	Yamaguchi/Japan
	L-9	Genetic Effects of HZE and Cosmic Radiation	Ikenaga/Japan
	L-10	Research on Perceptual-Motor Functions under the Zero Gravity Condition	Tada/Japan
	L-11	Study on the Biological Effect of Cosmic Radiation and the Development of Radiation Protection Technology	Nagaoka/Japan
	L-12	A Circadian Rhythm of Conidiation in <i>Neurospora Crassa</i>	Miyoshi/Japan

\*Primary Experiment Hardware provided by NASDA Japan as part of the L6 experiment.

TABLE 1. SL-J Payload Elements (Continued)

Discipline	Experiment Number/ Acronym	Title	PI Name/Country
Materials			
Science	PCG	Protein Crystal Growth	Bugg/USA
	SAMS	Space Acceleration Measurement System	DeLombard/USA
	M-1	Growth Experiment of Narrow Band-Gap Semiconductor PbSnTe Single Crystals	Yamada/Japan
	M-2	Growth of PbSnTe Single Crystal by Traveling-Zone Method in Low Gravity	Segawa/Japan
	M-3	Growth of Semiconductor Compound Single Crystal by Floating Zone Method	Nakatani/Japan
	M-4	Casting of Superconducting Composite Materials	Togano/Japan
	M-5	Formation Mechanism of Deoxidization Products in Iron Ingot Deoxidized with Two or Three Elements	Fukazawa/Japan
	M-6	Preparation of Ni Base Dispersion Strengthened Alloys	Muramatsu/Japan
	M-7	Diffusion in Liquid State and Solidification of Binary System	Dan/Japan
	M-8	High Temperature Behavior of Glass	Soga/Japan
	M-9	Growth of Si Spherical Crystals and the Surface Oxidation	Nishinaga/Japan
	M-10	Study on Solidification of Immiscible Alloy	Kamio/Japan
	M-11	Fabrication of Very-Low-Density, High-Stiffness Carbon Fiber/A1 Hybridized Composites	Suzuki/Japan
	M-12	Study on the Mechanism of Liquid Phase Sintering	Kohara/Japan
	M-13	Fabrication of Si-As-Te: Ni Ternary Amorphous Semiconductor in the Microgravity Environment	Hamakawa/Japan
	M-14	Gas-Evaporation in Low-Gravity Field (Congelation Mechanism of Metal Vapors)	Wada/Japan
	M-15	Drop Dynamics in Space and Interference with Acoustic Field	Yamanaka/Japan
	M-16	Study of Bubble Behavior in Weightlessness (Effects of Temperature Gradient and Acoustic Stationary Wave)	Azuma/Japan
	M-17	Preparation of Optical Materials Used in Non-Visible Region	Hayakawa/Japan
	M-18	Heat Transfer Under Marangoni Effect Induced Convection	Enya/Japan
	M-19	Solidification of Eutectic System Alloys in Space	Ohno/Japan
	M-20	Growth of Samarskite Crystal Under Microgravity Conditions	Takekawa/Japan
	M-21	Growth Experiment of Organic Metal Crystal in Low Gravity	Anzai/Japan
	M-22	Crystal Growth of Compound Semiconductors in a Low-Gravity Environment (InGaAs Crystals)	Tatsumi/Japan

## TABLE OF CONTENTS

	Page
SECTION I: Materials Science .....	1
Growth Experiment of Narrow Band-Gap Semiconductor PbSnTe Single Crystals in Space (M-1) .....	3
Growth of PbSnTe Single Crystal by Traveling-Zone Method in Low Gravity (M-2) .....	9
Growth of Semiconductor Compound Single Crystal InSb by Floating Zone Method (M-3) .....	15
Casting of Superconducting Composite Materials (M-4) .....	21
Formation of Deoxidization Products in Iron Ingot by the Addition of Al, Si, and/or Mn (M-5) .....	27
Preparation of Particle Dispersion Alloys (M-6) .....	31
Diffusion in Liquid State and Solidification of Binary System (M-7) .....	37
High Temperature Behavior of Glass (M-8) .....	41
Growth of Si Spherical Crystals and the Surface Oxidation (M-9) .....	45
Study on Solidification of Immisible Alloys (M-10) .....	51
Fabrication of Very-Low-Density, High-Stiffness Carbon Fiber/Aluminum Hybridized Composite with Ultra-Low Density and High Stiffness (M-11) .....	61
Study of the Mechanism of Liquid Phase Sintering (M-12) .....	69
Fabrication of Si-As-Te Ternary Amorphous Semiconductor in the Microgravity Environment (M-13) .....	75
Gas-Evaporation in Low-Gravity Field (Cogelation Mechanism of Metal Vapors) (M-14) .....	79
Drop Dynamics in Space and Interference with Acoustic Field (M-15) .....	83
Study of Bubble Behavior in Weightlessness (Effects of Thermal Gradient and Acoustic Stationary Wave) (M-16) .....	87
Preparation of Optical Materials Used in Non-Visible Region (M-17) .....	89

## TABLE OF CONTENTS (Continued)

	Page
Marangoni Effect Induced Convection in Material Processing Under Microgravity (M-18) .....	95
Solidification of Eutectic System Alloys in Space (M-19) .....	101
Growth of Samarskite Crystal Under Microgravity Conditions (M-20) .....	107
Growth Experiment of Organic Metal Crystal in Low Gravity (M-21) .....	113
Crystal Growth of Compound Semiconductors in a Low-Gravity Environment (InGaAs Crystals) (M-22) .....	117
Microgravity Acceleration Measurement Environment Characterization .....	121
Protein Crystal Growth .....	129
 SECTION II: Life Sciences .....	 137
Health Monitoring of Japanese Payload Specialist - Autonomic Nervous and Cardiovascular Responses Under Reduced Gravity Condition (L-0) .....	139
Endocrine and Metabolic Changes in Payload Specialist (L-1) .....	145
Neurophysiological Study on Visuo-Vestibular Control of Posture and Movement in Fish During Adaptation to Weightlessness (L-2) .....	151
Separation of Biogenic Materials by Electrophoresis Under Zero Gravity (L-3) .....	155
Comparative Measurement of Visual Stability in Earth and Cosmic Space (L-4) .....	161
Crystal Growth of Enzymes in Low Gravity (L-5) .....	165
Studies on the Effects of Microgravity on the Ultrastructure and Functions of Cultured Mammalian Cells (L-6) .....	171
Gravity, Chromosomes, and Organized Development in Aseptically Cultured Plant Cells .....	173
Effect of Low Gravity on Calcium Metabolism and Bone Formation (L-7) .....	177
Separation of the Animal Cellular Organella by means of Free-Flow Electrophoresis (L-8) .....	179



## TABLE OF CONTENTS (Concluded)

	Page
Genetic Effects of HZE and Cosmic Radiation (L-9) .....	181
Manual Control in Space Research on Perceptual-Motor Functions Under Zero Gravity Conditions (L-10) .....	185
Study on the Biological Effect of Cosmic Radiation and the Development of Radiation Protection Technology (L-11) .....	189
A Circadian Rhythm of Conidiation in <u>Neurospora Crassa</u> .....	197
Amphibian Fertilization and Development in Microgravity .....	201
Magnetic Resonance Imaging After Exposure to Microgravity .....	209
Countermeasure Reducing Post-Flight Orthostatic Intolerance .....	213
Bone Culture Research .....	223
Autogenic Feedback Training Experiment: A Preventative Method for Space Motion Sickness .....	227
In-Flight Demonstration of the Space Station Freedom Health Maintenance Facility Fluid Therapy System (E300/E05) .....	249



**SECTION I**  
**MATERIALS SCIENCE**



GROWTH EXPERIMENT OF NARROW BAND-GAP SEMICONDUCTOR  
PbSnTe SINGLE CRYSTALS IN SPACE  
M-1

Tomoaki Yamada  
NTT Basic Research Laboratories  
Japan

Abstract

An experiment on crystal growth of  $\text{Pb}_{1-x}\text{Sn}_x\text{Te}$  in microgravity is planned. This material is an alloy of the compound semiconductors PbTe and SnTe. It is a promising material for infrared diode lasers and detectors in the wavelength region between 6 and 30  $\mu\text{m}$ . Since the electrical properties of  $\text{Pb}_{1-x}\text{Sn}_x\text{Te}$  depend greatly on the Pb/Sn ratio and crystalline defects as well as impurity concentration, homogeneous, defect-free, high-quality crystals are anticipated. Although many growth methods, such as the pulling method, the Bridgman method, the vapor growth method, etc., have been applied to the growth of  $\text{Pb}_{1-x}\text{Sn}_x\text{Te}$ , large, homogeneous, low-defect-density crystals have not yet been grown on Earth. The unsuccessful results have been caused by buoyancy-driven convection in the fluids induced by the specific gravity difference between heated and cooled fluids on Earth.

Figure 1 shows a schematic view of  $\text{Pb}_{1-x}\text{Sn}_x\text{Te}$  crystal growth in this experiment. A crystal is grown by cooling the melt from one end of the ampoule.

In crystal growth from the melt, about 30% of the SnTe in the melt is rejected at the solid-liquid interface during solidification. On Earth, the rejected SnTe is completely mixed with the remaining melt by convection in the melt. Therefore, SnTe concentration in the melt, and accordingly in the crystal, increases as the crystal grows, as shown in Figure 2.

In the microgravity environment, buoyancy-driven convection is suppressed because the specific gravity difference is negligible. In that case, the rejected SnTe remains at the solid-liquid interface and its concentration increases only at the interface. If the growth rate is higher than the PbTe-SnTe interdiffusion rate, the amount of SnTe which diffuses from the interface into the melt increases as SnTe piles up at the interface, and finally it balances the amount of rejected SnTe during solidification, resulting in steady-state SnTe transportation at the interface. By using this principle, compositionally homogeneous crystals can be grown (Figure 2). Furthermore, low-defect-density crystals will be grown in microgravity, because convection causes crystalline defects by mixing hot and cold fluids and generating temperature fluctuations in them.

### Expected Results

Currently, the development of electronic technology is very rapid. This is due to the development of fabrication techniques for semiconductor materials and devices, called "Si-technology." Great improvements in device performance and large-scale integration of devices have been made based on crystal growth techniques for growing large, high-quality crystals. The quality of  $\text{Pb}_{1-x}\text{Sn}_x\text{Te}$  is presently much poorer than that of Si.

$\text{Pb}_{1-x}\text{Sn}_x\text{Te}$  is a promising material for infrared detectors and diode lasers. Growth of large, homogeneous and low-defect-density crystals will enable mass production of high performance devices at a cheaper cost and the development of integrated Si-like circuits. As a result, infrared detectors will be put into practical use as heat sensors in a variety of fields. For example, they may be used in heat controllers of furnaces, engines, machines, etc.; in security

instruments for automobiles, houses, factories, etc.; and in medical apparatuses for diagnosing diseased portions of the human body. Moreover, integration of detectors results in large-area image sensors and enables high-speed processing of infrared images. Such image sensors will be used for remote sensing instruments in resource satellites or Earth observation satellites and will greatly improve sensing ability. They will assist in assessing mining, marine, and agricultural products and in observing the Earth. Infrared diode lasers will be used in chemical analysis apparatuses and will serve to measure or monitor the gas concentration of  $\text{CO}_x$ ,  $\text{NO}_x$ ,  $\text{SO}_x$ ,  $\text{CH}_4$ , etc. in the air. Results obtained from the experiment will also assist in understanding the crystal growth mechanism and the behavior of fluids in microgravity.

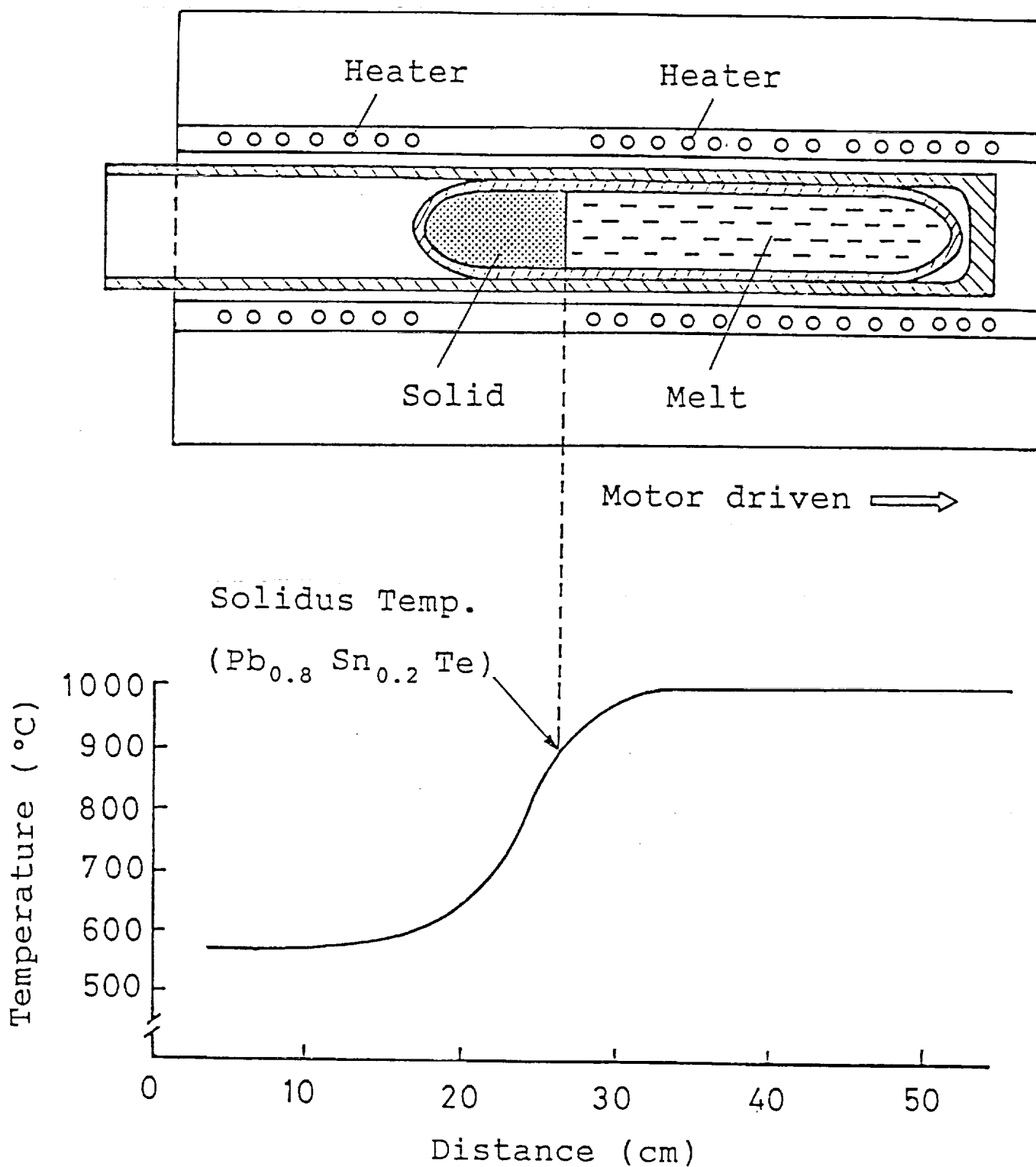


Figure 1. Schematic view of  $\text{Pb}_{1-x}\text{Sn}_x\text{Te}$  crystal growth using the Bridgman method.



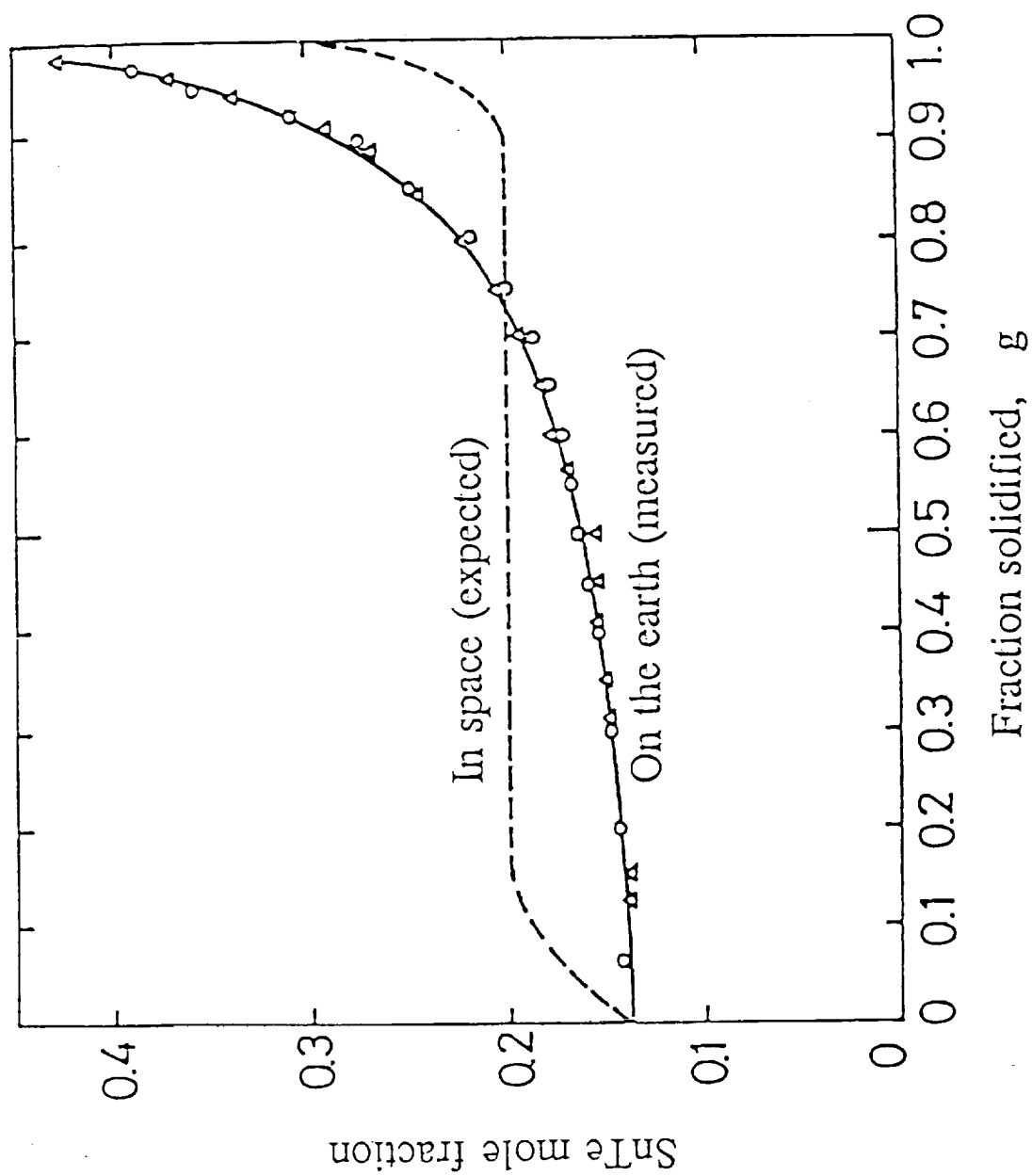


Figure 2. Comparison of compositional profiles between Earth-grown and space-grown crystals.



GROWTH OF PbSnTe SINGLE CRYSTAL BY TRAVELING-ZONE METHOD  
IN LOW GRAVITY  
M-2

Y. Segawa  
The Institute of Physical and Chemical Research  
Japan

The single-crystal lead tin telluride (PbSnTe) semiconductor is most promising as a laser radiation element and infrared detecting element in the far infrared region. However, it is very difficult to grow a large single crystal with a homogeneous composition on Earth because the elements have a very strong tendency to separate from each other in the molten phase due to differences in their specific gravities and melting points.

Experimental Purposes

- To grow a single crystal of PbSnTe by a traveling zone method in microgravity.
- To study the spatial fluctuation of the composition and the electrical properties of the crystal.

In this experiment, the image furnace will be used to melt a single PbSnTe crystal inside a quartz tube (Figure 1). The molten zone will be allowed to travel for 5 hours during the mission.

Expected Results

- The character of crystal growth under microgravity in comparison with crystal growth on Earth will be clarified.

- The fundamental mechanism of the crystal growth will be studied.
- A new method for crystal growth under microgravity may be proposed.

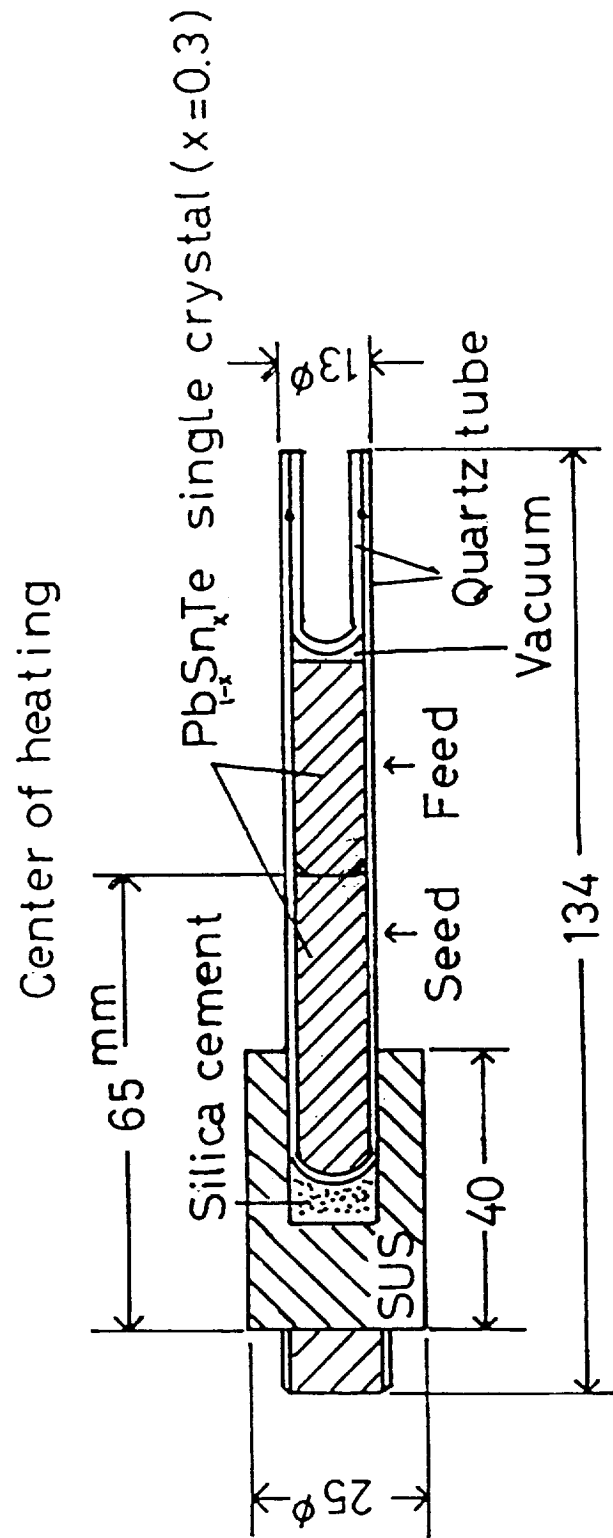


Figure 1. Quartz capsule.

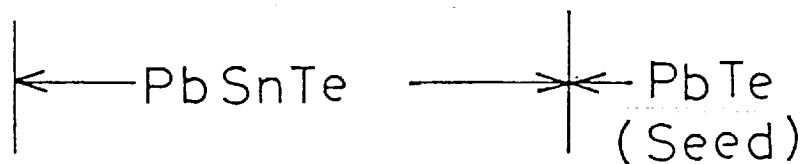
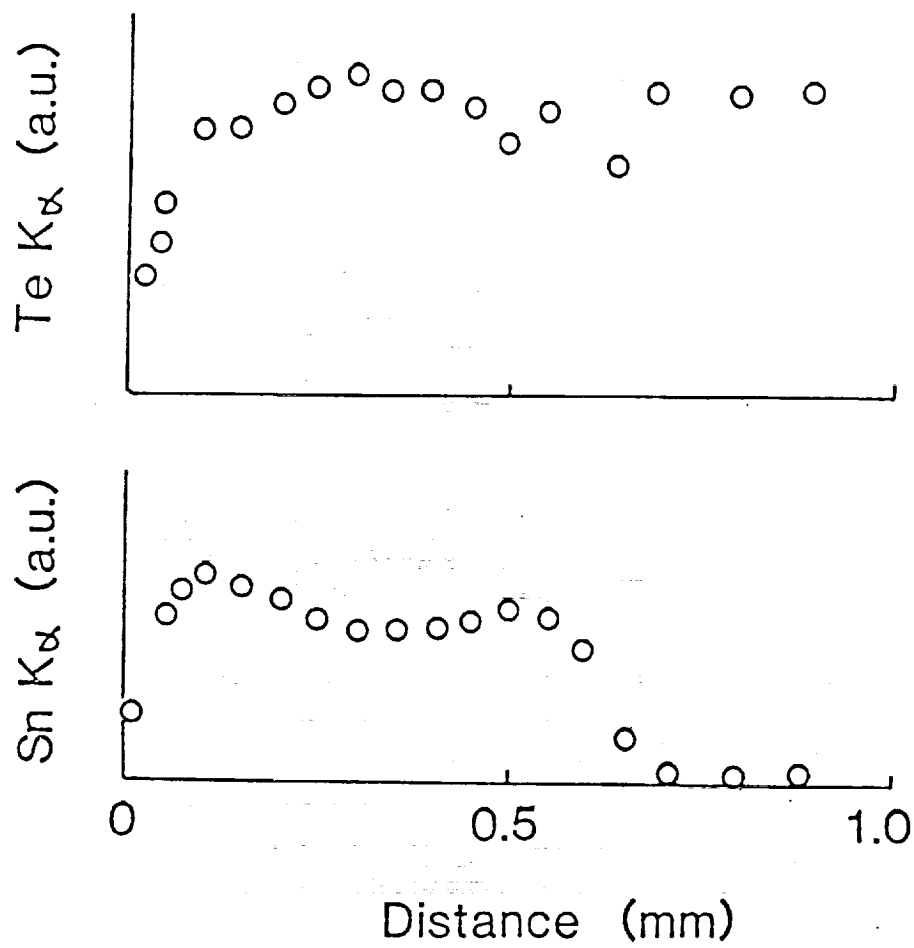


Figure 2.

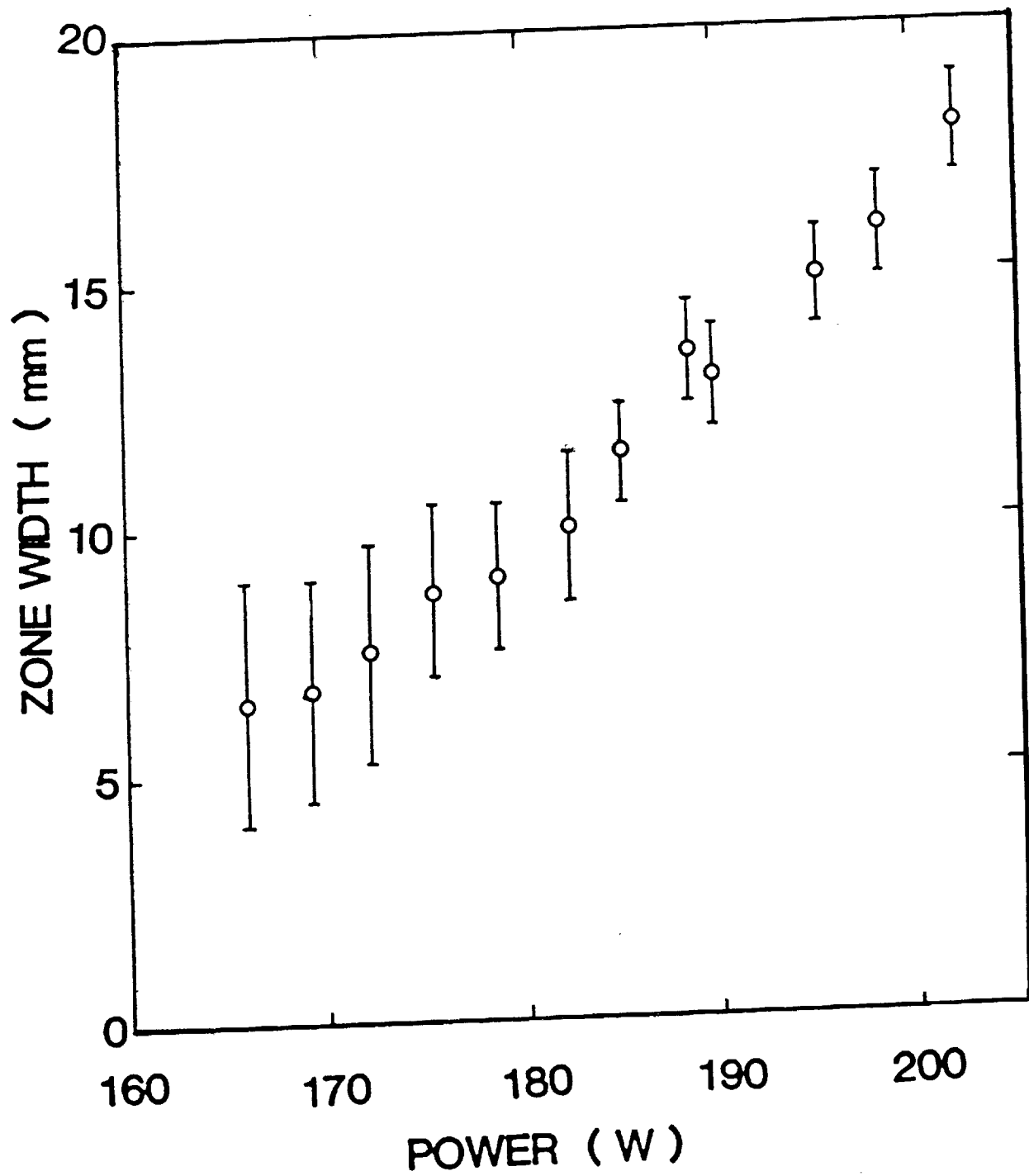


Figure 3.





GROWTH OF SEMICONDUCTOR COMPOUND SINGLE CRYSTAL InSb  
BY FLOATING ZONE METHOD  
M-3

I. Nakatani  
National Research Institute for Metals  
Japan

Floating zone methods have potential applications in growing single high-quality semiconductor crystals. In this method, melts can be sustained without containers and, therefore, are free from contamination from the containers. On the ground, however, the maximum stable length of the floating liquid column  $L_{\max}$  that can be sustained by its surface tension against the gravitational force is restricted as  $L_{\max} = 2.84 \sqrt{\gamma/\rho g}$ , where  $\gamma$ ,  $\rho$  are the surface tension and density of the liquid, respectively, and  $g$  the gravitational acceleration. This gravitational restriction makes it impossible to grow large diameter, single crystals of materials that have small surface tensions or high densities, e.g., InSb and GaSb, etc. In the microgravity environment, the maximum stable length of the liquid column dramatically increases and is written as  $L_{\max} = 2\pi R$ , where  $R$  is the radius of the cylindrical liquid column. The use of the floating zone method in the microgravity environment may allow growth of large diameter, single crystals of many materials. Moreover, the absence of the gravity-driven convection could reduce the temperature fluctuations at the growing interface and thus could lead to improvements in crystal quality.

The main objective of this project is to use the Image Furnace to study a large diameter, (20 mm) single crystal of InSb under microgravity conditions. The behavior of the liquid column is recorded on the VTR tapes and is compared with what is expected theoretically. The single crystal grown in space is characterized by comparing it with single crystals grown on the ground with respect to crystallographic and electronic properties. The goal of this project is to confirm the effects of the microgravity on the single crystals.

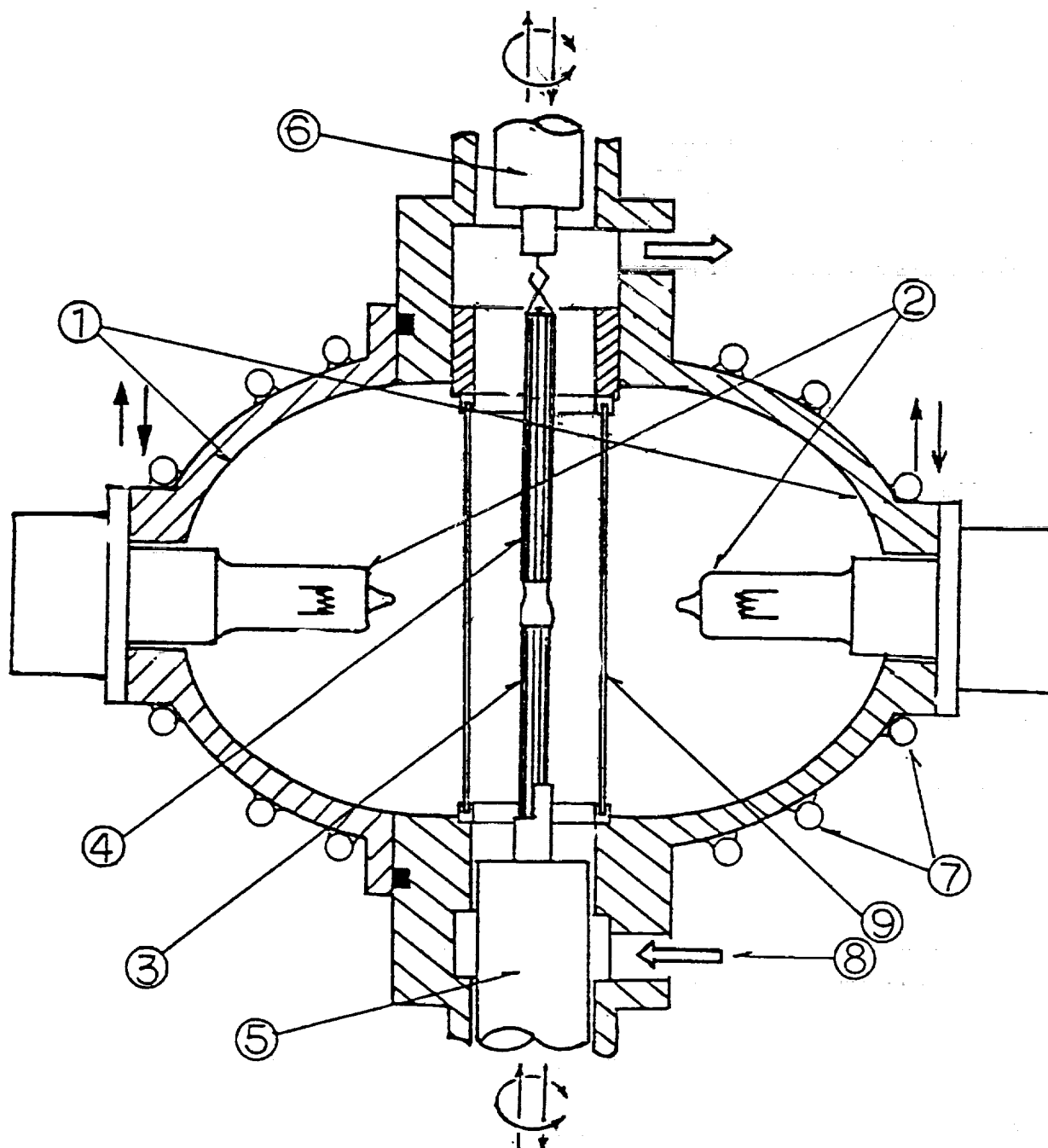


Figure 1. Schematic view of the double ellipsoidal image furnace: (1) double ellipsoidal mirror; (2) halogen lamps; (3) single crystalline rods of InSb; (4) polycrystalline rods of InSb; (5) upper shaft; (6) lower shaft; (7) cooling water; (8) atmospheric gas; (9) quartz tube.

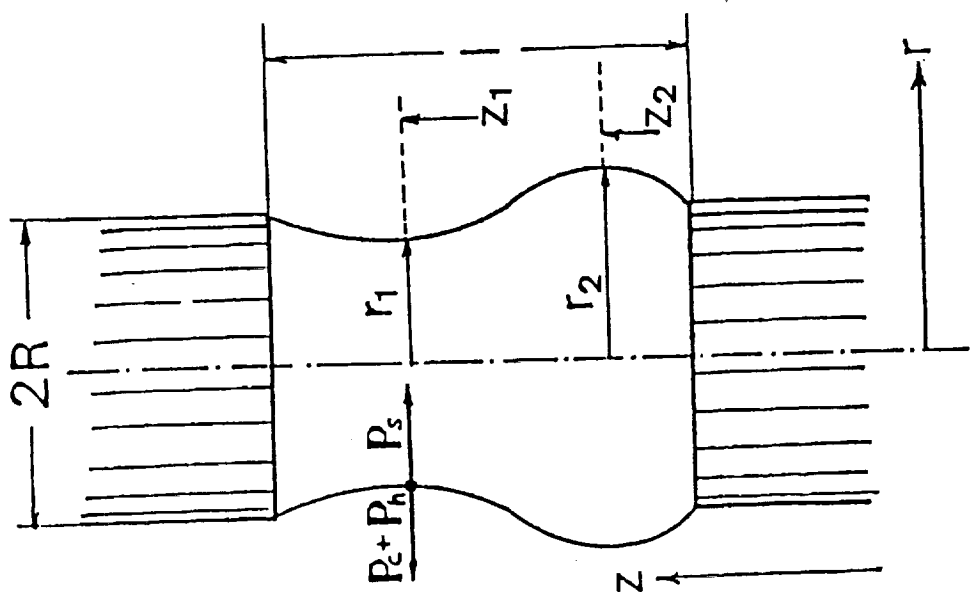


Figure 2. Bottle-shaped floating zone which exhibits a neck and a belly at the position of  $Z_1$  and  $Z_2$ , respectively.  $P_c$  denotes the pressure due to the centrifugal force,  $P_h$  the hydrostatic pressure, and  $P_s$  the pressure due to the surface tension.

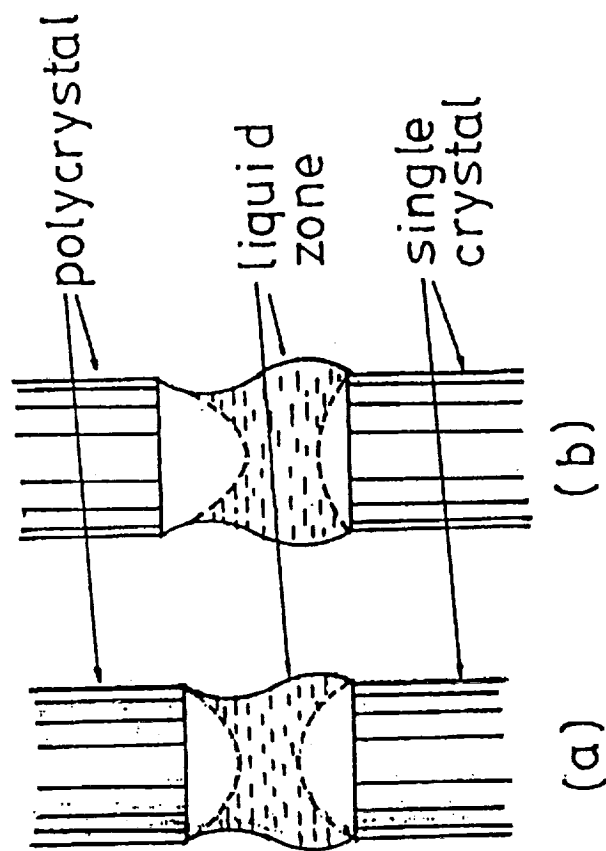


Figure 3. Solid liquid interfaces in floating zones: (a) the floating zone without travel; (b) the floating zone traveling with the velocity  $v$ .

1. formation of melt-drops at the both ends
2. joining the melts together
3. back-melting the seed end
4. floating zone growth
5. decreasing the diameter and pulling apart both the melts

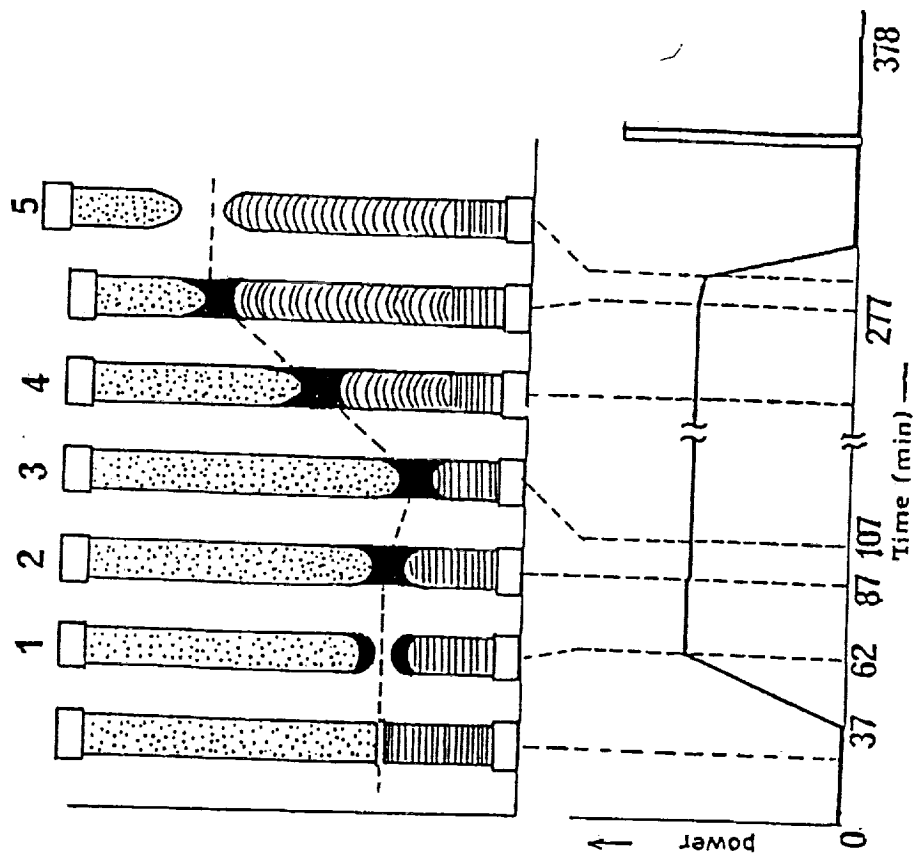


Figure 4

$$l = 5R ; V = \pi R^2 l$$

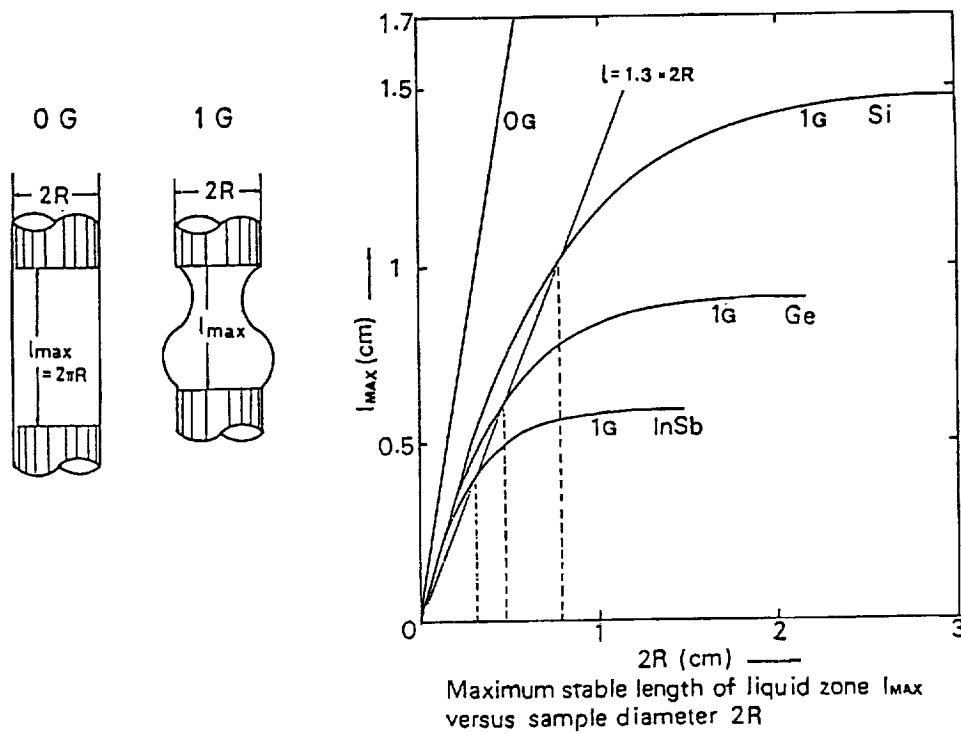
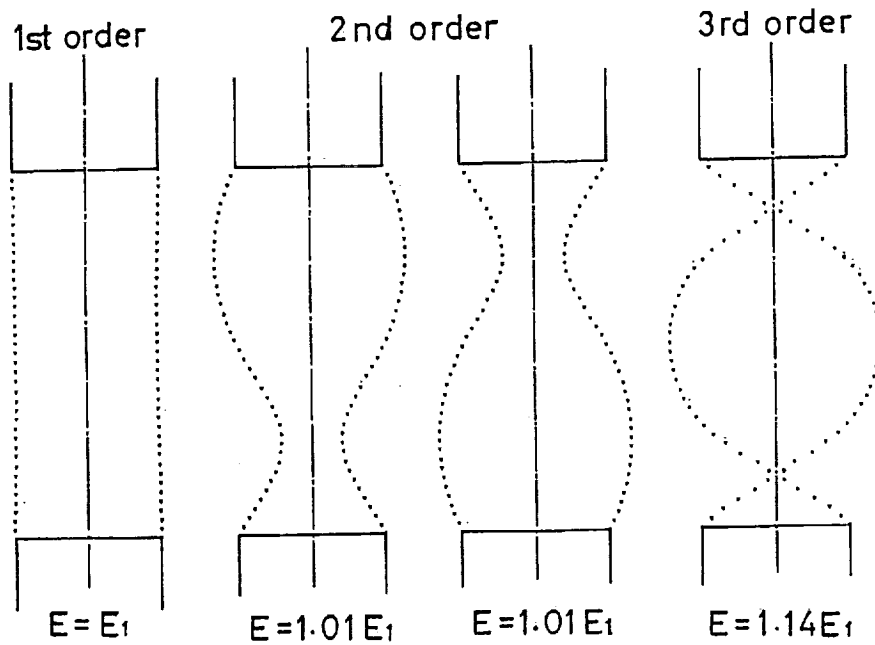


Figure 5.

[The page contains extremely faint, illegible text that appears to be a list or index of items, possibly names or titles, arranged in a structured format. The text is too light to transcribe accurately.]

**CASTING OF SUPERCONDUCTING COMPOSITE MATERIALS  
M-4**

**Kazumasa Togano  
National Research Institute for Metals  
Tsukuba, Japan**

An aluminum-lead-bismuth alloy is a flexible alloy and is promising for easily workable embedded-type, filament-dispersed superconducting wire material. It is difficult to produce homogeneous ingots of this material because it is easily separated into elements when melted on Earth due to the large specific gravity differences.

In this experiment, a homogeneous alloy will first be produced in molten state in microgravity. It will then be returned to Earth and processed into a wire or tape form. It will then be dispersed as the second phase in micro texture form into the primary phase of aluminum.

Superconducting wire material with high-critical-magnetic-field characteristics will be produced. The texture of the material will be observed, and its performance will be evaluated.

In addition to the above alloy, a four-element alloy will be produced from silver, a rare Earth element, barium, and copper. The alloys will be oxidized and drawn into wire after being returned to Earth. The materials are expected to be forerunners in obtaining superconducting wire materials from oxide superconductors.

The objectives of this experiment are as follows:

- To study the effects of microgravity on the solidification phenomena of monotectic and eutectic alloys.
- To form composite superconductors from the alloys.

## MATERIALS

### Monotectic Alloys

Al-Pb-Bi                      3

### Eutectic Alloys

Ag-Cu                      1

Ag-Y-Ba-Cu                      1

Ag-Yb-Ba-Cu                      1

### CRUCIBLE

Baron Nitride

### CAPSULES

Ta Double Layers

### CARTRIDGE Ta

### FURNACE

CHF

1300 °C x 17 min, gas jet cooling



## POST-FLIGHT EXPERIMENTS

### ANALYSES

Monotectic Alloys

Pb-Bi Particle Distribution in Al Matrix

Eutectic Alloys

Lamellar Spacing

### FORMATION OF COMPOSITE SUPERCONDUCTORS

Deformation of Al-Pb-Bi Alloy into Wire with Fine Distribution of Pb-Bi Superconducting Fibers in Al Matrix

Oxidation of Ag-Yb(Y)-Ba-Cu Alloy to Form YBaCuO HTSC Precipitates in Ag Matrix

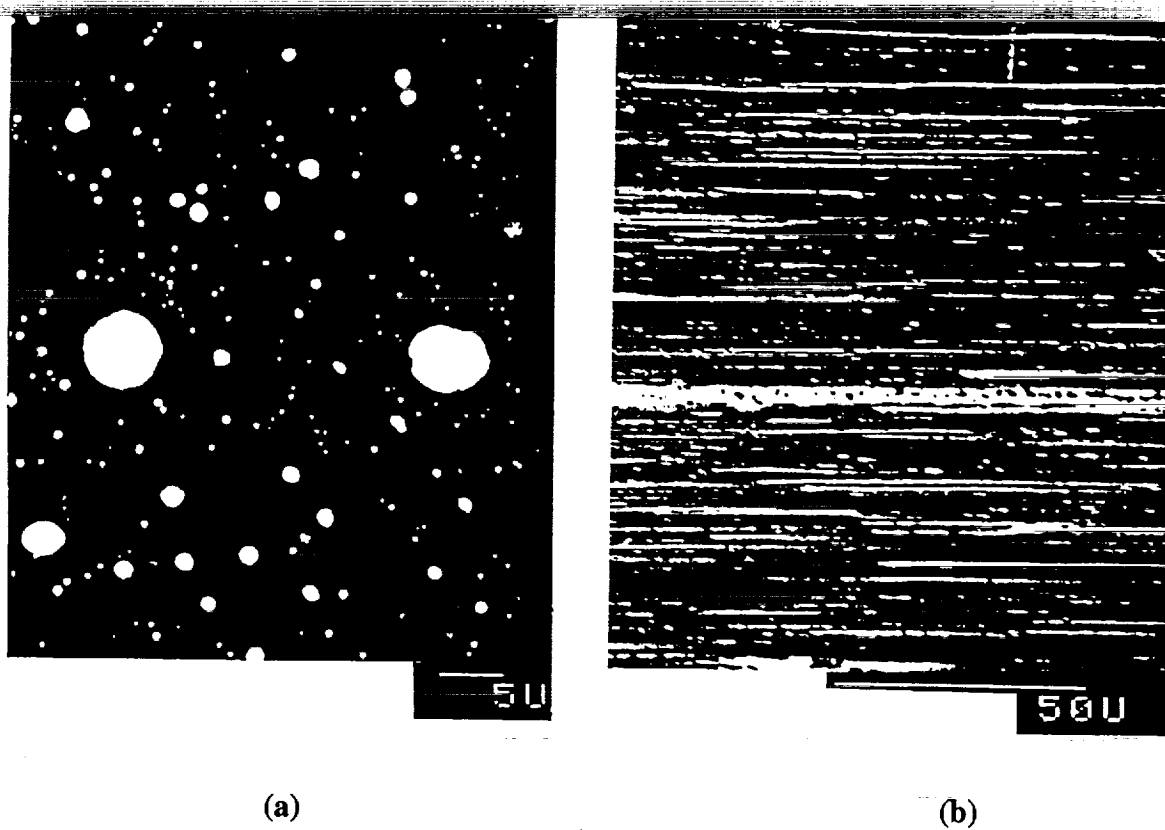


**Figure 1. M-4 casting of superconducting composite materials: (a) microphotograph of Al-Pb-Bi as-cast ingot and (b) microphotograph of wire made by deforming the ingot.**

FURNACE

TEM-01

AL-PB-BI ALLOY

BORON NITRIDE CRUCIBLE

NICKEL CARTRIDGE

(a) UNDER NORMAL GRAVITY

(b) UNDER LOW GRAVITY

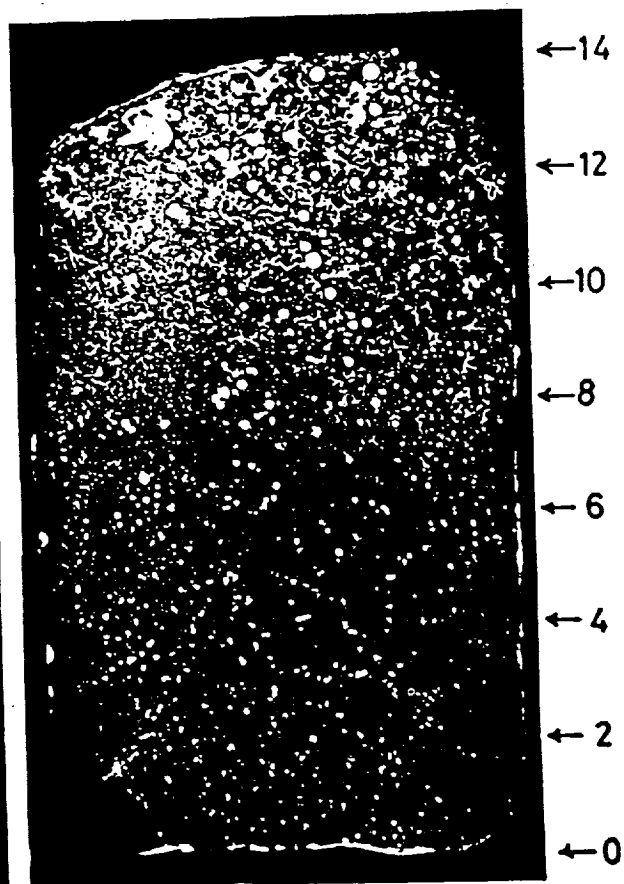
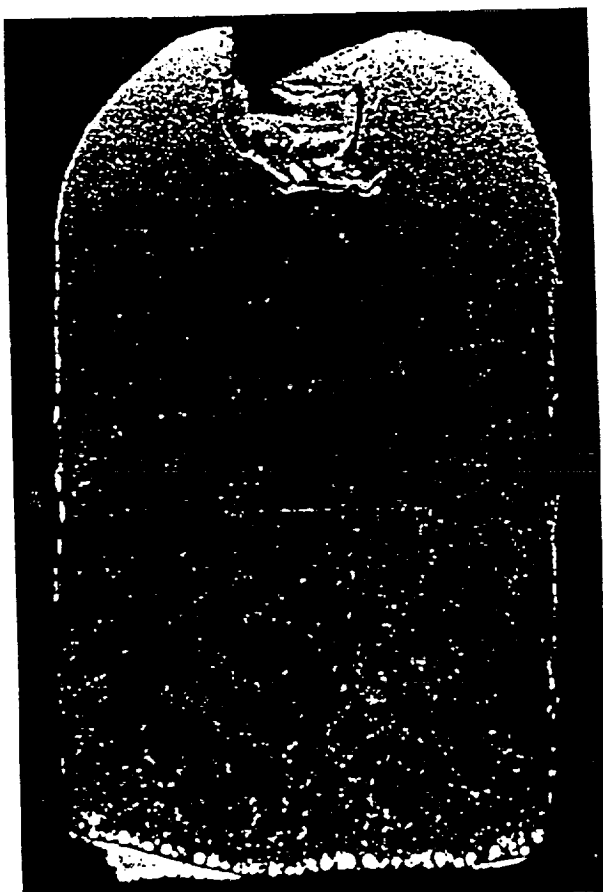
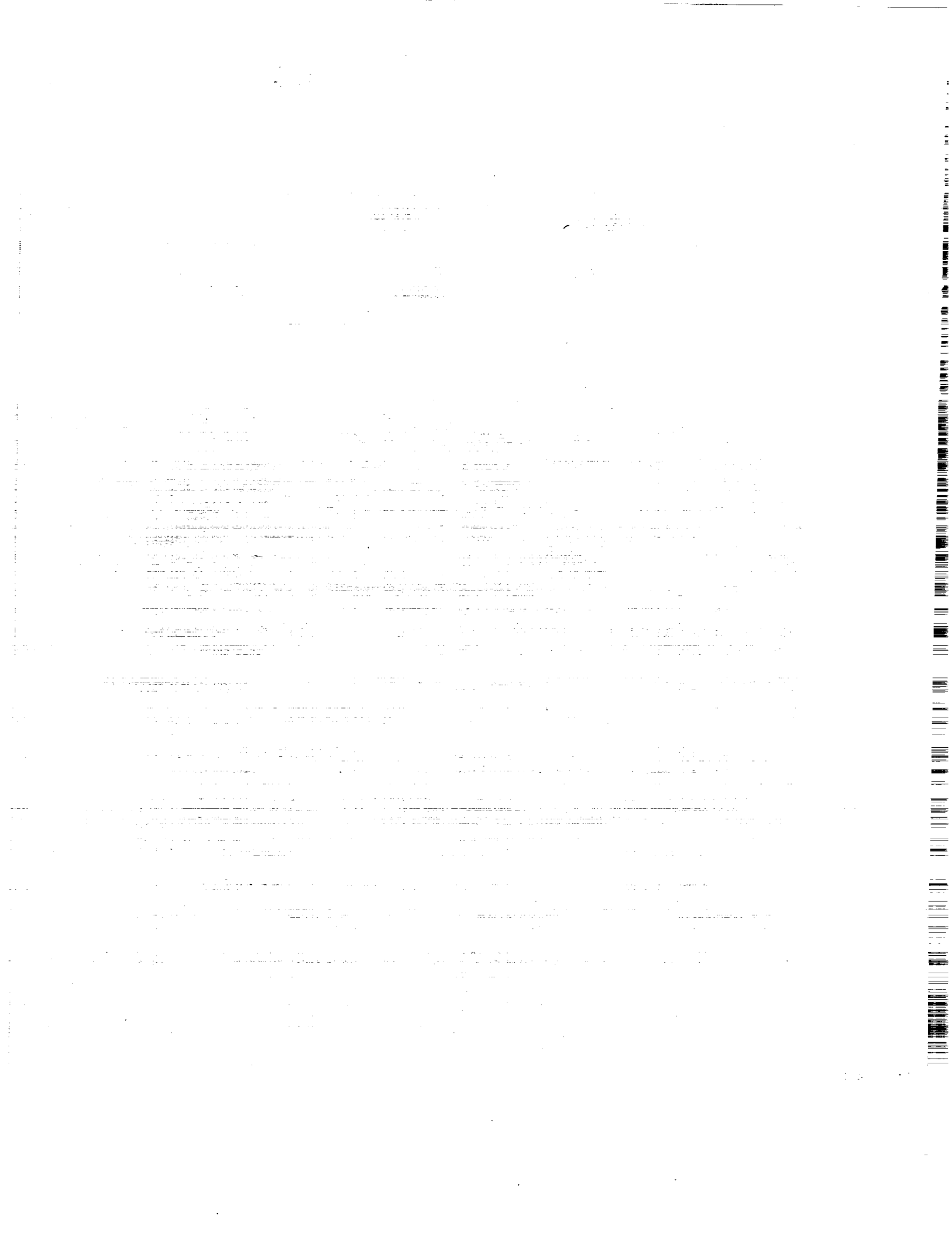


Figure 2. TEXUS 13 (1986) sounding rocket.



FORMATION OF DEOXIDIZATION PRODUCTS IN IRON INGOT  
BY THE ADDITION OF Al, Si, AND/OR Mn  
M-5

Akira Fukazawa  
National Research Institute for Metals  
Japan

The objective of this work is to examine the morphology, composition, and distribution of deoxidation products in iron and iron-10% Ni alloy ingots. The deoxidation agents Si, Mn, Al, and their mixtures are selected to investigate the formation mechanism of the deoxidation products and to compare the differences of oxide formation among these agents in microgravity.

The shape of the sample has been changed from a 12 mm $\phi$  sphere to a capillary type with 5 mm $\phi$  and a 25 or 10 mm length. As illustrated in Figure 1 the 25 mm sample is to be placed parallel with the axial direction of the Large Isothermal Furnace (LIF) and the 10 mm sample is set at a right angle to the axial line to check the effect of heat flow during solidification.

The samples are set in the A1203 crucible first, then the crucible is inserted into the 22 mm $\phi$ , 40 mm long BN chamber. Four sets of BN chambers (two sets for 25 mm samples and two sets for 10 mm samples) are put into the Mo container as shown in Figures 1-3. Finally, the Mo container is set into the Ta container. Both Mo and Ta containers are sealed by EB welding.

The profile for heating and cooling is as follows: the container is heated to 1550 °C for about 50 min; after the desired temperature is reached the container is heated for an additional 3 min, and then cooling starts. The power supply constantly provides 700 W during heating.

Iron with three levels of oxygen content is prepared: 10, 50, and 300 ppm. Deoxidizing elements Al, Si, and Mn are alloyed with 5N iron independently and are also coupled with each other; these seven kinds of deoxidizers are then rolled into a sheet about 0.2 mm thick. These 4.95 mm $\phi$  iron bars and deoxidizer sheets are inserted into the alumina crucible layer by layer like a sandwich. The layered sample is capped with an alumina disc, on which light pressure is applied by coiled fine Ta wire in order to fill up the vacant space between the BN chamber and the cap. In this way the alumina cap is expected to move with the expansion and shrinkage of the sample so as to avoid the occurrence of Marangoni effects. The shapes of BN chambers are shown in Figure 2. For the 10 mm sample a BN cylinder with three holes to set alumina crucibles is inserted. A total of 12 samples can be examined in space.

After the experiment in space, the tested specimens are going to be analyzed by the use of the latest physical and/or chemical analytical equipment, and the information obtained will be a great help for the comprehension of the formation of oxide inclusion in steel for practical purposes, and also for the study of the solidification mechanism theory in the theoretical field.

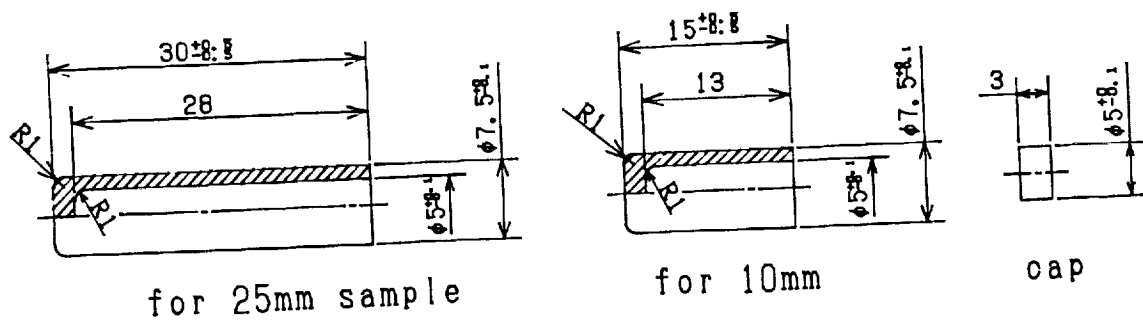
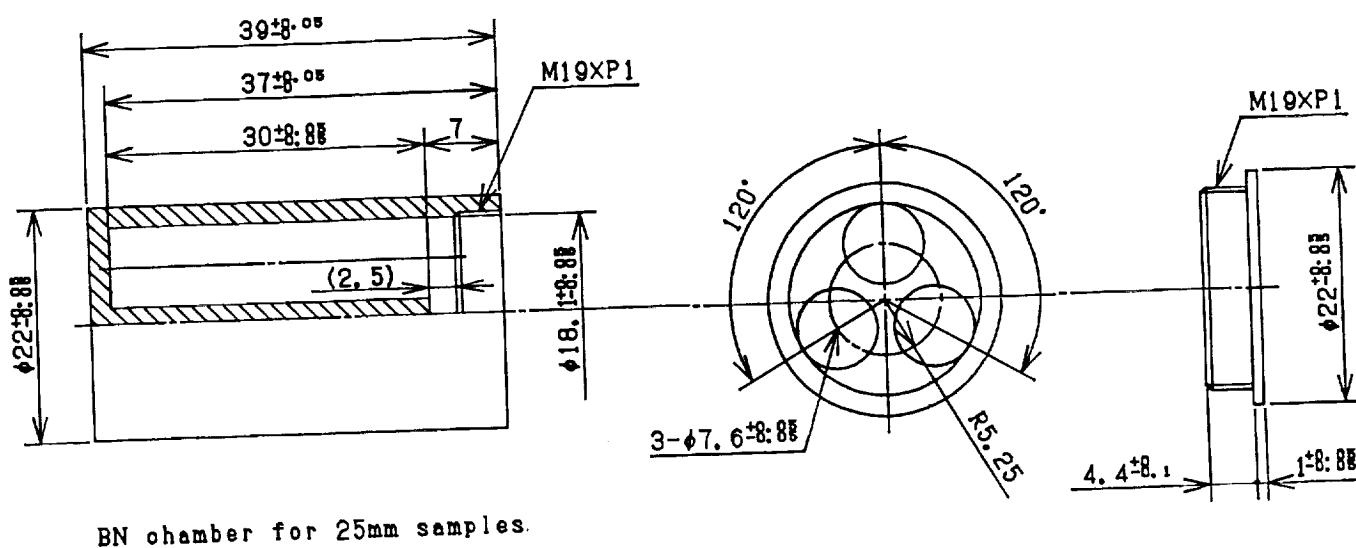
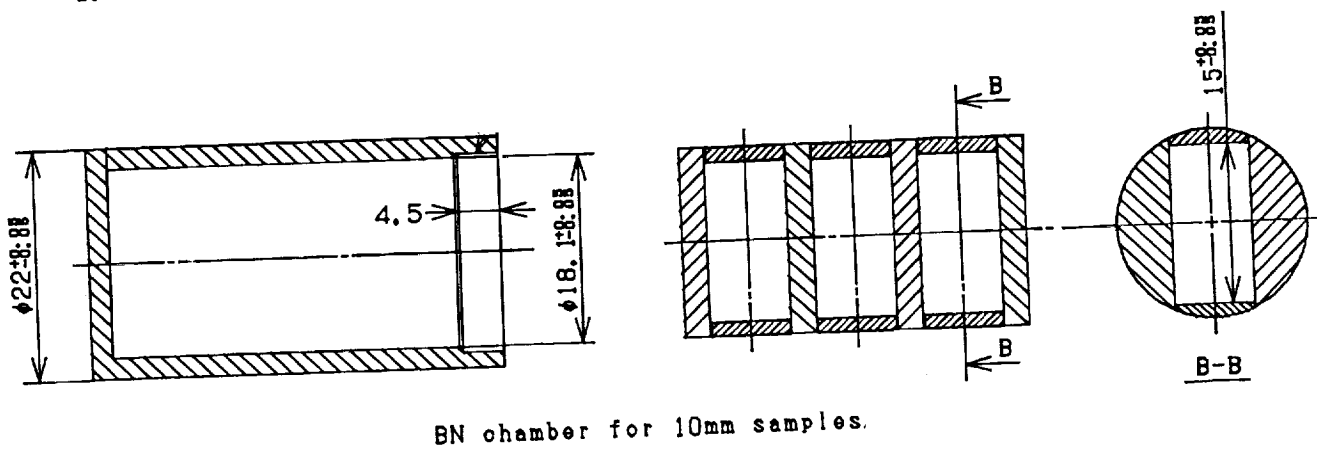


Figure 1. Alumina crucible.



BN chamber for 25mm samples.



BN chamber for 10mm samples.

Figure 2. BN chambers for 25 mm and 10 mm samples.

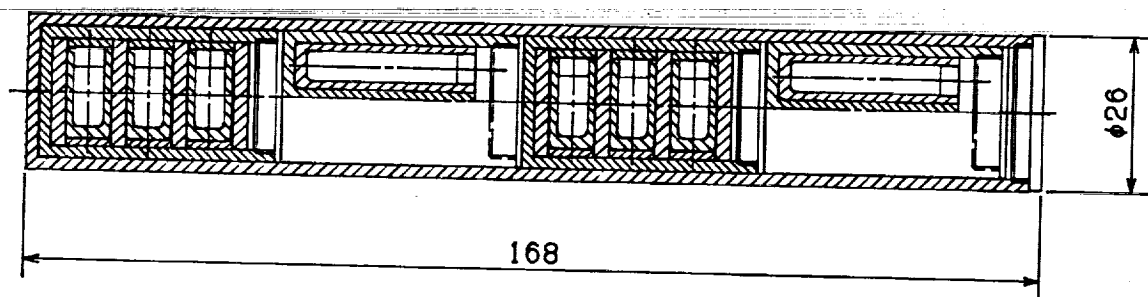


**Figure 3. Setup of Al<sub>2</sub>O<sub>3</sub> crucibles and BN chambers in Mo container.**



PREPARATION OF PARTICLE DISPERSION ALLOYS  
M-6

Yuji Muramatsu  
National Research Institute for Metals  
Japan

Objective

A particle dispersion alloy is one type of metal-ceramic composite material, and is used as heat resistance material, wear resistance material, and electrical material. This material consists of a metal matrix and dispersed particles, and for its unique structure it has both tenacity as a metal and hardness as a ceramic. Its properties improve when the particles become finer and disperse more uniformly.

Most of the particle dispersion alloys are produced by the powder metallurgical process. This process is favorable for uniform dispersion of particles, but it consists of complicated techniques such as mechanical alloying and hot extrusion, and has the following drawbacks:

1. It is difficult to fabricate large-sized products.
2. The amount of particles is limited to a few percent.
3. The process is complicated and expensive.

To overcome these drawbacks, recently special attention has been paid to conventional melting process. However, under terrestrial conditions, dispersions separate immediately due to the different specific gravities of the metal matrix and the particles and thermal convection

effects. The microgravity environment is, therefore, considered to be an attractive place for fabricating the dispersion alloy.

This space experiment is carried out to clarify the influence of microgravity on the properties of the particle dispersion alloy and to obtain a deeper understanding of the experiment under the microgravity environment.

### Outline of Experiment

The outline of the experiment is as follows:

#### 1. Sample

Samples used in this experiment are TiC-particle dispersion alloys. Their composition is given in Table 1. Molybdenum is an element used to improve the wettability of nickel and TiC. Chromium is added for improving oxidation and corrosion resistance, as well as for hardening the matrix. Cobalt is added for hardening the matrix.

These samples are prepared using powders of their constituents by the following procedure:

Weighing of powder→Mixing→Consolidation of mixed powder in high temperature.

#### 2. Sample Crucible

Figure 1 shows the cross-section of the sample crucible. It is made from graphite and is designed to process three samples simultaneously. To prevent leakage of the melt, a special glass developed in our laboratory is placed at both ends of the crucible as shown in Figure 1.

### 3. Sample Cartridge

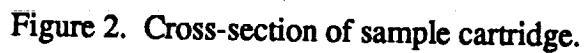
The cross-section of the sample cartridge is shown in Figure 2. The cartridge is made from tantalum and consists of a sample crucible holder and a pressurizing mechanism. The pressurizing mechanism is for squeezing the gas released from molten alloys, from the inside of the sample to the outside, so that it is very useful for fabricating solid samples free from voids.

After the cartridge is installed in the Large Isothermal Furnace, all of the operations such as heating, isothermal holding, pressurizing, etc. are carried out automatically by the aid of a computer.

### Related Experiment

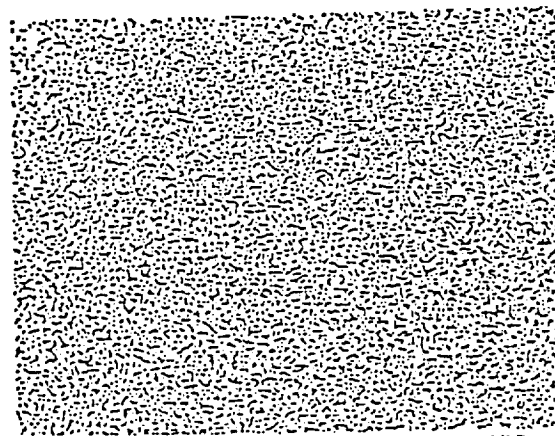
Related experiments were conducted by TT-500A Sounding Rocket (NASDA) in 1980, 1981, and 1982. These experiments have proved that a low-gravity environment is favorable for uniform dispersion of particles. Figure 3 illustrates the microstructures of the samples processed in space and on the ground. It is evident that the sample obtained in space has a structure more homogeneous than the sample obtained on the ground.

Sample	Ni	TiC	Mo	Cr	Co
No. 1	Bal	20	10	10	-
No. 2	Bal	20	10	-	10
No. 3	Bal	20	9	9	9





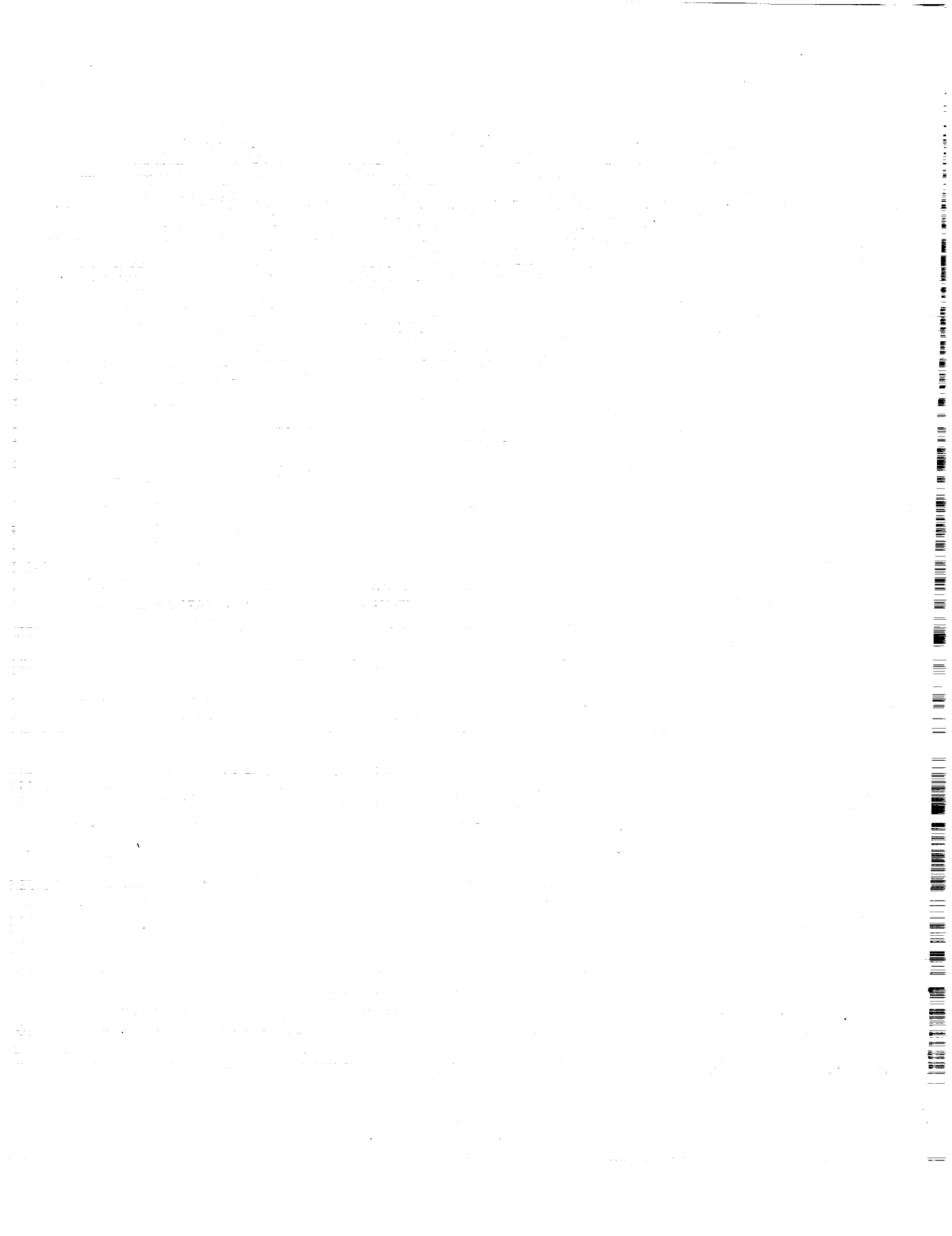
Processed on the ground



Processed in space



Figure 3. Microstructures of TiC-particle dispersion alloy.



DIFFUSION IN LIQUID STATE AND SOLIDIFICATION OF BINARY SYSTEM  
M-7

T. Dan  
National Research Institute for Metals  
Japan

Abstract

Diffusion is one of the most fundamental physical phenomena. It relates to the manufacturing processes of almost all materials. Therefore, the precise knowledge of diffusivities of relevant materials is necessary for the optimization of these processes. On the other hand, such knowledge is indispensable to understanding the diffusion mechanism and structure of liquid metal in the field of physical metallurgy.

Many diffusion experiments on solid metal have been undertaken and a lot of data have been accumulated. But on liquid metals there are few measurements because of experimental difficulties, such as thermal convection, induced by very slight temperature gradients in the specimen.

Under microgravity conditions, the movement of liquid metal due to density differences and thermal convection must be suppressed markedly. Therefore, the transportation process will be controlled only by the diffusion of constituent atoms. These conditions offer the optimum environments for the diffusion experiment.

We briefly describe the experimentals below. Diffusion couples are prepared by attaching end to end two rods of different pure metals using hot press equipment. These couples are inserted into a graphite crucible and then doubly enclosed by two silica ampoules, respectively

(Figure 1). The specimen is inserted into a tantalum cartridge, which is welded in a vacuum using an electron-beam apparatus. These cartridges are charged in the continuous heating furnace in space and held at a given temperature for a predetermined time and then solidified.

The concentration distribution of elements in these specimens will be measured along the rod axis by means of an electron probe microanalyzer. The counterdiffusivity of the liquid metal binary system is determined on the basis of the compensated concentration distribution profile for thermal contraction.

#### Expected Results

The results obtained by this experiment will contribute to the elucidation of the diffusion mechanism and the structure of liquid metal. Moreover, these results could be applied to both conventional and new manufacturing processes of materials not only in space but also on the ground in the near future.



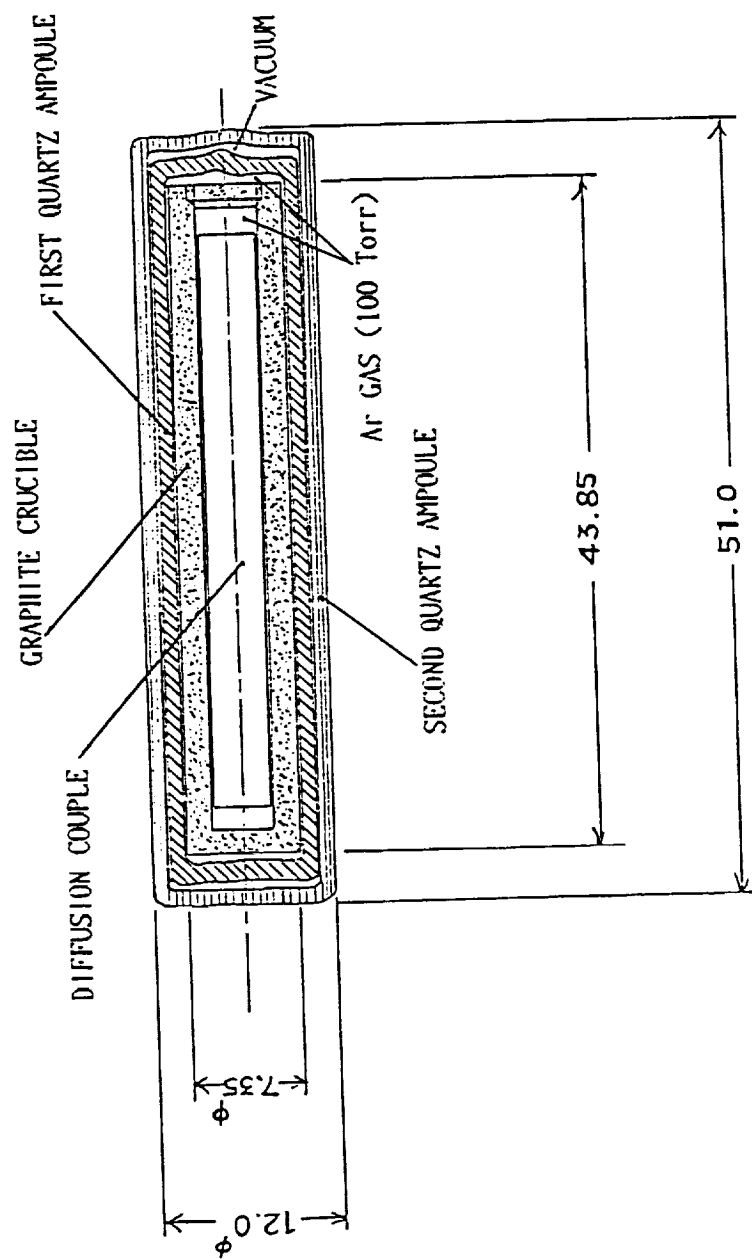


Figure 1. Configuration of M-7 specimen.



## HIGH TEMPERATURE BEHAVIOR OF GLASS M-8

Naohiro Soga  
Kyoto University  
Japan

### Outline of Experiment

The twofold purpose of this experiment is to obtain data on the occurrence of flow in a viscous glass sphere in microgravity, and to confirm data obtained on Earth for volume-temperature relationships of glass.

To do this, a cubic sample of glass laced with gold particles will be heated in the IMF. The sample's properties will be measured at high temperature, and the volume of the sample varied to measure the expansion coefficient. Movement of the gold particles, if any, will determine flow within the sample. The apparatus for this experiment is schematically shown in Figure 1. Figures 2 and 3 show the photographs of the image furnace with samples before and after melting, respectively. In this apparatus, shape and size of the sample are observed by video camera and recorded by video recorder. The recorded images of the sample are schematically shown in Figure 4. In this figure, symbols A, B, and C denote low, intermediate, and high temperatures, respectively. From these images, the volume of the sample is estimated and the temperature dependence of the volume, which is shown in Figure 5, is obtained.

If there is agreement between the data collected in this experiment and data obtained on Earth, it would tend to verify Earth-collected data.

### Expected Results

(1) The volume-temperature relationship obtained in space is compared with the Earth-bound data. The agreement between these data is taken as proof that all the Earth-bound data obtained on various glasses are good.

(2) From the movement, if any, of Au pieces, information about the occurrence of flow inside a viscous glass sphere can be obtained. This information is useful for obtaining homogeneous glass in space.

(3) The quenched sample is subjected to internal stress examinations when returned. This information is useful for examining the quenching and annealing processes in space.

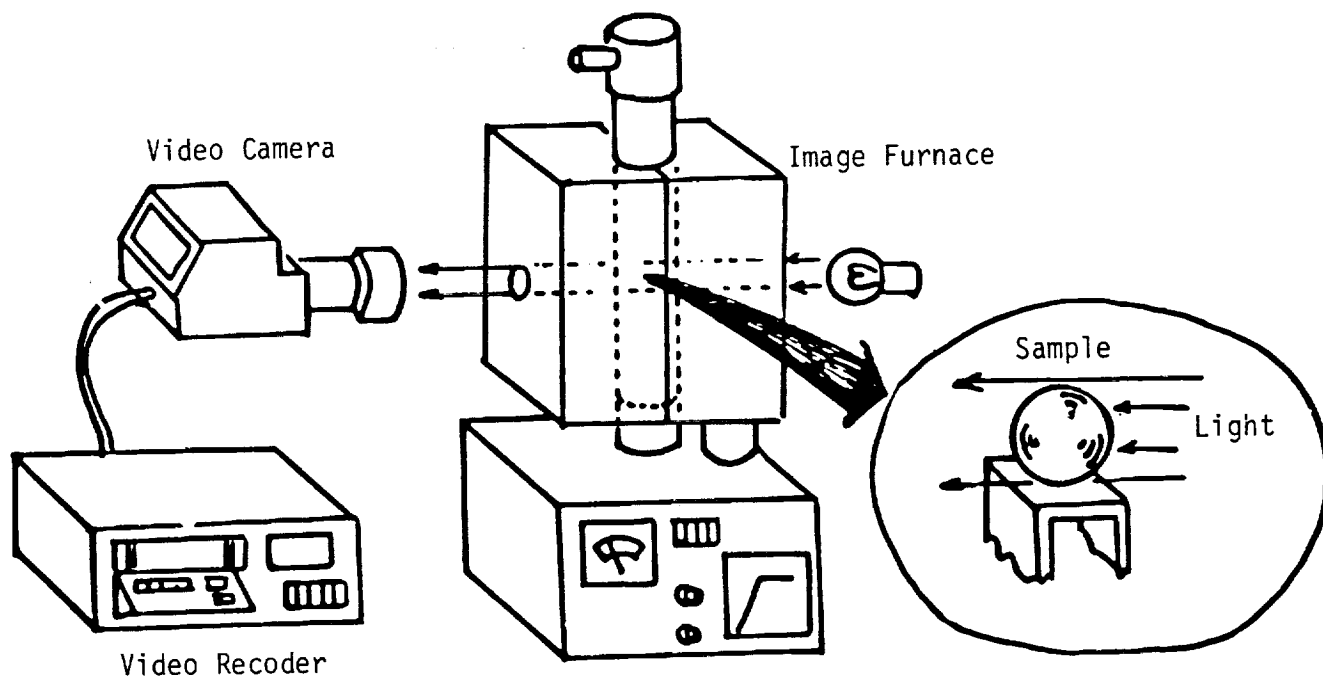


Figure 1. Apparatus for experiment.

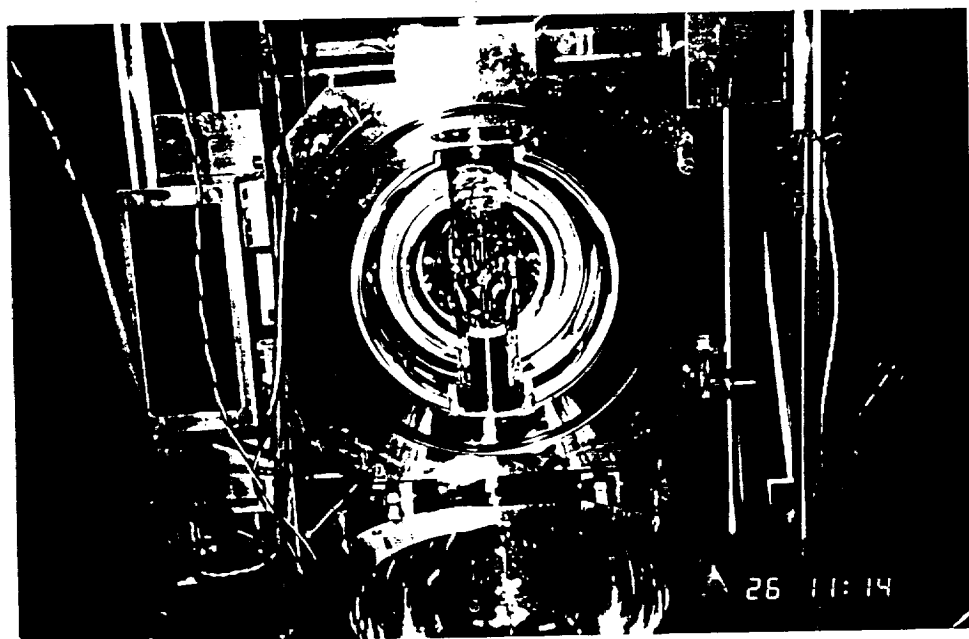


Figure 2. Photograph of image furnace with sample before melting.

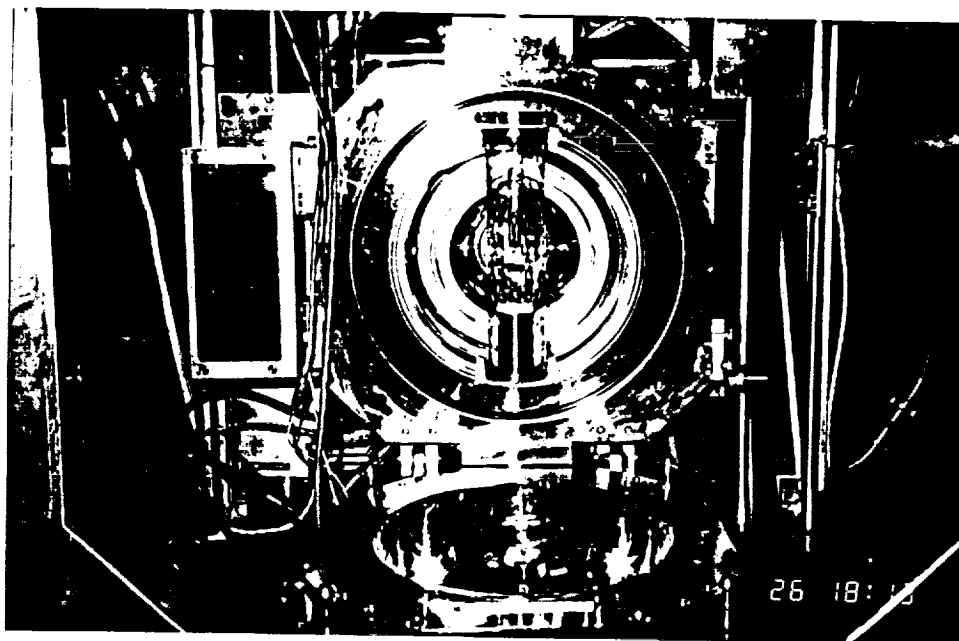


Figure 3. Photograph of image furnace with sample after melting.

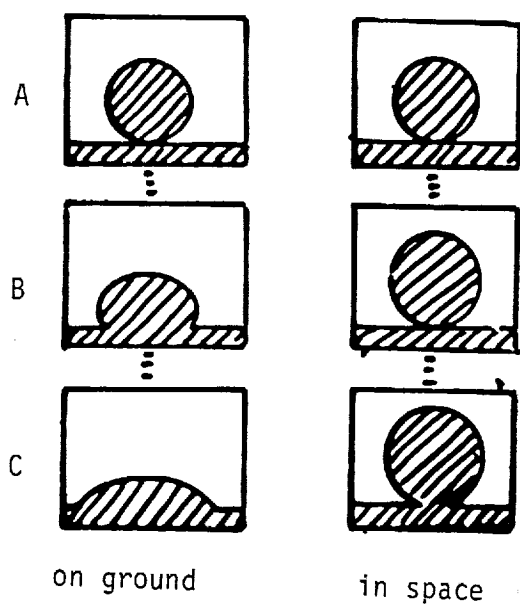


Figure 4. Images of the sample recorded by video recorder.

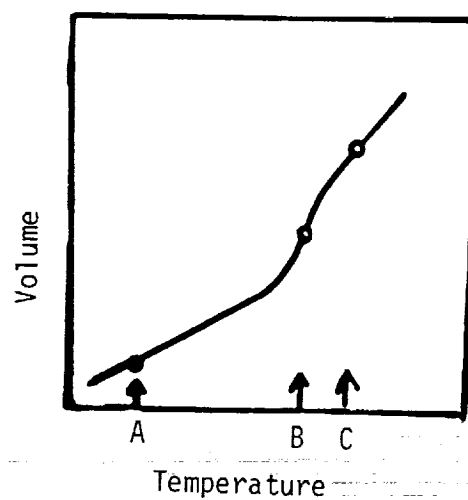


Figure 5. Temperature dependence of the glass sample.

## GROWTH OF Si SPHERICAL CRYSTALS AND THE SURFACE OXIDATION M-9

Tatau Nishinaga  
University of Tokyo  
Japan

Nearly 90% of semiconductor devices are produced with Si single crystals as the starting materials. For instance, the integrated circuits (IC), which are used in almost all electronic equipments such as TV, tape recorders, audio amplifiers, etc., are made after various processings of Si single crystal wafers. In these wafers, the same controlled amounts of impurities are added and the uniformities in their distributions are extremely important.

Growth under microgravity makes it possible to eliminate the buoyancy-driven convection in the melt, which is one of the main origins of convections which results in non-uniformity of the impurity. Another source of convection is known as Marangoni convection which is driven on the free surface when a temperature gradient occurs. One of the merits of microgravity experimentation is that the detailed study of this convection becomes possible. Another important advantage of microgravity is that growth of crystals without a crucible is possible. This makes it possible to study melt growth without the strain which is usually introduced on the ground. Nevertheless, we should repeat and analyze many growth experiments in space to get reliable results. However, since in the FMPT, the time for the experiment is limited, we plan to carry out two kinds of very simple and basic experiments as the first step for the semiconductor growth experiment.

In the first experiment, we use single crystal Si sphere as the starting material and as shown in Figures 1 and 2, this sphere is heated in the furnace at a slightly higher temperature

than the melting point. After the melting front moves nearly half way to its center, the temperature is decreased to stop the melting and to start the growth from the seed for which we use the unmelted solid part of the sphere. The sphere is centered by quartz protuberances inside of the quartz crucible. There exists the possibility of temperature fluctuations being introduced when the molten sphere occasionally touches the protuberances. The total time needed for the melting and the growth processes is estimated to be 30 minutes. Infrared emission from the sphere is monitored in order to prevent the accidental loss of the central solid core.

The schematical illustration of the second experiment is shown in Figure 3. Here, a single crystal, Si rod is used as the starting material. In the first stage, the rod is melted from one end to obtain a liquid sphere. In the second stage, the single crystal is grown by decreasing the temperature from the unmelted part of the rod which is used as the seed. The second experiment somewhat resembles the Czochralski method used on the ground; however, in the space experiment, no crucible is employed and the temperature uniformity is much superior.

In both experiments, phosphorus is doped to allow observation of the change in the shape of the liquid solid interface during crystal growth and the impurity striations, if any.



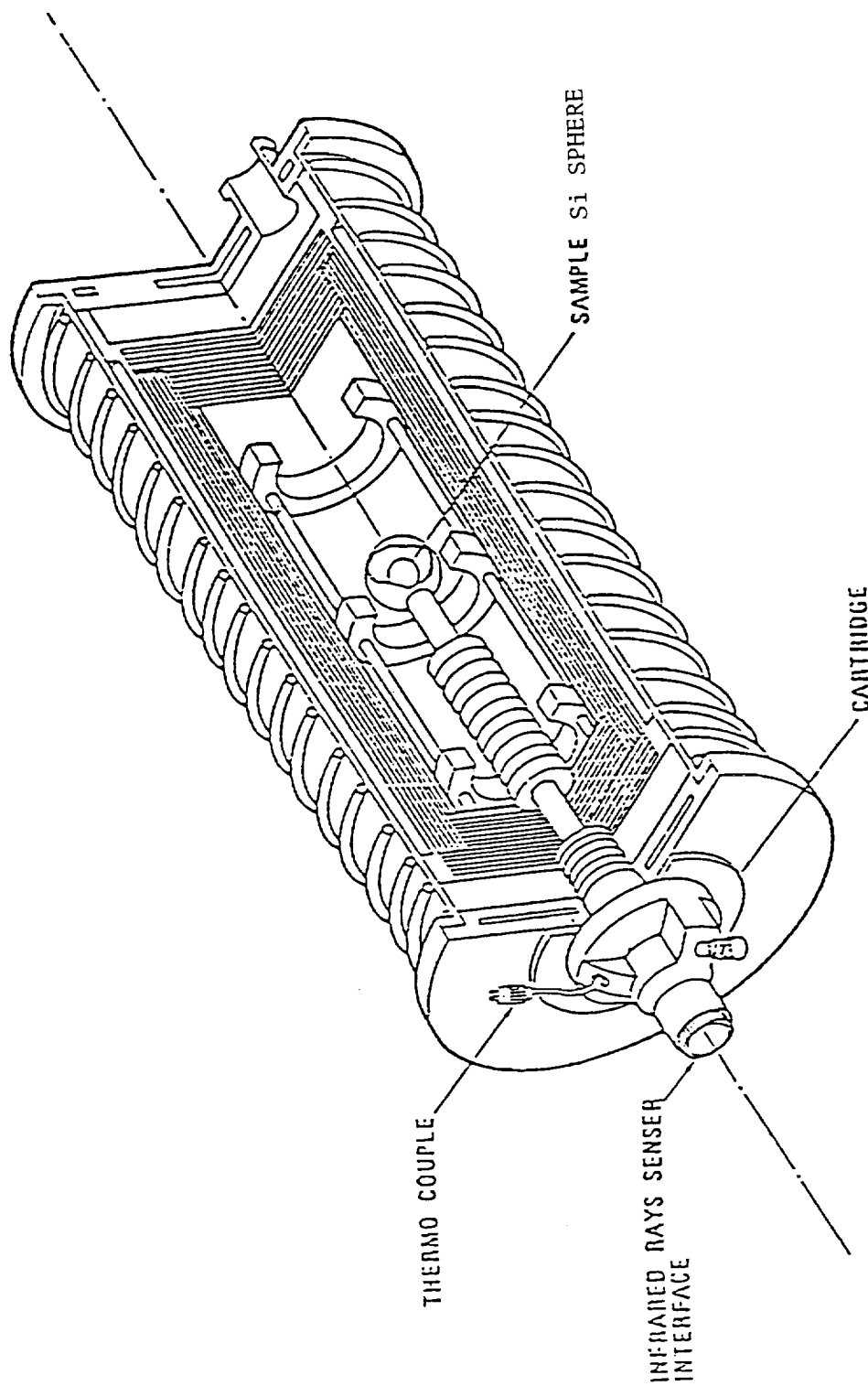


Figure 1. Crystal Growth Experiment Facility concept.

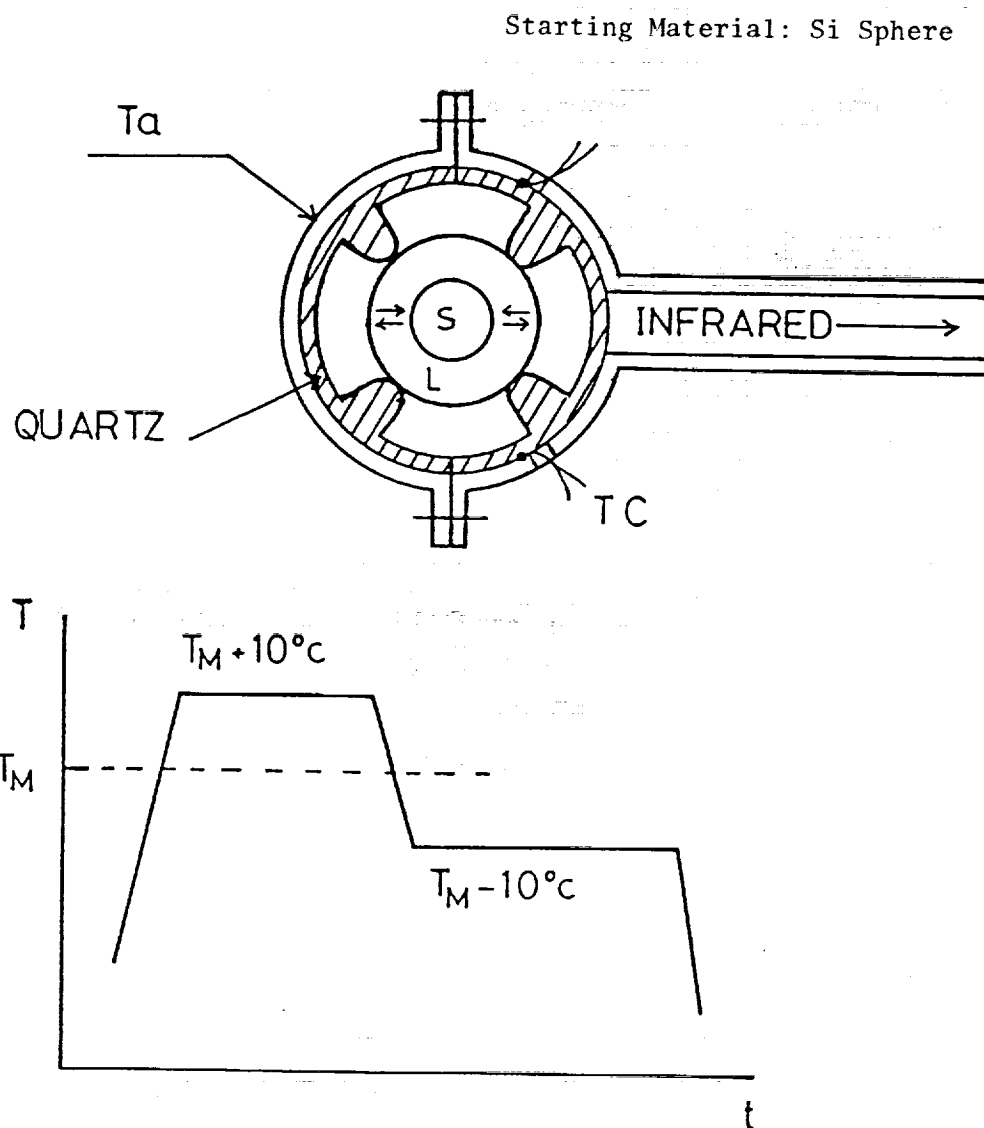


Figure 2. Growth of spherical crystal.

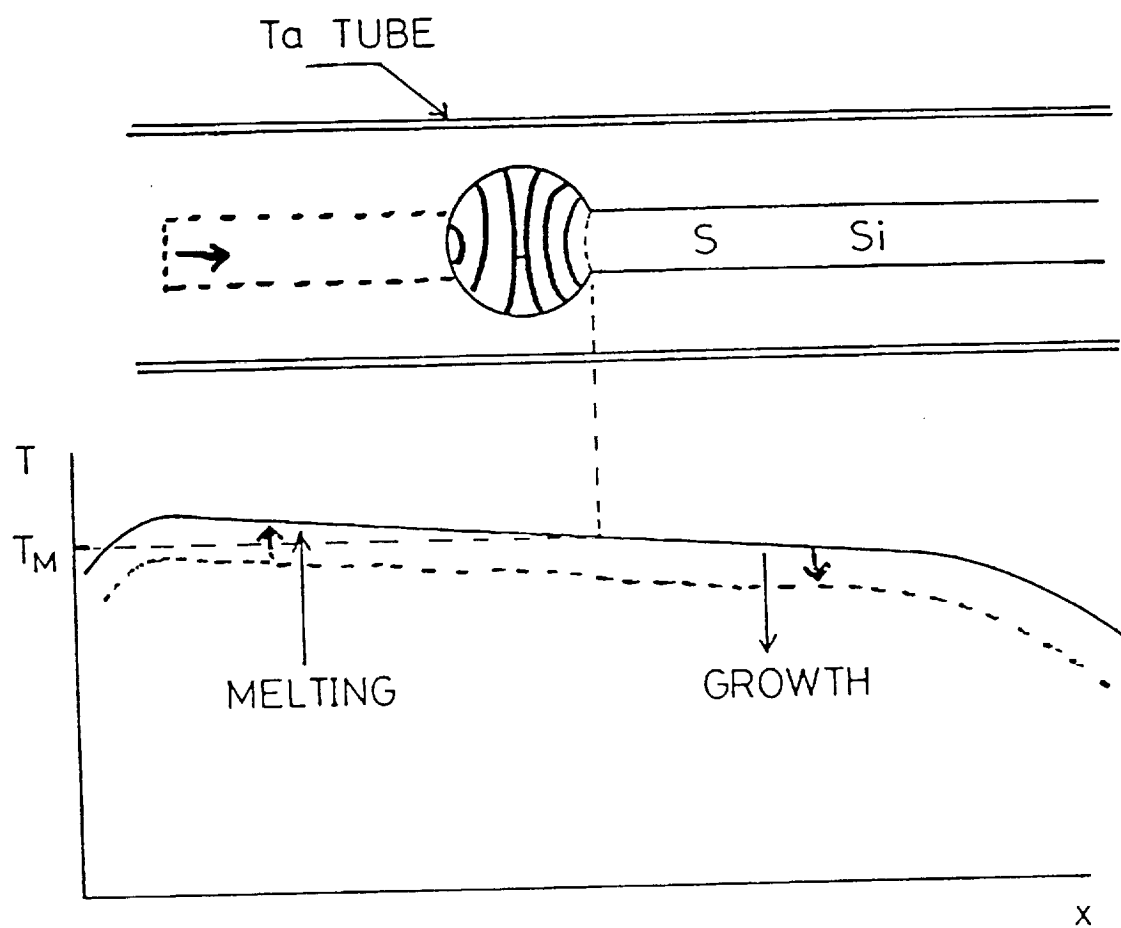


Figure 3. Growth of HEMI-spherical crystal with external seed.



STUDY ON SOLIDIFICATION OF IMMISIBLE ALLOYS  
M-10

Akihiko Kamio  
Dept. of Metallurgical Engineering, Tokyo Institute of Technology  
Japan

Alloying of immiscible alloys under microgravity is of interest in metallurgical processes. Several experiments investigating the alloying of immiscible alloys, such as Al-In, Al-Bi, Zn-Bi and Zn-Pb, have been done in space. Homogeneous distribution of small  $L_2$  particles in the matrix, such as an emulsion structure, was expected in the space-solidified alloys. However, the alloys demonstrated an extremely segregated structure. To date insufficient information has been obtained to explain these unexpected results. We proposed our experiment to clarify the solidification manner of immiscible alloys and to obtain fundamental information concerning structural control of the alloys. In space, density differences between the two liquids separated in immiscible regions can be neglected, so that no sedimentation of  $L_2$  phase will take place. When the growth of the alloys is interrupted and this status is frozen by an adequate rapid cooling procedure, it will provide much information concerning decomposing homogeneous liquid and the interaction between the monotectic growth front morphology and the distribution of  $L_2$  phase. It is anticipated that the results will be useful for elucidating the monotectic solidification manner and it will be instructive to explain the segregated structures obtained in the past space experiments.

## Equipment Functions

Separation Chamber	62 x 10h (cm)
Thickness	4.0 (mm)
Electric Field Grad.	100 V/cm Max.
	Const. Volt.
Electric Current	100 mA Max.
Buffer Flow Rate	2-10 cm/min
Sample Flow Rate	2-10 cm/min
Operating Temperatures	<5 °C (wall)
Number of Fractions	2.5 ml x 60 Max.
Detector System	Real Time Monitor
Wavelength	280 nm
Resolution	512 ch (0.1 mm)
Scale	0-1.02 OD
Sensitivity	<0.005 OD
Buffer Capacity	>1200 ml

### Experiment Objectives

1. Mixing of immiscible melts of Al-In and Cu-Pb alloys by ultrasonic vibration
2. Unidirectional solidification of Al-In and Cu-Pb hyper-monotectic alloys
3. Observation of distribution of immiscible  $L_2$  liquid phases ahead of monotectic growth front.

### Expected Results

1. Techniques to obtain homogeneous liquid in melting of immiscible alloys under microgravity
2. Alloying of immiscible alloys having uniform dispersion of small unsolutionable particles
3. Separating manner of  $L_2$  liquid in miscibility gap of monotectic system alloys
4. Interaction between monotectic growth front and separated  $L_2$  liquid phase
5. Formation mechanism of solidification structure in monotectic and hyper-monotectic alloys
6. Production of in situ composite materials having arrayed structure under microgravity.

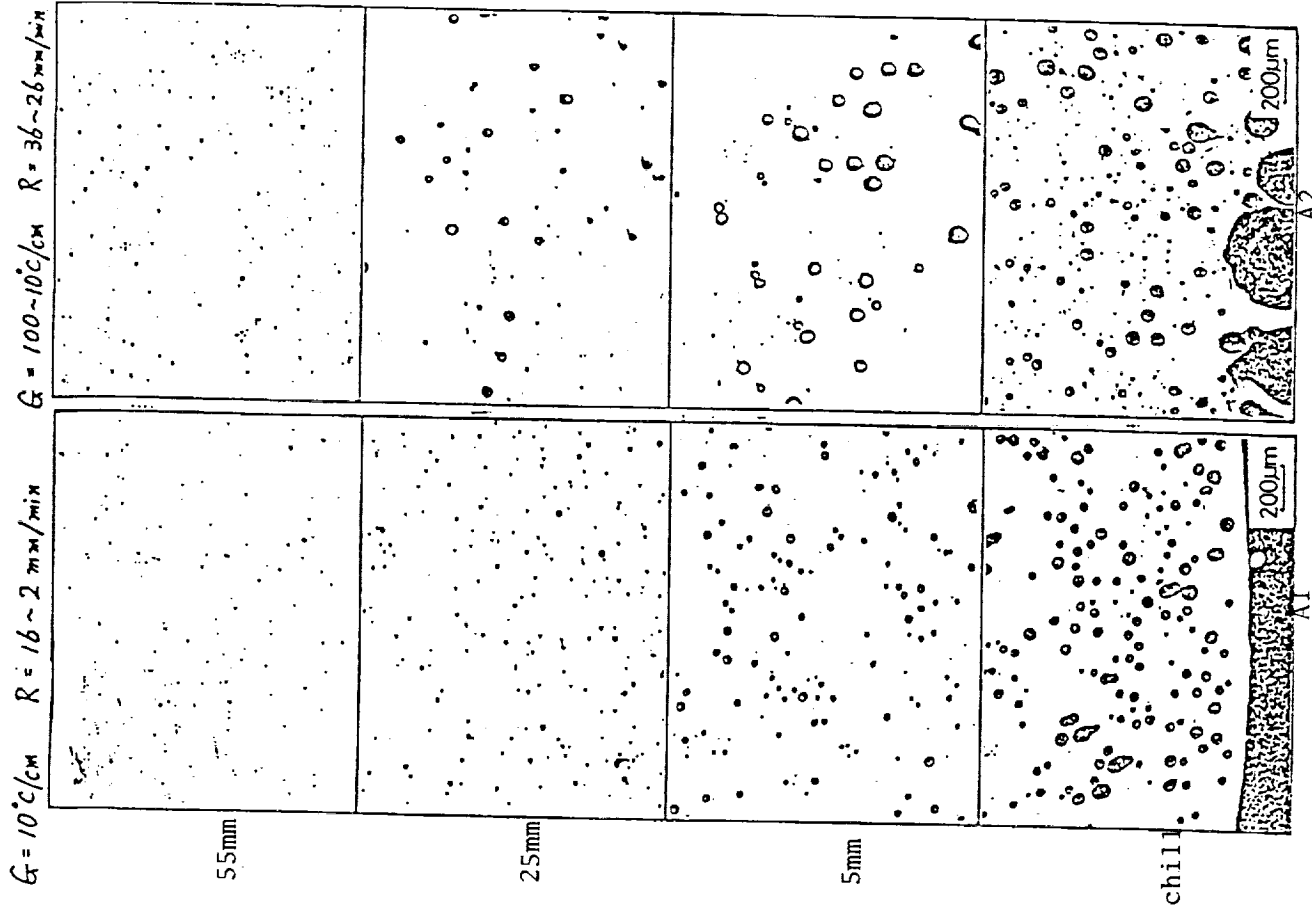


Figure 3. Microstructures of Al-10%Pb alloy solidified unidirectionally.

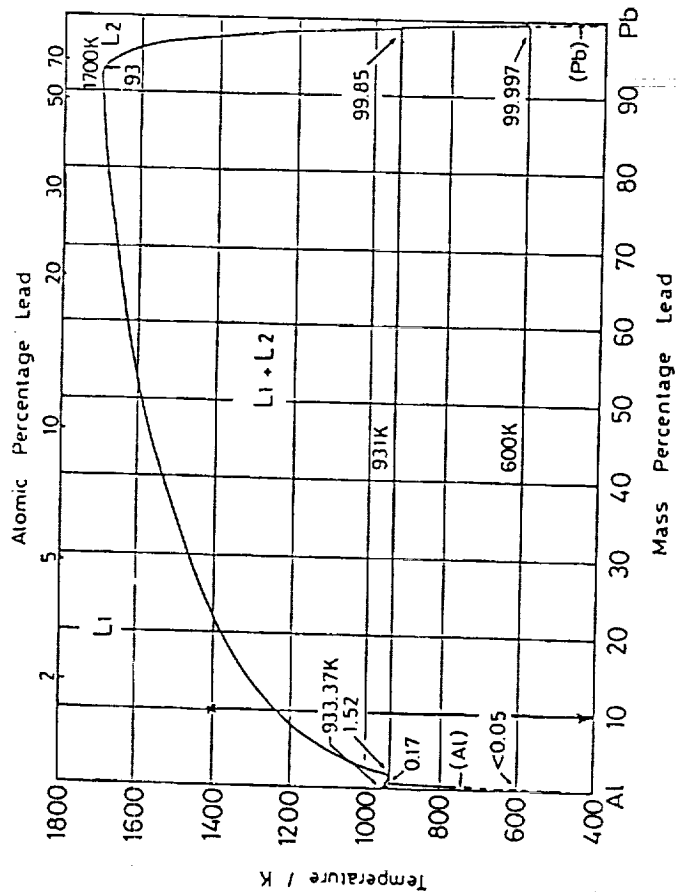


Figure 1. Al-Pb phase diagram.

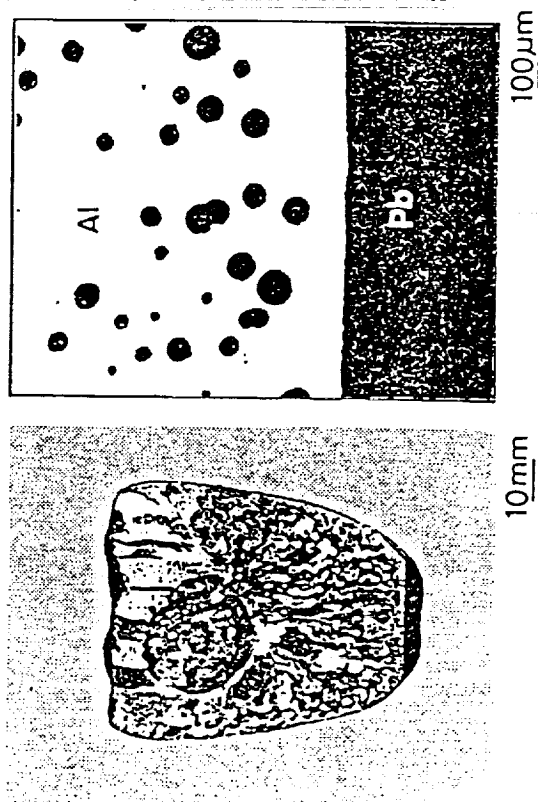


Figure 2. Macro- and microstructure showing gravity segregation in hypermonotectic Al-10 mass%Pb alloys solidified non-directionally.



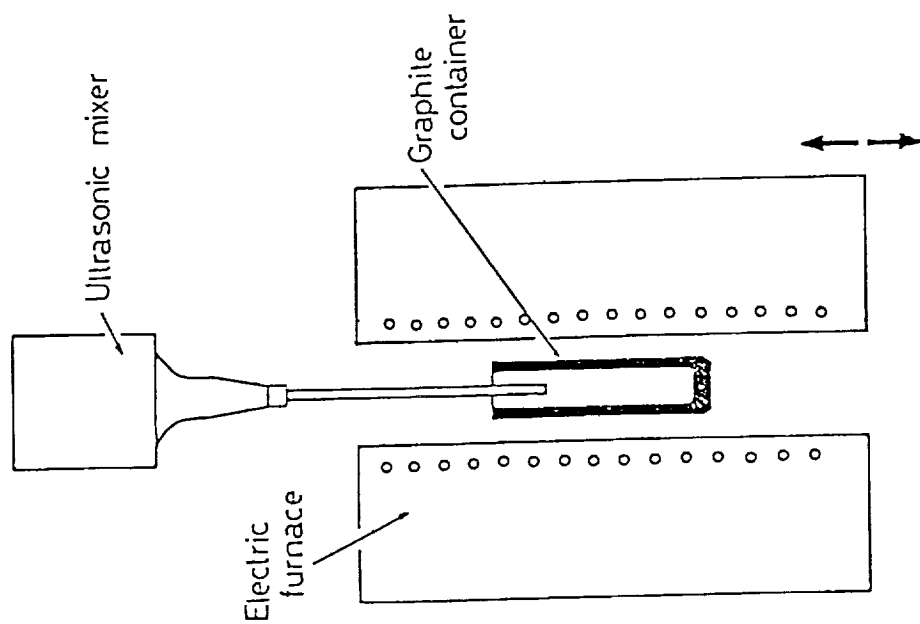


Figure 4. Apparatus for alloying under terrestrial conditions.

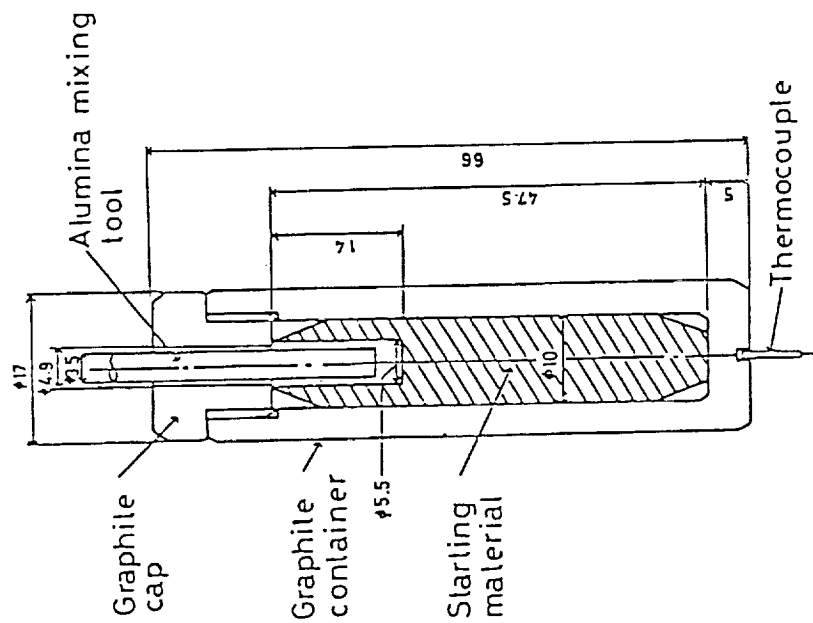


Figure 5. Dimensions of starting material and graphite container.

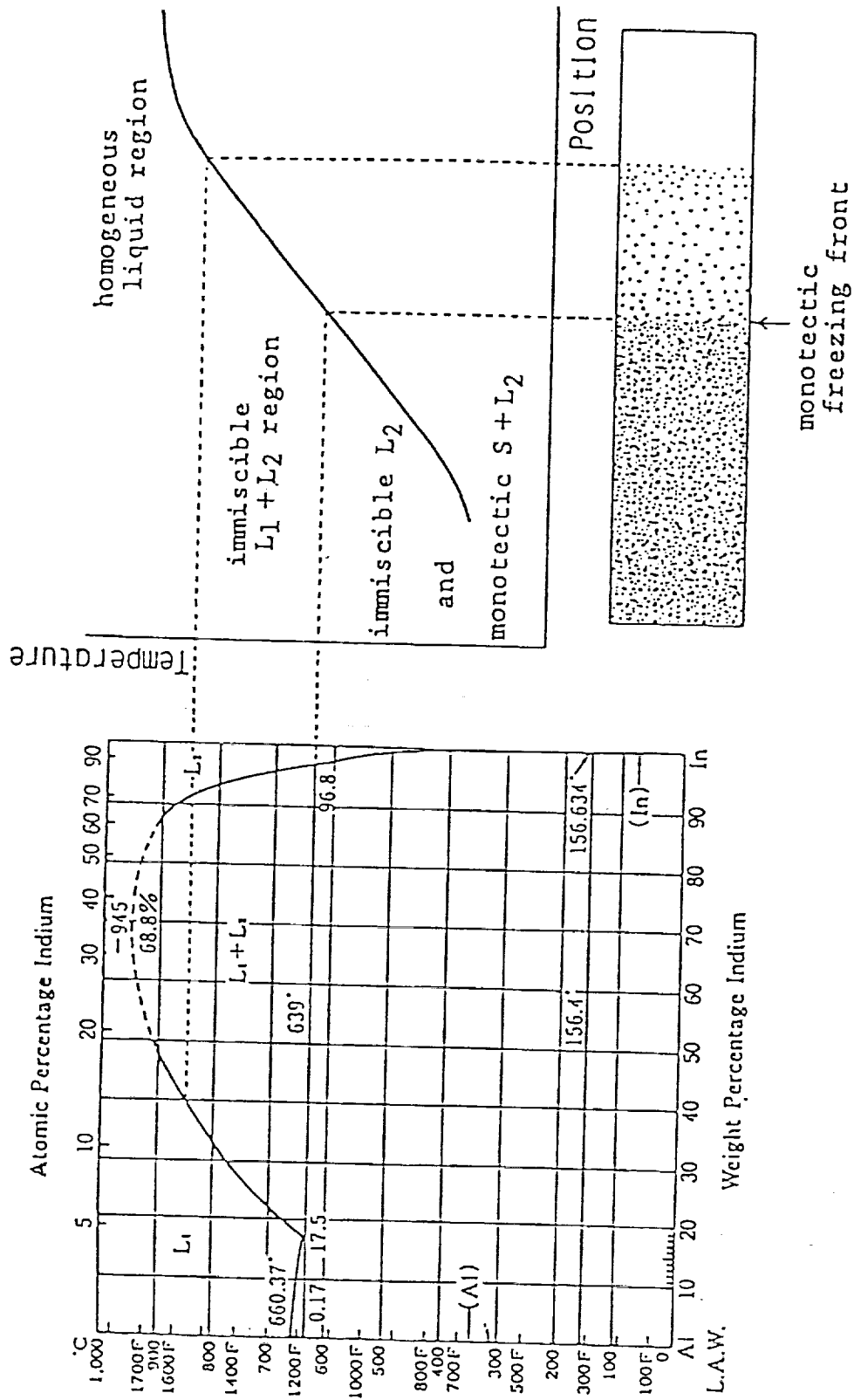


Figure 6. Unidirectional solidification of hypermonotectic Al-In alloy.

Table 1. Composition of Samples

A1-40 mass%In alloy	( $\phi$ 9 x 65 mm)
A1-17.5 mass%In alloy	( $\phi$ 4 x 67 mm)
A1-20 mass%In alloy	( $\phi$ 4 x 67 mm)
A1-40 mass%In alloy	( $\phi$ 4 x 67 mm)
Cu-36 mass%Pb alloy	( $\phi$ 4 x 67 mm)

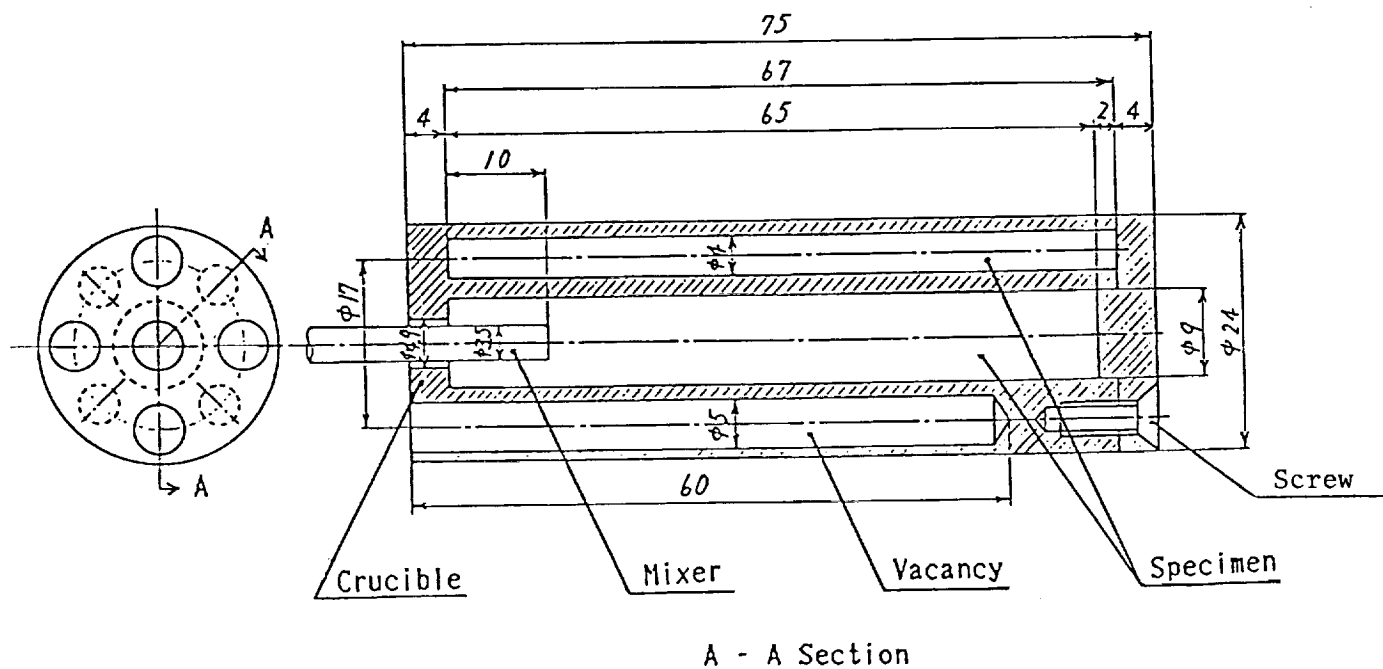


Figure 7. Specimen and crucible size.

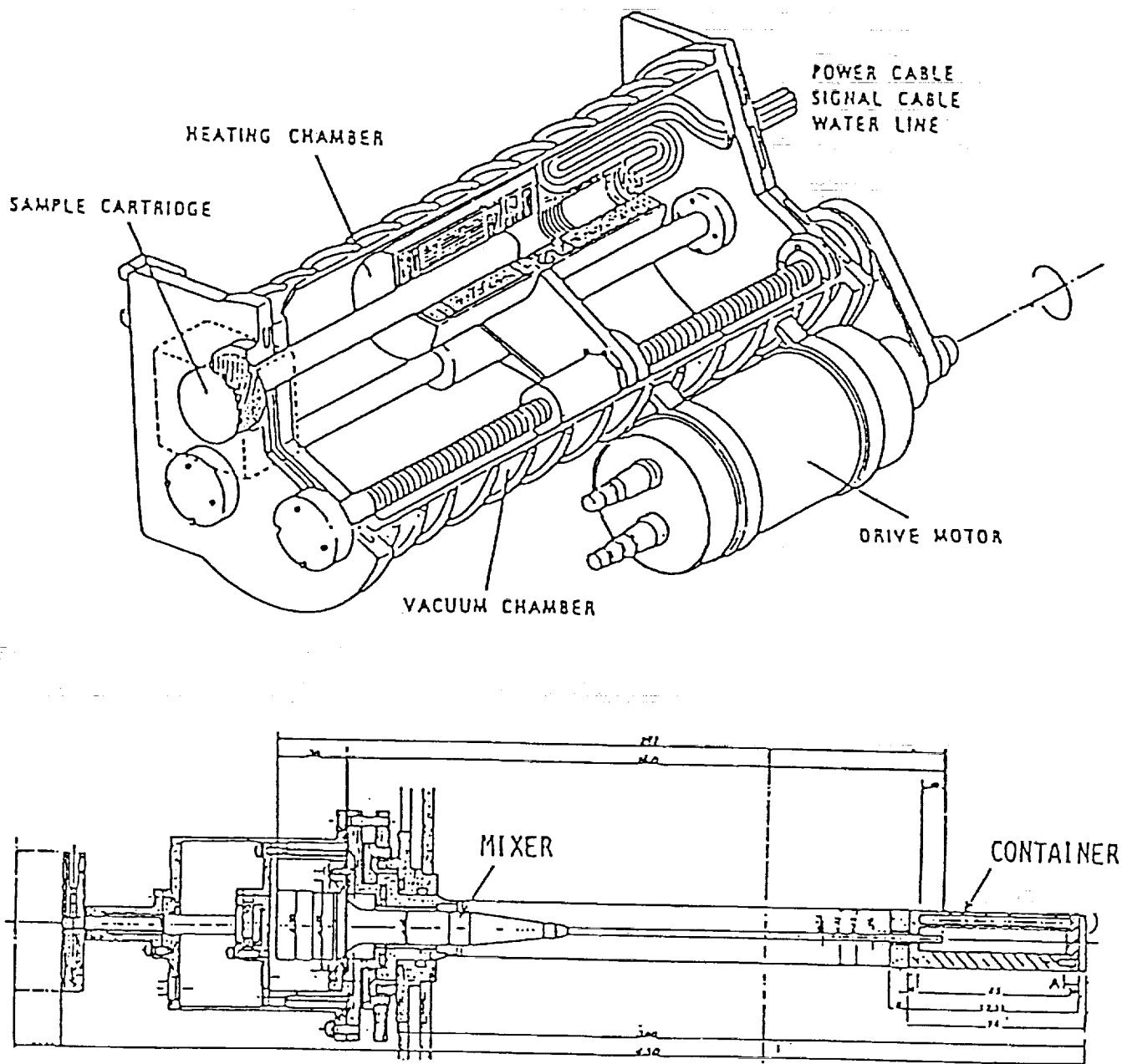
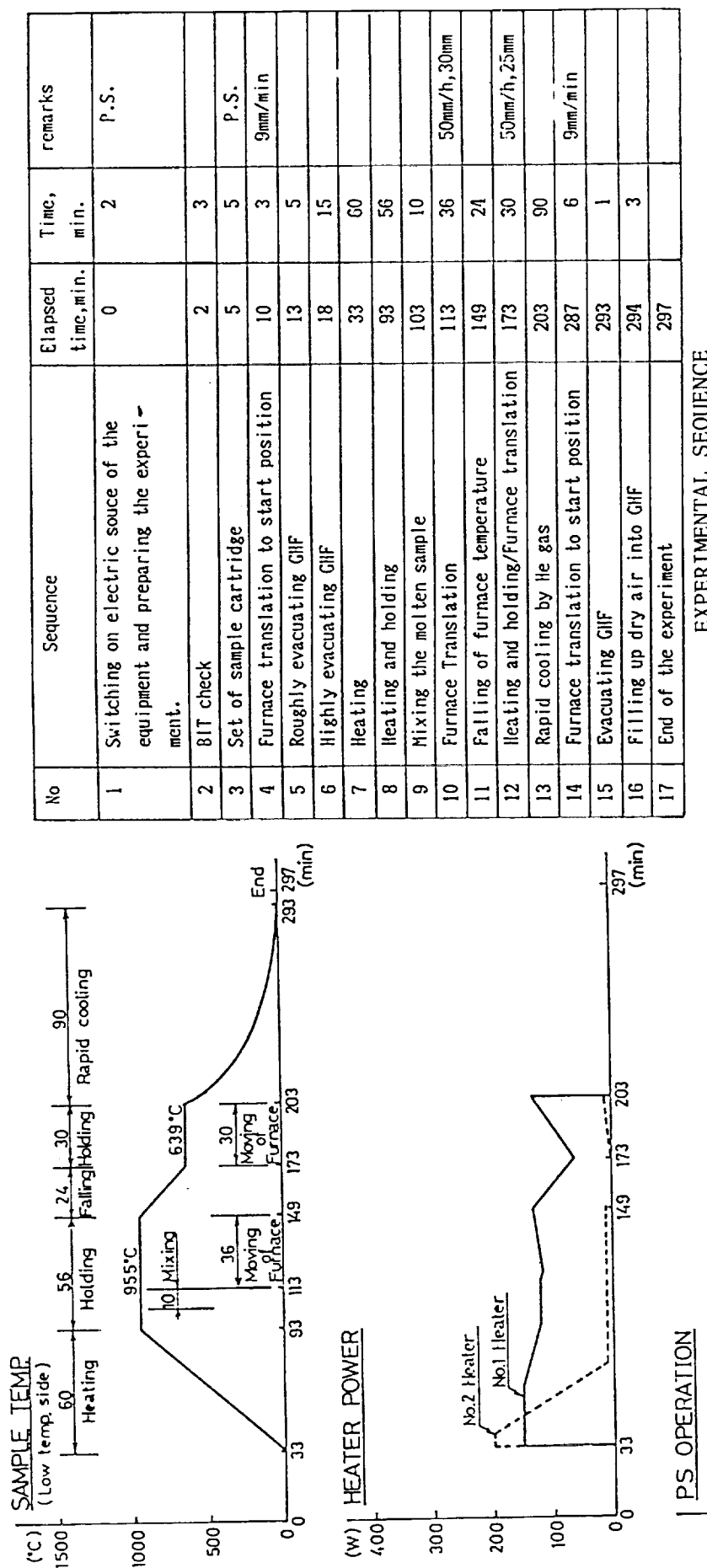
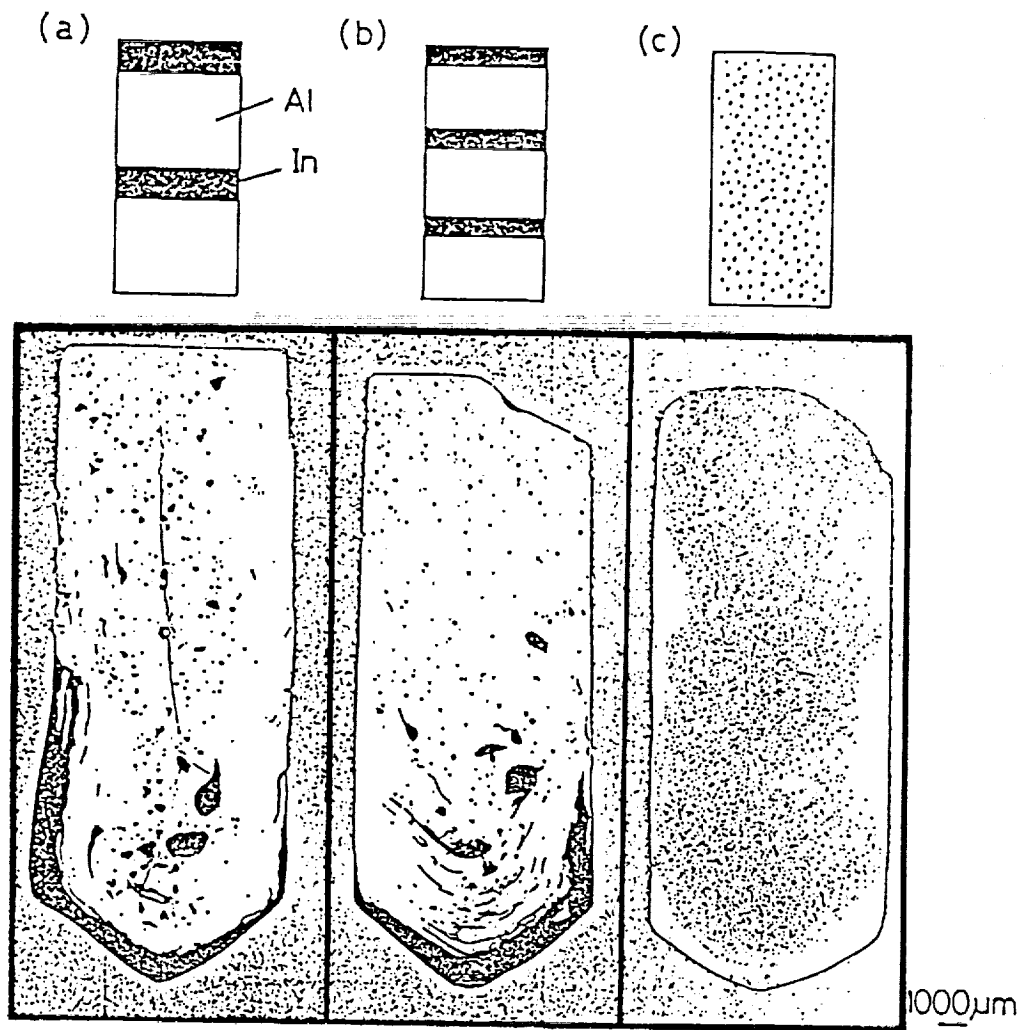


Figure 8. GHF-MP Furnace.



\* Sample cartridge is taken out of GHF after landing.

Figure 9. Experimental procedure and sequence.



**Figure 10. Influence of configuration of starting materials on alloying of Al-30 mass% In alloys under terrestrial condition.**

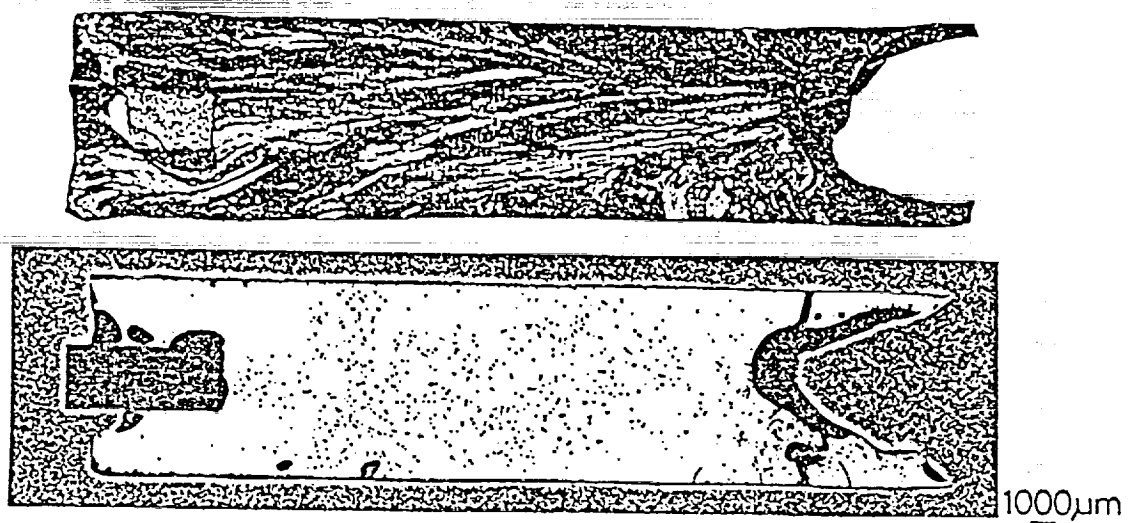


**Figure 11. Macro- and microstructure of Al-30 mass% In alloy melted and solidified under microgravity condition.**

FABRICATION OF VERY-LOW-DENSITY, HIGH-STIFFNESS CARBON  
FIBER/ALUMINUM HYBRIDIZED COMPOSITE WITH ULTRA-LOW DENSITY  
AND HIGH STIFFNESS

M-11

Tomoo Suzuki  
Department of Metallurgical Engineering, Tokyo Institute of Technology  
Japan

Fabrication of a composite material with ultra-low density and high stiffness in microgravity is the objective of the present investigation. The composite structure to be obtained is a random three-dimensional array of high modulus, short carbon fibers bonded at contact points by an aluminum alloy coated on the fibers. The material is highly porous and thus has a very low density. The motivation toward the investigation, simulation experiments, choice of the component materials, and on-flight experiment during ballistic trajectory of a NASDA rocket, are described herein.

Introduction

Structural materials in space are desired to possess high specific strength, stiffness, and resistance to buckling. Also it is desirable that the materials be fabricated on-orbit. Such requirements can be met, in principle, by a material such as a finely foamed, metal-ceramic composite where the macroscopic buckling load can be raised by an increase in the second moment of area of the cross section at a constant mass, while the microscopic buckling at the metal walls between small cavities is prevented by fine ceramic particles or fibers dispersed in the metal matrix. Fabrication of such materials was our original proposal for the current FMPT project. However, preliminary investigation revealed two difficulties to overcome, which are: (a) to

confine cavities to an isolated fine state in a molten metal even under microgravity since metals have generally very low viscosity and very high surface tension in the molten state and (b) to find a suitable constituent which will act as a foaming agent in a molten metal and is yet safe in carrying out the fabrication.

An alternate method to obtain a similar type of structure which would have the properties stated above was then proposed. The structure consists of short high modulus ceramic fibers and a small amount of filler metal of relatively low density. The fibers are aligned as random three-dimensional arrays and are bonded at contact points by the metal that is coated on the surface of the fibers. Such a structure is highly porous and cavities are surrounded by the metal walls to resemble the structure of the foamy hybrid composite in the original proposal. The fabrication procedure in this case involves fiber coatings with a metal or an alloy encapsulation of chopped fibers and heating the material to a temperature above the melting point of the metal coating, followed by cooling to ambient temperature. The procedure is simple and thus has an advantage for possible on-orbit fabrication. Microgravity during fabrication is essential for two reasons: (a) keeping short fibers in a random three-dimensional configuration instead of collapsing to near two-dimensional configuration under the effect of gravity, and (b) keeping the molten metal from slipping down and separating away along the direction of gravity due to a difference in densities of the fibers and the metal.



### Simulation Experiment

In order to provide a better picture of the structure under consideration, results of a simulation experiment are briefly shown. In the experiment, nylon threads to 0.8 mm in diameter are used as fibers which are coated with wax to a thickness of some 0.2 mm. The coated threads are chopped into pieces of 5 mm in length and then heated in a Pyrex glass container until the wax coatings melt. To simulate a microgravity environment, coated threads are placed in an aqueous solution of alcohol of which the density is adjusted to be that of the wax. Upon heating and subsequent cooling, the threads are bonded at contact points. Figure 1a shows composites obtained under the microgravity simulation, and Figure 1b shows those prepared under the effect of gravity. In Figure 1a, a random three-dimensional array of the short threads bonded at contact points is achieved, whereas in Figure 1b the wax has separated from the nylon threads and is deposited at the bottom of the container. The difference is clearly seen when the height of the specimen is compared because the same amount of materials was used for each case of fabrication.

### Choice of Component Materials

A high modulus carbon fiber was chosen for this experiment and an aluminum alloy was developed as a coating substance for the fibers. An aluminum-based alloy was selected because of its relatively low density and its moderate melting temperature where fabrication is practical and feasible with non-expensive, simple electric furnaces. It was recognized, however, that the wettability between carbon fiber and pure aluminum is known to be extremely poor. However, the wettability between them is known to be improved at temperatures above 1273 K due to the

formation of aluminum carbide ( $\text{Al}_4\text{C}_3$ ) at the interface [2,3]. The chemical reaction is also known to occur even at lower temperatures, at 773 K for example, upon prolonged exposure [2-7]. At any rate, the occurrence of the carbide formation has been known to cause severe degradation of the fiber strength. In the present investigation, therefore, a systematic investigation was first undertaken to improve the compatibility between carbon fiber and aluminum by alloying the aluminum.

Aluminum alloys containing a small amount of various alloying elements (up to 5 at%) were prepared by arc-melting under an argon atmosphere. These alloys were coated onto the carbon fiber surface by vacuum deposition. The fibers were then heated to 1073 K in vacuum encapsulated silica tube to melt the alloys. After cooling the surface of the fibers was examined by scanning electron microscopy to judge the degree of wettability. As is shown in Figure 2a, the surface of the fibers coated with pure aluminum has a number of metal droplets indicating the poor wettability. It was found that when addition of such elements as thallium, indium, and lead by only 1 at% was made, the wettability was significantly improved as shown in Figure 2b for the case of lead addition. Moreover, tensile tests of the coated fibers after the heat treatment revealed that room temperature strength of the fiber was not deteriorated by such alloy coatings. Through the investigation, a wetting reagent which could be added to aluminum was found so that the composite fabrication under consideration became realistic. Details of the investigation are describe elsewhere [8].

### Flight Experiment

A flight experiment was carried out in August 1983 using a NASDA TT-500A-13 rocket. The details of the materials preparation and the fabrication experiment are as follows.

Carbon fibers of a high modulus type being approximately 7 to 8  $\mu\text{m}$  in diameter were coated on the surface with an Al-1 at% Ti alloy to a thickness of 1  $\mu\text{m}$  using a vacuum evaporation technique. The coated fibers were cut into short pieces of 0.5 to 1 mm in length and vacuum encapsulated in a silica tube with an inner diameter of 10 mm. Prior to the encapsulation, a piece of lid made of silica pipe was welded onto the inner wall of the tube to slightly compact the materials. The height of the specimen in the silica tube was then ca. 15 mm. The whole specimen capsule, ca. 45 mm in length as shown in Figure 3, was then packed in a graphite container and placed in an electric furnace. The TT-500A rocket provided a microgravity environment for 6 min during its ballistic trajectory and the heat treatment of the specimen was scheduled for this time period. The maximum temperature was scheduled to be 1023 K for 2 min while the melting point of the aluminum alloy was about 943 K.

Unfortunately, during the on-flight experiment temperature control of the electric furnace was unsuccessful and the temperature went up to above 1743 K. Examination of the retrieved specimen showed obvious damage on the surface of the fibers due to the overheating and the whole composite was found to be brittle. This is probably due to the chemical reaction between the fiber and aluminum alloy to form  $\text{Al}_4\text{C}_3$  and also due to partial evaporation of the aluminum alloy. SEM observation, however, revealed the structure of the specimen to be a random three-dimensional configuration of the short fibers and the contact-point bonding was mostly successful making the entire specimen rigid.

### References

- [1] Y. Mishima, M. Hori, T. Suzuki, and S. Umekawa: J. Mater. Sci., 21, 2763 (1986).
- [2] C. Manning and T. Gurganus: J Amer. Ceram. Soc., 52, 115 (1969).
- [3] S. Rhee: *ibid.*, 53, 386 (1970).
- [4] A. A. Baker and C. Shipman: Fibre Sci. Technol., 5, 285 (1972).
- [5] G. Blankenburgs: J. Aust. Inst. Met., 14, 26 (1969).
- [6] P. W. Vackson, D. M. Branddick, and D. J. Walker: Fibre Sci. Technol., 5, 219 (1972).
- [7] S. J. Baker and W. Bonfield: J. Mater. Sci., 13, 1329 (1978).
- [8] Y. Kimura, Y. Mishima, S. Umekawa, and T. Suzuke: *ibid.*, 19, 3107 (1984).

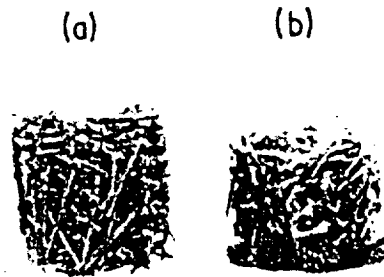


Figure 1. Structure of Nylon threads-wax composites fabricated under (a) microgravity simulation and (b) the effect of gravity.

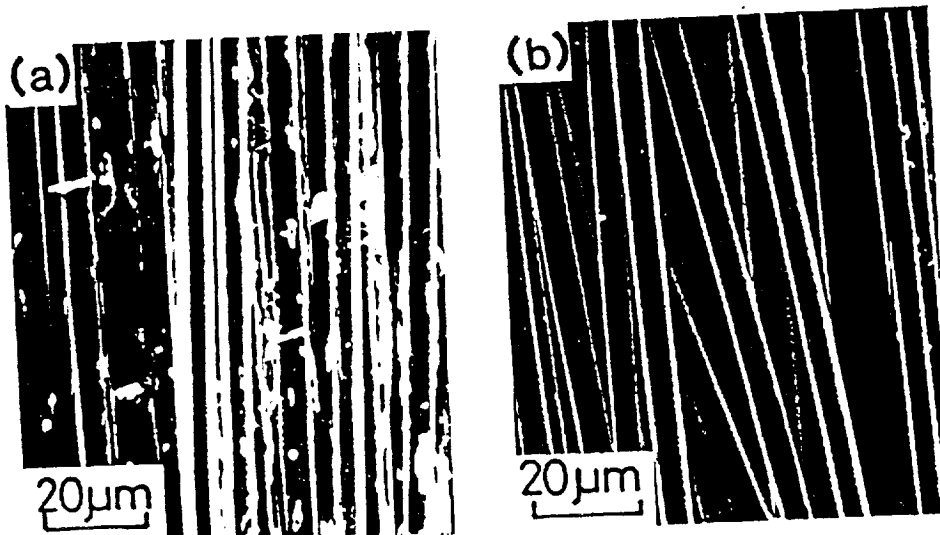


Figure 2. Scanning electron micrographs of carbon fibers after heating at 1073 K for 30 min coated with (a) pure aluminum and (b) Al-1 at% Pb alloy.

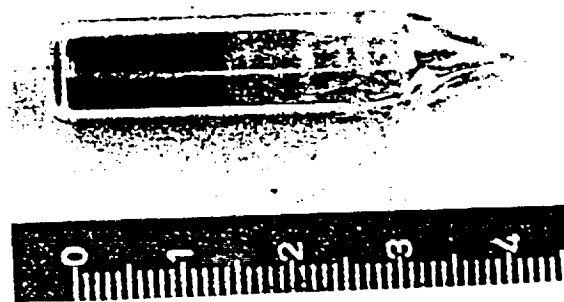


Figure 3. Appearance of the specimen capsule for the in-flight experiment.



STUDY ON THE MECHANISM OF LIQUID PHASE SINTERING  
M-12

S. Kohara  
University of Tokyo  
Tokyo, Japan

Description of the Project

Objectives:

- (1) To obtain the data representing the growth rate of solid particles in a liquid matrix without the effect of gravity.
- (2) To reveal the growth behavior of solid particles during liquid phase sintering using the data obtained.

Background of the Experiment:

Sintering means the particle coalescence of a powdered aggregate accomplished by heating at an elevated temperature. When a powdered aggregate composed of two kinds of constituent metals is heated and kept at a temperature higher than the melting point of one constituent metal, the metal with the lower melting point melts down and forms a liquid phase. Sintering is accelerated by the existence of a liquid phase compared to the sintering in a solid phase. This technique in powder metallurgy is called liquid phase sintering.

The properties of sintered products are dependent on the size distribution of the second phase particles. However, the solid particles in a liquid matrix grow larger during sintering. Therefore, it is important to reveal the growth behavior of the solid particles during sintering to

control the properties of sintered products in industrial applications. However, the study on the growth behavior of solid particles during liquid phase sintering is difficult on Earth because of the gravitational segregation of solid particles.

In the present experiment, nickel and tungsten are used as the constituent materials in liquid phase sintering. The properties of the constituent metals are given in Table 1. When a compact of the mixture of tungsten and nickel powders is heated and kept at 1550 °C, nickel melts down but tungsten stays solid. As the density of tungsten is much greater than that of nickel, the sedimentation of tungsten particles occurs in the experiment on Earth. Figure 1 illustrates the difference between the experiments on Earth and in space. The tungsten particles sink to the bottom and are brought into contact with each other. The resulting pressure at the contact point causes the accelerated dissolution of tungsten. Consequently flat surfaces are formed at the contact sites. As a result of dissolution and reprecipitation of tungsten, the shape of particles changes to a polygon. This phenomenon is called "flattening." An example of flattening of tungsten particles is shown in Figure 2. Thus, the data obtained by the experiment on Earth may not represent the exact growth behavior of the solid particles in a liquid matrix. If the experiments were done in a microgravity environment, the data corresponding to the theoretical growth behavior of solid particles could be achieved.



### Experimental Procedure:

The mixtures of tungsten powder and nickel powder with the compositions of 3.5, 7, 15, 20, and 30 mass % Ni are prepared and compacted into cylindrical specimens. As illustrated in Figure 3, each specimen is inserted in an alumina ( $\text{Al}_2\text{O}_3$ ) receptacle and five receptacles are put in a boron nitride (BN) container. The container is enclosed in a tantalum (Ta) capsule. The capsule is evacuated and filled with argon gas. Last, the capsule is put in a tantalum cartridge.

Two cartridges will be prepared and heated at 1550 °C in space (one for 1 h and the other for 3 h) in the FMPT experiment. The furnace and cartridge for the experiment is shown in Figure 4. The profiles of PS operation, sample temperature, heater power, and gas supply are shown in Figure 5.

The specimens will be cut and polished for metallographic measurement after return to Earth. Then the distribution curves of solid particle size will be determined and analyzed.

Table 1. Properties of Tungsten and Nickel

Tungsten	3410 °C	19.3 g/cm <sup>3</sup>
Nickel	1453 °C	8.9 g/cm <sup>3</sup>

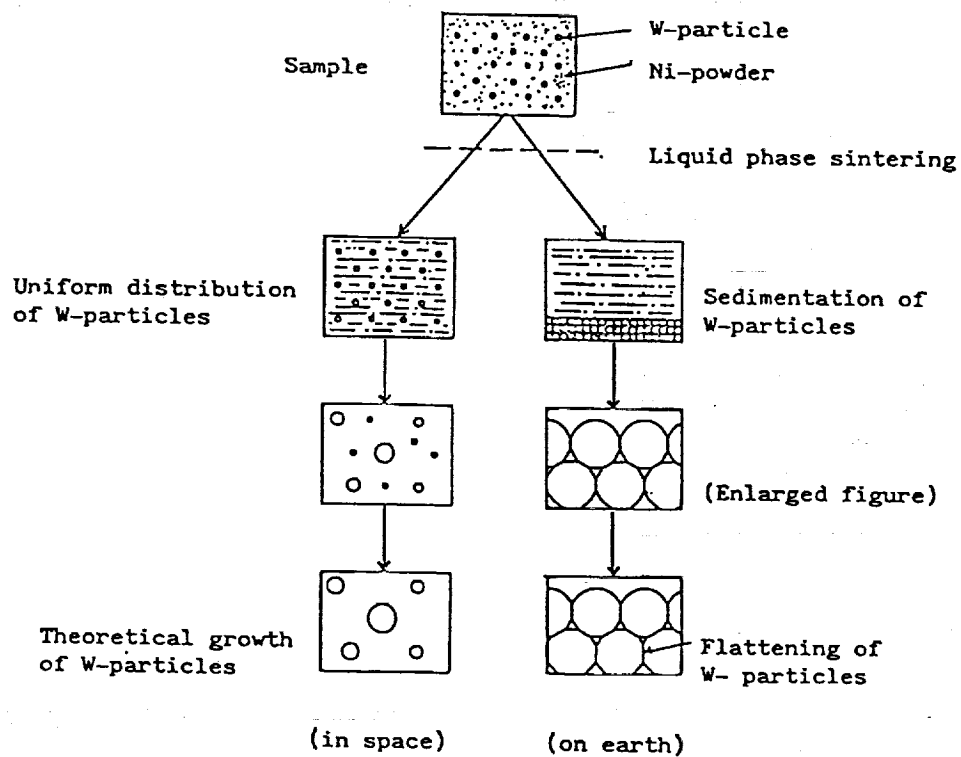


Figure 1. Illustration of the experiment.



Figure 2. Flattening of tungsten particles.

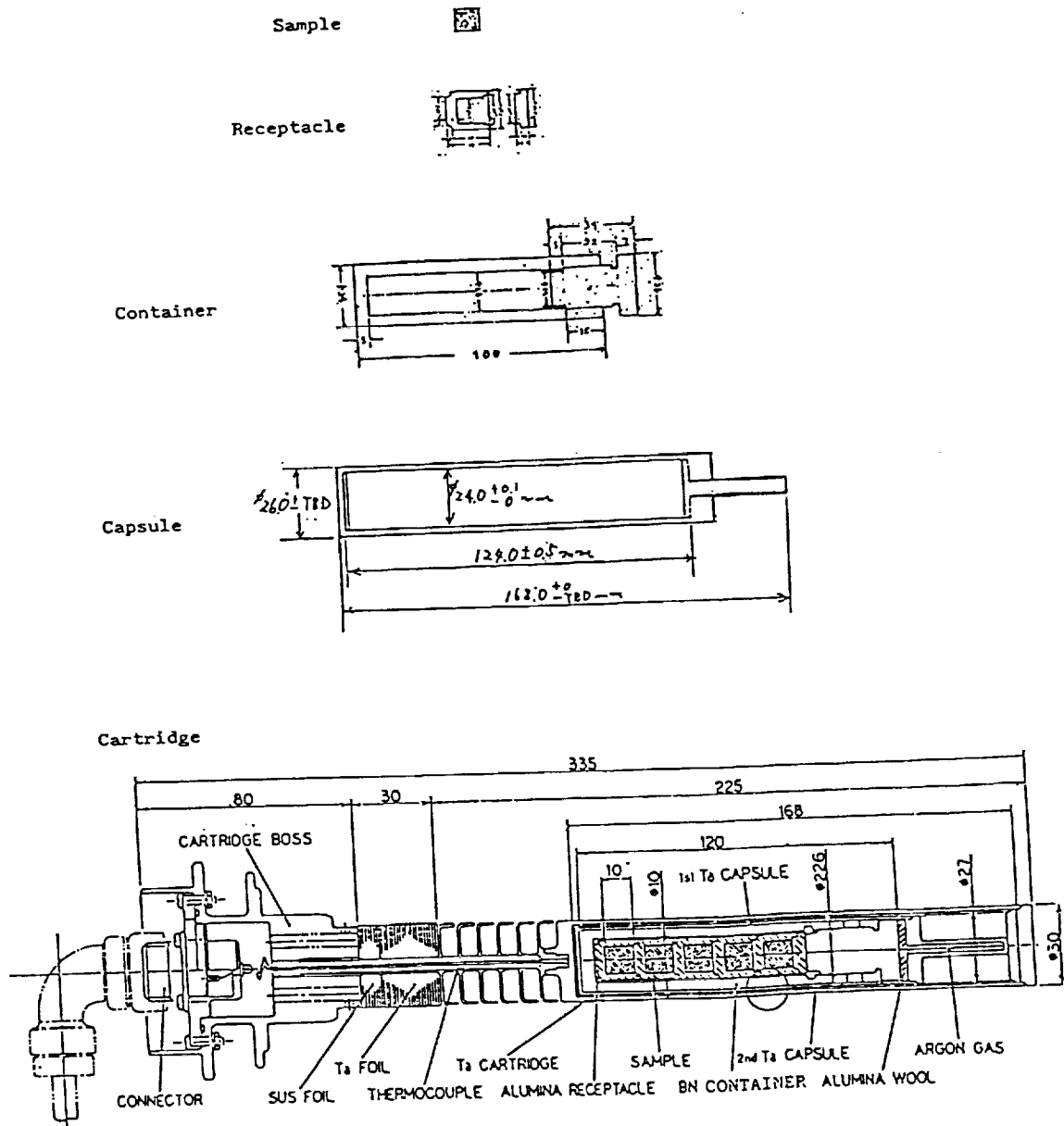


Figure 3. Setting of samples in a cartridge.

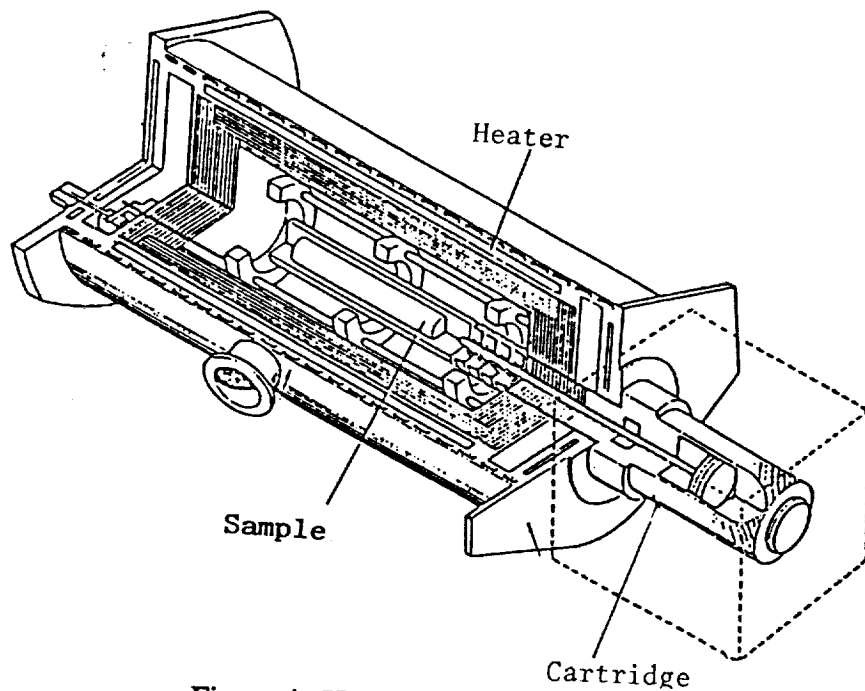


Figure 4. Heating furnace and cartridge.

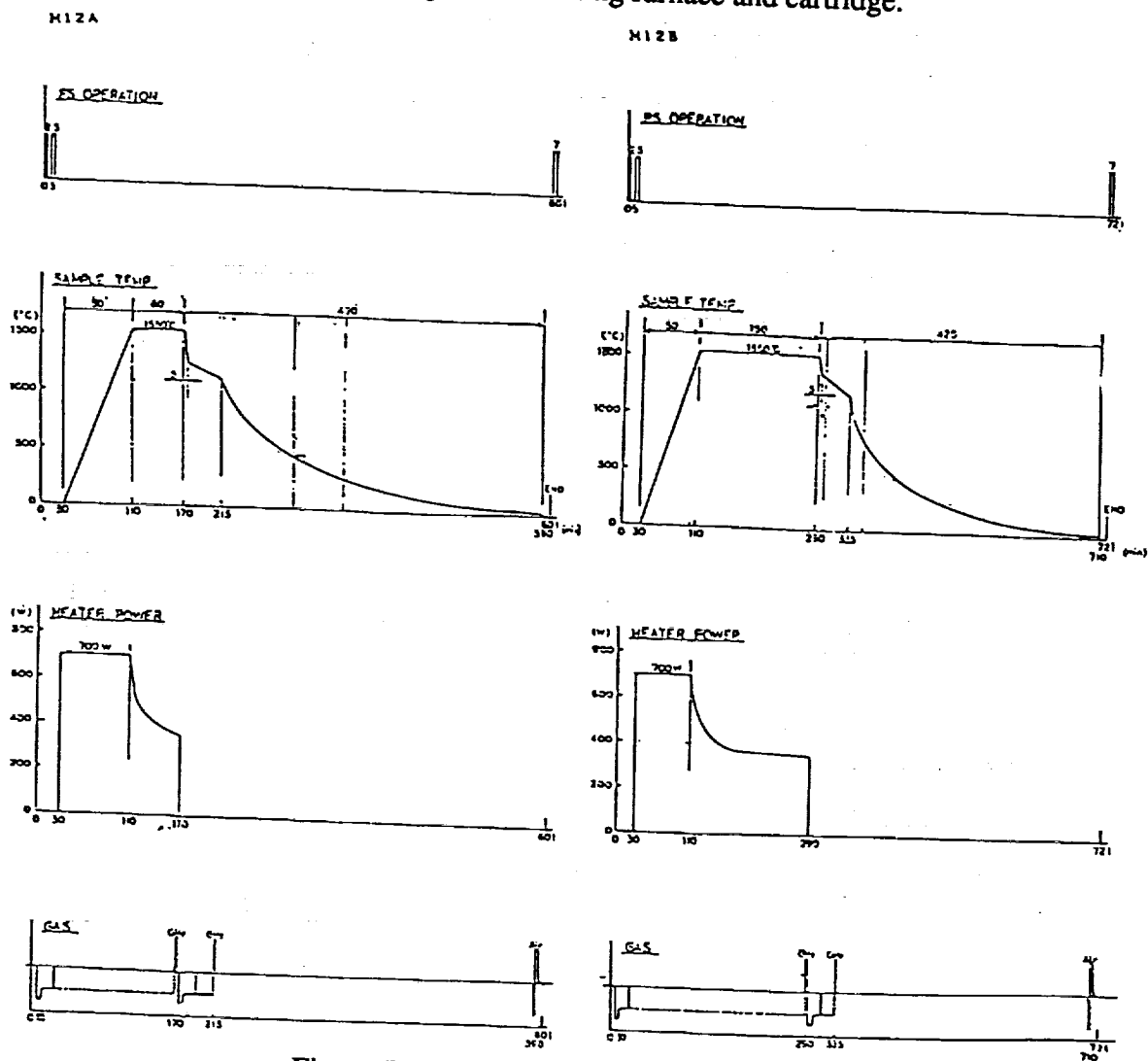


Figure 5. Experiment resource utilization profiles.

FABRICATION OF Si-As-Te TERNARY AMORPHOUS SEMICONDUCTOR  
IN THE MICROGRAVITY ENVIRONMENT  
M-13

Yoshihiro Hamakawa  
Osaka University  
Toyonaka, Osaka 560, Japan

Outline of FMPT Experiment

Ternary chalcogenide Si-As-Te system is an interesting semiconductor from the aspect of both basic physics and technological applications. Since a Si-As-Te system consists of a IV-III-II hedral bonding network, it has a very large glass forming region with a wide physical constant controllability as shown in Figure 1. For example, its energy gap can be controlled in a range from 0.6 eV to 2.5 eV, which corresponds to the classical semiconductor Ge (0.66 eV), Si (1.10 eV), GaAs (1.43 eV), and GaP (2.25 eV). This fact indicates that it would be a suitable system to investigate the compositional dependence of the atomic and electronic properties in the random network of solids.

In spite of these significant advantages in the Si-As-Te amorphous system, a big barrier impeding the wide utilization of this material is the huge difficulty encountered in the material preparation which results from large differences in the weight density, melting point, and vapor pressure of individual elements used for the alloying composition.

The objective of the FMPT/M13 experiment is to fabricate homogeneous multi-component amorphous semiconductors in the microgravity environment of space, and to make a series of comparative characterizations of the amorphous structures and their basic physical constants on the materials prepared both in space and in normal terrestrial gravity.

On the basis of systematic investigations on the Si-As-Te amorphous semiconductor system in terrestrial experiments, a proposal to FMPT/M-13 project has been planned. Samples to be fabricated in this experiment were selected from the terrestrial experimental data for compositions  $\text{Si}_x(\text{As}_3\text{Te}_3)_{1-x}$  in which  $x$  is varied from 0.25 to 0.75. In order to examine the valence electron controllability, a trial will be made of impurity doping with Mn and Ni elements of several atomic percent on  $\text{Si}_9\text{As}_{14}\text{Te}_{21}$  glass, on which the electronic properties have been most intensively investigated.

The Si-As-Te samples already synthesized with Si, As, and Te mixture of designed atomic fractions are employed for the starting material. This procedure is likely to be essential to avoid the possible break down of material sealings due to a rapid increase in vapor pressure, particularly of decomposed As, upon an accidental extreme overheating. Ground powder samples are sealed three-fold with silica ampoules, and encapsulated in the Ta universal cartridge. They are heated to 1300 °C continuously for 1 hour using the CHF apparatus. After that, a rapid quenching is accomplished in the cooling chamber using He gas flow; from 1300 °C down to below 45 °C in less than 10 minutes. A systematic investigation will be carried out on the structure and electronic properties of Si-As-Te amorphous semiconductors thus fabricated, with particular emphasis placed on the differences between the space-fabricated semiconductors and those fabricated under the normal terrestrial gravity environment.

### Expected Results

In modern civilization we are surrounded by electronic devices - telephones, television, desk calculators, video taperecorders, microwave ovens, business computers, etc. Electronics

have become an indispensable tool in today's life. The marvelous growth of semiconductor electronics in the past 35 years was made possible by the well-established single crystalline foundation of solid state physics.

Amorphous materials are solids in which the atomic sites are randomly arranged. They lack long-range ordering in their lattice networks. The amorphous semiconductor will someday have a similar impact on modern life as have the crystalline semiconductors. This material is provided with wide controllability of physical constants and of fractions of the composed elements, doped impurity and defect compensator atoms. These features are a result of a lack of long-range order in the atomic structure. Being free from the constraints of periodicity in the atomic array, amorphous semiconductors lend themselves to relatively low-cost fabrication of large-area and thin film electronic devices with a good mass producibility.

Among a wide variety of amorphous semiconductors, the Si-As-Te system offers us the greatest opportunity for carrying out systematic investigations on the compositional dependence of structural and electronic properties. On the other hand, from the technological standpoint, this material is expected to be applied to multi-layered heterojunction devices and also optoelectronic functional elements in a wide spectral region from near-infrared to visible light region. The issue for making the best use of these advantages is to fabricate homogeneous Si-As-Te alloy materials, which would be possible if they were synthesized in the microgravity environment of space. The FMPT/M-13 experiment has been planned on this background idea. The results from the FMPT experiment will contribute to the physics of disordered materials as well as to the development of new materials for semiconductor electronics.

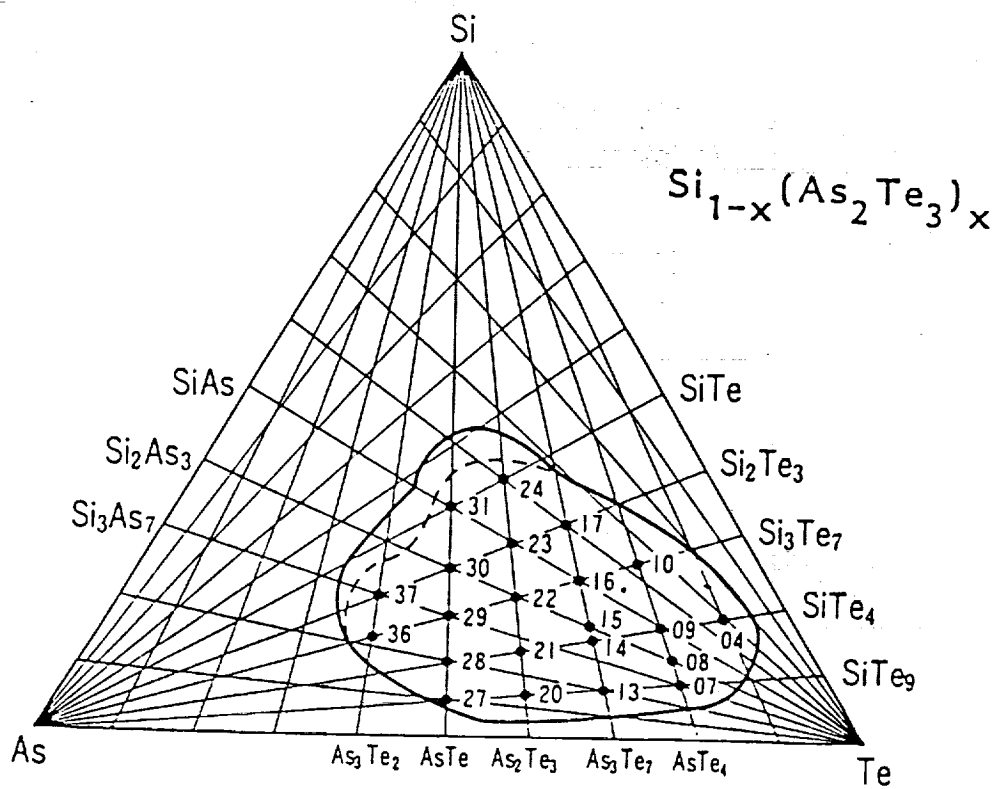


Figure 1. Glass forming region of Si-Te-Te system.



GAS-EVAPORATION IN LOW-GRAVITY FIELD  
(COGELATION MECHANISM OF METAL VAPORS)

M-14

N. Wada  
Nagoya University, Faculty of Science  
Nagoya, Japan

When metal and alloy compounds are heated and vaporized in a rare gas such as helium, argon, or xenon, the vaporized substances diffused in the rare gas are supersaturated resulting in a smoke of fine particles of the material congealing as snow or fog. The gas vaporizing method is a fine particle generation method. Though the method has a variety of applications, the material vapor flow is disturbed by gravitational convection on Earth. The inability to elucidate the fine particle generation mechanism results in an obstruction to improving the method to mass production levels.

As no convection occurs in microgravity in space, the fine particle generation mechanism influenced only by diffusion can be investigated. Investigators expect that excellent particles with homogeneous diameter distribution can be obtained. Experiment data and facts will assist in improving efficiency, quality, and scale of production processes including element processes such as vaporization, diffusion, and condensation.

Experiment Objectives

The objective of this experiment is to obtain important information related to the mechanism of particle formation in the gas atmosphere (smoke particles) and the production of sub-micron powders of extremely uniform size.

### Experimental Procedures

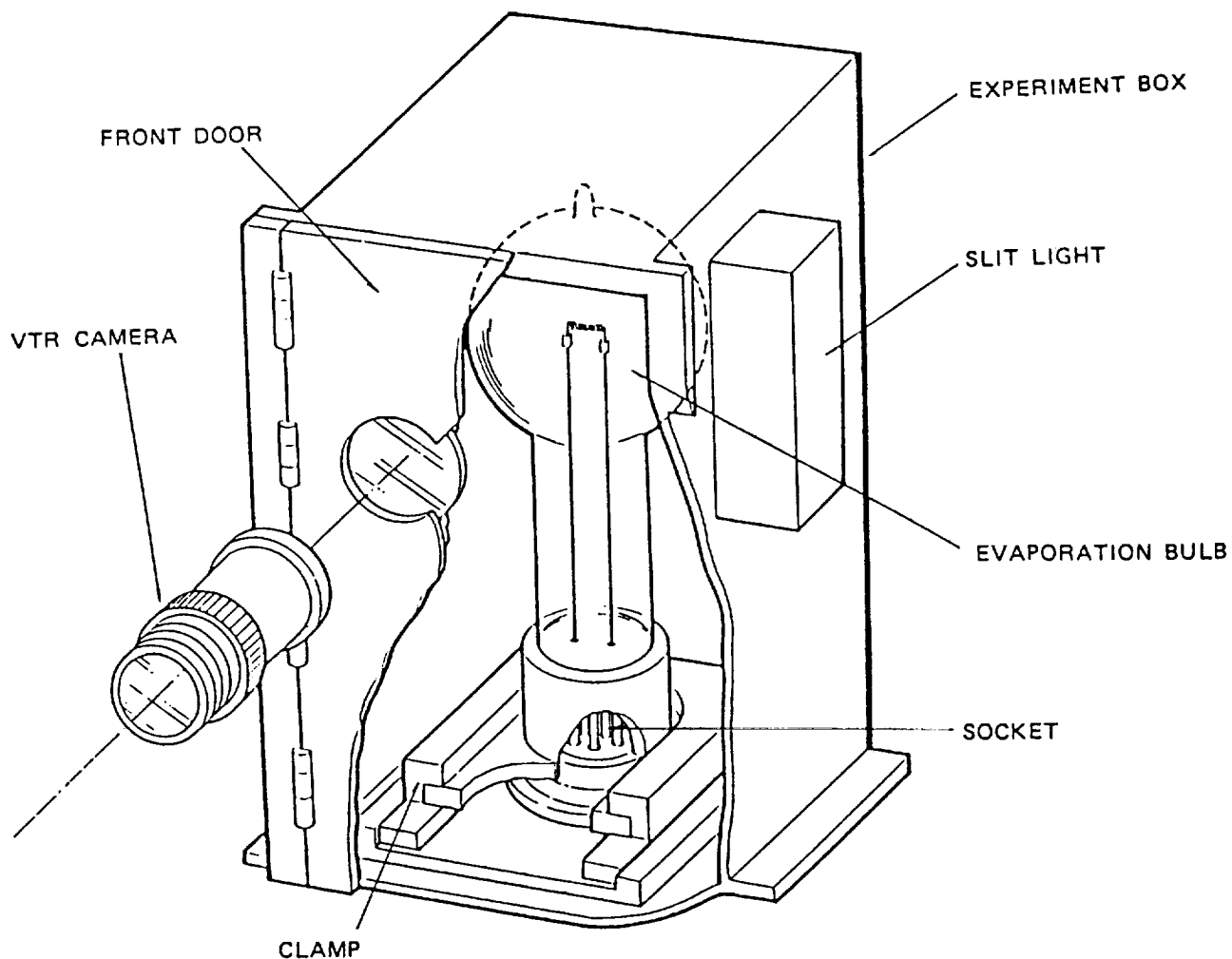
Several glass chambers (Evaporation Bulbs) with evaporation sources (as on the filament) at the centers are prepared and filled with He or Xe gas of various pressure.

Heated by the filament, the metal is evaporated and the motion of the smoke produced is recorded by the VTR. The variations of the heating temperature, pressure, etc. are recorded simultaneously.

After the experiment each bulb will be brought back to the ground and the deposited particles observed using an electron microscope.

### Expected Results

In the gravity field, the particle generation mechanism becomes complicated and results in various configurations and sizes of the particles because the vaporizing process is disturbed by convection. In the low-gravity field, the situation is much more simplified, provided that the vaporation is carried out at the center of spherical chamber. The diffusion of vapors into the gas atmosphere and the condensation into fine particles takes place in a spherical symmetric way.



### EVAPORATION BULB

- 1) Protection Cover (poly-carbonate)
- 2) Evaporation Bulb (glass 80  $\phi$ , sealed He or Xe)
- 3) Filament (W, Ta) with Metal sample (Ag or Al)
- 4) Thermo-couple (WRe-W)
- 5) Thermo-couple (PtRh-Pt)
- 6) Pressure Detector (quartz)
- 7) Stem (W-rod 2  $\phi$ )
- 8) Getter
- 9) Thermal reflector (quartz disk)
- 10) Electrode-Base (poly-carbonate)

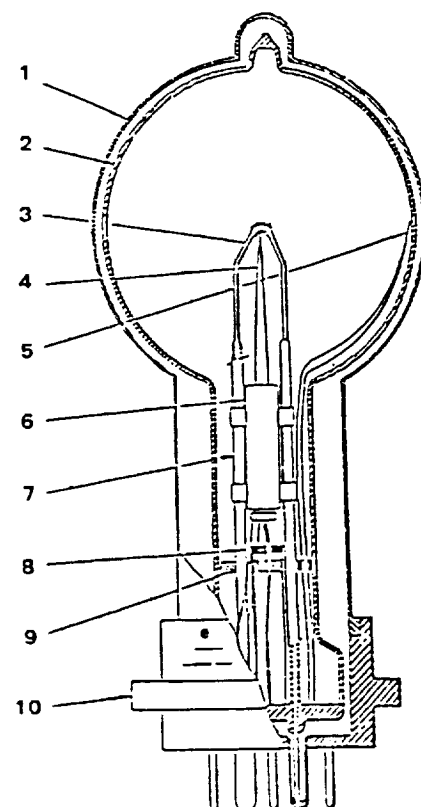


**Figure 1. Gas Evaporation Experiment Facility.**

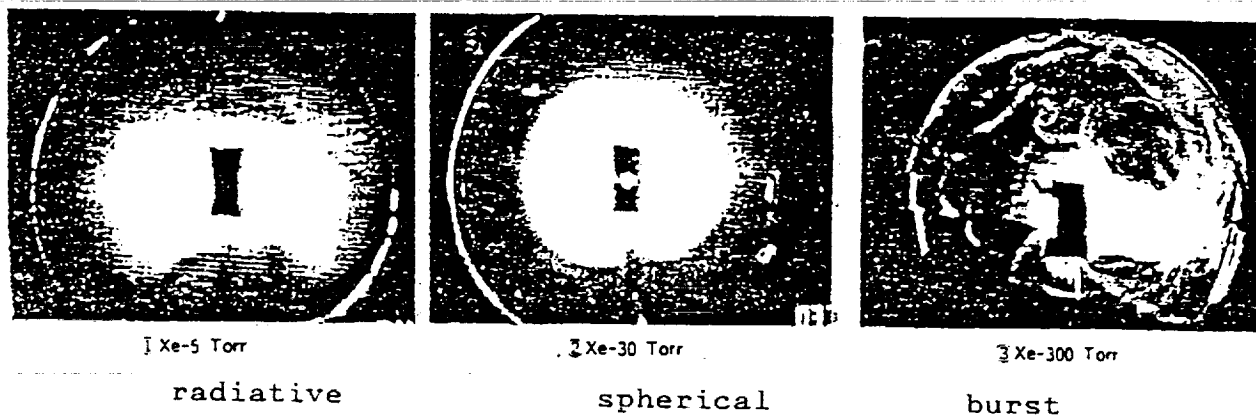


Figure 2. Deference of smoke shapes for the pressure difference of E.B (by airplane).

## DROP DYNAMICS IN SPACE AND INTERFERENCE WITH ACOUSTIC FIELD M-15

Tatsuo Yamanaka  
National Aerospace Laboratory  
Tokyo, Japan

The objective of the experiment is to study contactless positioning of liquid drops, excitation of capillary waves on the surface of acoustically levitated liquid drops, and deformation of liquid drops by means of acoustic radiation pressure.

Contactless positioning technologies are very important in space materials processing because the melt is processed without contacting the wall of a crucible which can easily contaminate the melt specifically for high melting temperatures and chemically reactive materials. Among the contactless positioning technologies, an acoustic technology is especially important for materials unsuceptible to electromagnetic fields such as glasses and ceramics.

The shape of a levitated liquid drop in the weightless condition is determined by its surface tension and the internal and external pressure distribution. If the surface temperature is constant and there exist neither internal nor external pressure perturbations, the levitated liquid drop forms a shape of perfect sphere. If temperature gradients on the surface and internal or external pressure perturbations exist, the liquid drop forms various modes of shapes with proper vibrations. A rotating liquid drop has been specifically studied not only as a classical problem of theoretical mechanics to describe the shapes of the planets of the solar system, as well as their arrangement, but it is also more a contemporary problem of modern non-linear mechanics.

In the experiment, we are expecting to observe various shapes of a liquid drop such as cocoon, tri-lobed, tetrapod, multi-lobed, and doughnut.

Wave-wave coupling is also one of the major problems of non-linear mechanics. Various electromagnetic phenomena accompanied by an aurora, the microwave heating in the nuclear fusion, an implosion by means of laser excitation, the rf discharge of an ion thruster, etc., are the relevant subjects. To study the interference of the capillary waves with acoustic fields is one of the objectives of this experiment.

If a large liquid drop is levitated by an acoustic resonance chamber in a weightless condition of an in-orbit space shuttle, the above-mentioned various non-linear phenomena are actually observed. Further, if an acoustic radiation pressure is actively applied to a liquid drop, the drop forms a flattened shape such as liquid disk, a liquid flat tape, and a liquid thread by means of much more sophisticated acoustic manipulation. By various modes of vibrating, rotating, and flattening liquid drops are largely deformed from the original sphere. The theoretical prediction of such kinds of greatly deformed shapes is also another important subject of modern mechanics. The experiment will provide plentiful data for modern theoretical mechanics.

If cocoon, tri-lobed, tetrapod, multi-lobed, and ring-shaped glasses are manufactured in space exactly as the theory predicts, it will not only serve to inspire young scientists but will also contribute much to advancement of science and technology.

The applications aspect of the experimental results may prove productive. Contactless positioning technology promises glassification processing of high melting temperature materials

such as tungsten, tantalum, molybdenum, rhenium, and their alloys. For such processes, a contactless mixing technology will be necessary. An acoustic excitation technology of the capillary waves will perform the function of a contactless mixer.

An acoustic contactless technology for forming liquid thread and flat tape also has promise for the manufacturing of amorphous metal tapes and fluoride glass fibers, because the melt is rapidly solidified soon after forming a fine thread or tape. Earth-based fluoride glass fibers are difficult to manufacture because, due to the high reactivity of fluorine with other materials, their chemical reactions are violent which prevents formation of glasses.

If the fluoride glass fibers are manufactured in the future by means of an acoustic technology, the space-based manufactured optical fibers will drastically impact the state-of-the-art optical communications networks because of their very low attenuation characteristics of transmission.





STUDY OF BUBBLE BEHAVIOR IN WEIGHTLESSNESS (EFFECTS OF THERMAL  
GRADIENT AND ACOUSTIC STATIONARY WAVE)

M-16

H. Azuma  
National Aerospace Laboratories  
Japan

The aim of this experiment is to understand how bubbles behave in a thermal gradient and acoustic stationary wave under microgravity. In microgravity, bubble or bubbles in a liquid will not rise upward as they do on Earth but will rest where they are formed because there exists no gravity-induced buoyancy. We are interested in how bubbles move and in the mechanisms which support the movement. We will try two ways to make bubbles migrate.

The first experiment concerns behavior of bubbles in a thermal gradient. It is well known that an effect of surface tension which is masked by gravity on the ground becomes dominant in microgravity. The surface tension on the side of the bubble at a lower temperature is stronger than at a higher temperature. The bubble migrates toward the higher temperature side due to the surface tension difference. The migration speed depends on the so-called Marangoni number, which is a function of the temperature difference, the bubble diameter, liquid viscosity, and thermal diffusivity. At present, some experimental data about migration speeds in liquids with very small Marangoni numbers have been obtained in space experiments, but cases of large Marangoni number are rarely obtained. In our experiment a couple of bubbles are to be injected into a cell filled with silicon oil, and the temperature gradient is to be made gradually in the cell by a heater and a cooler. We will be able to determine migration speeds in a very wide range of Marangoni numbers, as well as study interactions between the bubbles. We will observe bubble movements affected by hydrodynamical and thermal interactions, the two kinds of interactions

which occur simultaneously. These observation data will be useful for analyzing the interactions as well as understanding the behavior of particles or drops in materials processing.

The second experiment concerns bubble movement in an acoustic stationary wave. It is known that a bubble in a stationary wave moves toward the node or the loop according to whether its diameter is larger or smaller than that of the main resonant radius. In our experiment fine bubbles will be observed to move according to an acoustic field formed in a cylindrical cell. The existence of bubbles varies the acoustic speed, and the interactive force between bubbles will make the bubble behavior collective and complicated. This experiment will be very useful to the development of bubble removal technology as well as to the understanding of bubble behavior.

**PREPARATION OF OPTICAL MATERIALS USED IN NON-VISIBLE REGION  
M-17**

**J. Hayakawa  
Government Industrial Research Institute, Osaka  
Japan**

**Purpose of Experiment**

- Development of containerless glass melting technique
- Fabrication of high purity glass
- Development of acoustic levitation technique

**SAMPLE:** For the space experiment, glass  $65\text{CaO} \cdot 25\text{Ga}_2\text{O}_3 \cdot 10\text{GeO}_2$   
was selected out of various types of glasses.

**Expected Results**

- Ultra-high purity glass
- Manipulation by acoustics

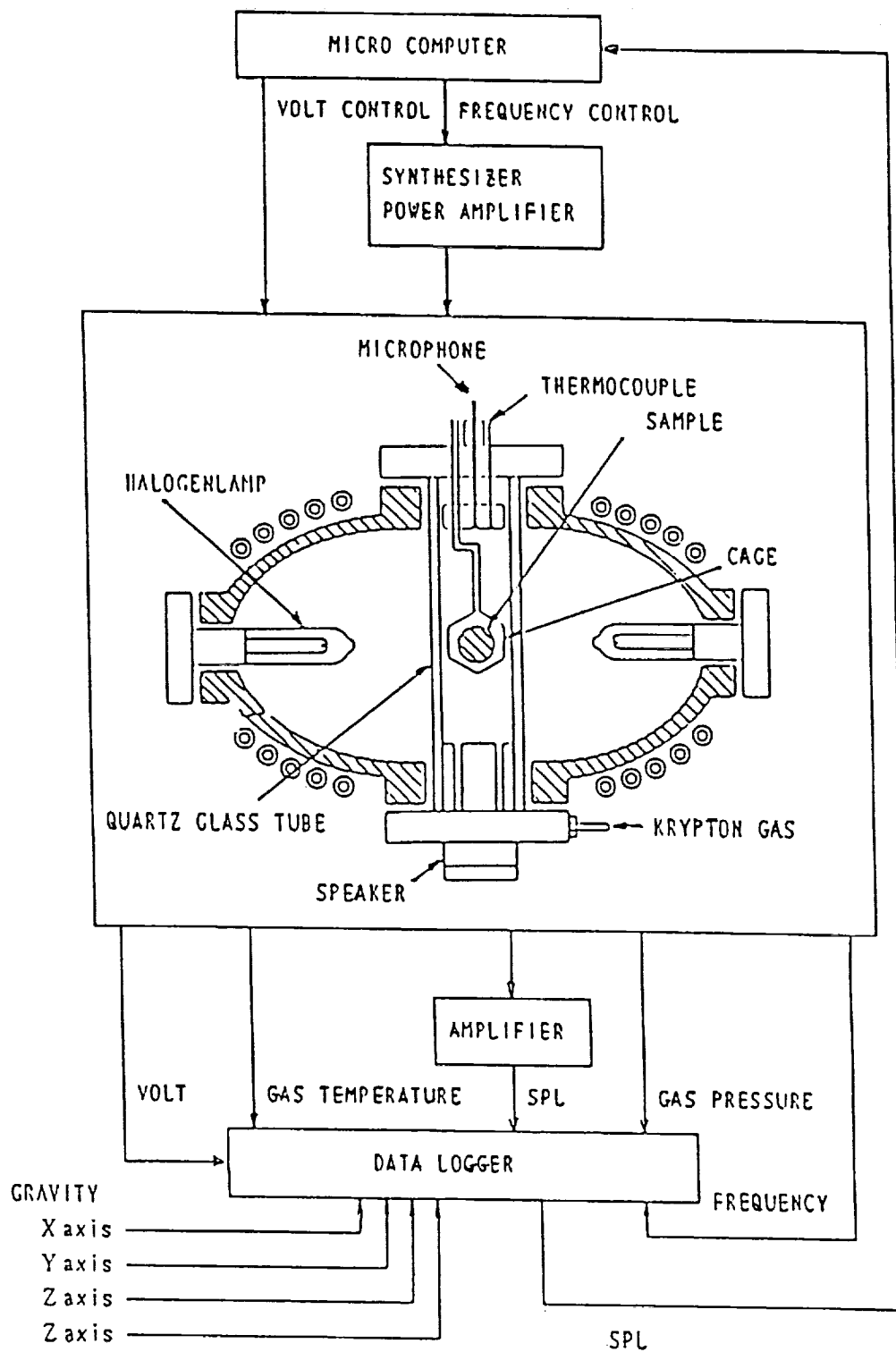
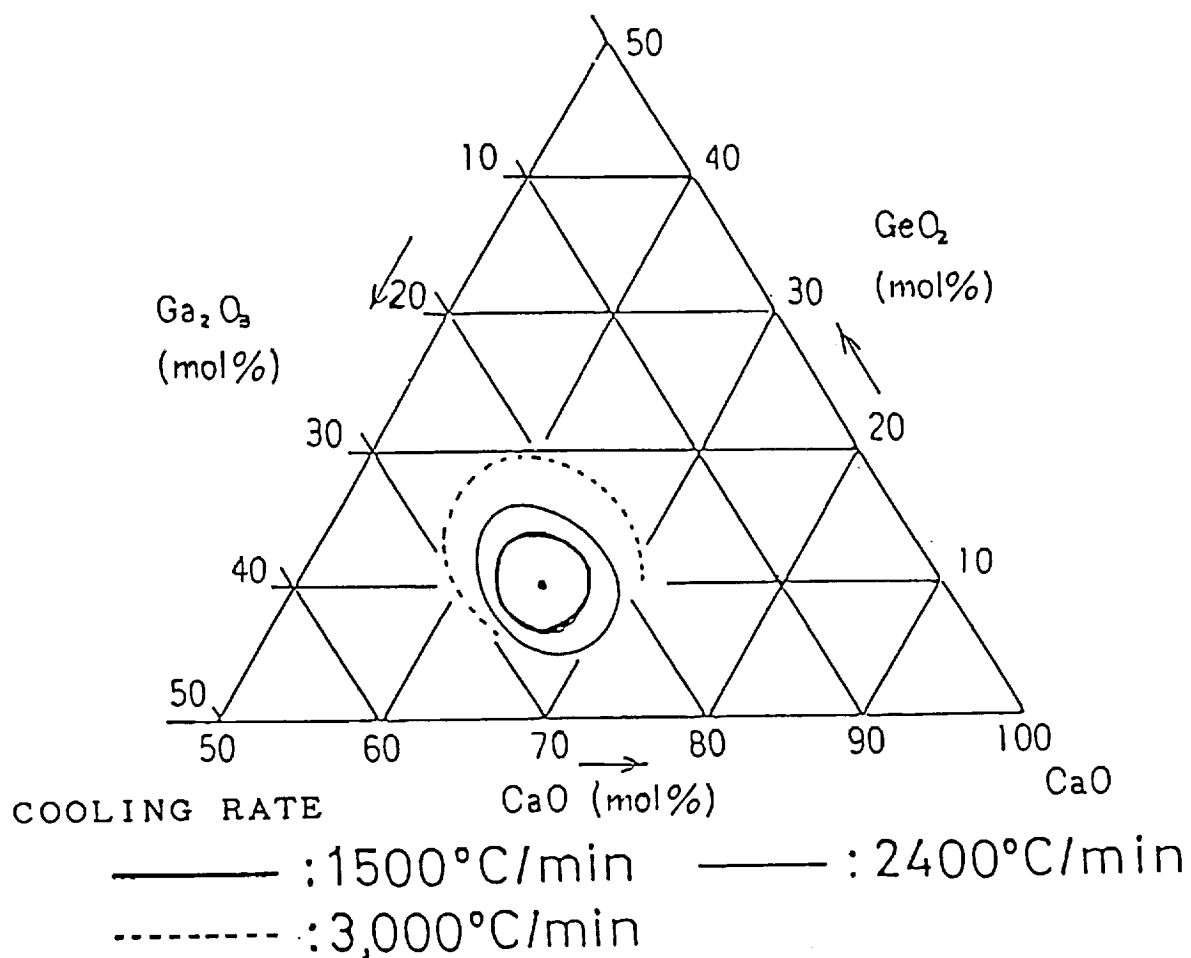


Figure 1. Schematic diagram of acoustic levitation furnace.



Glass Composition



Figure 2. Glass formation range of CaO-Ga<sub>2</sub>O<sub>3</sub>-GeO<sub>2</sub>

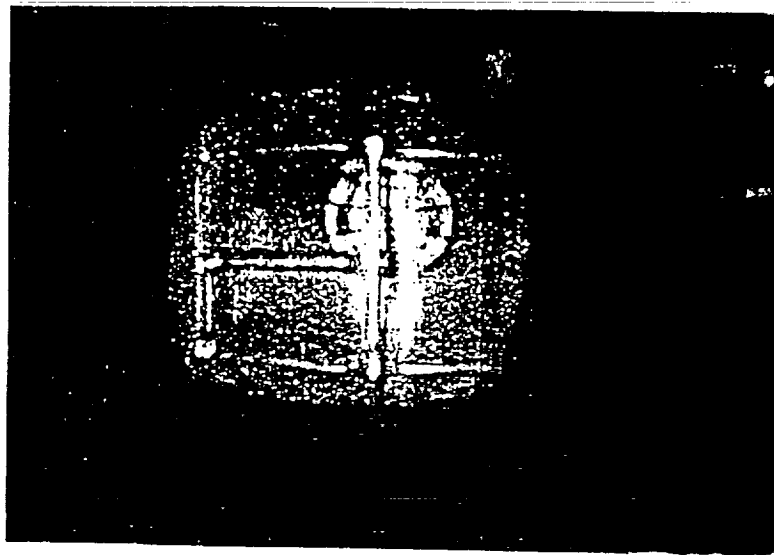


Figure 3. Molten glass under microgravity on the board.



Figure 4. Levitating the glass sample under low gravity.

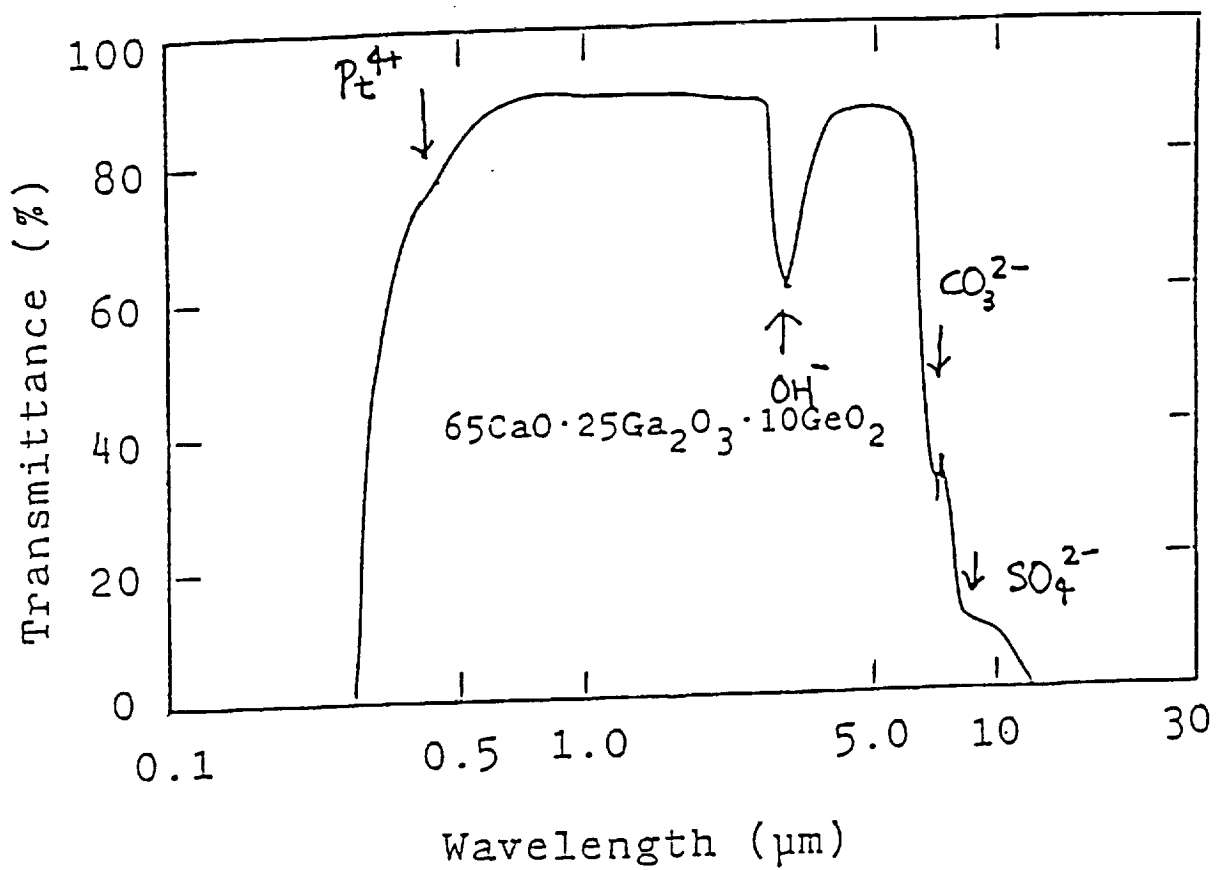


Figure 5.

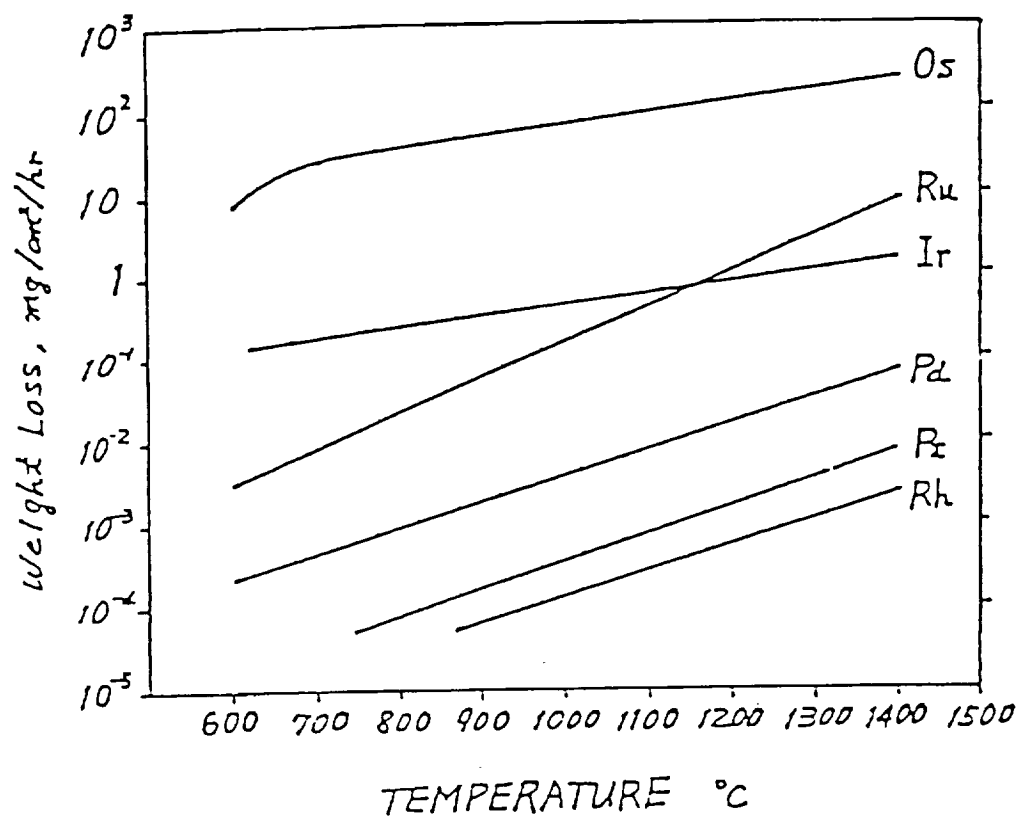


Figure 6.





MARANGONI EFFECT INDUCED CONVECTION IN MATERIAL PROCESSING  
UNDER MICROGRAVITY  
M-18

S. Enya  
Ishikawajima-Harima Heavy Industries Co., Ltd.  
Japan

Objective of Flight Experiment

On the ground the upper layer of the liquid in a vessel heated from below becomes hotter than the lower layer. This well-known phenomenon results from buoyancy-induced convection. Though this means that the buoyancy-induced convection is not dominant under microgravity conditions in space, another convection called Marangoni convection may possibly occur. This convection results from an intermolecular force which acts on a free surface, that is surface tension. Since it is stronger at lower temperatures, the liquid surface near the heated wall is pulled to the cooled side as shown in Figure 1. This surface movement causes the inner convection. Marangoni convection, however, may be negligible on the Earth, for the molecular force is generally smaller than buoyancy.

Various tests on material processing have recently been conducted in space and some high quality crystals free from buoyancy convection were obtained. But, at the same time, others proved to be less uniform than expected in the components' distribution. This nonuniformity seems to be mainly caused by Marangoni convection. It is, therefore, very important to know how to control the convection by studying its characteristics, but the problem is that on the ground it is impossible to carry out the experiment without gravity. That is why a space experiment aboard the space shuttle is planned as the First Material Processing Tests (FMPT) of Japan.

The experiment on Marangoni flow visualization is being performed in order to investigate the characteristics of convection in uni-dimensional melt growth under microgravity conditions.

### Outline of Flight Experiment

The configuration simulates a possible case of the melt state in Bridgman growth as shown in Figure 2(a). We use a paraffin (n-eicosane) as a transparent liquid sample and fill the cylindrical space enclosed by glass cover, cold top wall, and hot bottom wall with the liquid. The free surface is formed just below the cold top wall, and the temperature gradient on the surface generated by controlling both the heater and the cooler drives Marangoni convection.

The convective motions in the liquid column can be visualized by tracers, fine aluminum flakes, and the optical fibers used to observe a section in the liquid column in two different angles as shown in Figure 2(b). The flow field is recorded on video tape. Three experiment runs of 40 minutes each, with different temperature gradients shown in Figure 3, are planned. In the third run the cold wall will be cooled under the melting point of liquid and the solidification front will move slowly from the cold to the hot wall. A schematic view of the Marangoni Convection Unit (MCU) is shown in Figure 4. From the visualized data the velocity and stream line are obtained. Temperature distribution and Nusselt number will be analyzed later.

### Future Contribution of the Experimental Results

By data analysis of Marangoni convection in the space experiment, the flow pattern, the velocities, and their distribution can be determined. The boundary flow near the cooled side of

the wall is particularly important, for the wall is situated at the solidification front in crystal growth. Since the experiment for producing semiconductors by the Bridgman method is also planned in the FMPT, the flow difference between the model liquid and the melted semiconductor will be made clear. The numerical simulation can be modified by the results, and it will become easy to predict a liquid flow field in crystal manufacturing.

The Bridgman method is often used for the production of the compound semiconductors, which can be applied to such devices as light emission/absorption elements of infrared rays. When Marangoni convection is sufficiently understood and controlled, large-sized crystals of high quality will be able to be produced. The technique is also useful for manufacturing other semiconductors and alloys at a lower cost on the ground.

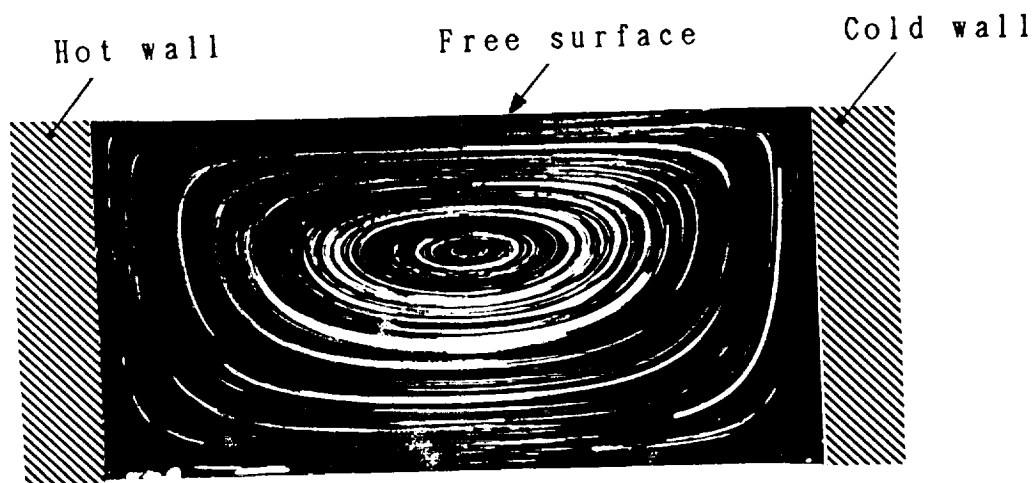
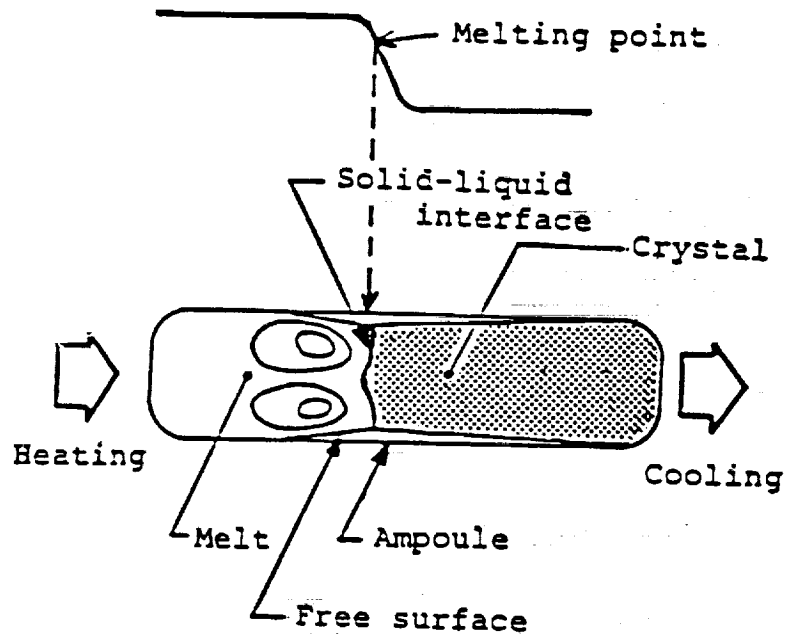
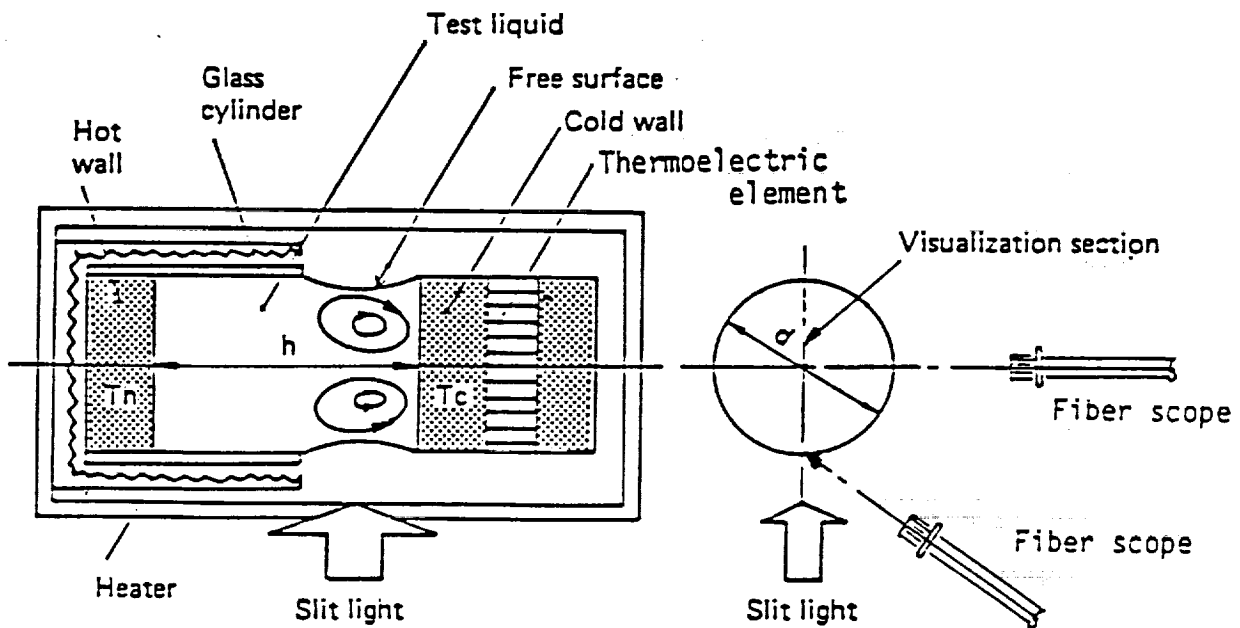


Figure 1. Flow visualization of Marangoni convection on the ground.



(a) Bridgman method



(b) Experimental apparatus of Marangoni convection in space

Figure 2. Schematic diagram of Marangoni convection experiment in FMPT.

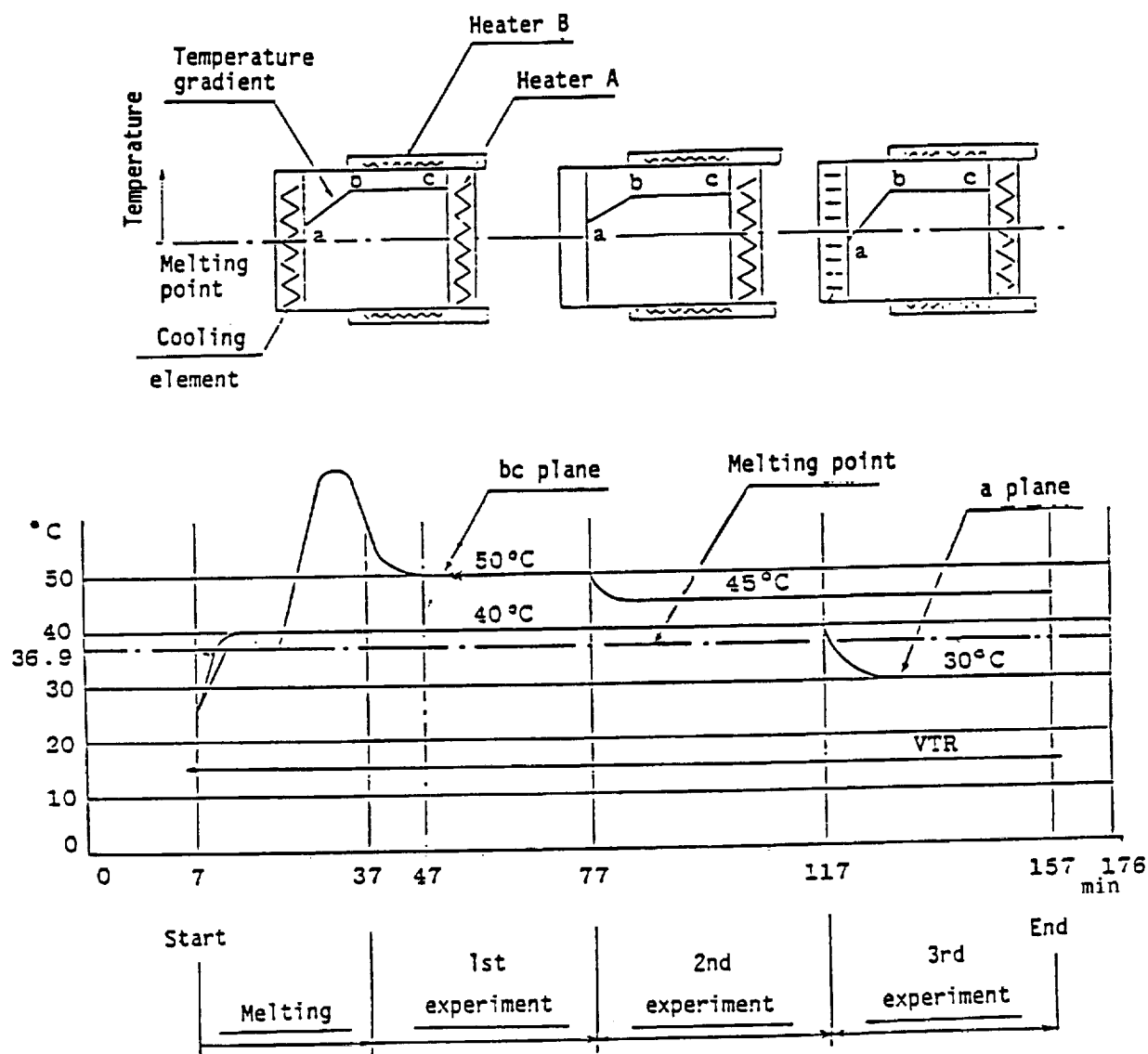


Figure 3. Experiment sequence of M18.

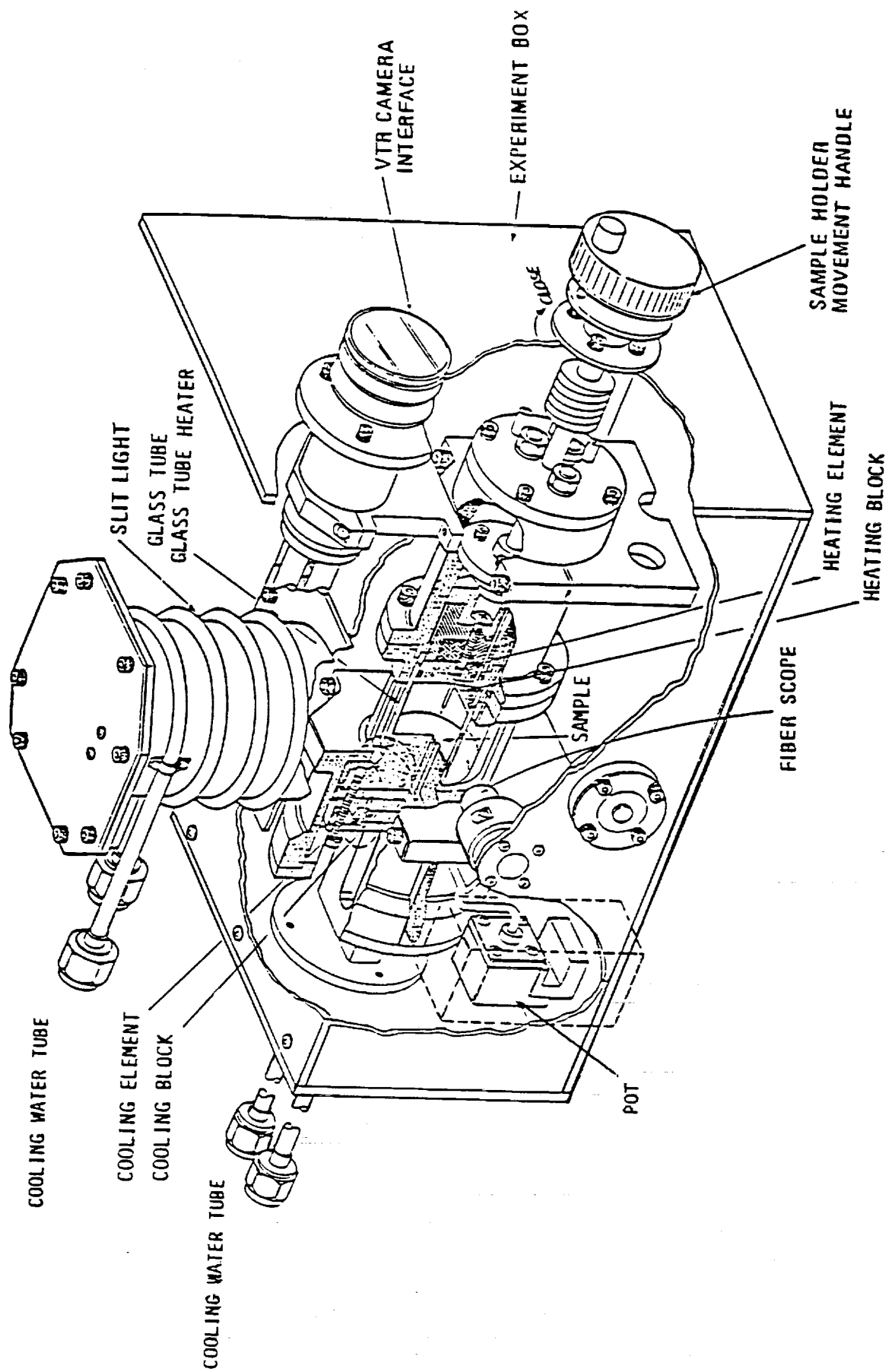


Figure 4. Marangoni Convection Unit.

SOLIDIFICATION OF EUTECTIC SYSTEM ALLOYS IN SPACE  
M-19

Atsumi Ohno  
Chiba Institute of Technology  
Japan

It is well known that in the liquid state eutectic alloys are theoretically homogenous under 1 g conditions. However, the homogeneous solidified structure of this alloy is not obtained because thermal convection and non-equilibrium solidification occur. The present investigators have clarified the solidification mechanisms of the eutectic system alloys under 1 g conditions by using the in situ observation method; in particular, the primary crystals of the eutectic system alloys never nucleated in the liquid, but instead did so on the mold wall, and the crystals separated from the mold wall by fluid motion caused by thermal convection as shown in Figure. 1. They have also found that the equiaxed eutectic grains (eutectic cells) are formed on the primary crystals. In this case, the leading phase of the eutectic must agree with the phase of the primary crystals as shown in Figure 2.

In space, no thermal convection occurs so that primary crystals should not move from the mold wall and should not appear inside the solidified structure. Therefore no equiaxed eutectic grains will be formed under microgravity conditions.

Past space experiments concerning eutectic alloys have been classified into two types of experiments: one with respect to the solidification mechanisms of the eutectic alloy and the other to the unidirectional solidification of this alloy. The former type of experiment has the problem that the solidified structures between microgravity and 1 g conditions show little difference. This is why the flight samples have been prepared by the ordinary cast techniques on Earth. Therefore

it is impossible to ascertain whether or not the nucleation and growth of primary crystals in the melt occur and the if primary crystals influence the formation of the equiaxed eutectic grains.

In this experiment, hypo- and hyper-eutectic aluminum copper alloys which are near eutectic point are used. The chemical compositions of the samples are Al-32.4mass%Cu (hypo-eutectic) and Al-33.5mass%Cu (hyper-eutectic). Long rods for the samples are cast by the Ohno Continuous Casting Process and they show the unidirectionally solidified structure as shown in Figure 3. Each flight and ground sample has been made of these same rods. The dimensions of all samples are 4.5 mm in diameter and 23.5 mm in length. Each sample is put in a graphite capsule and then vacuum sealed in a double silica ampoule. Then the ampoule is put in the tantalum cartridge and sealed by electron beam welding.

For onboard experiments, a Continuous Heating Furnace (CHF) will be used for melting and solidifying samples under microgravity conditions. Six flight samples will be used. Four samples are hypo-eutectic and two are hyper-eutectic alloys. The surface of the two hypo-eutectic alloy samples are covered with aluminum oxide film to prevent Marangoni convection expected under microgravity conditions. Each sample will be heated to 700 °C and held at that temperature for 5 min. After that the samples will be allowed to cool to 500 °C in the furnace and then they will be taken out of the furnace for He gas cooling. Figure 4 shows the heating and cooling diagrams for the flight experiments.

After collecting the flight samples, the solidified structures of the samples will be examined and the mechanisms of eutectic solidification under microgravity conditions will be determined.



**It is likely that successful flight experiment results will lead to production of high quality eutectic alloys and eutectic composite materials in space.**

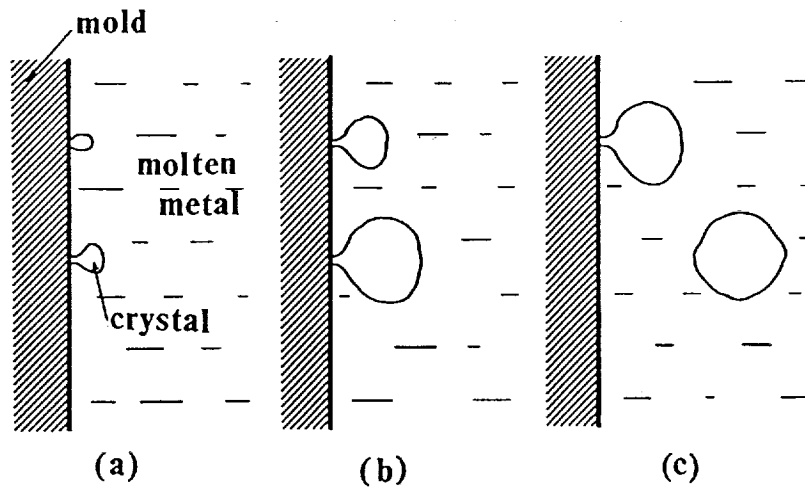


**Figure 1.** Schematic illustrations of the separation of primary crystals from the mold wall observed directly in some eutectic alloys under 1 g: (a) nucleation, (b) growth, (c) separation.

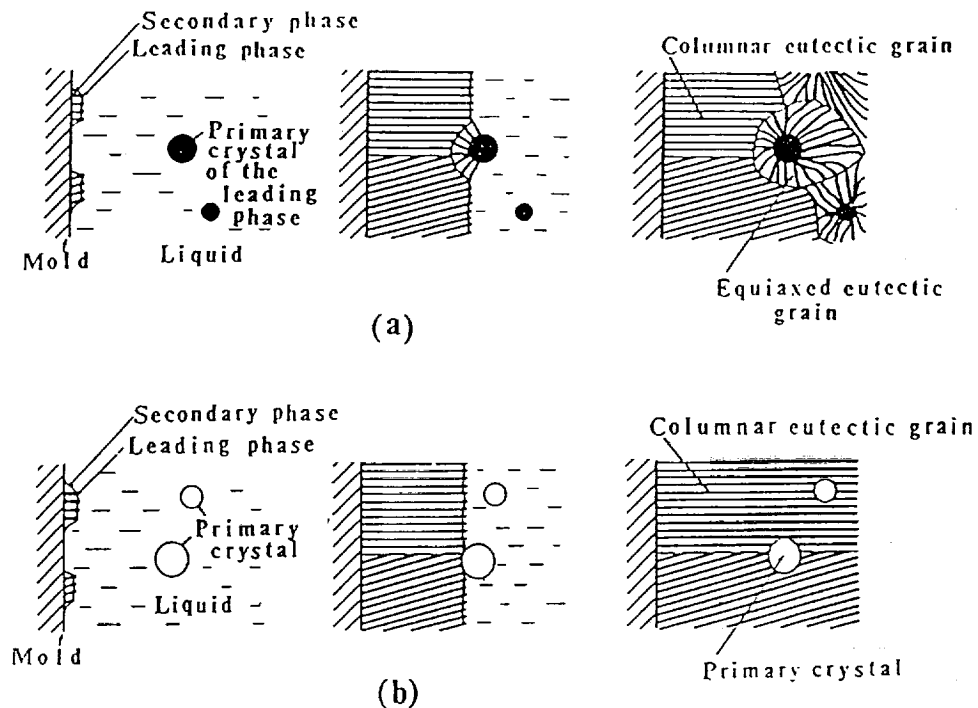


**Figure 2.** Schematic illustrations of the relation between the primary crystals and the eutectic grains. (a) Equiaxed eutectic grains formed on the primary crystals when the leading phase of the eutectic agrees with the phase of the primary crystal. (b) Formation of columnar eutectic grains are independent of the primary crystals. In this case the leading phase of the eutectic does not agree with the phase of the primary crystal.

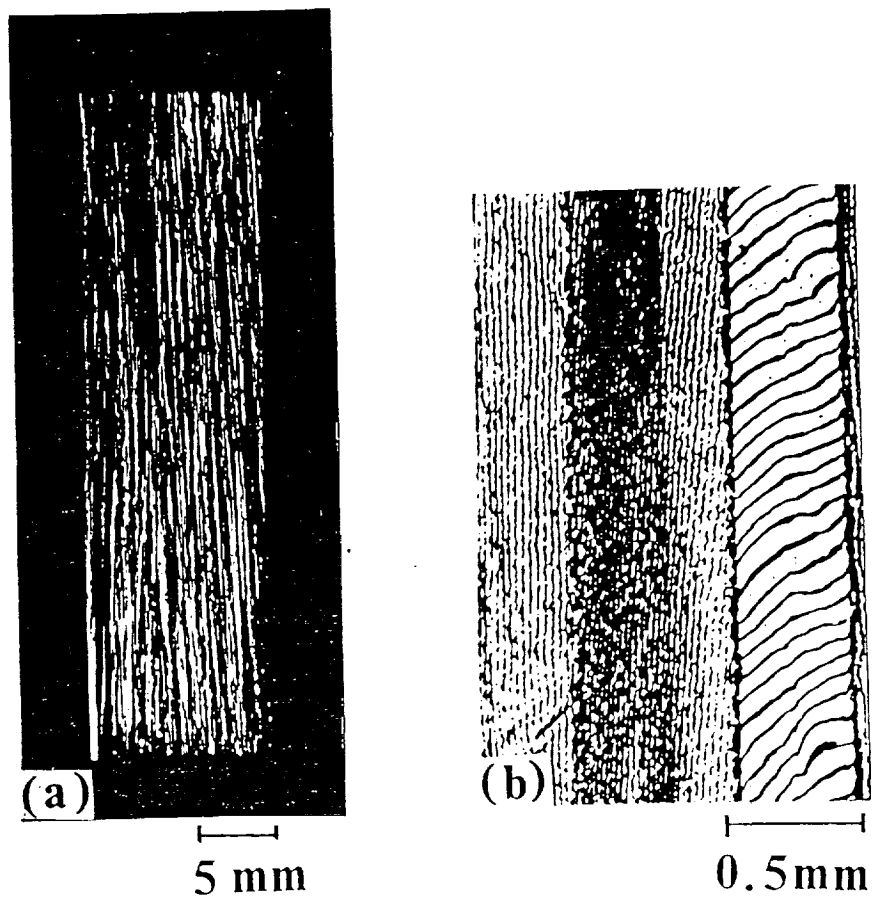


Figure 3. Unidirectionally solidified structures of Al-32.4 mass%Cu alloy used for sample:  
(a) macrostructure, (b) microstructure.

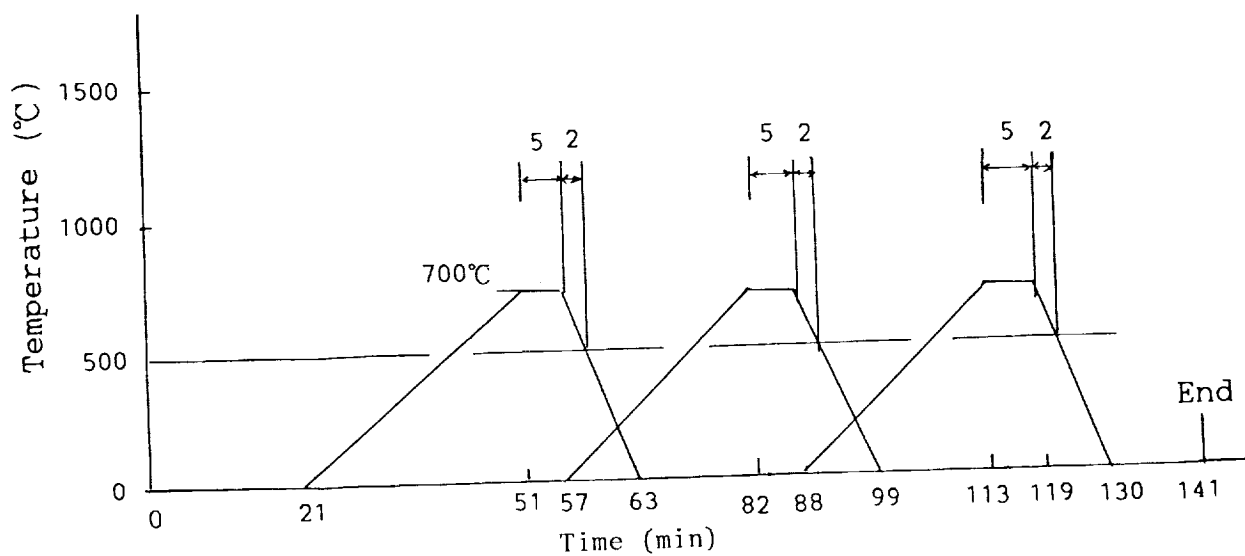


Figure 4. Heating and cooling curves for the samples.



# GROWTH OF SAMARSKITE CRYSTAL UNDER MICROGRAVITY CONDITIONS M-20

S. Takekawa  
National Institute for Research in Inorganic Materials  
Japan

## Purpose of the Experiment

To grow single crystals of samarskite under microgravity conditions by the traveling solvent float zone (TSFZ) method.

To study the phase relations in the samarskite-related systems involving liquid phases by the slow cooling float zone (SCFZ) method.

Samarskite is one of the minerals in a metamict state and is composed of Ca, Fe, Y, U, Th, Nb, Ta, O, etc.  $\alpha$ -particles radiating from uranium and/or thorium in the samarskite itself has destroyed its original structure without damaging its chemical composition and its external form. Consequently its structure has been converted into a vitreous structure.

## The TSFZ Method

The TSFZ method is for growing a single crystal (B) of an incongruently melting compound from the high temperature solution having the composition (S) which coexists with the solid phase (B). B denotes the composition of the compound B in Figure 1. S denotes the composition of the high temperature solution coexisting with the compound B in Figure 1.

### The SCFZ Method

The SCFZ method is for investigating the phase relations in the system involving liquid phases. The samples are melted and solidified in the controlled solidification process by using a float zone apparatus. The whole solidification sequence of the solidified phases and the concentration distribution in the solidified bodies are disclosed by means of EPMA technique. The phase relations are revealed by using the information obtained with the procedure described above. The scheme for explaining the method is shown in Figure 2.

The chemical formula of our sample is expressed by  $\text{Ca}_{0.24}\text{U}_{0.20}\text{Y}_{0.84}\text{Fe}_{1.56}\text{Nb}_{5.04}\text{O}_{16}$  and the shape is shown in Figure 3. The weight of uranium in the sample is 0.0669 g and its radioactivity is 0.0223  $\mu\text{Ci}$ .

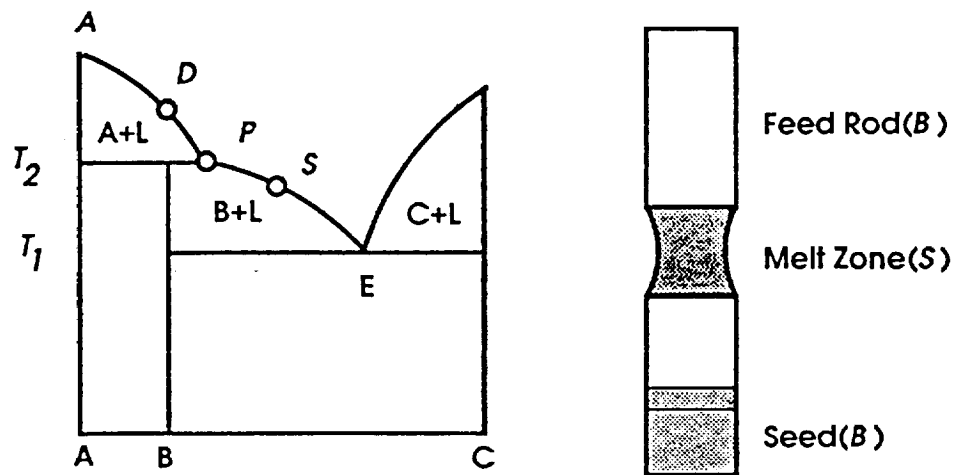


Figure 1. TSFZ method.

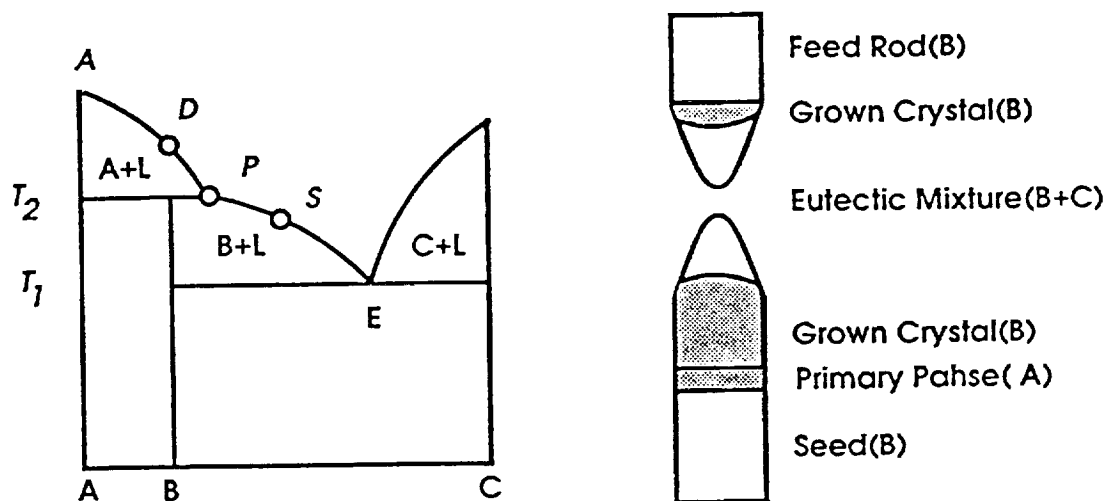
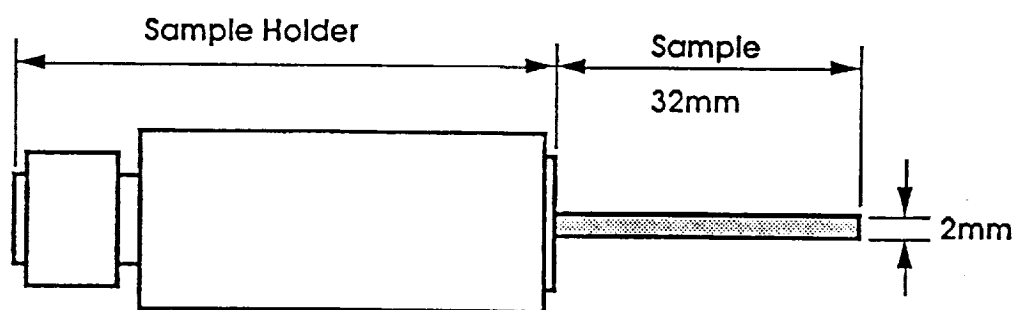
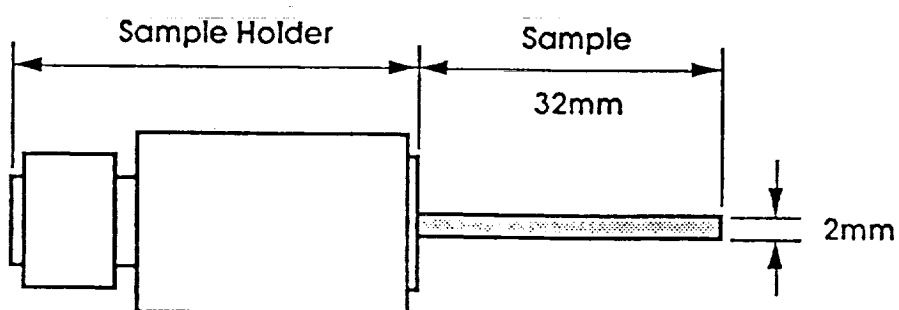


Figure 2. SCFZ method.



Upper Sample



Lower Sample

Figure 3. Samples.



### Stages in the Experiment

The experiment is consists of 7 stages(shown in Fig.4). The function in each stage is shown in below.

- ① Prepare the experimental environment such as setting up samples, quartz tube, IMF.
- ② Lamp power is automatically increased up to 260W. No PS task.
- ③ Build melt zone. If necessary, increase or decrease lamp power.
- ④ Single crystal growth by the TSFZ method. If necessary, adjust the shape of melt zone.
- ⑤ Study of phase relations by SCFZ method. No PS task.
- ⑥ Upper shaft moves upward rapidly to cut off the melt zone with certainty and Lamp power is automatically decreased down to 0W. No PS task.
- ⑦ Restore samples, quartz tube etc. and make IMF into the initial condition.

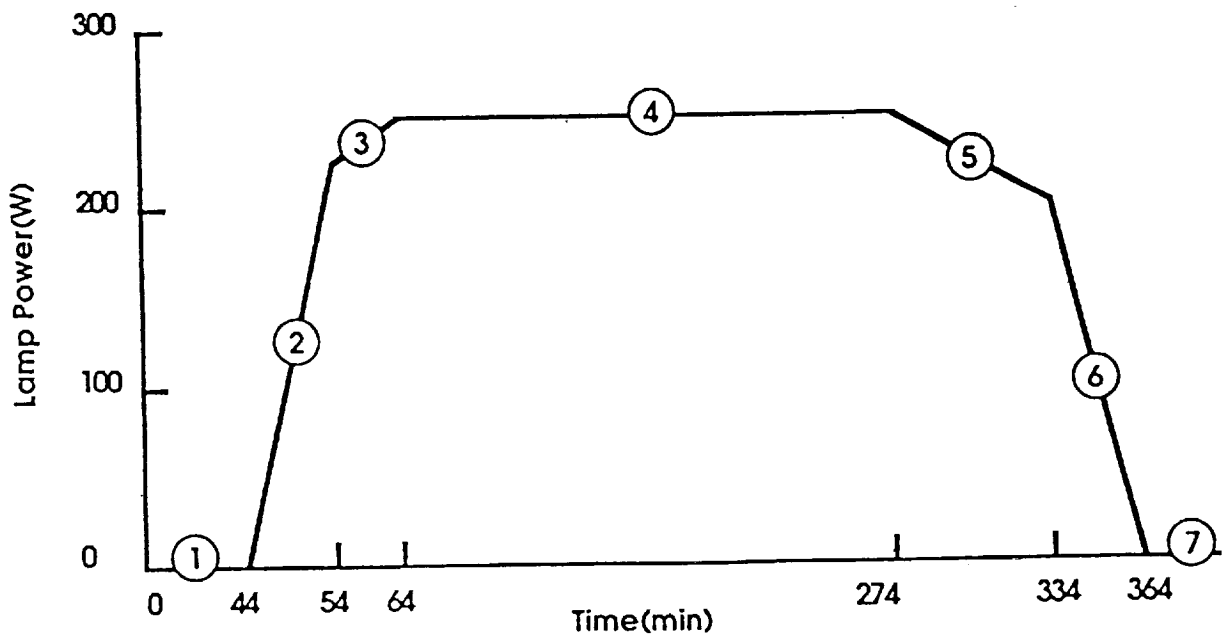


Figure 4. Experiment stages.



## GROWTH EXPERIMENT OF ORGANIC METAL CRYSTAL IN LOW GRAVITY M-21

Hiroyuki Anzai  
Electrotechnical Laboratory  
Tsukuba, Japan

The purpose of this experiment is to grow large, high-quality single crystals of the organic metal (TMTTF-TCNQ) by the diffusion method without thermal fluctuation due to convection and gravitational sedimentation, and to evaluate the difference in properties between such crystals grown in low gravity and the ones obtained on Earth.

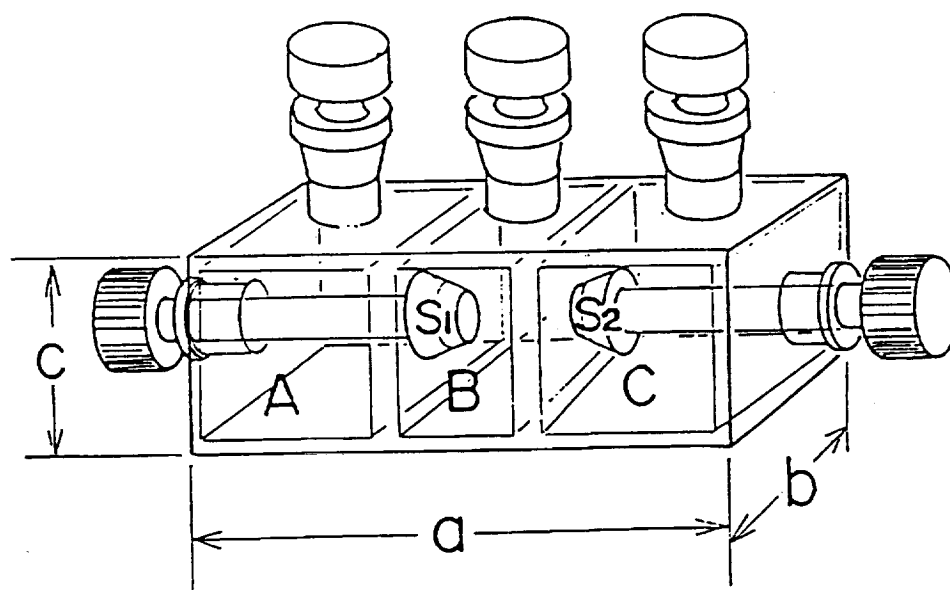
The expected results may fix several physical properties of TMTTF-TCNQ, lead to the discovery of new phenomena, and enable us to analyze diffusion processes in a precise way. The result will contribute to the development of research on organic metals and, generally, on crystal growth.

### Outline of Flight Experiment

The crystal growth apparatus for operation on the space shuttle is composed of three adjoining chambers each equipped with cocks. One side chamber is filled with the anisole solution of electron acceptor, TCNQ, the other side chamber is filled with the anisole solution of electron donor, TMTTF, and the center chamber is filled with pure anisole and seed crystals. When the space shuttle enters a state of microgravity, both side cocks are opened simultaneously, and from both side chambers, TMTTF and TCNQ molecules enter into the center chamber, react with each other, and produce the complex TMTTF-TCNQ. After a concentration of the complex

reaches saturation, crystals form around the seed crystals, growing by pure diffusion in microgravity. The physical properties of these space-grown crystals will be evaluated and compared with the properties of crystals grown on the Earth.

Solvent :  $C_6H_5OCH_3$   
 Donor :  $C_{10}H_{12}S_4$  (TMTTF)  
 Acceptor :  $C_{12}H_4N_4$  (TCNQ)



Dimension (mm)

	Small Cell	Large Cell
a	42	102
b	16	34
c	16	54

Figure 1. Crystal growth cell for organic metals.

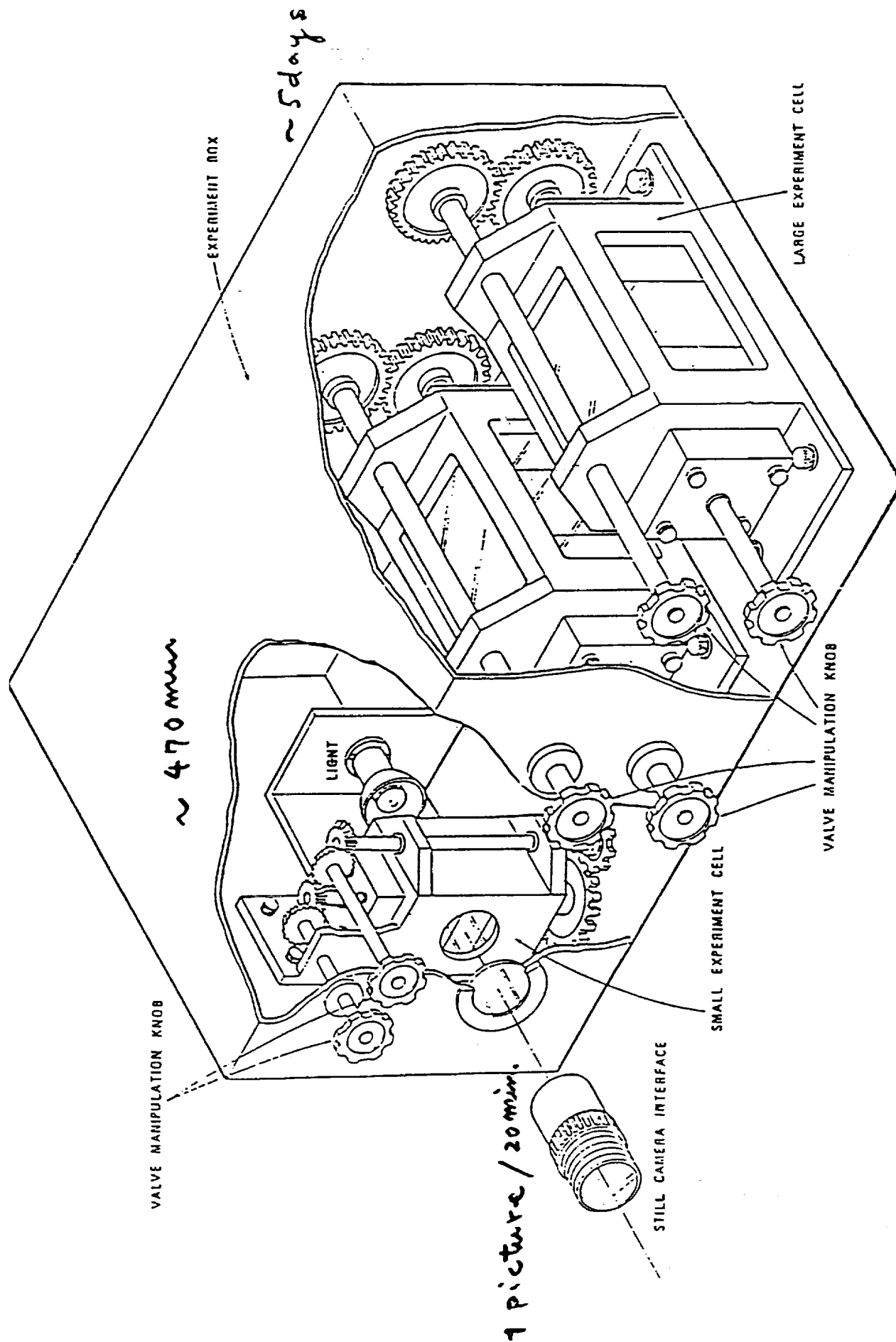


Figure 2. Organic Crystal Growth Experiment Facility concept.

CRYSTAL GROWTH OF COMPOUND SEMICONDUCTORS IN A LOW-GRAVITY  
ENVIRONMENT (InGaAs CRYSTALS)  
M-22

Masami Tatsumi  
Sumitomo Electric Industries, LTD  
Japan

Outline

Compound semiconductor crystals, such as gallium arsenide and indium phosphide crystals, have many interesting properties that silicon crystals lack, and they are expected to be used as materials for optic and/or electro-optic integrated devices. Generally speaking, alloy semiconductors, which consist of more than three elements, demonstrate new functions. For example, values of important parameters, such as lattice constant and emission wavelength, can be chosen independently. However, as it is easy for macroscopic and/or microscopic fluctuations of composition to occur in alloy semiconductor crystals, it is difficult to obtain crystals having homogeneous properties.

Macroscopic change of composition in a crystal is caused by the segregation phenomenon. This phenomenon is due to a continuous change in the concentration of constituent elements at the solid-liquid interface during solidification. On Earth, attempts have been made to obtain a crystal with homogeneous composition by maintaining a constant melt composition near the solid-liquid interface, through suppression of the convection flow of the melt by applying a magnetic field. However, the attempt has not been completely successful. Convective flow does not occur in microgravity because the gravity in space is from four to six orders of magnitude less than that on Earth. In such a case, mass transfer in the melt is dominated by the diffusion phenomenon. So, if crystal growth is carried out at a rate that is higher than the rate of mass

transfer due to this phenomenon, it is expected that crystals having a homogeneous composition will be obtained. In addition, it is also possible that microscopic composition fluctuations (striation) may disappear because microscopic fluctuations diminish in the absence of convection.

We are going to grow a bulk-indium gallium arsenide (InGaAs) crystal using the gradient heating furnace (GHF) in the first material processing test (FMPT). The structure of the sample is shown in Figure 1 where InGaAs polycrystals in a crucible are doubly sealed in two quartz tubes for safety. As shown in Figure 2, the GHF consists of two zones, namely, high temperature and low temperature zones, which results in a large temperature gradient at the interface. Crystal growth is performed by moving the furnace (i.e. the temperature profile) from the left to right at a definite rate. Thus, we will grow crystals both on Earth and in space under the same conditions. As previously described, it is possible to obtain good quality crystals which are homogeneous in composition both macroscopically and microscopically due to the lack of convection in space. We are planning to study effects of convection on crystal growth from a melt by comparing and characterizing the properties of crystals grown on Earth with those grown in space.

### Expected Results

It is important to control convection during crystal growth, especially from a melt. However, the effects of convection in a melt during crystal growth are not clear. In order to control convection in melt on Earth, various methods have been attempted, for example, imposing a magnetic field in a melt and adding forced convection by rotation, but the effects of these methods are also not clear.



Because the magnitude of gravity is small enough in space it is possible to completely suppress convection resulting from gravity. Accordingly, we can control convection in microgravity and study the effects. In the FMPT we are planning to study the effects of convection on crystal growth from a melt by comparing the properties of crystals grown on Earth and in space under the same conditions. The results will help to control convection in melts and to grow crystals on Earth. If a high quality crystal with uniform composition is obtained, InGaAs will be even more important as a material for optic devices for optical communication using quartz fiber. This experiment in the FMPT will also provide information for obtaining good crystals on Earth.

If we can control convection in a melt, we can grow big compound semiconductor crystals of any composition, and even crystals having few defects. Such crystals would not only lower production costs greatly but allow easy fabrication of many kinds of light emitting diodes, laser diodes, and electron devices for rapid calculation. Also, the realization of optical integrated circuits and optical computers would be possible.

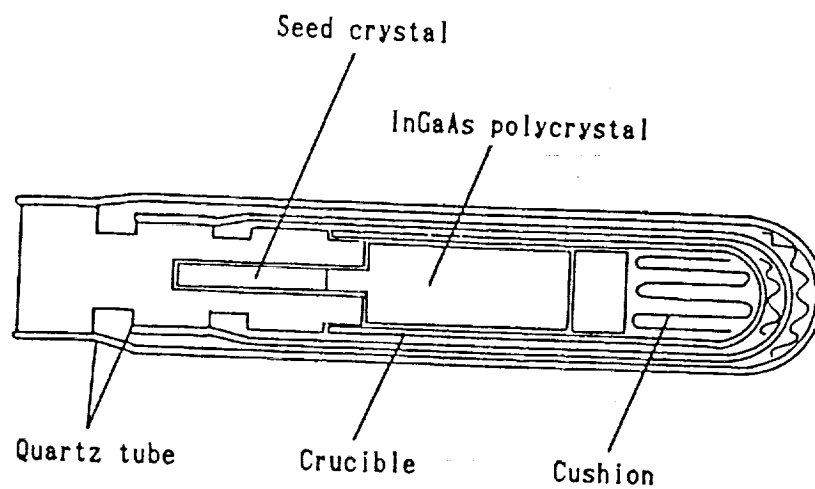


Figure 1. Sample structure.

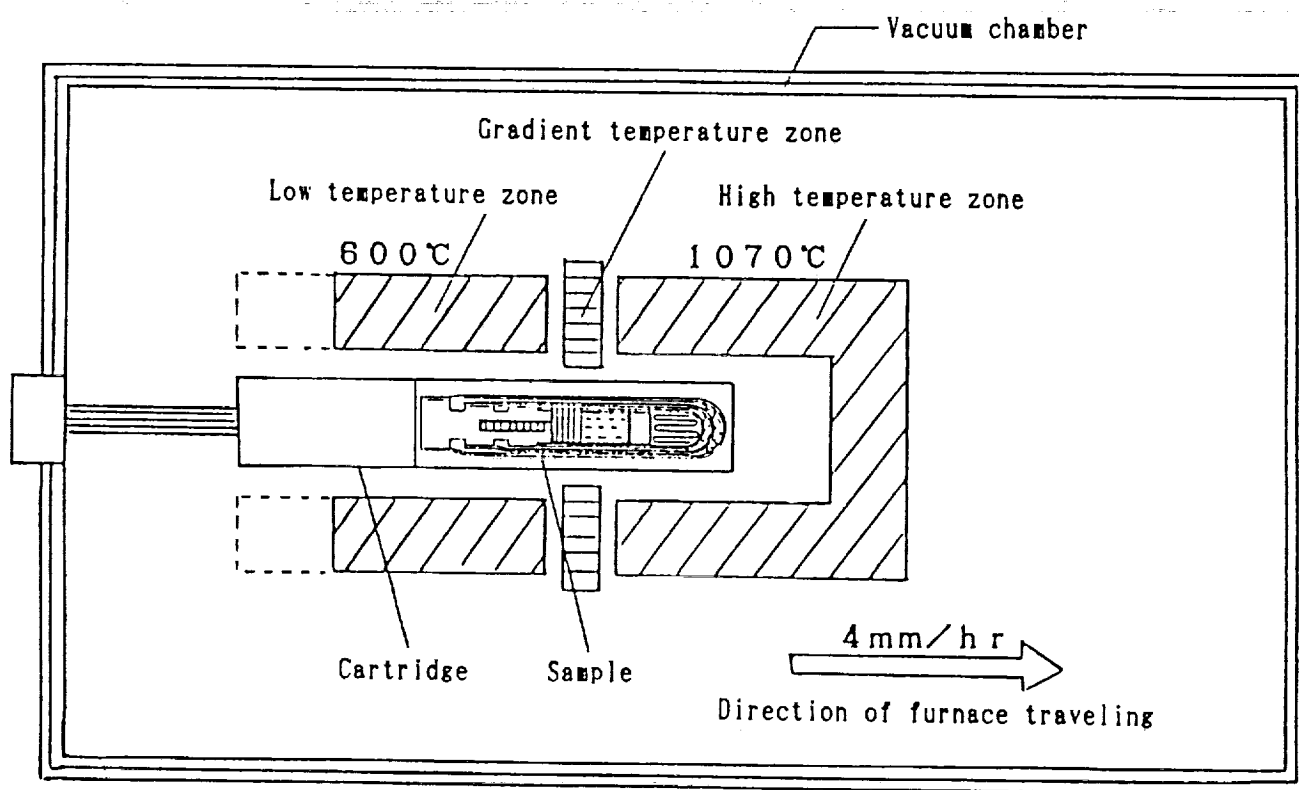


Figure 2. Crystal growth by the GHF.

## MICROGRAVITY ACCELERATION MEASUREMENT ENVIRONMENT CHARACTERIZATION

Richard DeLombard  
Lewis Research Center  
Cleveland, Ohio

### Science

The Space Acceleration Measurement System (SAMS) is a general-purpose instrumentation system designed to measure the accelerations onboard the shuttle Orbiter and shuttle/Spacelab vehicles (see Figure 1). These measurements are used to support microgravity experiments and investigations into the microgravity environment of the vehicle. Acceleration measurements can be made at locations remote from the SAMS main instrumentation unit by the use of up to three remote triaxial sensor heads. The SAMS was developed by NASA's Lewis Research Center (LeRC) in support of NASA's microgravity science programs.

In the past, numerous acceleration measurement systems have flown on various space missions. These systems were tailored to measure accelerations for a narrow set of requirements and were limited in bandwidth, dynamic range, and recording capability. In addition, these systems were mission-peculiar and not easily modified for other applications or missions. The result has been an inability to accurately assess the expected microgravity environment prior to a mission for a particular experiment and/or location.

The prime science objective for SAMS on the SL-J mission will be to measure the accelerations experienced by a multitude of experiments in the two racks of the Japanese First Materials Processing Test (FMPT). The FMPT consists of a variety of materials science and life

science experiments contained in racks #7 and #10. The SAMS data will be made available to the FMPT principal investigators after the mission for their analysis with the FMPT data.

A secondary science objective for SAMS will be the characterization of the acceleration environment of the Spacelab module. This will include an analysis of the acceleration transfer function of the Spacelab module which will utilize the FMPT acceleration measurements along with measurements at the rack #9 structure. Another analytical effort to be undertaken is a general characterization of the acceleration environment of the Spacelab as an orbiting laboratory. These analysis efforts will be in conjunction with similar measurements and analyses on other SAMS Spacelab missions.

### Instrument

SAMS configurations are available for the Orbiter middeck locker area, Spacelab SMIDEX rack, and Spacelab center aisle. The configuration for the Orbiter cargo bay is presently under development. These configurations of the same instrument will enable microgravity measurements at nearly any desired payload location.

A SAMS unit consists of a main unit (shown in Figure 2) with one triaxial sensor head and up to three remote triaxial sensor heads. The main unit is comprised of the crew interface, optical disk data storage devices, and control and processing electronics. The remote triaxial sensor heads are comprised of three single-axis acceleration sensors, preamplifiers, and filters. Each head is connected to the main unit by an umbilical cable which has a maximum length of 20 feet.

The low-pass bandwidth for a triaxial sensor head is independent of the bandwidth of the other two heads and is chosen to match the requirements of the supported experiment. Standard choices for the low-pass bandwidth of a head are 0 to 2.5 Hz, 5 Hz, 10 Hz, 25 Hz, 50 Hz, and 100 Hz.

The standard SAMS triaxial sensor head employs the Sundstrand QA-2000 sensors, having a sensor resolution of 1 micro-g. Two triaxial sensor heads utilizing Bell XI-79 sensors are also available having a sensor resolution of 0.01 micro-g. The SAMS uses simultaneous sample and hold circuits to maintain phase coherence in the three axis measurements of a given triaxial sensor head. Similarly, the outputs of the three sensors of a given triaxial sensor head are digitized by the same 16-bit analog-to-digital converter. The signal processing for each triaxial sensor head has filtering characteristics matched to the data sampling rate for that triaxial sensor head. The preamplifier has four decade gain ranges and the capability for an electronic calibration mode.

The triaxial sensor head digitized data are formatted and transferred to optical disk for permanent storage. The optical disk drive enables crew-tended disk changes which allow essentially unlimited data storage during a mission. With 200 Mb of storage per optical disk side, typical times between disk change operations are from hours to days, depending on the triaxial sensor head sampling rates.

To support the FMPT life science experiments on SL-J, one SAMS head will be mounted in rack #7. This triaxial sensor head will utilize Sundstrand model QA2000 sensors and will be set for 50 Hz and 250 samples per second. This will result in measuring the acceleration environment experienced by the equipment mounted in rack #7.

To support the FMPT material science experiments on Spacelab-J, one SAMS head will be mounted in rack #10. This triaxial sensor head will also utilize Sundstrand model QA2000 sensors and will be set for 50 Hz and 250 samples per second. This will result in measuring the acceleration environment experienced by the equipment mounted in rack #10.

To measure the low-frequency accelerations experienced by the Spacelab, the third head will be mounted toward the bottom of rack #9 and will be set for 2.5 Hz and 12.5 samples per second. This triaxial sensor head will utilize one of the Bell model XI-79 sensor heads (if available) and will be set for 2.5 Hz and 12.5 samples per second. If a Bell sensor head is unavailable, a Sundstrand sensor head will be utilized.

The three separate sensor head locations will allow a continued characterization of the Spacelab module acceleration transfer function as well as contribute to a data base for characterizing the Spacelab acceleration environment.

SAMS units are currently manifested on the SLS-1, IML-1, SL-J, USML-1, USMP-1, and IML-2 Spacelab missions and STS-43 in the middeck. There will be eight flight units fabricated to support the expected flight rate of four microgravity science missions (e.g., IML-3, USML-2, USMP-2) per year.

#### Data Processing and Analysis

Post-mission processing of data by the SAMS project will be limited to data extraction, compensation, identification, format conversion, archival, and dissemination. The processed data

will be provided to the principal investigators involved with the particular mission and other interested organizations, as required.

In conjunction with the SAMS project, the Acceleration Characterization and Analysis Project will assist the PIs in the SAMS data conversion as well as performing analyses of the SAMS mission data. The SAMS acceleration data from the numerous missions will allow a better prediction of the acceleration environment for future microgravity missions.

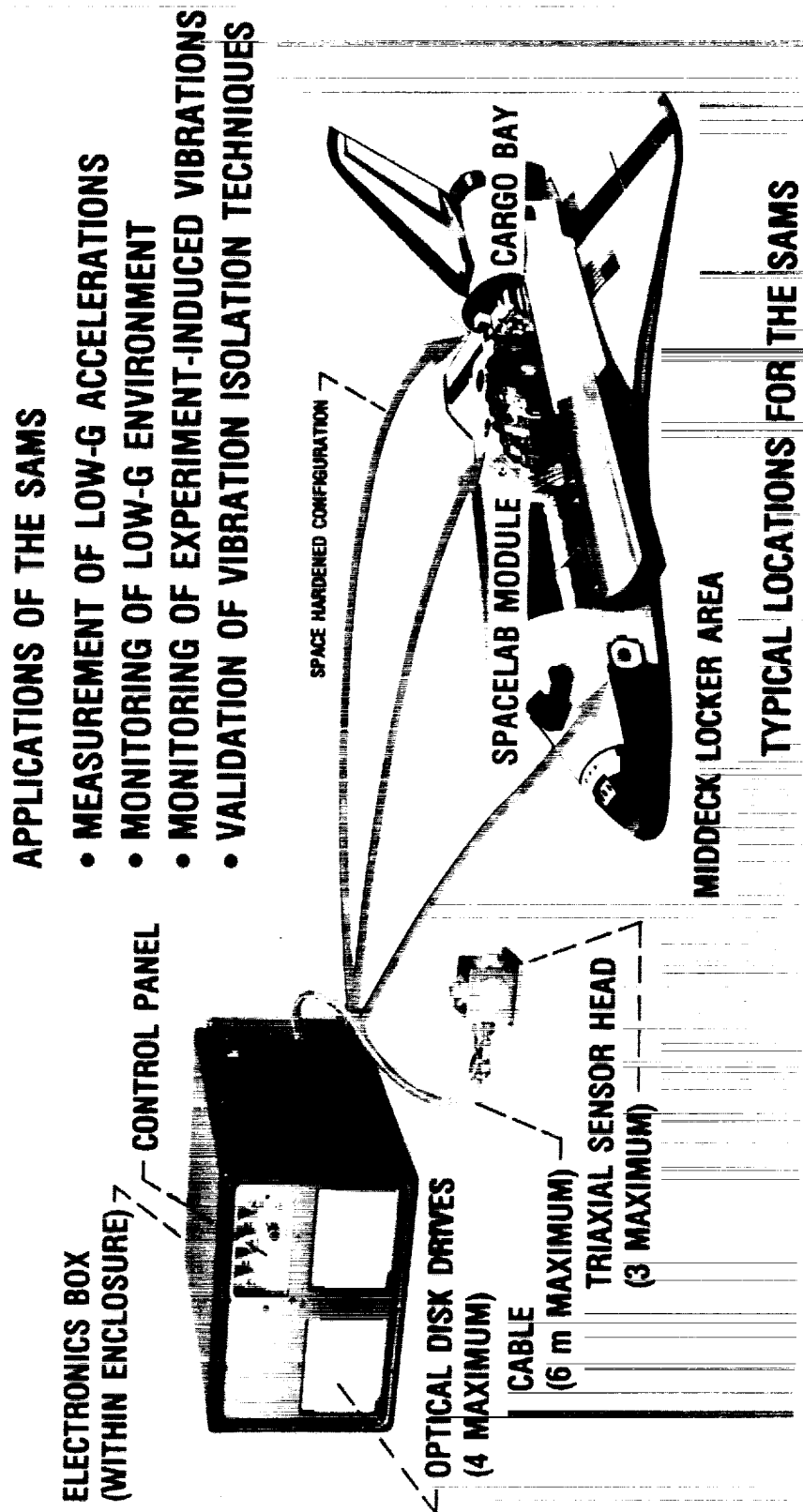


Figure 1. Space Acceleration Measurement System (SAMS).



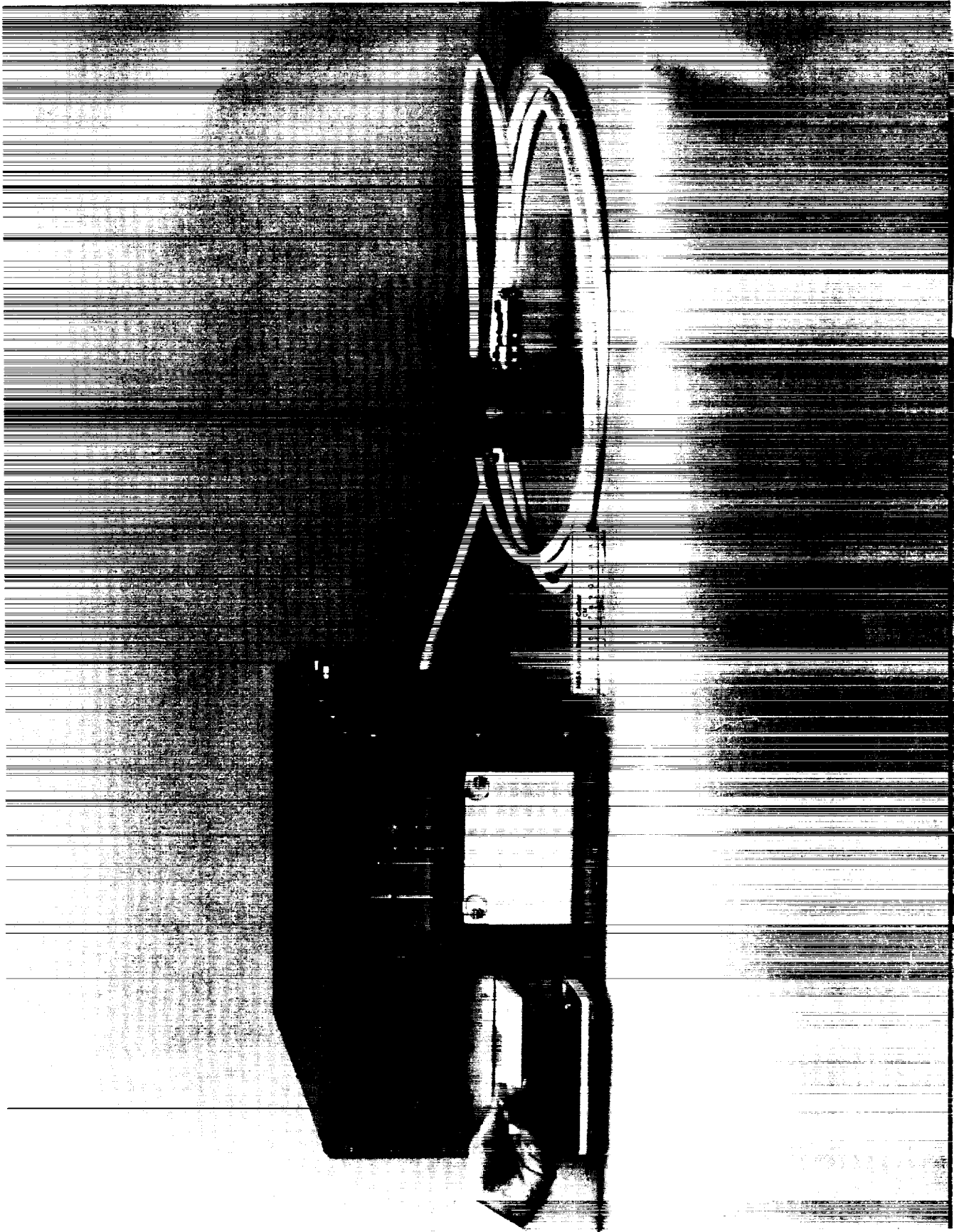


Figure 2. Space Acceleration Measurement System (SAMS).

ORIGINAL PAGE  
BLACK AND WHITE PHOTOGRAPH



## PROTEIN CRYSTAL GROWTH

Charles E. Bugg  
University of Alabama at Birmingham  
Birmingham, AL

Proteins (enzymes, hormones, immunoglobulins, and numerous other types) account for 50% or more of the dry weight of most living systems and play a crucial role in virtually all biological processes. Since the specific functions of essentially all biological molecules are determined by their three-dimensional structures, it is obvious that a detailed understanding of the structural makeup of a protein is essential to any systematic research pertaining to it. At the present time, protein crystallography has no substitute: it is the only technique available for elucidating the atomic arrangements within complicated biological molecules.

Most macromolecules are extremely difficult to crystallize, and many otherwise exciting and promising projects have terminated at the crystal growth stage. Single crystals that have dimensions of 0.2-1.0 mm on a side are generally required for x-ray crystallographic analyses of macromolecular structures and much larger crystals are required for neutron diffraction analyses. Proteins and other biological macromolecules often yield small micro-crystals readily, but it might then take several years of trial and error experimentation before these micro-crystals can be induced to grow large enough for a complete structural analysis. Even when large crystals are obtained, the crystals of essentially all biological macromolecules diffract rather poorly due to internal disorder. Thus, there is a pressing need to better understand protein crystal growth, and to develop new techniques that can be used to enhance the size and quality of protein crystals.

In principle, there are several aspects of microgravity that might be exploited to enhance protein crystal growth. According to theoretical considerations and experiment results, the major factor that might be expected to alter crystal growth processes in space is the elimination of density-driven convective flow. Convection in solution growth is caused by density gradients that occur when solute is depleted from the solution at the growing crystal surfaces. The density-dependent convection might be expected to affect protein crystal growth from aqueous solutions in several different ways. Convection will force solution to flow past the crystal, thus bringing material to the growing crystal surfaces at a rate that is significantly different from the steady-state diffusion rate that would be predominant in quiescent solutions. The flow patterns may generate significant variation in concentration at different parts of a crystal, thus leading to non-uniform growth rates. Also, convection may lead to significant physical stirring of growth solutions; in general, it is expected that such stirring effects might alter nucleation in growth processes.

Another factor that can be readily controlled in the absence of gravity is the sedimentation of growing crystals in a gravitational field. When a protein crystal grows from aqueous solution on Earth, it generally migrates to the top or the bottom of the crystallization vessel (depending on whether its density is greater or less than the density of the solution). Therefore, protein crystals often grow from solution at an interface where all sides of the crystal are not equally accessible to the crystallizing solution. (In most cases, sedimentation causes proteins to crystallize as fused masses that contain highly disordered crystalline arrays.) Under microgravity conditions, it is expected that protein crystals will not display this tendency to migrate away from initial nucleation sites, and can thus grow in isotonic environments, forming discrete, independent nucleation in sites.

Another potential advantage of microgravity for protein crystal growth is the option of doing containerless crystal growth. Contacts with vessel walls often lead to heterogeneous nucleation in crystal growth solutions. In the microgravity environment, it may be possible to form stable spherical droplets of crystallizing materials, which might be suspended by acoustical levitation or other methods. It is definitely possible to form relatively large stable droplets of protein solutions by extruding solutions from a pipette or a syringe; thus, protein crystals might be grown under microgravity conditions in relative large droplets adhering to syringe tips, without the extensive wall effects that generally accompany crystallization experiments on Earth.

As a result of the above theories and facts, one can readily understand why the microgravity environment established by Earth-orbiting vehicles is perceived to offer unique opportunities for the protein crystallographer. This perception led to the establishment of the Protein Crystal Growth in a Microgravity Environment (PCG/ME) project that continues today under NASA sponsorship. This project has advanced from simple hand-held devices (containing only a few protein solutions) to a more complex system involving 60 individual protein experiments in a thermally-conditioned environment. The results of experiments already performed during STS missions have in many cases resulted in protein crystals being grown that are significantly larger and more structurally correct than the best specimens produced on Earth. Thus, the near-term objective of the PCG/ME project is to continue to improve the techniques, procedures, and hardware systems used to grow protein crystals in Earth orbit. A large number of industrial guest investigators and co-investigators are involved in the project and multiple flight opportunities are obviously required to accomplish these objectives.

During the mission, protein crystals will be grown by vapor diffusion which is a technique that uses the diffusion of water vapor to establish equilibrium between protein solutions and more concentrated reservoir solutions. The protein and precipitant solutions will be contained separately in double-barrelled syringes located within small experiment chambers. The experiment chambers will also contain absorbent reservoirs saturated with precipitant solutions at higher concentrations.

The PCG payload flying on SL-J will include three vapor diffusion trays (VDAs) contained in a Refrigerator/Incubator Module (R/IM) at 22 °C (Figure 1). Each VDA tray (Figure 2) will contain 20 experiment chambers, each containing a double-barrelled syringe and a containment plug. Each syringe is made of polysulfone and is operated by a ganging mechanism. Prior to launch, the syringes will be loaded with a maximum of 40 µl of protein solution in one barrel and a maximum of 40 µl of precipitant solution in the other barrel, and the absorbent reservoir will be saturated with precipitant solution. The syringes will then be installed in the experiment chambers and capped by containment plugs for launch. One VDA tray will be modified to accommodate seeding of the protein droplets with Seed Insertion Devices (SIDs). Seeding is a technique used to initiate and enhance crystal growth by the introduction of seed crystals into equilibrated protein droplets. During the pre-flight loading procedure, a few protein seed crystals will be loaded into each SID, and then the SIDs will be stowed in the PCG equipment locker.

Shortly after achieving orbit, a crew member will activate the PCG experiments. A handwheel will be attached to a ganging mechanism that retracts the containment plugs from the double-barrelled syringes. Next, the handwheel will be relocated on the tray to operate the syringe ganging mechanism, resulting in the simultaneous movement of the pistons attached to

each syringe. This will force the protein and precipitant solutions from their respective barrels, causing the two solutions to mix as they form a droplet on the tip of each syringe. The pistons will be retracted and extended through several cycles to ensure mixing of the two solutions. At a prescribed time, shortly after PCG activation, the SIDs will be inserted into the appropriate chambers and the seed crystals injected into the protein droplets.

After activation, each protein droplet is surrounded by a saturated atmosphere that is in contact with a reservoir containing a precipitant solution. Water vapor will gradually move from the droplet to the reservoir because the precipitant concentration in the reservoir is higher than that in the drop. This diffusion of water out of the drop causes the concentrations of protein and precipitant to increase in the drop. When appropriate concentrations are reached in the drop, the protein molecules will begin to nucleate, causing crystals to form in the droplet.

Prior to landing, a crew member will deactivate the payload by first turning the hand-wheel to draw the droplets back into the syringes and then plugging the syringe tips with the containment plugs to protect the crystals during landing.

Protein crystals produced by experiments such as these enable investigators to determine each protein's three-dimensional structure, thus leading to new information about the structure and function of protein molecules. Previous PCG experiments have produced many protein crystals, that once analyzed by x-ray crystallography, were found to be larger and more perfect than their ground-based counterparts. Potential applications of the structural information gained from these protein crystals include treatment of organ transplants and HIV infection, production of dietary protein for human and domestic animals, and transfer of genetic materials.

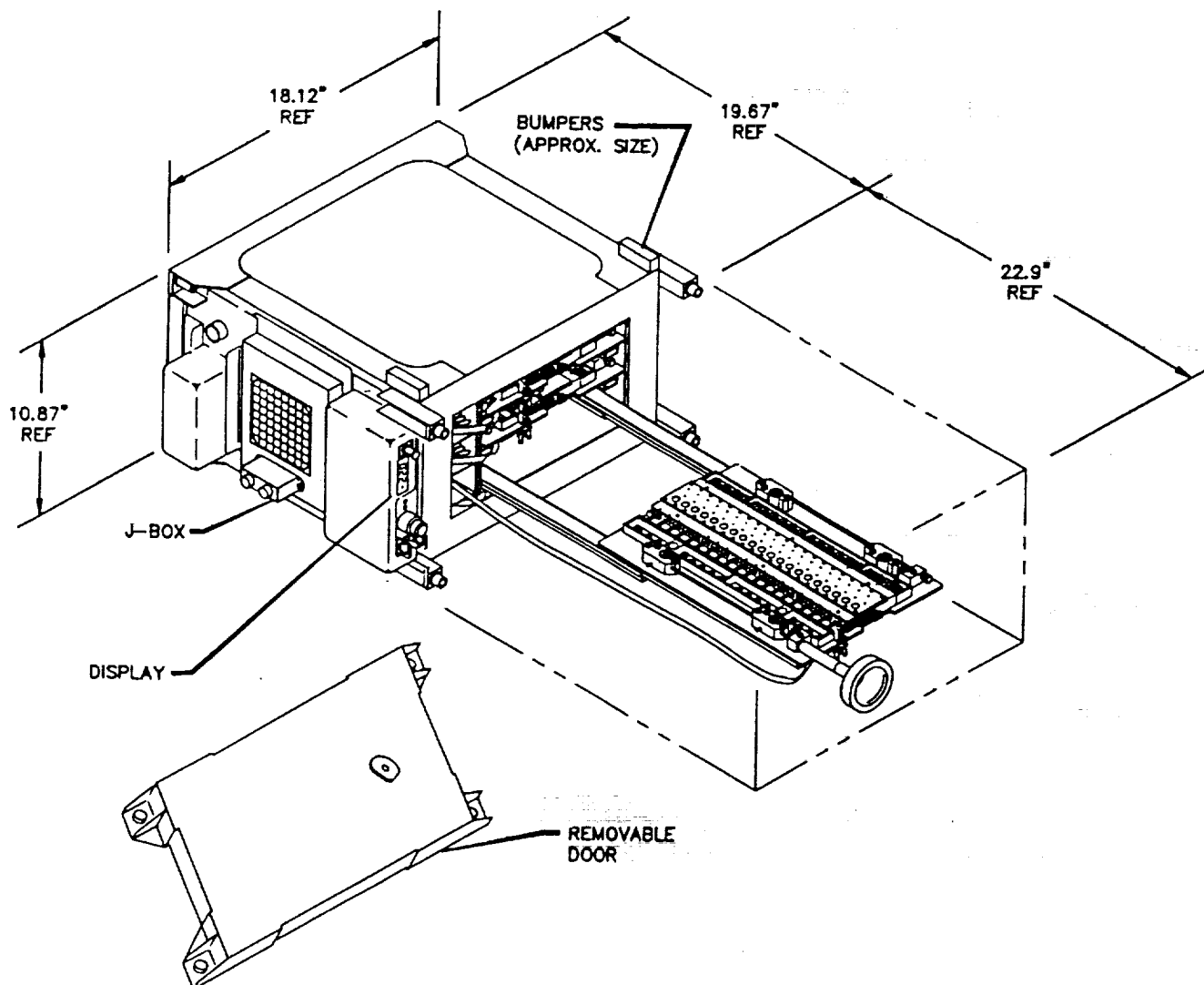


Figure 1. Refrigerator/Incubator Module (R/IM).



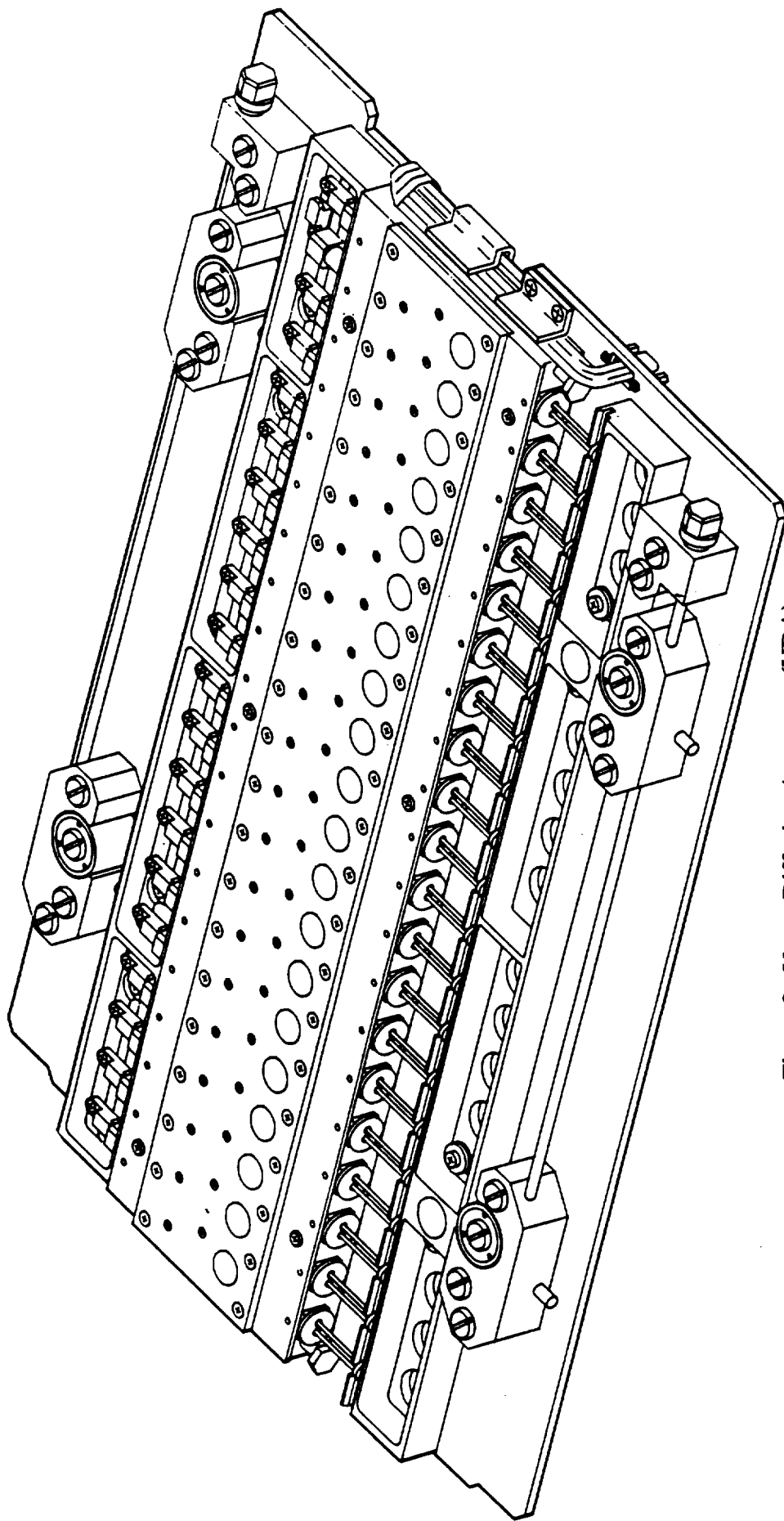


Figure 2. Vapor Diffusion Apparatus (VDA).



**SECTION II  
LIFE SCIENCES**



**HEALTH MONITORING OF JAPANESE PAYLOAD SPECIALIST - AUTONOMIC  
NERVOUS AND CARDIOVASCULAR RESPONSES UNDER  
REDUCED GRAVITY CONDITION  
L-0**

**Chiharu Sekiguchi  
National Space Development Agency of Japan  
Japan**

**Introduction**

In addition to health monitoring of the Japanese Payload Specialist (PS) during the flight, this investigation also focuses on the changes of cardiovascular hemodynamics during flight which will be conducted under the science collaboration with the Lower Body Negative Pressure (LBNP) Experiment of NASA. For the Japanese, this is an opportunity to examine firsthand the effects of microgravity on human physiology. We are particularly interested in the adaptation process and how it relates to space motion sickness and cardiovascular deconditioning.

By comparing data from our own experiment to date collected by others, we hope to understand the processes involved and find ways to avoid these problems for future Japanese astronauts onboard Space Station Freedom and other Japanese space ventures.

**Objectives**

The primary objective of this experiment is to monitor the health condition of Japanese Payload Specialists to maintain a good health status during and after space flight. The second purpose is to investigate the autonomic nervous system's response to space motion sickness. To achieve this, the function of the autonomic nervous system will be monitored using non-invasive

techniques. Data obtained will be employed to evaluate the role of the autonomic nervous system in space motion sickness and to predict susceptibility to space motion sickness. The third objective is evaluation of the adaptation process of the cardiovascular system to microgravity. By observation of the hemodynamics using an echocardiogram we will gain insight on cardiovascular deconditioning. The last objective is to create a data base for use in the health care of Japanese astronauts by obtaining control data in experiment L-0 in the SL-J mission.

### Experiment Description

The experiment consists of on-orbit data collection phase and ground data collection phase including KC-135 parabolic flight experiment and pre- and post-flight data collection. Parabolic flight data collection sessions are scheduled to familiarize PS crew members with donning and doffing of PMS equipment in microgravity. We will assure adequate mobility and performance of PS while wearing PMS. Baseline physiological data such as EKG, electrooculogram (EOG), finger plethysmogram, skin potential reflex (SPR), and respiratory wave (RW), with and without specific vestibular stimuli, will be collected.

Pre-flight and post-flight data collection will be obtained for blood and urine for electrolyte, hormone, and chemistries. In addition to the sample collection, hemodynamics will be measured under LBNP stress.

On-orbit experimental protocol consists of two parts: one is continuous physiological monitoring using PMS and the other is observation of hemodynamic changes using an echocardiograph, the LBNP, and related equipment. The continuous recording of basic physiological

data using a NASA/PMS is conducted while the PS is working at launch day, mission day (MD) 1, 2, 5, and 6 (re-entry day). Signals of ECG, RW, and SPR are transmitted to the ground via an infrared telemetry system three times a day when physiological data are monitored.

Echocardiographic parameters, central venous pressure, leg volume, blood pressure, and ECG are measured without LBNP stress at MD 2 and 5 and with LBNP stress at MD 4.

### Hardware

**Physiological Monitoring System Back Pack.** The Physiological Monitoring System (PMS) Back Pack consists of PMS, respiratory wave signal conditioner, infrared telemetry system, and cassette data tape recorder. The PMS acquires blood pressure, ECG, SPR, and heart rate information. It consists of an arm cuff with a microphone to measure blood pressure, chest electrode leads to acquire the heart signals, and forearm electrodes to obtain the SPR signal. Infrared telemetry system downlinks some physiological parameters such as ECG, respiration, and SPR through the Data Interface Unit to the ground. The PMS displays blood pressure and heart rate on a numerical display unit.

**Cassette Data Tape Recorder.** The Cassette Data Tape Recorder (CDTR) is a battery-powered recorder that records the subject's ECG, respiration, and SPR. This is also installed in a PMS backpack.

**Echocardiography.** The Echocardiography (AFE) uses ultrasound (high frequency sound above hearing range), computer imaging, and data storage to produce multiple two-dimensional,

realtime pictures of the heart. This image provides information on heart dimensions and a basis for multiple measurements relating to the function of the heart.

**Lower Body Negative Pressure Device.** The components of the Lower Body Negative Pressure Device (LBNPD) are an inflatable cylinder assembly, a control console assembly, and a cover/stowage container. During launch and landing operation, the LBNPD is compressed into a compact unit, stowed in its nomex cloth container, and attached to a floor section of the Spacelab. The control console assembly contains a pressure/vacuum pump, switches, digital logic, pressure/vacuum and pressure relief valves, pressure/vacuum hoses, and a pressure gauge. The pressure/vacuum pump operates on 28 volts dc and pressurizes the walls of the cylinder to inflate it to its full height. After inflation, a negative pressure is created within the cylinder by operation of the pump in the vacuum mode. A manually-operated pressure regulator is used to obtain pressure in a range from 0 to -60 mmHg. A LED digital readout displays the level of vacuum in the cylinder. A latex rubber waist seal on the LBNPD forms an airtight seal around the subject. The LBNPD can be easily purged to ambient pressure by the operator.

**Automatic Blood Pressure System.** The Automatic Blood Pressure System (ABPS) is a flight-qualified model of the Puritan-Bennett Infrasonde series of blood pressure monitors. It is an electronic sphygmomanometer which, when used with cuff and transducer, comprises a system for measuring both systolic and diastolic arterial blood pressure using a patented infrasonic pulse-detection method. The ABPS incorporates a digital printer, a RS-232 communications interface, an ECG input connector, a heart rate monitor, and a series of buffer amplifiers to provide data outputs.



**Central Venous Pressure Device and Data Recorder.** The Central Venous Pressure Device (CVPD) consists of a non-invasive Doppler blood flow probe mounted in an aluminum enclosure along with an electronic pressure meter, hardware circuitry, and LCD display. A mouthpiece/pressure transducer plugs into the pressure meter. The probe is placed over the jugular vein in the neck. The subject expires into the restricted mouthpiece while listening through stereo headphones to the flow sounds and watching the pressure meter to generate various target pressures. Flow and pressure data are recorded onto the TEAC 7-channel cassette data recorder. The TEAC cassette data recorder is an off-the-shelf seven channel recorder, powered by a single 9-volt alkaline battery, used to record data from medical experiments.

**Ultrasonic Limb Plethysmograph.** The Ultrasonic Limb Plethysmograph (ULP) is a self-contained device which uses pulses of ultrasound to determine chord lengths through the calf at one or two levels. The instrument has ultrasound transducers which are attached to the skin over the calf muscle using double-sided adhesive tape rings. An ultrasonic pulse is produced by exciting the transmitter crystal with a fast-rising voltage pulse. The pulse propagates through the tissue to the receiver crystal. The receiver output is sensed by a high-gain amplifier and threshold detector.

ORIGINAL PAGE  
BLACK AND WHITE PHOTOGRAPH



Figure 1. Photograph of PMS system performance test onboard the KC-135 aircraft. Payload Specialist Dr. Mohri, who was wearing the PMS device (left), and the author were checking the performance of the system.

## ENDOCRINE AND METABOLIC CHANGES IN PAYLOAD SPECIALIST L-1

Nobuo Matsui  
Nasoya University  
Japan

### Background

The endocrine system plays an important role in the adaptation to unusual environments by secreting hormones to control metabolism. Since human beings have long evolved on the surface of the Earth under a gravity environment, the weightless environment must be quite unusual for them. The purpose of this experiment is to study the mechanisms of human adaptation to a weightless environment from endocrine and metabolic changes.

Our study plan is focused on four major physiological changes which have been reported during past space flights or which may be expected to occur under that condition.

1. Hormone and metabolic changes associated with fluid shift. It is well-established that exposure to weightlessness results in significant redistribution of body fluids. As shown in Figure 1, on arrival at zero gravity, body fluid shifts from the lower part of the body to the upper part, resulting in overhydration of the upper body. The change can be partly ameliorated by hormonal adjustment of fluid metabolism such as increased urine flow. This change causes a decrease in plasma volume. Therefore, on return to Earth, gravity-induced downward fluid shift may elicit cardiac deconditioning. Thus, investigation of body fluid metabolism and its regulating mechanism has been thought to be one of the most important subjects in space medicine.

2. Bone demineralization and muscle atrophy. On the Earth, bone and muscle function to sustain body weight and to exercise against gravitational force. Under the weightless condition, the load on them is greatly reduced. Thus, bone and muscle atrophy are commonly observed in the astronauts after space flight. These changes are accompanied by increased urinary calcium excretion and loss of muscle proteins. Since loss of calcium continues for the entire stay in space, bone demineralization has been thought to be one of the major limiting factors of long-term space flight. Up to now, these changes in bone and muscle have been attributed to gravitational unloading, but the involvement of the endocrine system also should be considered. It is widely known that increased secretion of glucocorticoids such as occurs in Cushing's syndrome or their administration for a variety of diseased states causes bone and muscle atrophy, while various kinds of anabolic steroids are used by athletes to strengthen bone and muscle. Thus, changes in catabolic glucocorticoids and anabolic testicular steroids during space flight should be examined.

3. Altered circadian rhythm. Various physiological functions of living organisms on the Earth show remarkable rhythmical changes which are concordant with the Earth's rotation. Among these physiological functions, circadian rhythmicity of some hormone secretion is prominent ensuing circadian variation of metabolic parameters. It has been suggested that alteration of circadian rhythm may cause disease. The alteration of the circadian rhythm of adrenocortical hormone secretion is known in patients with depression. On the other hand, eastward or westward air travel causes so-called jet lag. This well-experienced phenomenon is a result of discordance between the acquired rhythm at the original location and rhythm of the new

location. Therefore, the effect of space flight free from influence of Earth's rotation on circadian rhythm of endocrine and metabolic function is interesting.

4. Stress reaction during space flight. When living organisms are exposed to unusual environments, stress reaction which accompanies increased secretion of adrenocortical hormones occurs. Since stress reaction modifies the regulation of water and electrolyte metabolism as well as gonadotropic hormone secretion, evaluation of the stress reaction is indispensable. The elucidation of the interrelationship between stress reaction and above the three subjects is most interesting.

#### Procedures of the Experiment

Timed urine samples will be consecutively collected from the seventh pre-flight day to the third post-flight day, with a 2-day interruption during the in-flight period. Blood samples will be obtained at pre- and post-flight periods. Body weight will be measured every morning before breakfast. Fluid intake of all kinds will be recorded. Various parameters will be measured, for example, water- and electrolyte-regulating hormones, adrenal and testicular hormones, catecholamines and metabolic parameters such as Na, K, Cl, Mg, Ca, P, hematocrit, osmolality, etc. Simultaneous determination of various hormones and metabolic indices and consecutive collection of urine characterize this experiment.

#### Influential Effects of this Experiment on Biomedical Science

In spite of wide variations of environment that surround living organisms, composition of body fluid is maintained within relatively narrow ranges. Thus, cells which are fundamental

components of organisms, are bathed by stable body fluid and keep their function. The maintenance of constant internal milieu, homeostasis, is essential for life. The endocrine system plays an important role in homeostasis. Thus, investigations of the endocrine system under unusual environments offer fundamental knowledge to biomedical science. The weightless environment is a novel unusual environment which has been experienced by few human beings. Therefore, the proposed experiment may offer new results on the mechanism of human adaptation to various environments.

Expectations on each topic: (1) Disturbances of water and electrolyte metabolism comprise not only edematous disorders but also hypertensive disorders which are the most common adult diseases. Since changes in water- and electrolyte-regulating hormones during space flight differed from what was expected by simulated weightless experiments on the Earth, the control of these hormones may be modulated by other factors so far not fully realized. This experiment may elucidate them. (2) Atrophy of bone and muscle is an important problem in geriatric medicine. Elucidation of the mechanism of atrophy during space flight should greatly contribute to the understanding of pathogenesis of bone and muscle atrophy in aged people. (3) Recent development of aircraft and popularization of world travel has made jet lag common. The mechanism of circadian rhythmicity of physiological functions, however, has not been clarified yet. Investigation on the rhythmicity of hormone secretion in space where the influence of the Earth's rotation is absent may contribute to understanding the basic mechanism of the rhythm and may offer countermeasures against jet lag. (4) Stress reaction affects various endocrine systems. Studies on the influence of stress reaction induced by space flight upon endocrine and metabolic systems are important to understand the control mechanisms of living organisms.

Thus, this experiment may be important not only for maintenance of good health of astronauts but also for basic and clinical medicine on the Earth, and it may contribute to understanding of the basic phenomena of life.

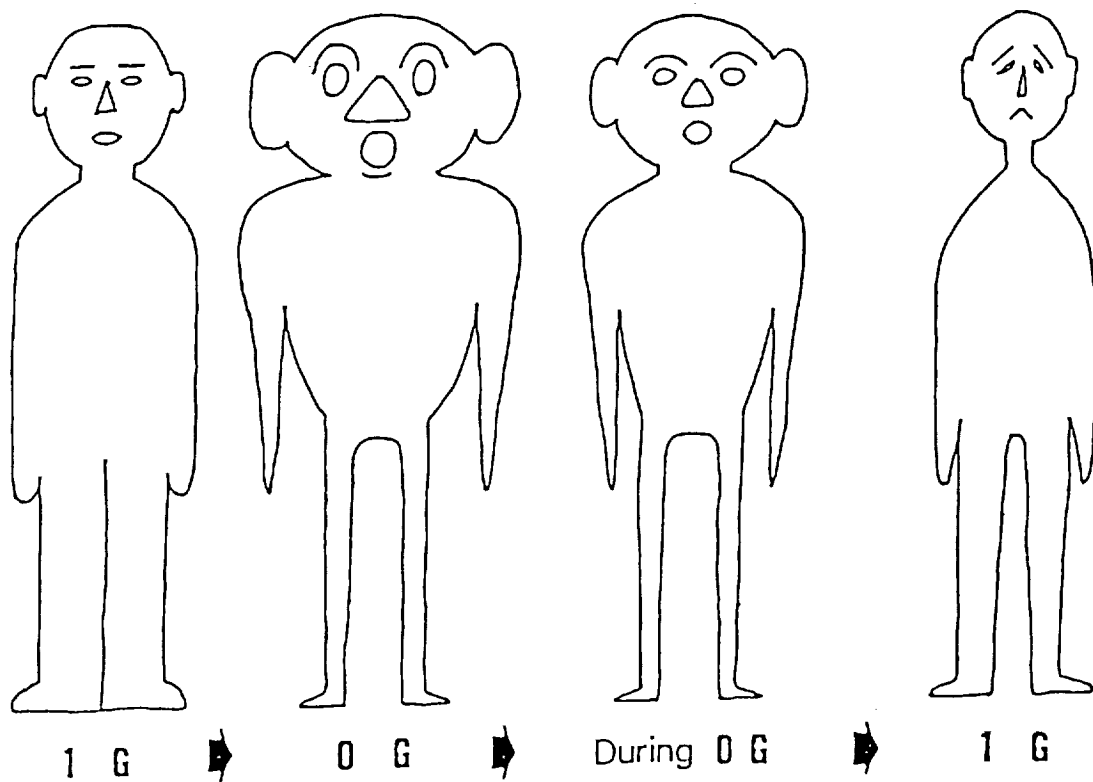


Figure 1. Body fluid shift caused by space flight.





NEUROPHYSIOLOGICAL STUDY ON VISUO-VESTIBULAR CONTROL OF POSTURE  
AND MOVEMENT IN FISH DURING ADAPTATION TO WEIGHTLESSNESS  
L-2

Shigeo Mori  
Research Institute of Environmental Medicine, Nagoya University  
Japan

We can stand upright and walk smoothly without paying any particular attention to it. This is because we have established in ourselves an integration center that controls our body subconsciously in response to input from eyes, muscles, joints, foot soles, and also from the gravity sensor in the inner ear (the otolith organ). It has been shown that the cerebellum plays an important role for the establishment of the integration center and that the control pattern is comparable to that of a highly sophisticated computer system.

The programming for the control, however, may well be acquired for the 1-g ground condition and does not cover the 0-g in space. Although each of the above organs function as it does on the ground, the signal pattern sent to the center must be different under 0-g and, in addition, complementary signals from the otolith organ are missing, leading to confusion in the integration center and causing a variety of symptoms similar to those of car-sickness or sea-sickness. After exposure to microgravity an immediate process of re-programming will begin and be completed in 2-4 days. There is strong supporting evidence for this sensory conflict theory as an explanation for space motion sickness (SMS) episodes.

Fish were selected as test organisms for this investigation because they swim around freely in three dimensions and have well-developed organs for vision and gravity detection. They also have an innate nature to orient their back toward a light source. Actually, on the

ground, the fish tilts its vertical axis toward the light when illuminated laterally, and the tilt angle is a function of the intensity of light and the magnitude of gravity, while its posture is completely light-dependent in the low-gravity environment produced by aircraft parabolic flight or when the otolith organs are removed. This implies that fish posture is entirely under visual and otolithic control. In this case, the cerebellum will also contribute to the control.

In the space shuttle experiment, two fish (one with the otolith-removed and the other with intact otoliths) are onboard for 7 days. The arrangement of the experiment is shown in Figure 1. Lamps illuminate each fish alternately from different directions at a duration of 20 seconds for 10 minutes totally, twice a day. The video images and the brain waves from the cerebellum are analyzed later. If the sensory conflict theory is acceptable, then the confusion at the onset and the following recovery process will be manifested both in the light-dependent behavior and also in the cerebellar activity. In addition, there should be some variation in response between the two fish.

Even if the results are positive in the present fish experiment, they would not be extensive enough to allow us to understand the complete mechanism of SMS. However, what is currently needed is a collection of evidence based on animal experiments on which to base future investigations.

Countermeasures for SMS are mandatory since SMS-induced vomiting occurring within a space suit could be fatal for a crew member during extravehicular activities. We expect that countermeasures will be developed before the space station era starts, and that the results of these studies will be applied to improving human welfare.

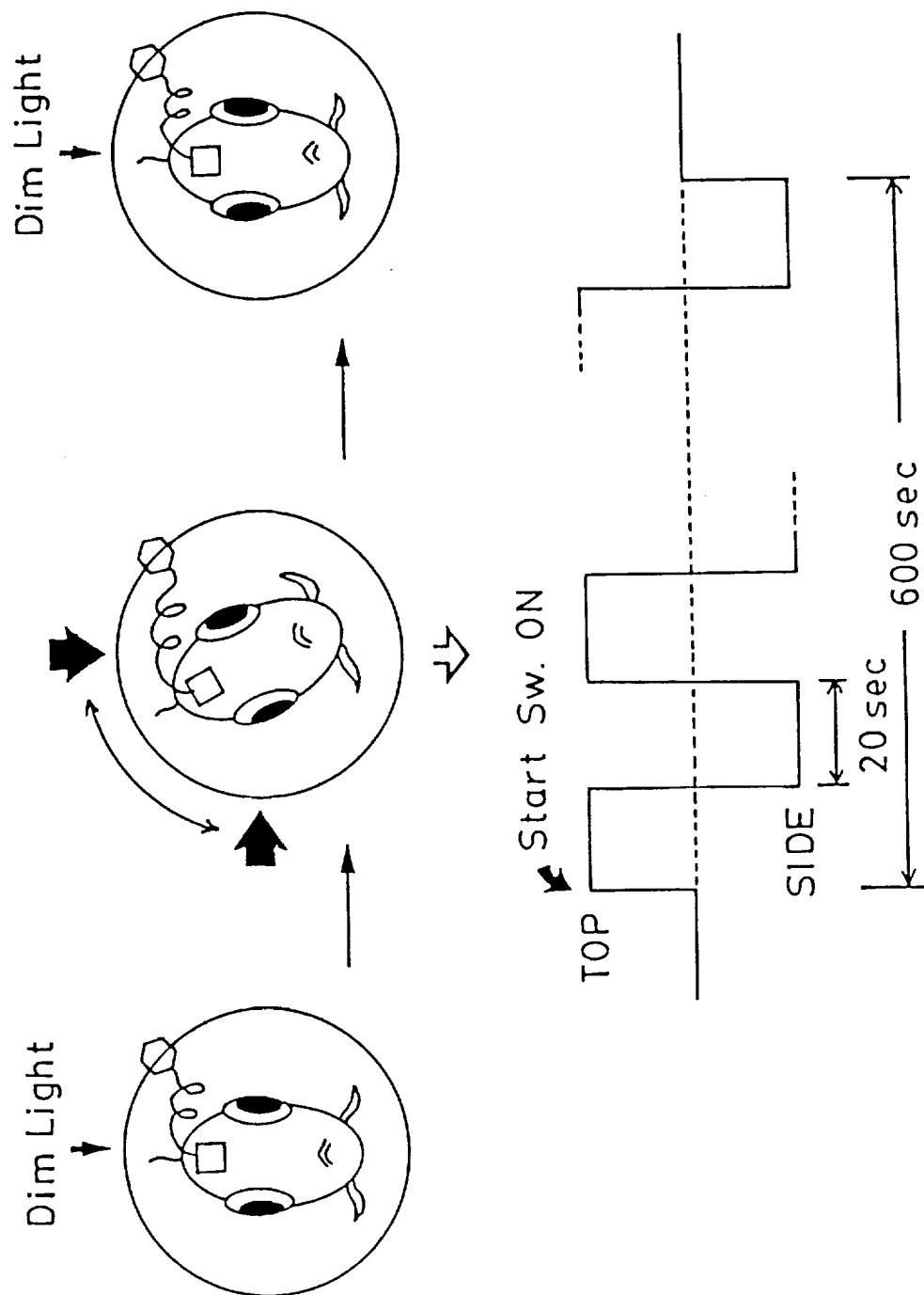


Figure 1. Carp experiment in space. Ten-minute recordings of light-dependent carp behavior and the electrical activity of the cerebellum are collected twice a day during the 7-day mission.



SEPARATION OF BIOGENIC MATERIALS BY ELECTROPHORESIS  
UNDER ZERO GRAVITY  
L-3

Masao Kuroda  
Osaka University Medical School  
Japan

Outline of Flight Experiment

Electrophoresis separates electrically charged materials by imposing a voltage between electrodes. Though free-flow electrophoresis is used without carriers such as colloids to separate and purify biogenic materials including biogenic cells and proteins in blood, its resolving power and separation efficiency is very low on Earth due to sedimentation, floatation, and thermal convection caused by the specific gravity differences between separated materials and buffer solutions.

The objective of this experiment is to make a comparative study of various electrophoresis conditions on the ground and in zero-gravity in order to ultimately develop a method for separating various important "vial" components which are difficult to separate on the ground.

A schematic of a free-flow electrophoresis apparatus is shown in Figure 1. Several free-flow electrophoresis devices have been developed. Since all electrophoresis devices utilize an electric field, Joule heat is generated. This heating causes convection currents in the sample solution, which disrupts the separated sample bands and therefore limits the separation ability.

In space we may be able to obtain improved separations of important biological samples which are difficult to separate on the ground because of the absence of floating or sedimentation of the sample due to concentration differences, or the convection current due to Joule heat.

In the FMPT experiment, we will examine the differences in separations obtained on Earth and those performed in microgravity, and investigate the effects of various separative conditions using samples composed of several mixed proteins.

### Ground-Based Experiments

Preliminary ground-based experiments were performed in a small free-flow electrophoresis chamber (width 60 mm, height 100 mm, thickness 0.8 mm). The chamber thickness is less than that of the flight chamber to allow more efficient cooling of the chamber buffer which is necessary to control Joule heating.

In the preliminary experiment, we tested the electrophoresis of a mixture of various proteins (Cytochrome C, Bovine Serum Albumin, Trypsin-inhibiter, etc.) in preparation for the flight experiment.

The results obtained are shown in Figures 2 and 3. These results are as expected. Since separation ability was still not optimum, we plan to examine how these proteins separate in space.

## Objectives of the Flight Experiment

We will use a sample composed of a mixture of proteins to investigate the effects of varying the following experiment parameters on the separation efficiency.

1. Comparison of separation ability by the change of the velocity of a flowing buffer liquid.
2. Comparison of separation ability based on the change of the electrophoresis voltage.
3. Comparison of separation ability by the change of the volume of infusing sample.

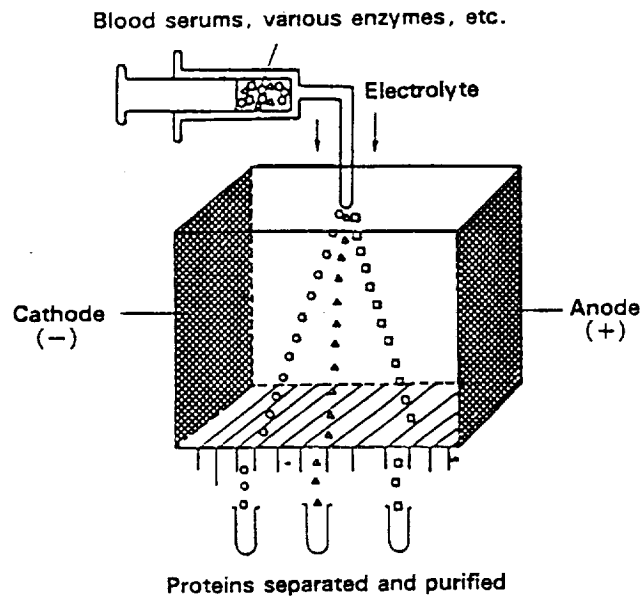


Figure 1. Schematic of Electrophoresis Chamber.

4 種混合蛋白 (各 20mg/ml)

Cytochrome C (PI 10.1)

Conalbumin (PI 8.4)

B S A (Bovine Serum Albumin PI 4.8)

Trypsin inhibitor (PI 4.5)

流量 B: 2400  $\mu$ l/min (B 40)

S: 2.00  $\mu$ l/min

ABS 0.05

温度 20 °C

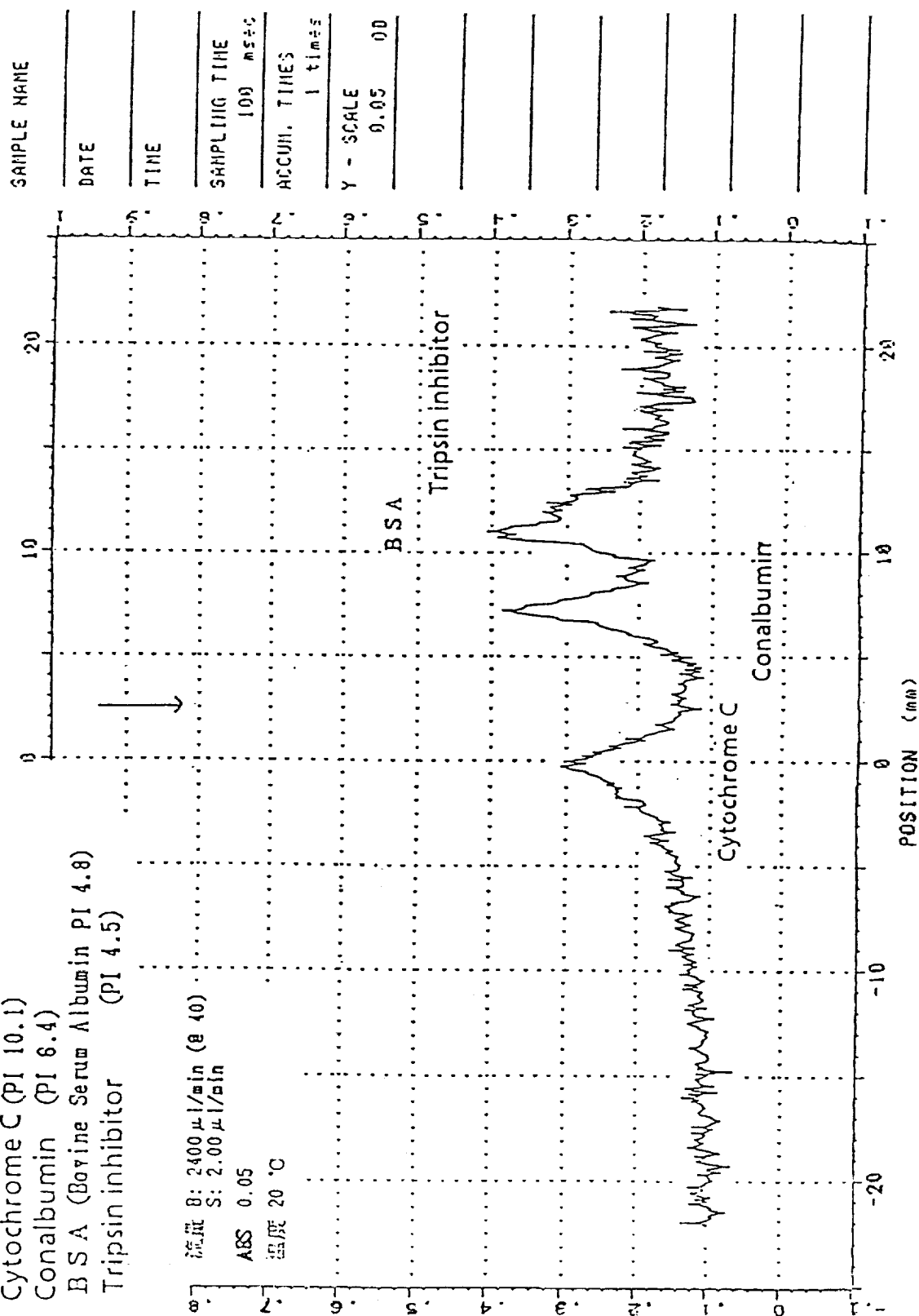


Figure 2. Electrophoresis separation of mixed proteins (BBM).



### 3种混合蛋白

Cytochrome C (PI 10.1)

Conalbumin (PI 8.4)

BSA (Bovine Serum Albumin PI 4.8)

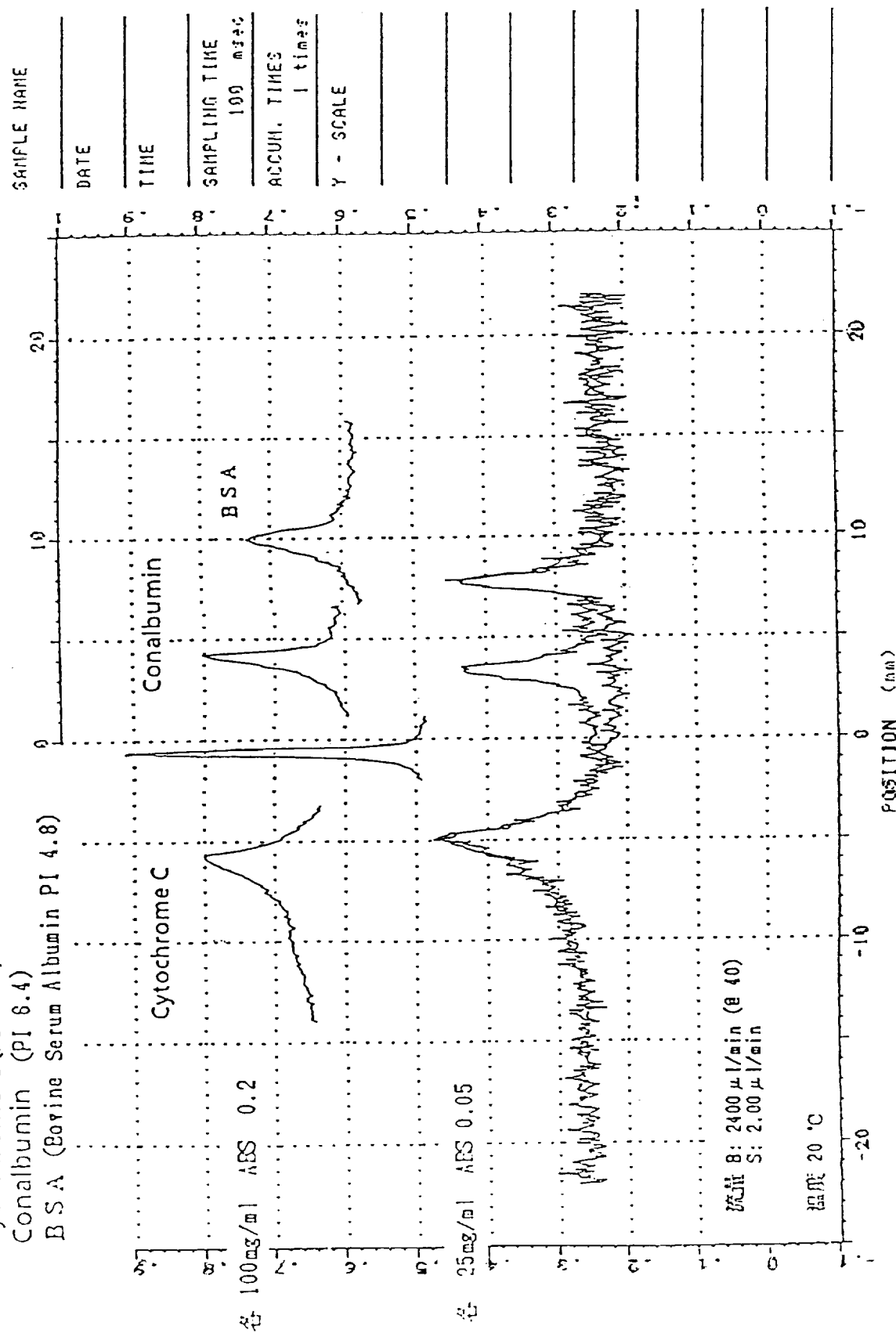


Figure 3. Electrophoresis separation of mixed proteins (BBM).

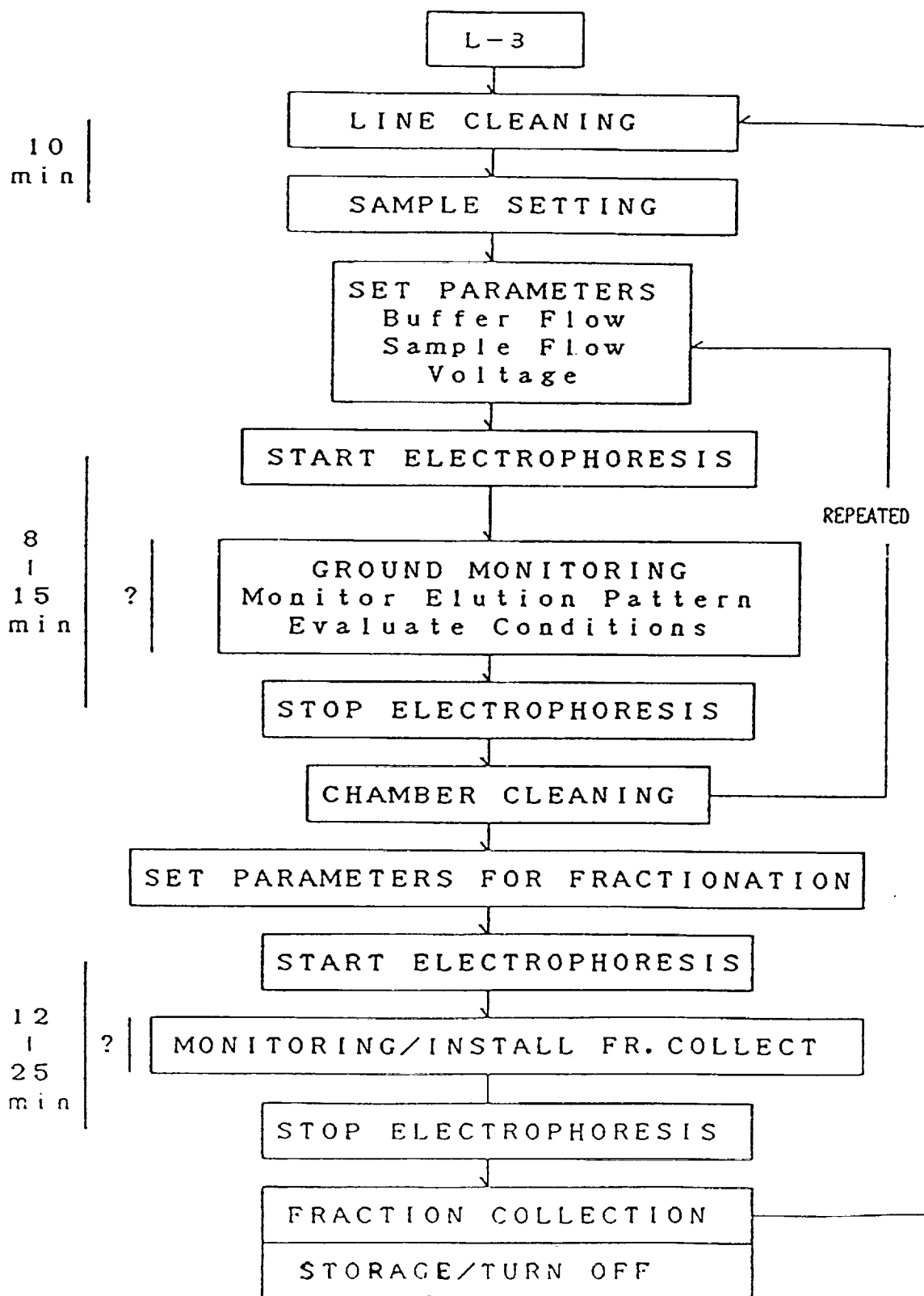


Figure 4. Electrophoresis experiment operations.

COMPARATIVE MEASUREMENT OF VISUAL STABILITY  
IN EARTH AND COSMIC SPACE  
L-4

Kazugo Koga  
Magoya University  
Japan

Purpose of the Research

The frequency and the intensity of space motion sickness has been reviewed and investigated (Treisman, 1977). Unusual induced-gravity situations, such as rotation, linear acceleration, parallel swinging (Guedry, 1966; Lackner, 1976; Melvill Jones, 1970), etc. have been investigated as well. Visually-induced motion sensation or distorted perception have been evaluated with respect to visual stability by many investigators (Rock, 1966; Grabiell, 1974; Howard, 1966, 1974, 1988; Snyder & Pronko, 1952; Dichgans & Brandt, 1973; Dolezal, 1982; Gibson, 1958, 1966, 1979). These studies are all concerned with the effect of gravity and the induction of motion sickness through human visual perception. Direct investigation under the microgravity situation, such as parabolic flight, Skylab, and Spacelab, have been carried out (von Baumgarten, 1986; Vogel, 1986; Young, 1986, Koga, 1988, 1989). These studies focused on how human visual stability is established through various sensory afferents in specific gravity conditions. Results from these investigations indicate that sensory mismatch probably plays an important role in space motion sickness.

The interaction of visual, vestibular, and somatosensory perception is smoothly coordinated under normal gravitational conditions on the Earth in our daily life. When the cooperation is destroyed or a mismatch occurs among them, motion sickness may develop not only on the

Earth but also in microgravity. The latter case may be the cause of space motion sickness or space adaptation syndrome.

How human beings obtain visual stability even with posture changes on the ground has been investigated. Visual stability can be categorized as static or dynamic. Static visual stability is concerned with orientation and dynamic stability is concerned with object motion perception. The perception of visual stability is modified by many other sensations, such as somatosensory, vestibular, and muscle tension. We will mainly focus on modifications by vestibular inputs to visual perception produced by eye movements in microgravity. The Vestibular-Ocular Reflex (VOR) is a well-known characteristic which results from the relationship between eye mobility and vestibular afferent inputs. Eye movements also modify dynamic visual perception, such as perceived object motion velocity. The VOR is constantly stimulated under 1-g conditions here on Earth. In fact, human beings have been habituated and "programmed" for orientation (visual stability) in their everyday, 1-g environment. When humans are exposed to a different gravity situation, this programmed behavior must change; that is, it is reprogrammed. This is called habituation or familiarization. We hope to examine how object motion perception is perturbed and subsequently adapted in the microgravity environment.

### Expected Results

This experiment is focused on the cooperation of visual, vestibular, and somatosensory perception coordination and how it is changed or reduced in space compared to 1-g environment. We will obtain information on the coordination between eye movement and neck muscle activity

by using EOG and EMG. We will also collect data from Payload Specialists using a self-diagnostic questionnaire concerned with perceptual abnormality. When each sensory input function and its integration in the higher nervous system are well-characterized, then more effective techniques to control SAS may be developed.



CRYSTAL GROWTH OF ENZYMES IN LOW GRAVITY  
L-5

Yuhei Morita  
Tsukuba R & D Center, Fuji Oil Co., Ltd.  
Japan

Recent developments in protein engineering have expanded the possibilities of studies of enzymes and other proteins. Now such studies are not limited to the elucidation of the relationship between the structure and function of the protein. They also aim at the production of proteins with new and practical functions, based on results obtained during investigation of structure and function. For continuing research in this field, investigation of the tertiary structure of proteins is important. X-ray diffraction of single crystals of protein is usually used for this purpose. The main difficulty is the preparation of the crystals. The theme of the present research is to prepare such crystals at very low gravity, with the main purpose being to obtain large single crystals of proteins suitable for x-ray diffraction studies.

Single crystals of protein are prepared in a low-gravity field in space by use of the conditions found suitable on Earth for the growth of single crystals of protein and the crystals grown in space must be compared with those grown on Earth. Furthermore, x-ray crystallographic analysis of single crystals of protein grown at low gravity should be done at high resolution. The influence of low-gravity fields on the protein structure can be studied by comparison with the already published structures of crystals grown at one gravity.

Large single crystals of proteins of 5 mm in each dimension that would be difficult to grow on Earth might be prepared and used in physical measurements such as neutron diffraction, as well as in x-ray diffraction analysis.

The results of these experiments should make a practical contribution to the invention of new protein foodstuffs and to the development of medical supplies. Also, studies will help to clarify protein structures, especially the surface structure of the protein molecule, which cannot yet be completely elucidated.

The airtight cell for enzyme crystallization shown in Figure 1 was designed and produced for use in the Spacelab experiment and is adapted for operation at very low gravity. It is composed of the middle part on which metal fittings are fixed for photography, a knob, and two pairs of cylinders, and pistons located on both ends of the cell.

For the preparation of single crystals of protein, several principles have been proposed, and investigators have been conducting trials of the principles by using a variety of procedures. In the present experiment, we decided to use the batch method in which a supersaturated solution is left undisturbed, taking into account that single crystals must be grown at 20 °C during the 7-day flight of the shuttle. Outline and merits of the present method are as follows: The crystallization solution contains a salt such as sodium chloride or ammonium sulfate, and it produces a supersaturated solution when mixed with the protein solution (Figure 2). The concentration and pH of the buffer used, the concentration of the protein solution, and the concentration of salt of the crystallization solution are selected to give a mixture suitable for crystal formation. The two solutions are mixed and then allowed to stand. This method is suitable for crystallization within a short time because the conditions necessary for crystallization are fulfilled soon after the solutions are mixed. Irrespective of the large volume of the solution, the procedures are simple and time-saving.



We selected three functional proteins and three kinds of enzymes as samples for this experiment. The functions of these proteins are as follows:

1. Lysozyme from hen egg white. Lysozyme is an enzyme that catalyzes the hydrolysis of  $\beta$ -(1-4) glycoside linkages between N-acetylmuramic acid and N-acetylglucosamine (Figure 3). These are basic components of bacterial cell walls. This enzyme also hydrolyzes chitin, a biopolymer of N-acetylglucosamine.

2. Myoglobin from horse skeletal muscle. Myoglobin is a functional protein found in skeletal muscle cells (Figure 3). It is particularly abundant in diving mammals such as whales, seals, and walruses. It serves not only to store oxygen but also to enhance the rate of diffusion of oxygen through the cell.

3.  $\omega$ -amino acid: pyruvate aminotransferase from *Pseudomonas* sp. F-126.  $\omega$ -amino acid transferase is an enzyme that is involved in the reversible transfer of amino group from  $\omega$ -amino acids to amino acceptors with the aid of pyridoxal 5'-phosphate as a coenzyme (Figure 3c). For this enzyme, pyruvate is the only amino acceptor, and  $\beta$ -alanine is used as the best amino donor among the various  $\omega$ -amino acids.

4. Glucoamylase from *Rhizopus delemar*. Glucoamylase is an exo-splitting enzyme that consecutively removes the glucose unit from the non-reducing of starch and related malto-oligosaccharides. This enzyme is found in various microorganisms, and it occurs almost exclusively in fungi, but far less in bacteria and yeasts. Fungal glucoamylase is very useful for industrial production of glucose or oligo-saccharides.

5. Ovotransferrin from hen egg white. Transferrins are a family of iron-binding glycoproteins found in serum, secretory fluids, milk, and egg white. They are dimeric proteins and each monomer can reversibly bind to two atoms of iron. The high affinity for iron of ovotransferrin can retard microbial growth by making the iron relatively unavailable.

6. Insulin from humans. Insulin is a polypeptide hormone secreted by the B cells of the islets of Langerhans. It affects the entire intermediary metabolism, especially of the liver adipose tissue and muscle. Insulin is the only hormone that decreases the blood glucose concentration, and is concerned with the regulation of the rate of carbohydrate metabolism.

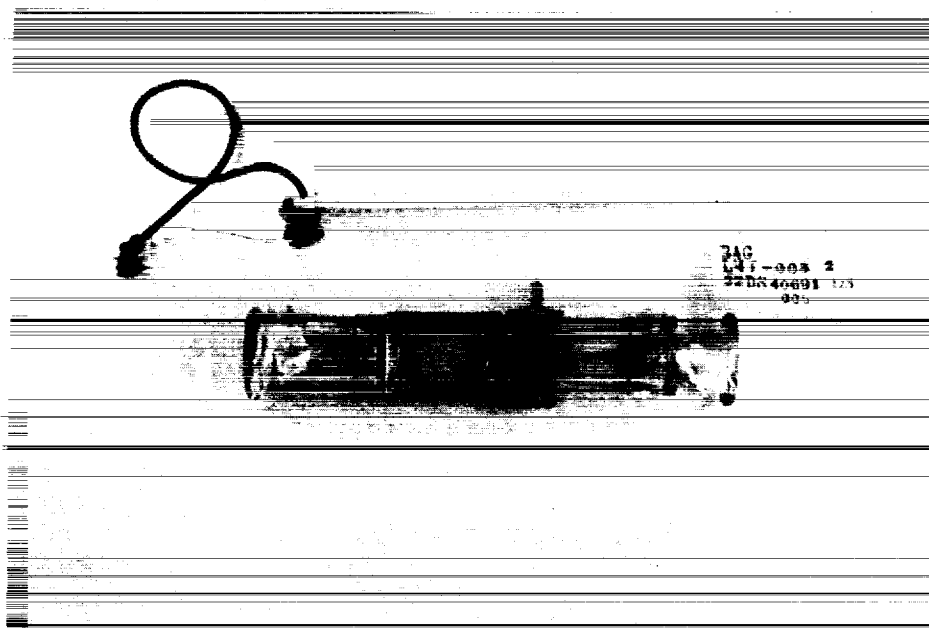


Figure 1. Enzyme crystallization cell.

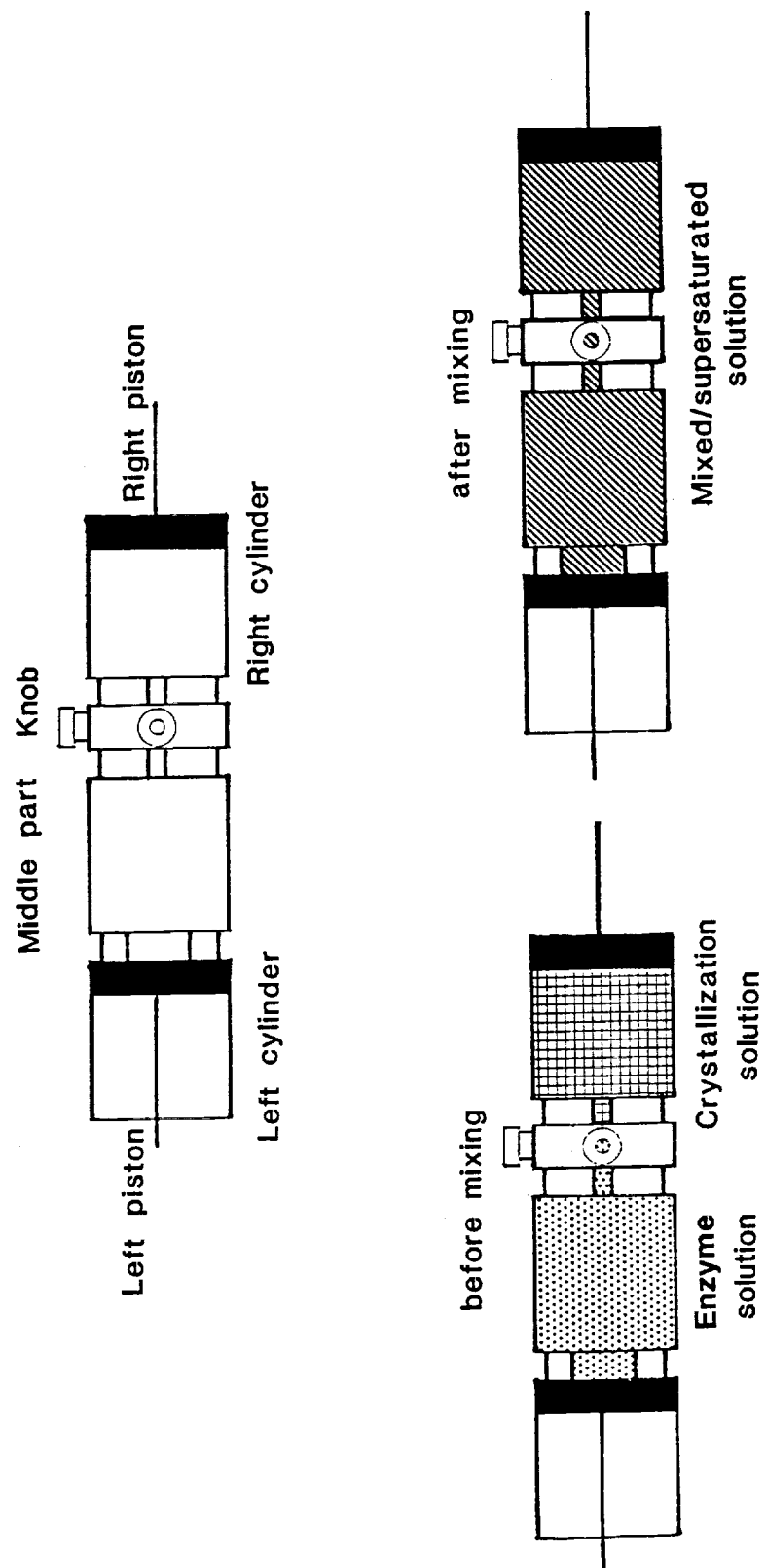
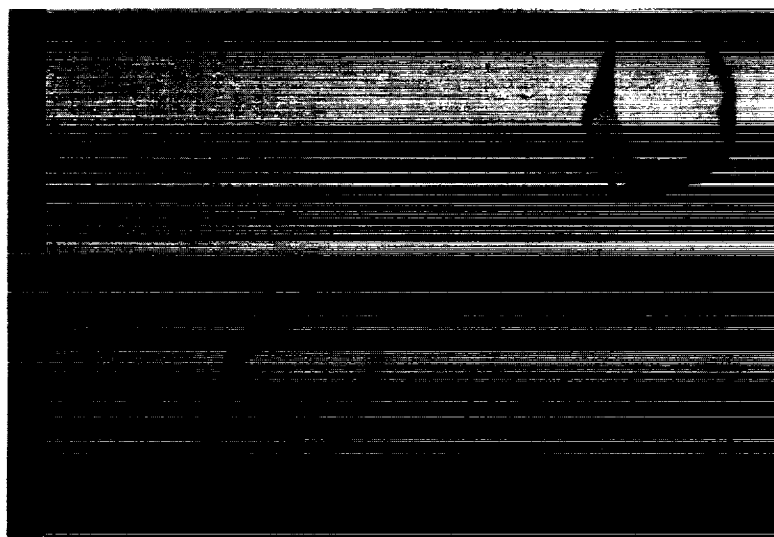
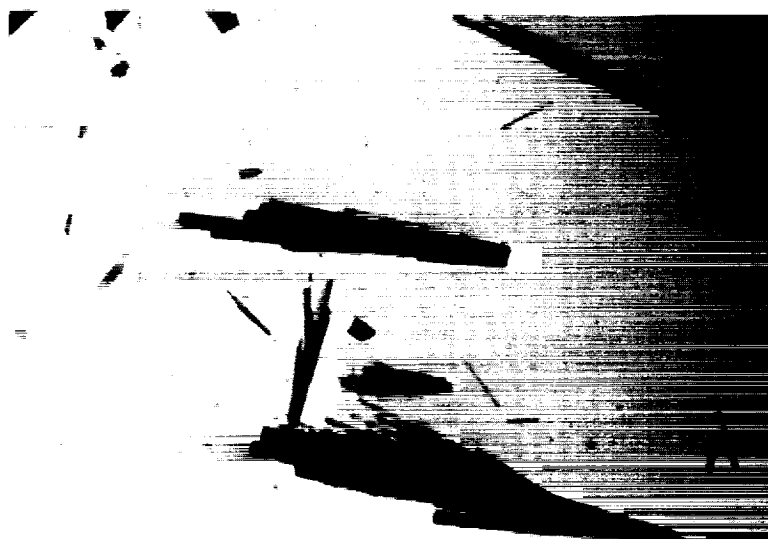


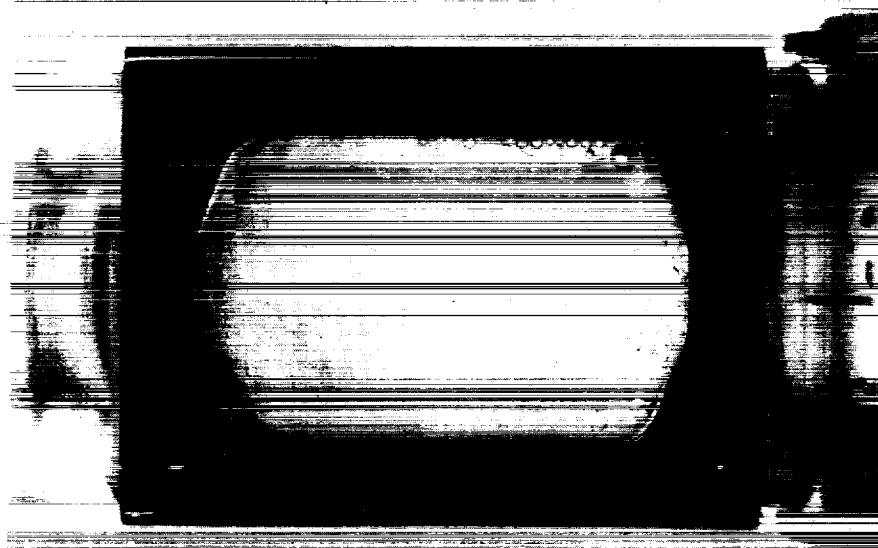
Figure 2. Operations of enzyme crystallization cell.



(a)



(b)



(c)

**Figure 3. Single crystals of: (a) hen egg lysozyme, (b) horse skeletal muscle myoglobin, and (c) *Pseudomonas*  $\omega$ -amino acid: Pyruvate Aminotransferase.**

STUDIES ON THE EFFECTS OF MICROGRAVITY ON THE ULTRASTRUCTURE AND  
FUNCTIONS OF CULTURED MAMMALIAN CELLS  
L-6

Atsushige Sato  
Tokyo Medical and Dental University  
Japan

The human body consists of  $10^{13}$  cells. Understanding the mechanisms by which the cells sense and respond to microgravity is very important as the basis for space biology. The cells were originally isolated aseptically from mammalian bodies and cultured in vitro. A set of cell culture vessels has been developed to be applied to three kinds of space flight experiments.

Experiment I is to practice the cell culture technique in a space laboratory and obtain favorable growth of the cells. Aseptic handling in trypsin treatment and medium renewal will be tested. The cells, following space flight, will be returned to the ground and cultured continuously to investigate the effects of space flight on the cellular characteristics.

Experiment II is to examine the cytoskeletal structure of the cells under microgravity conditions. The cytoskeletal structure plays essential roles in the morphological construction, movements, axonal transport, and differentiation of the cells. The cells fixed during space flight will be returned and the cytoskeleton and ultrastructure observed using electron microscopy and fluorescence microscopy.

Experiment III is to study the cellular productivity of valuable substances. The waste medium harvested during space flight are returned and quantitated for the cellular products. The effects of microgravity on mammalian cells will be clarified from various aspects.

### Expected Results

Cell culture is a basic method used in biology, medicine, pharmaceuticals, agriculture, and biotechnology. The establishment of the cell culture technique in a space laboratory is expected to be applicable in various fields of science. It will be of particular use to help clarify some of the basic phenomena concerning living things in space, which is difficult to elucidate using entire animals or plants. For example, it will be determined in a simplified experimental system whether the bone metabolic alterations occurring in astronauts reflect the direct action of microgravity on bones. In addition, some of the cultured cells produce valuable autacoids and physiologically important bioactive substances which can be utilized pharmaceutically. It is possible that highly purified substances can be produced using the continuous free-flow electrophoresis device in a space laboratory. This experiment will hopefully give definitive results concerning the effectiveness of separations conducted in the microgravity environment.

GRAVITY, CHROMOSOMES, AND ORGANIZED DEVELOPMENT  
IN ASEPTICALLY CULTURED PLANT CELLS

Abraham D. Krikorian  
State University of New York at Stony Brook, New York  
USA

Background and Hypothesis

Plant development entails an orderly progression of cellular events both in terms of time and geometry (dimensional space). Work done by us on Soviet Kosmos 782 and 1129 biosatellites using totipotent carrot cells which could undergo somatic embryo formation showed that while the broad events of asexual embryogenesis could and did occur, the transition from one stage to another was slowed down significantly. The cell system used for the Kosmos experiments involved the generation of so-called embryogenic cells, their induction on Earth to produce proembryos, and their subsequent exposure to space conditions so as to evaluate their capability of expressing their capacity to form later stage somatic embryos. The normalcy of the developmental pathway of cells to proembryos to later stages of embryogeny could thus be scored. Similarly, the broad temporal aspects could be traced. The experimental design was, however, not optimal insofar as the temporal aspects were concerned (there was no onboard fixation), neither was a 1-g centrifuge available on the 1129 flight. Moreover, no attempt was made to carry out karyological observations, chromosomal and detailed cell biological and biochemical analysis.

Since then, a much-improved in vitro system for carrot somatic embryogenesis has been developed by us. The advantages of the new system include: (1) simulation of zygotic

embryogenesis with high fidelity; we now have the ability to expose cells to the space environment that show no obvious polarity and to "turn on" the "embryogenic switch" in space by means of the very simple procedure of a change in medium; (2) not requiring external growth regulators to be manipulated at any stage of the entire process of obtaining or modulating embryogenic cells; (3) being 100% responsive; i.e., all preproglobular somatic embryos go on to yield proembryos and later stage embryos; (4) no selection or mechanical cell sorting is required to prepare test specimens; i.e., they are selected very early in the culture process; (5) being readily amendable to automation; (6) having potential for selection of adaptive cells (mutants?); (7) controllably providing an open-ended system; i.e., the system can be made to cycle so that new test specimens do not have to be prepared de novo for successive experiments. Not only will answers gotten from such a system be of interest to developmental plant biologists but they will have significance for those seeking to use biotechnological procedures and manipulations in space for a variety of reasons. Indeed, the ability to use and manipulate plant cells and other kinds of propagules in vitro reliably in space will be a necessary prerequisite to many projected or hypothesized commercialization schemes.

### Objectives

The more specific objectives of the PCR experiment are:

- To test the hypothesis that microgravity will in fact affect the pattern and developmental progression of embryogenically competent plant cells from one well-defined, critical stage to another.



- To determine the effects of microgravity in growth and differentiation of embryogenic carrot cells grown in cell culture.

- To determine whether microgravity or the space environment fosters an instability of the differentiated state.

- To determine whether mitosis and chromosome behavior are adversely affected by microgravity.

### Methods

The methods employed will consist of the following:

- Special embryogenically competent carrot cell cultures will be grown in cell culture chambers provided by NASDA.

- Four cell culture chambers will be used to grow cells in liquid medium.

- Two dishes (plant cell culture dishes) will be used to grow cells on a semi-solid agar support.

- Progression to later embryogenic stages will be induced in space via crew intervention and by media manipulation in the case of liquid grown cell cultures.

- Progression to later stages in case of semi-solid cultures will not need crew intervention.

- Embryo stages will be fixed at a specific interval (day 6) in flight only in the case of liquid-grown cultures.

- Some living cells and somatic embryos will be returned for continued post-flight development and "grow-out." These will derive from the semi-solid grown cultures.

### Post-Flight Analysis

Post-flight analysis will concentrate on the following general features:

- General cellular morphology
- Scoring of embryogenesis according to stage
- Light microscopy at the level of embryogenic cells
- Electron microscopy (SEM, scanning electron microscopy)
- Chromosome analysis and karyotype determination by examining directly fixed materials
- Evaluation of non-fixed materials by post-flight behavior in vitro for continued growth and adaptation post-flight.

The above should unequivocally establish whether there are developmental phase-related disturbances in a critical event stage of embryogenesis, i.e., from the preproglobular to the globular stage proembryo. Also, it should go far to establish whether the fidelity and frequency of embryonic progression both morphologically and cytologically (chromosomally) are adversely affected or enhanced.

EFFECT OF LOW GRAVITY ON CALCIUM METABOLISM  
AND BONE FORMATION  
L-7

Tatsuo Suda  
Showa University, Tokyo  
Japan

Outline and Expectation of the Experiment

Recently, attention has been focused on the disorders of bone and calcium metabolism during space flight. The skeletal system has evolved on the Earth under 1-g. Space flights under low gravity appear to cause substantial changes in bone and calcium homeostasis of the animals adapted to 1-g. We have proposed a space experiment for FMPT to examine the effects of low gravity on calcium metabolism and bone formation using chick embryos loaded in a space shuttle. We proposed this space experiment based on the following two experimental findings. First, it has been reported that bone density decreases significantly during prolonged space flight. The data obtained from the US Skylab and the U.S.S.R. Salyut-6 cosmonauts have also documented that the degree of bone loss is related to the duration of space flight. Second, the US-Soviet joint space experiment has demonstrated that the decrease in bone density under low gravity appears to be due to the decrease in bone formation rather than the increase in bone resorption (Science 201: 1138, 1978). The purpose of our space experiment is, therefore, to investigate further the mechanisms of bone growth under low gravity using fertilized chick embryos.

In our space experiment, 30 fertilized chicken eggs are preincubated for 7 to 11 days on Earth (Table 1). The preincubated eggs are further incubated for an additional 7 days during

space flight. Thus, 7-, 9-, and 11-day-old chick embryos will be 14, 16, and 18 days old, respectively, when the space shuttle returns to Kennedy Space Center (KSC) in Florida. In each group, half of the eggs (5 eggs each) are subjected to the following experiments immediately after the space shuttle returns to KSC. The rest of the eggs are further incubated until hatching at KSC. Another batch of 30 fertilized eggs is incubated at KSC as the controls under 1 g. After the eggs are recovered from the space shuttle at KSC, cartilage growth, bone formation and resorption, differentiation of chondroblasts, osteoblasts and osteoclasts, biosynthesis of actin and myosin, muscle fiber formation, collagen biosynthesis, and calcium and vitamin D metabolism are compared morphologically as well as biochemically between the chick embryos recovered from the shuttle and the control embryos incubated on the Earth. It is expected that a counterplan for preventing bone loss due to prolonged space flight (for example, space station experiments) and immobilization (for example, disuse atrophy and bedridden, older people) may be obtained from this space experiment.

**Table 1. Flight Protocol of 30 Fertilized Chicken Eggs in our Space Experiment (L7)**

Stages of the Fertilized Chicken Eggs Loaded			
Taking off		Landing	Number of eggs
7 days old	7 days flight ----->	14 days old	10*
9 days old	7 days flight ----->	16 days old	10*
11 days old	7 days flight ----->	18 days old	10*

\*In each group, 5 of 10 eggs are further incubated on Earth until hatching after they are recovered at KSC.

# **SEPARATION OF THE ANIMAL CELLULAR ORGANELLA BY MEANS OF FREE-FLOW ELECTROPHORESIS**

**L-8**

**Tokio Yamaguchi  
Tokyo Medical and Dental University  
Tokyo, Japan**

## **Purpose of Experiment**

**To demonstrate the effectiveness of a weightless environment to separate cells and cellular organelle by FFE.**

## **Experiment Status**

- 1. Sample is a mixture of microbial cells of lipopolysaccharide defective mutants derived from a gram-negative bacterium.**
- 2. The bacterial cells show different mobilities in electrolyte.**
- 3. The bacterial cells are stable and viable in electrolyte for mission period.**
- 4. The bacterial cells are quite sensitive to antibiotics and disinfectants (alcohols, detergents, etc.).**

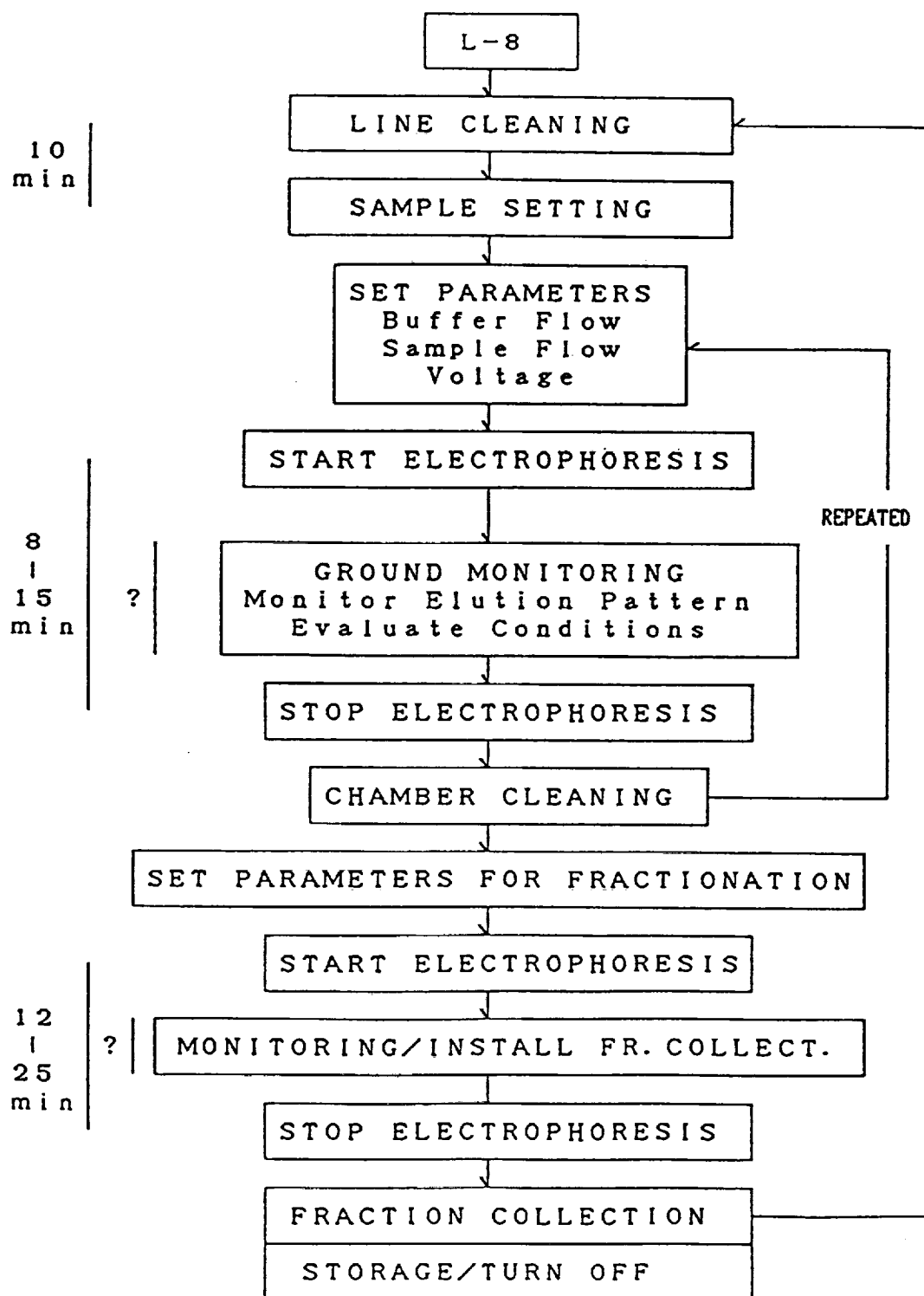


Figure 1. Experiment and operations.

GENETIC EFFECTS OF HZE AND COSMIC RADIATION  
L-9

Mituo Ikenaga  
Radiation Biology Center, Kyoto University  
Japan

Background and Outline of the Experiment

Space radiation like cosmic rays originates both from distant sources in the universe and from the Sun. A fraction of such cosmic rays reaches the surface of the Earth. Fortunately, all the organisms on the Earth are well protected from cosmic rays by the thick layer of atmosphere, as well as by the Earth's magnetic field deflects low-energy cosmic particles falling on the Earth. But, if we go into space these protectors against cosmic rays are no longer available, and the dose (amount) of space radiation will increase several hundred-fold over what we routinely encounter on Earth. Nevertheless, the radiation dose in space is still too small to cause any serious effects on astronauts, so the risk of space radiation has been neglected so far.

Our knowledge obtained with experimental animals has indicated that low or medium doses of radiation cause two major delayed effects of radiation, namely, induction of cancers among exposed animals and induction of mutations among descendants of exposed animals. Genetic properties of each individual, such as ABO blood type and hair color in humans, are determined by each specific gene located on the chromosomes in the cell nucleus. These properties usually do not change at all and are transmitted through many generations from parents to children and also from a parent cell to daughter cells within the same body. However, on very rare occasions, radiation or toxic chemicals produce an alteration of a gene, resulting in the

acquisition of a new property among descendant individuals or cells, the property different from their parents. Such a change in genetic property is called "mutation." In fact, in 1927, Dr. H. J. Mueller of the University of Texas first discovered that x-ray irradiation can induce mutations in Drosophila, a small fruit fly widely used for study of genetics. For this outstanding discovery, he was awarded the Nobel Prize in 1946. It is also known that human cancers arise from mutations that occur in "proto-oncogenes" in cells constituting a human body. Of course, such cancerous mutations which occur in a cell of a certain organ, like the lung, liver and stomach of a particular person will not be transmitted to a child. This type of "non-heritable mutation across generations" is called "somatic mutation," and it appears as a change observable with a portion of cells in a body.

As mentioned above, the effects of space radiation on astronauts, such as high-charge and high-energy particles (HZE) and other cosmic radiation, are believed to be very small, at least during the short-term flight by the space shuttle. However, in theory, even those small doses of radiation will certainly elevate the frequency of mutations, including specific somatic mutations leading to cancer induction. Although the possible increase in cancer incidence due to space flight may be practically negligible, we should have the knowledge of "theoretical mutation risk" caused by space radiation.

The purpose of our experiment is to detect mutations in Drosophila possibly induced by space radiation during the SL-J mission, so that we will be able to obtain basic information about "the genetic (mutational) risk of space radiation" which can be used to estimate human risk of cancer induction by space flight. As an example of somatic mutation, we will analyze mor-



phological changes in hair growing on the surface of the wing of an adult fly. A piece of wing consists of about 30 thousand wing cells and in the wild type Drosophila a long single piece of hair is growing on the surface of each wing cell. When Drosophila is exposed to radiation at its early stage of development, such as embryonic stage or larval (maggot) stage, some mutations will appear in the wing hair of the adult fly with a certain low frequency, depending on the radiation dose. Among the mutations, the most frequent one is a change in the number of hairs per cell, that is, usually three or more hairs are coming out from a single wing cell.

In the actual SL-J flight, we will install thousands of Drosophila larvae (maggots) into the Space Shuttle Discovery and expose them to space radiation during the 7-day mission. Immediately after the re-entry to the ground, these larvae are expected to develop (emerge) into adult flies. Then the wings will be fixed by ethylalcohol and permanent samples will be prepared. Finally, we will analyze the wing samples microscopically in order to detect mutations.

#### Future Prospect Derived from Experimental Results

As mentioned in the previous section, the total radiation dose during the SL-J mission may be very small, probably the same order of dose which we usually receive after a single exposure to medical x-rays for health screening, such as chest x-rays. Therefore, we do not have to worry about any effect on crew members of such low dose of radiation during the space shuttle flight.

However, during the late 1990's Space Station Freedom will usher in a new era of space programs. The Space Station Freedom is planned to make an orbital flight with an altitude of

460 km, a much higher altitude than the space shuttle program. In addition, it is projected that the crew members of the Station may be replaced every 6 months. With these flight conditions, the approximate possible radiation dose accumulated for 6 months may be in the range of 10 to 20 rem (0.1 to 0.2 Sv). This value seems to be quite large. It is true that there are still considerable debates as to whether or not such a dose range of radiation (10 to 20 rem) would cause appreciable health effects in humans. Yet it is also clear that necessary precautions must be taken to minimize radiation dose inside the spacecraft in order to protect crew members (or general public who will expand into space in the distant future) from unnecessary exposure to radiation.

The results of this experiment may provide basic, important information which will enable us to calculate "the necessary radiation shielding of the spacecraft to ensure crew safety."

MANUAL CONTROL IN SPACE  
RESEARCH ON PERCEPTUAL-MOTOR FUNCTIONS  
UNDER ZERO GRAVITY CONDITIONS  
L-10

Akira Tada  
National Aerospace Laboratory  
Japan

Are human abilities to control vehicles and other machines the same in space as those on Earth? The L-10 Manual Control Experiment of FMPT started from this question.

Suppose a pilot has the task to align the head of a space vehicle toward a target. His actions are to look at the target, to determine the vehicle movement, and to operate the manipulator. If the activity of the nervous system were the same as on Earth, the movements of the eye and hand would become excessive because the muscles do not have to oppose gravity. The timing and amount of movement must be arranged for appropriate actions. The sensation of motion would also be affected by the loss of gravity because the mechanism of the otolith, the major acceleration sensor, depends on gravity. The possible instability of the sensation of direction may cause mistakes in the direction of control of manipulator movement. Thus, the experimental data can be used for designing man-machine systems in space, as well as for investigation of physiological mechanisms.

In this experiment, the direction of vehicle heading is expressed by a light spot of an array of light emitting diodes and the manipulator is of a finger stick type. As the light spot moves up and down, the Japanese Payload Specialist, as the subject, must move the manipulator forward

and backward to keep the movement of the light spot within the neighborhood of the central point of the display. The position of the light spot is computed in such a manner that when the stick is kept at the neutral position, the light spot moves randomly, and that when the manipulator is deflected from the neutral position, a motion whose acceleration is proportional to the angle of deflection is added to the movement of the light spot.

The Operator Describing Function, which is an expression of human control characteristics, can be calculated from 2 minutes of raw data of the light spot position and stick deflection. The 2 minutes of operation is called a run, and 8 runs with resting periods composes a session.

The on-orbit experiment will be conducted on the second, fourth, and seventh days. One session of experiment on each of these days is conducted following the L-4 experiment, which uses the same apparatus. The Payload Specialist, aided by a Mission Specialist, will take our apparatus from a rack container, set up the apparatus, attach electrodes for measurements of eye movement and muscle activity, conduct the L-4 Visual Stability Experiment, conduct one session of the manual control experiment, and then disassemble and stow the apparatus.

In addition to the flight experiment, pre-flight and post-flight experiments will be conducted. The data of three sessions on orbit will reflect adaptation of physiological systems to microgravity. The data of post-flight experiments, on the other hand, will reflect re-adaptation of physiological systems to the gravity condition on the ground. Control data collected with and without psychological tension will be scheduled just prior to and long before launch.

### Expected Results

Automation such as automatic control systems for vehicles, robots for industrial manufacturing, etc., is rapidly developing. The more automation develops, however, the more understanding of human abilities becomes necessary. In space activities, automation is being performed when feasible, however, it has also been realized that system performance, safety, and efficiency is largely enhanced by use of human activity at appropriate system interfaces.

The investigation of manual control in space is expected to lead to development of man-machine systems with higher performances and safety and with lower costs. If phenomena such as frequent mistakes in direction and/or close correlation between the Operator Describing Function and adaptation of physiological systems to the space environment is found, it would be an important cue to understanding the mechanism of such adaptation.



STUDY ON THE BIOLOGICAL EFFECT OF COSMIC RADIATION  
AND THE DEVELOPMENT OF RADIATION PROTECTION TECHNOLOGY  
L-11

Shunji Nagaoka  
National Space Development Agency of Japan  
Japan

Background

As the era of Space Station Freedom and solar system travel approaches, it becomes increasingly important to develop radiation protection for the people who will live and work in space for long durations. The space environment surrounding the Earth is known as the geosphere where the magnetic field of the Earth traps the so-called solar wind which results in a giant torus of radiation field of highly energized electrons and protons such as the Van Allen Belt. In addition, high-energy ionized particles are coming from the Sun and the cosmic galaxy. The latter is usually of extremely high energy which can easily penetrate a protected spacecraft.

Most of the human activities inside and outside the spacecraft occur in such a radiation field where the radiation environment, on the average, is remarkably high compared to that on the ground; because the Earth's atmosphere, a dense blanket of air, effectively protects us from most of the radiation, particularly against the high-energy radiation at levels lethal to most living species.

From the accumulated data in past space flights, we know the average radiation dose at the lower Earth orbit (300 - 500 km); for example, in the case of Skylab in 1973, the total dose for the astronauts during 84 days was measured by a conventional method to be approximately

7.7 rem which corresponds to 90 mrem/day. Similar results have been obtained from several recent missions of Spacelab. One can estimate from such data, based upon the altitude and inclinations, that the total dose for astronauts during the longest Mir Mission (366 days) was approximately 80 rem at skin level and 30 rem at bone marrow. The level is almost at the allowable limit (50 rem/year) for astronauts recommended by NCRP. It is well known that exposure to ionized radiation over a certain level can become suddenly toxic to living systems. Since the majority of studies on radiation effects and risks have been based on x-ray, gamma ray, or neutron studies on the ground, the question then arises, "Can the effects of such space radiation on biological systems be extrapolated from the results studied on the ground?" Recent developments, based on the ground-based-studies, as well as space experiments, have suggested that the Relative Biological Effectiveness (RBE) of the heavy ions may be much higher than that of gamma-rays ( $>20$ ). Then, beyond the Earth's atmosphere, what and how can we protect life from such damaging radiation? Radiation research at NASDA has been undertaken to give answers to the questions above. The detailed analysis on the biological effects and data accumulated from those analysis must be used for precise risk estimations and for the development of the radiation protection technology necessary for the human occupation of the space radiation environment.



## Flight Experiments

### Equipment and Specimens

NASDA is now participating in a series of flight experiments on Spacelab missions. The first experiment was carried out on the first International Microgravity Laboratory Mission (IML-1) January 1992, and the second experiment will be conducted on the Spacelab-J Mission (FMPT). The equipment or Radiation Monitoring Container Devices (RMCD) (Figure 1) includes passive dosimeter systems shown in Table 1 and biological specimens. The experiments using this hardware are designed by NASDA to measure and investigate the radiation levels inside spacecraft like space shuttle and to look at the basic effects of the space environment from the aspect of radiation biology. The data gathered will be analyzed to understand the details of biological effects as well as the physical nature of space radiation registered in the sensitive Solid-State Track Detectors (SSTD).

Table 1. Flight Equipment List

Radiation Monitoring Container*		2 sets
Solid State Track Detectors TS-16, CR-39		50 sheets/cont.
Physical Dimensions	12.5 x 12.5 x 10.4 cm	
Sample Holders	3 types/cont.	
Dosimeter Package**		14 sets
TLD (LiF, MgSiO:Tb, LiF:Hg:Cu:P)		24/cont.
Physical Dimensions	12.1 x 12.1 x 0.9 cm	

\*Set in aft-end cone of Spacelab

\*\*Set in incubator, stowage container, refrigerator, etc.

In this experiment, layers of the radiation detectors and biological specimens, bacterial spores (*Bacillus subtilis*), shrimp eggs (*Artemia salina*), and maize seeds (*Zea mays*) (Table 2) are sandwiched between the track detectors in the Radiation Monitoring Container. The detectors, sheets of plastic material called TS-16 and CR-39, register the nuclear track of cosmic radiation. The dosimeter package contains conventional detectors made of lithium fluoride or magnesium-silica-terbium. These are thermoluminescent materials (TLD) which, when heated moderately after radiation exposure, emit luminescent photons linearly depending upon the dose of radiation. The experiment consisting of the box-like container is mounted on the aft end cone of the Spacelab, where there is somewhat less radiation than at other locations.

Table 2. Biological Samples

Maize seeds ( <i>Zea mays</i> ) (Y <sub>g2</sub> x yg <sub>2</sub> )	100-120/holder	4 Sets
Brine shrimp eggs ( <i>Artemia salina</i> )	2000-3000/holder	6 Sets
Bacterial spores ( <i>Bacillus subtilis</i> 168)	10 <sup>4</sup> -10 <sup>5</sup> /holder	6 Sets

### Outline of Experiment Operations

The experiment operations including the pre- and post-specimen preparation are summarized below. The in-flight procedure is very simple, major activities are stowage and unstowage operations. The results are analyzed at Japanese laboratories after the specimens retrieval.

#### (1) Sample Preparation (Japan)

L-3 weeks: Prepared and fixed on sample holders

L-2 weeks: Shipped to KSC (while being protected from radiation) including biological samples/track detectors TLD with dosimeters.

**(2) Hanger-L Operation (KSC)**

**L-1 weeks: Packed into radiation monitoring containers and kept in refrigerator  
until late access**

**L-13 hrs.: Late access to STS middeck**

**(3) Onboard Operation**

- a. Transfer the containers/dosimeters to SL after the activation.**
- b. Assemble containers/dosimeters/temp. sensor and set at aft end cone.**
- c. Set dosimeter near fly container, incubators, refrigerator and fungi growth chamber, and middeck locker.**
- d. All devices remain in position until SL deactivation.**
- e. The container/dosimeters are removed and restored.**

**(4) Post-Flight Operations (landing site and KSC)**

- a. Early removal from STS middeck and transfer to KSC.**
- b. Store at Hanger-L refrigerator until shipment.**

## Post-Flight Analysis

Each plastic detector in the device can register individual nuclear tracks in three dimensions, and the TLD accumulates integrated radiation energy. The biological specimens in the device are exposed to cosmic radiation for 7 to 8 days during the mission. All specimens and radiation detectors are analyzed after the mission to correlate the radiation characteristics and biological effects. The plastic detectors are etched chemically to visualize the radiation tracks, called "etch-pits." The geometric properties of the etch-pits can reveal the physical characteristics of the radiation, such as incident angle, energy, and nucleon type. Three-dimensional trajectories are analyzed by a computerized microscopic image handler with a three-dimensional stage controller, and reconstructed through the piled detector sheets in relation to the positions of the biological specimens. The specimens will be evaluated by biological and biochemical methods using their intrinsic natures for radiation effects during the processes of development, sporulation, hatching, and germination. Primary genetic studies will also be conducted at the cellular, organ, and individual levels.

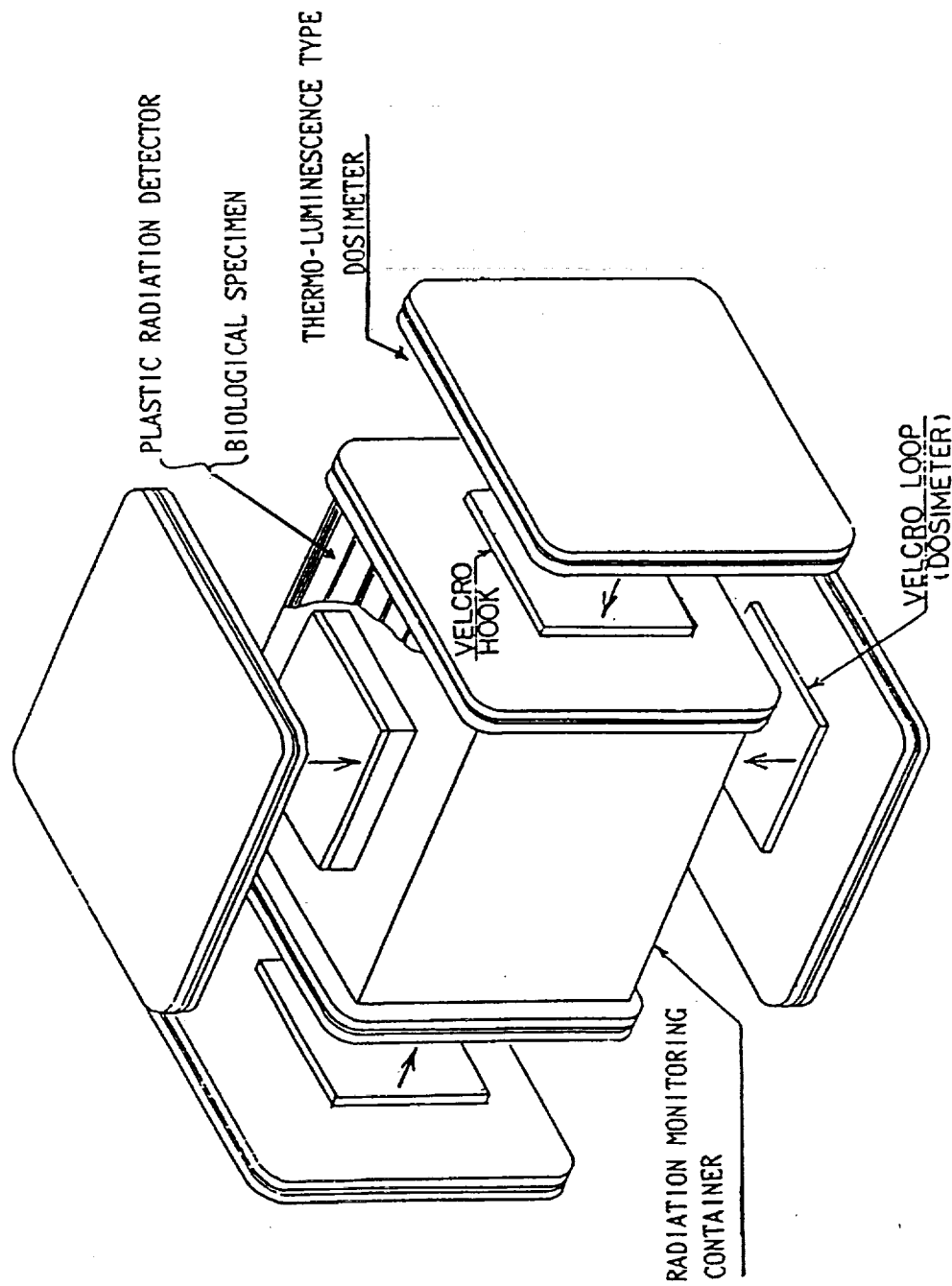


Figure 1. Monitoring container - dosimeter.

A CIRCADIAN RHYTHM OF CONIDIATION IN NEUROSPORA CRASSA  
L-12

Prof. Yashuhiro Miyoshi  
University of Shizuoka  
Japan

Outline of Experiment

Two fungi growth chambers containing six growth tubes each are used in this experiment. One chamber is for the space experiment; the other is for the simultaneous ground control experiment. The hyphae of Neurospora crassa band A mutant are inoculated at one end of each tube. Both the chambers are kept at  $3^{\circ}\text{C} \pm 1.5^{\circ}\text{C}$  to stop hyphae growth until the Spacelab is activated. After the activation, each chamber is transferred simultaneously to the Spacelab and a phytotron in KSC and kept in continuous light at the same temperature. After about 24 hours of light exposure, each chamber is inserted into a growth chamber bag to keep it in constant darkness. The circadian rhythm of conidiation is initiated by this light to dark transition. After the dark incubation for 5 days at room temperature, both the growth chambers are kept at  $3^{\circ}\text{C} \pm 1.5^{\circ}\text{C}$  to stop growth of the hyphae. After the space shuttle lands, both conidiation patterns are compared and analyzed.

Purpose of Experiment

It has been known that numerous physiological phenomena show circadian rhythms. They are characterized by the fact that the oscillation can persist under constant conditions of light and temperature. Therefore, it has been accepted by most investigators that the generation

mechanism of the circadian rhythm is endogenous. However, one cannot reject the possibility that these rhythms are caused by some geophysical exogeneous factor having a 24-hour period, such as atmospheric pressure, gravity, or electromagnetic radiation.

In this study, we use Neurospora crassa band A mutant which shows an obvious circadian rhythm in its spore-forming (conidiation) on the ground, and we intend to attempt the conidiation of this mutant in the Spacelab where 24-hour periodicity is severely attenuated and to elucidate the effect of the geophysical exogeneous factor in the generation mechanism of the circadian rhythm.



D A Y	T I M E	DESCRIPTION OF CREW OPERATION
0	4	Transfer Fungi growth chamber to SL and attach to SSC#1 door. set up Temp. sensor.
	8	
	12	
	16	
	20	
1	4	Report time on voice.
	8	
	12	
	16	
	20	
2	4	Take close up photo, cover Fungi growth chamber with growth chamber bag.
	8	
	12	
	16	
	20	
3	4	Report time on voice.
	8	
	12	
	16	
	20	
4	4	Uncover and take close up photo.
	8	
	12	
	16	
	20	
5	4	Report time on voice
	8	
	12	
	16	
	20	
6	4	Stow close up apparatus, Temp. sensor. Transfer Fungi growth chamber to MD and stow in Refrigerator.
	8	
	12	
	16	
	20	

Figure 1. L-12 time line.

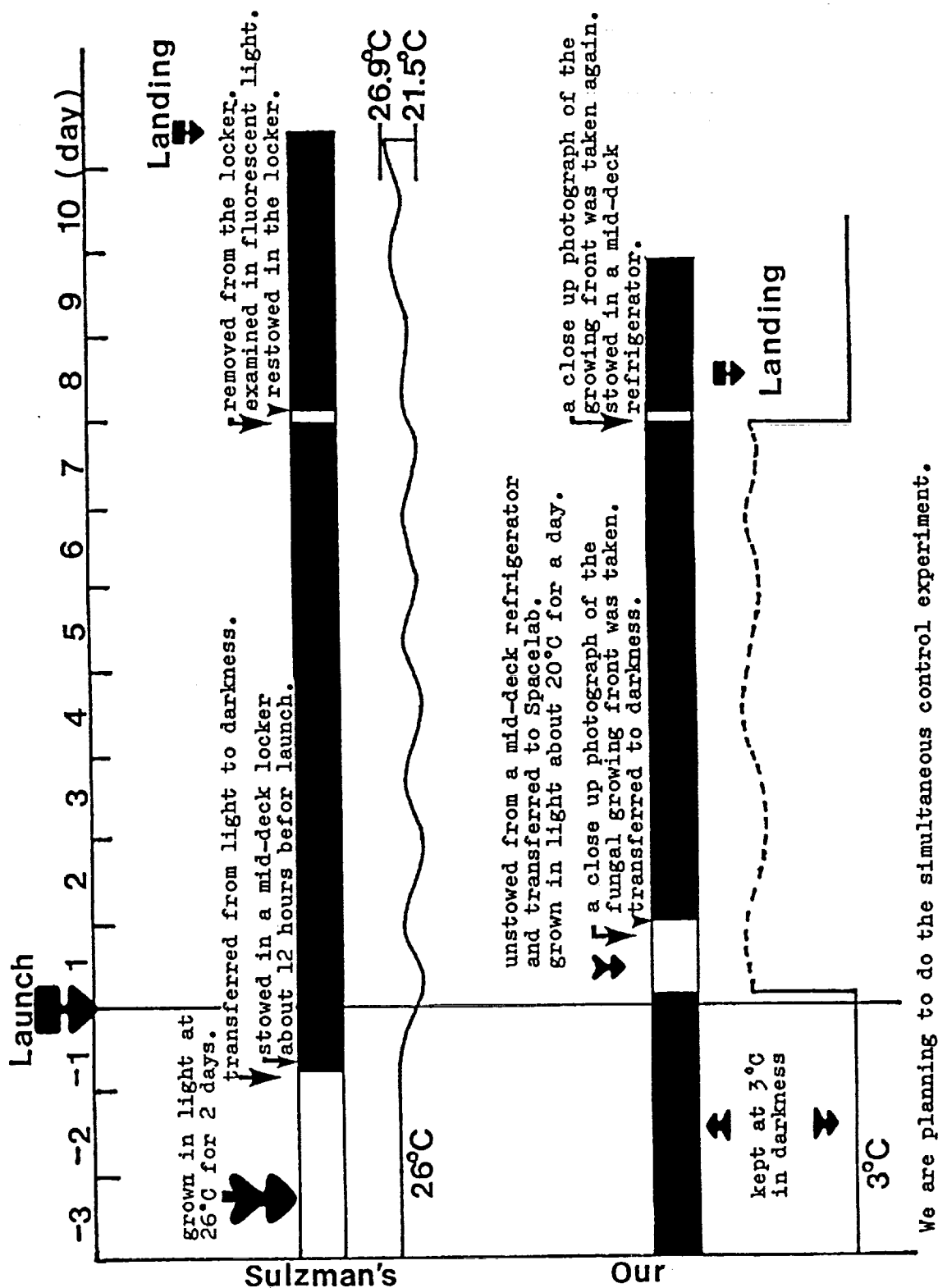


Figure 2. Some differences between Sulzman's and our procedures.

## AMPHIBIAN FERTILIZATION AND DEVELOPMENT IN MICROGRAVITY

Kenneth A. Souza  
Space Life Sciences Payloads Office, NASA-Ames Research Center  
Moffett Field, CA 94035

Introduction

The frog egg is a small 1-2 mm spherical cell surrounded by several gelatinous layers which swell when they contact water. The egg is divided into hemispheres, one of which is lightly pigmented and contains a high concentration of yolk platelets; the other hemisphere is darkly pigmented and is filled with cytoplasm of a lighter density. When the female frog sheds her eggs into the aquatic medium, the eggs are randomly oriented with respect to the gravity vector. Once fertilized, the eggs rotate such that the heavy lightly pigmented hemisphere is down and the opposite hemisphere is up.

Is the geotropic response exhibited by fertilized frog eggs required for normal amphibian development? Over the past century, many developmental biologists attempted to answer this question using a variety of approaches, including forcibly inverting the eggs between glass slides, tumbling them in streams of water, rotating them on clinostats and centrifuges, and using a variety of immobilizing agents like agar and gelatin to hold them in place (1-9). These experiments indicated that gravity and centrifugal force can definitely affect amphibian development. For example, eggs immobilized and held in a position  $90^\circ$  inclined from the gravity vector will form the dorsal structures of the body axis from the uppermost side of the egg (2). This topography is seen even if the point on the egg where the sperm penetrated (Sperm Entry Point, SEP), the prospective ventral side of the egg, is held uppermost. Thus gravity can be used to ex-

perimentally override the normal mechanisms that specify the position of the dorsal structures relative to the SEP. However, in spite of a plethora of ground-based research, it is not known if gravity has a role in the development of a normal egg, i.e., an egg that is free to rotate inside its fluid filled membrane and gelatinous coating. The SL-J Frog Embryology Experiment (FEE) will attempt to conclusively answer the question, "Is gravity required for normal amphibian development?"

### Experimental Design

During the year before launch, female frogs will be tested every 3 months for the quantity and quality of eggs produced. Two weeks or more prior to launch, male and female frogs will be transported to the John F. Kennedy Space Center (KSC). During the few weeks before launch, groups will be periodically tested for egg quality to assure that the frogs have adapted to the KSC laboratory environment.

About 27 hours before launch, four females will be placed in a damp foam-lined box, called the Adult Frog Box (AFB), through which 100 cc/min of air will be circulated. The AFB will be lowered into the Spacelab and loaded into the Frog Environmental Unit (FEU) (Figure 1) during the final pre-launch preparations. A sperm suspension, for use in flight to fertilize the eggs, will also be prepared and loaded during the pre-launch period. The sperm suspension, together with a kit of syringes containing Human Chorionic Gonadotropin (HCG), will be stored in a refrigerator aboard the shuttle until needed in flight.

On the first day of flight, the AFB will be transferred from the FEU to the General Purpose Work Station (GPWS), which is a type of glove box specially designed to allow the crew to use chemicals and biological materials during the flight without contaminating the shuttle/Spacelab environment. Inside the GPWS the four adult frogs will be injected with the HCG hormone and returned to the FEU. Approximately 16 hours after injection, ovulation should have taken place and 15 to 20 eggs from each frog will be placed on each of two egg baskets and covered with sperm for 10 minutes. The egg baskets are inserted into acrylic egg chambers and 50 ml of "pond water" (20% strength Modified Ringers solution) is added. One of the chambers from each frog will be placed on a centrifuge within the FEU and rotated to simulate normal terrestrial gravity (1 g). The remaining chambers are incubated under microgravity conditions within the FEU. Forty minutes after fertilization, the four chambers exposed to 1 g will be removed and observed within the GPWS using a dissecting microscope and camera system. On the basis of egg rotation and egg appearance, the "best" and "second best" frogs will be selected to contribute additional eggs.

Using the two best frogs, 22 egg chambers will be loaded with eggs and fertilized. Eleven chambers will be incubated at microgravity and eleven will be incubated on the centrifuge. At various times during the flight, chambers will be removed from the FEU and transferred to the GPWS where a formaldehyde-based fixative will be injected in order to preserve important developmental stages for in depth study following the flight.

Five of the 22 chambers plus the eight fertilization test chambers will be returned to Earth with live tadpoles. The swimming behavior of these free swimming tadpoles will be examined

within several hours of landing and some will be fixed for a detailed analysis of their inner ear, the otolith, the animals "balance system." Lychakov and Vinikov (10,11) reported an increase in otolith size in tadpoles that developed (but were not fertilized) in space. Live tadpoles from the SL-J flight will be raised through metamorphosis for studies of maturation including an analysis of the effects of space flight on their ability to produce normal progeny.

Following the flight, the fixed embryos will be serially sectioned and stained using procedures that were developed for this experiment. The embryos fixed at the 2- to 4-cell stage will be examined for the distribution of cytoplasmic contents, including the various classes of yolk platelets, and the location and shape of the cleavage furrows. The gastrulae will be assessed for the normality of the complex cellular rearrangements that constitute blastopore formation and involution, i.e., the differentiation of the embryo into its specialized body parts. Using a new procedure, the gastrulae will be bleached which will enable the initial sperm entry point (SEP) to be located. The correlation between the SEP and the dorsal lip of the blastopore will be determined. Under normal terrestrial conditions it has been shown that the SEP typically is located on the side of the egg opposite the future dorsal side of the embryo (2). The neurulae will be examined for the normality and completeness of the neural plate and archenteron expansion. The tadpole stages will be used to study the allometry and morphology of the various organ systems.

#### Expected Results

We expect that the amphibian embryos developing at microgravity will have essentially normal morphology. This expectation is based on the results of previous space flight data (albeit

from embryos fertilized at 1 g and launched at various stages of development) (12,13), random motion experiments (4), and clinostat experiments (7,9) in which most embryos developed normally. Moreover, a recent IML-1 experiment has exposed amphibian embryos to microgravity during the gravity-sensitive period between fertilization and first cell division and most embryos appear normal although no embryos were fixed after gastrulation and none were allowed to develop to hatching due to the constraints of the hardware (G. Ubbels, personal communication). The SL-J frog embryology experiment will assess the normality of the complete ontogeny of the organism including behavioral analyses.

Swimming behavior of tadpoles fertilized on the ground and launched prior to the formation of their otolith systems are expected to exhibit abnormal behavior in microgravity based on our experiments with short-term exposure to microgravity during parabolic flights on NASA's KC-135 airplane (14) and previous experiments with tadpoles and fish aboard the Skylab and Apollo spacecraft. We are far less certain that this behavior will persist throughout the 7-day flight and for how long it may persist post-flight. Similarly, we are less certain about the swimming behavior of tadpoles which were fertilized and developed at microgravity. Never having been exposed to gravity, their swimming behavior may be quite different than normal tadpoles, both at microgravity and at 1 g post-flight.

Regarding the SEP-dorsal axis topography, we expect that the correlation will be normal; i.e., the dorsal structures will form on the side of the egg opposite the SEP. We base this assessment on recent findings that the normal topography depends on cytoplasmic rearrangement that can actually work against gravity in an experimental situation. However, other scientists predict

a disruption of the normal cytoplasmic rearrangements (7). If they are correct, a randomization of the SEP-dorsal structures relationship will occur. The Spacelab J Frog Embryology Experiment should resolve this issue.

### References

1. Ancel, P., and P. Vintemberger (1948) Bull. Biol. Suppl., 31, 1.
2. Black, S., and J. Gerhart, (1985) Dev. Biol., 108, 310.
3. Born, G. (1885) Arch. Mikrosk. Anat., 24, 475.
4. Morgan, T. (1904) Anat. Anz., 25, 94.
5. Pasteels, J. (1964) Adv. Morphog., 3, 363.
6. Neff, A., M. Wakahara, A. Juraud, and G. Malacinski (1983) J. Embryol. Exp. Morph., 80, 197.
7. Neff, A., G. Malacinski, and H.-M. Chung (1985) J. Embryol. Exp. Morph., 89, 259.
8. Pfluger, E. (1883) Pflugers Arch., 32, 1.
9. Tremor, J., and K. Souza (1972) Space Life Sci., 3, 179.
10. Lychakov, D., and Y. Lavrova (1985) Sp. Biol. Aerosp. Med., 19(3), 70.
11. Vinikov, Ya., O. G. Gazenko, D. V. Lychakov, and L. R. Palmbakh (1974) Zhurnal Obshchey Biologii, 44(2), 147.
12. Young, R., and J. Tremor (1968) Bioscience, 18, 609.
13. Souza, K. A. (1987) Biological Sciences in Space, International Symposium on Biological Sciences in Space, Nagoya, Japan. Editors: Watanabe, S., G. Mitarai, and S. Mori, MYU Research, Tokyo.
14. Wassersug, R. J., and K. A. Souza (1990) Naturwissenschaften 77, 443.



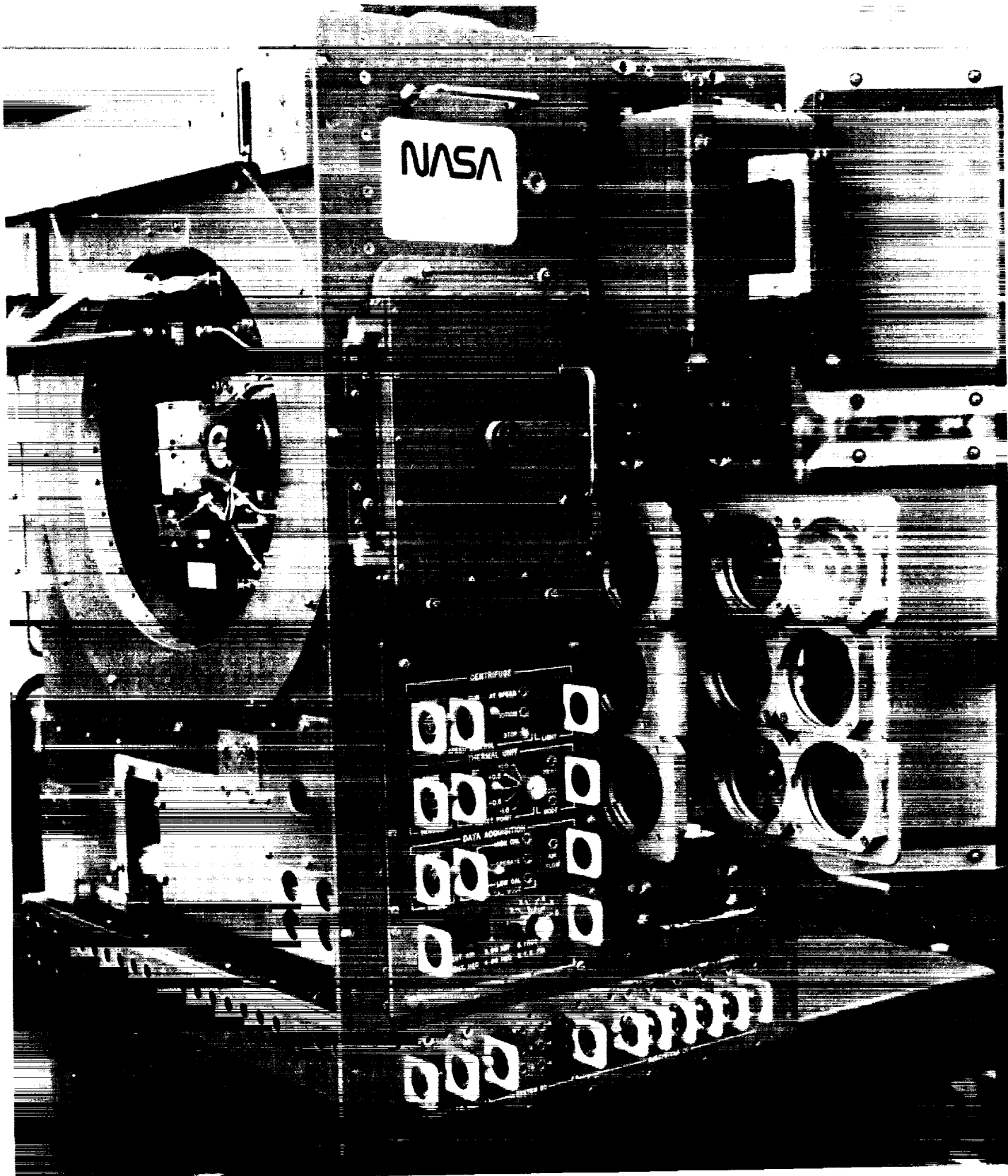


Figure 1. Frog environmental unit.



## MAGNETIC RESONANCE IMAGING AFTER EXPOSURE TO MICROGRAVITY

Adrian LeBlanc, Ph.D.  
Department of Medicine, Baylor College of Medicine  
Houston, TX

A number of physiological changes have been demonstrated in bone, muscle, and blood from exposure of humans and animals to microgravity. Determining mechanisms and the development of effective countermeasures for long-duration space missions is an important NASA goal. Historically, NASA has had to rely on tape measures, x-ray, and metabolic balance studies with collection of excreta and blood specimens to obtain this information. The development of magnetic resonance imaging (MRI) offers the possibility of greatly extending these early studies in ways not previously possible; MRI is also non-invasive and safe; i.e., no radiation exposure. MRI provides both superb anatomical images for volume measurements of individual structures and quantification of chemical/physical changes induced in the examined tissues. This investigation will apply MRI technology to measure muscle, intervertebral disc, and bone marrow changes resulting from exposure to microgravity.

Limb volume changes associated with exposure to microgravity probably involves two factors: (1) changes in fluid amount and distribution and (2) muscle atrophy. Both processes involve fluid shifts, the first mostly extracellular, the second intracellular. MRI techniques are ideal for measuring changes in water content of tissues and are both non-invasive and quantitative. Muscle wasting would be expected to produce muscles less able to perform work. Muscular deconditioning was documented during Apollo and Skylab missions and in ground-based simulation bed rest studies. The loss in muscle mass and strength produced by weightless

exposure affects some muscles more than it does others, i.e., differential muscle atrophy. In Skylab, this was suggested by the observed differences between the leg flexors and extensors. Animals flown in space or subjected to simulated weightlessness have demonstrated differential muscle atrophy. MRI will be used to measure volume changes of individual muscle groups of the calf, thigh, and back of Spacelab crewmen.

Marrow fat increases in immobilized patients (bone biopsy of paraplegics) and animals. Rats flown aboard Cosmos also had dramatic changes in marrow fat. The exact function of marrow adipose cells and their relation to bone metabolism and hematopoiesis is unknown; however, the metabolic activity of the marrow adipose cells appear to be coupled to the hematopoietic activity of the marrow. Therefore, the study of marrow fat as it relates to hematological changes in weightlessness could provide new information concerning the loss of red cell mass during space flight. The possible association of changes in marrow fat and trabecular bone loss is also of scientific interest. We will measure the relaxation times of the lumbar spine bone marrow before and after space flight to determine if changes in marrow composition are occurring.

Research studies indicate that normal ambulation is necessary for intervertebral disc health. Unloading the discs in weightlessness may adversely affect disc physiology. Our bed rest studies indicate changes in the lumbar discs during bed rest and reambulation. Our studies suggest an expansion of the disc during bed rest followed by relatively rapid changes following reambulation. The exact nature and significance of these changes is under investigation.

MRI imaging of the crew members of the Spacelab mission, SL-J, will be performed prior to flight on days F-90, F-60, F-30 and post-flight on days R+1 and R+30. The equipment will be the Siemens 1.5 Tesla magnet located at the Methodist Hospital, Department of Radiology. Multi-slice images, using a spin echo technique, will be obtained to measure muscle volume changes in the calf, thigh, and back. A single, 1 cm sagittal slice through the center of the lumbar spine will be obtained with a spin echo sequence for calculating T2 of the lumbar spine bone marrow and intervertebral discs. Changes in disc shape will also be quantitated from these images. In addition, a series of thin sagittal slices through the lumbar disc will be obtained to document disc volume changes.



COUNTERMEASURE FOR REDUCING POST-FLIGHT  
ORTHOSTATIC INTOLERANCE

LOWER BODY NEGATIVE PRESSURE (LBNP) EXPERIMENT E140

John B. Charles  
Space Biomedical Research Institute  
NASA, Johnson Space Center

Investigators have shown that after 1-2 weeks of bed rest ingestion of 1000 ml of a salt water solution during 4 hours of continuous exposure to 30 mm Hg of lower body negative pressure will protect plasma volume and orthostatic function for up to 24 hours. We hypothesize that a similar countermeasure will reduce the effects of fluid loss induced by headward fluid shift during space flight. The objective of this flight experiment is to evaluate the efficacy of the proposed countermeasure in reversing these effects on the cardiovascular system.

Experimental Procedures

Lower Body Negative Pressure (LBNP) involves exposing the legs and lower abdomen to reduced air pressure. The LBNP device is an air-tight chamber that seals the subject's waist to enclose the lower body. As used in this experiment, LBNP provides both the candidate treatment as well as the means of assessing the effectiveness of the treatment.

## 1. LBNP Response Tests ("RAMPS")

LBNP response tests ("ramps," Figure 1) will be conducted to measure orthostatic responses three times inflight for each participating crewmember. During this LBNP test, after 6 minutes of control data collection, the pressure will be decreased in 10 mm Hg steps every 3 minutes until a pressure of 50 mm Hg below ambient is attained. After 3 minutes at -50 mm Hg, the vacuum will be released and 3 minutes of recovery data will be collected. ECG, echocardiographic parameters, and calf dimensions will be monitored continuously; blood pressure measurements will be made at every minute of the "ramp"; leg volume measurements will be made immediately before and after each LBNP "ramp" test. Real-time medical monitoring of ECG, blood pressure, and LBNPD pressure is required throughout the ramp test.

Each LBNP "ramp" test is a 2-crew member operation. One crew member serves as the LBNP subject and will also operate the LBNP device. The other crew member is the prime hardware operator for the echocardiograph (AFE) and automatic blood pressure system (ABPS), both of which are described in detail below.

## 2. LBNP Treatment ("SOAK")

The treatment protocol ("soak," Figure 2) will be conducted inflight once for each participating crewmember. After 6 minutes of baseline data collection, the pressure in the LBNP device is decreased in 10 mm Hg steps every 3 minutes until a pressure of 50 mm Hg below ambient is attained. After 3 minutes at -50 mm Hg, the vacuum will be partially released to 30 mm Hg below ambient for the "soak" period. During the first hour of the soak period, the crew



member will ingest 8 salt tablets and 4 beverage containers of water (128 oz, total). This pressure level (-30 mm Hg) will be maintained for 225 minutes. Then, the pressure will be reduced in 10 mm Hg steps every 3 minutes until a pressure of 50 mm Hg below ambient is attained. After 3 minutes at this pressure step, the vacuum will be released and 6 minutes of recovery data will be collected.

During the ramp-like portions of the protocol, measurements will be made and described above. During the soak portion (e.g., the 225 minutes at 30 mm Hg), echo and blood pressure measurements will be continuously made for 10 minutes at scheduled times (one 10-min session occurs every 50-60 minutes). In addition, one blood pressure measurement will be taken every 15 minutes throughout the soak. ECG will be monitored continuously and will be available onboard for crew member reference. Leg volume measurements will be made immediately before the pre-soak ramp and after the post-soak ramp. Real-time medical monitoring of ECG, blood pressure, and LBNPD pressure is required during the soak period.

The LBNP "soak" is a 2-crew member operation. One crew member serves as the LBNP subject and will also operate the LBNP device. The other crew member serves as the prime hardware operator for the AFE and ABPS. During periods of the soak when no measurements are being made on the LBNP subject, the second crew member can perform other tasks but must continue to monitor the subject.

For an overview of all LBNP experiment operations on SL-J, please refer to Figure 3.

## In-flight Hardware Description

### 1. Lower Body Negative Pressure Device

The components of the Lower Body Negative Pressure Device (LBNPD) are an inflatable cylinder assembly, a control console assembly, and a cover/stowage container (Figure 4). During launch and landing, the LBNPD collapses into a compact unit and stows in its Nomex cloth container attached to a floor section of the Spacelab. The stowage container has flaps with zippers to enclose and stow the control console and the compressed cylinder assembly.

The control console assembly contains a pressure/vacuum pump, switches, digital logic, pressure/vacuum and pressure relief valves, pressure/vacuum hoses, and a pressure gauge. The pressure/vacuum pump operates on 28 volts dc and pressurizes the walls of the cylinder to inflate it to its full height. After inflation, a negative pressure is created within the cylinder by operation of the pump in the vacuum mode.

### 2. American Flight Echocardiograph

The American Flight Echocardiograph (AFE) is an off-the-shelf medical ultrasonic imaging system modified for space shuttle compatibility. The AFE has flown on STS 51-D (April 1985) and STS-32 (January 1990) and SLS-1 (June 1991). It is an ultrasound instrument designed to acquire real time (30 frames per second) two-dimensional images of the heart. The non-invasive scan procedure provides data on cardiac structure and dynamic function. The power supply is optimized for use with three-phase, 400 Hz, 100-volt ac shuttle power.

Structural-packaging modification allows for operation from within a middeck locker.

### **3. Automatic Blood Pressure System**

The Automatic Blood Pressure System (ABPS) is an electronic sphygmomanometer which, when used with cuff and transducer, comprises a system for measuring both systolic and diastolic arterial blood pressures using a patented infrasonic pulse-detection method. The ABPS incorporates a digital printer, an RS-232 communications interface, an ECG input connector, a heart rate monitor, and a series of buffer amplifiers to provide data outputs. The main unit controls inflation and deflation of the cuff while calculating and displaying blood pressure. It contains a microprocessor and other electronics, a dc air pump to inflate the cuff, a cuff-pressure transducer, and a keyboard and various other controls. Results appear on three liquid crystal displays (LCDs). The ABPS also incorporates an ECG medical isolation amplifier/signal conditioner to provide ECG in conjunction with blood pressure information.

### **4. Central Venous Pressure Device and Data Recorder**

The Central Venous Pressure Device (CVPD) consists of a non-invasive Doppler blood flow probe (8 MHz continuous wave) mounted in an aluminum enclosure along with an electronic pressure meter, hardware circuitry, and LCD display. A mouthpiece/pressure transducer plugs into the pressure meter. The probe is placed over the jugular vein in the neck. The subject expires into the restricted mouthpiece while listening through stereo headphones to the flow sounds and watching the pressure meter to generate various target pressures. The mouthpiece

pressure which transiently interrupts jugular flow is taken as an estimate of central venous pressure. Flow and pressure data are recorded onto a TEAC 7-channel cassette data recorder.

#### 5. Ultrasonic Limb Plethysmograph

The Ultrasonic Limb Plethysmograph (ULP) is a self-contained device which uses pulses of ultrasound to determine chord lengths through the calf at two levels. Ultrasound transducers are attached to the skin over the calf muscle. An ultrasonic pulse (2.5 MHz frequency) propagates through the tissue from the transmitter crystals to the receiver crystal. The transit time is converted to distance representing chord length, displayed in millimeters on a numeric indicator, and stored on a microcassette recorder integral to the ULP.

#### 6. Stocking (Leg) Plethysmograph

The leg plethysmograph is a stocking-like device pulled over the lower portion of the leg. The material is slightly elastic to maintain contour and grip on the leg. Integral circumferential tapes are pulled snug and marked with a colored pen for post-flight analysis. Longitudinal tapes aid in donning and insure the location of the circumferential tapes.

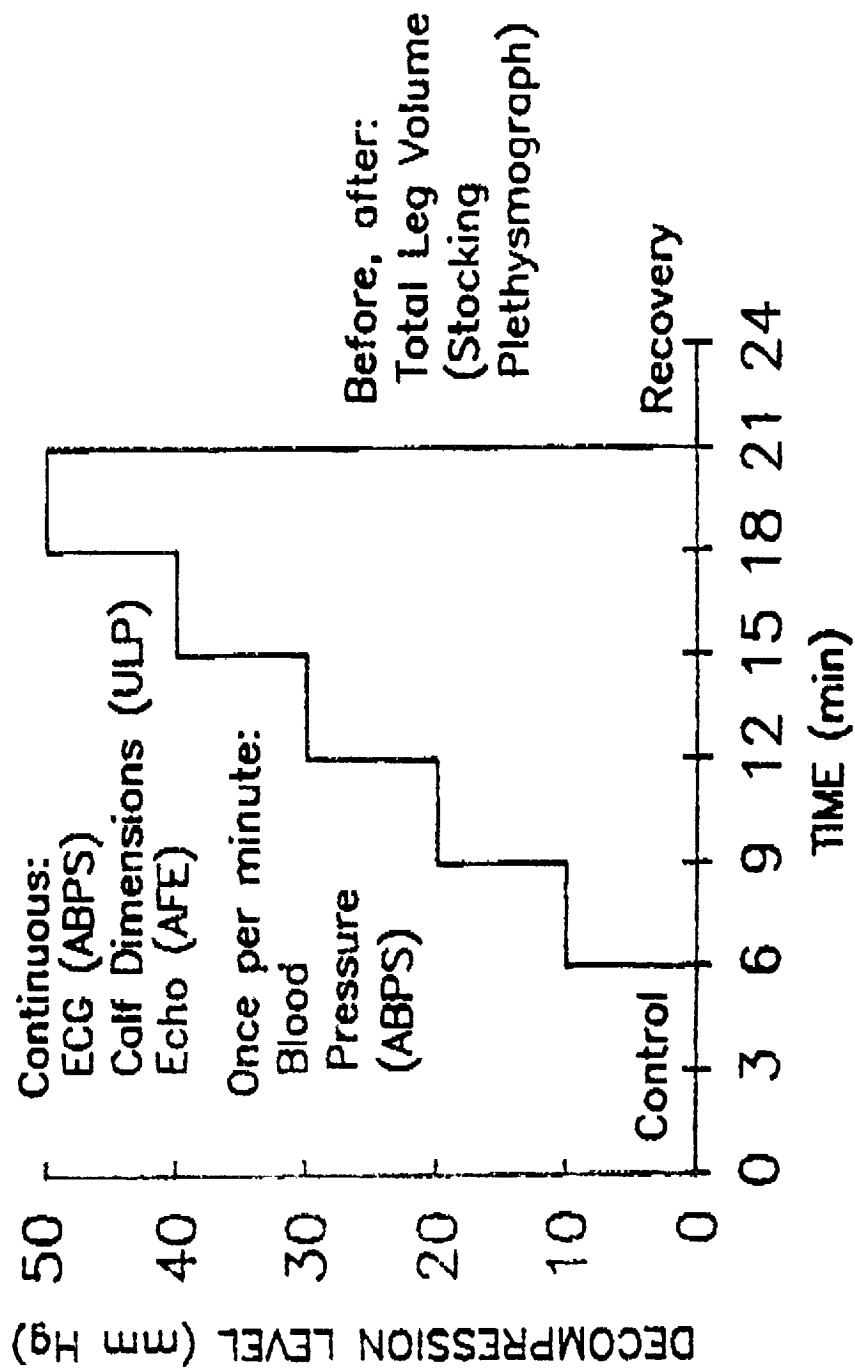


Figure 1. LBNP test protocol ("RAMP").

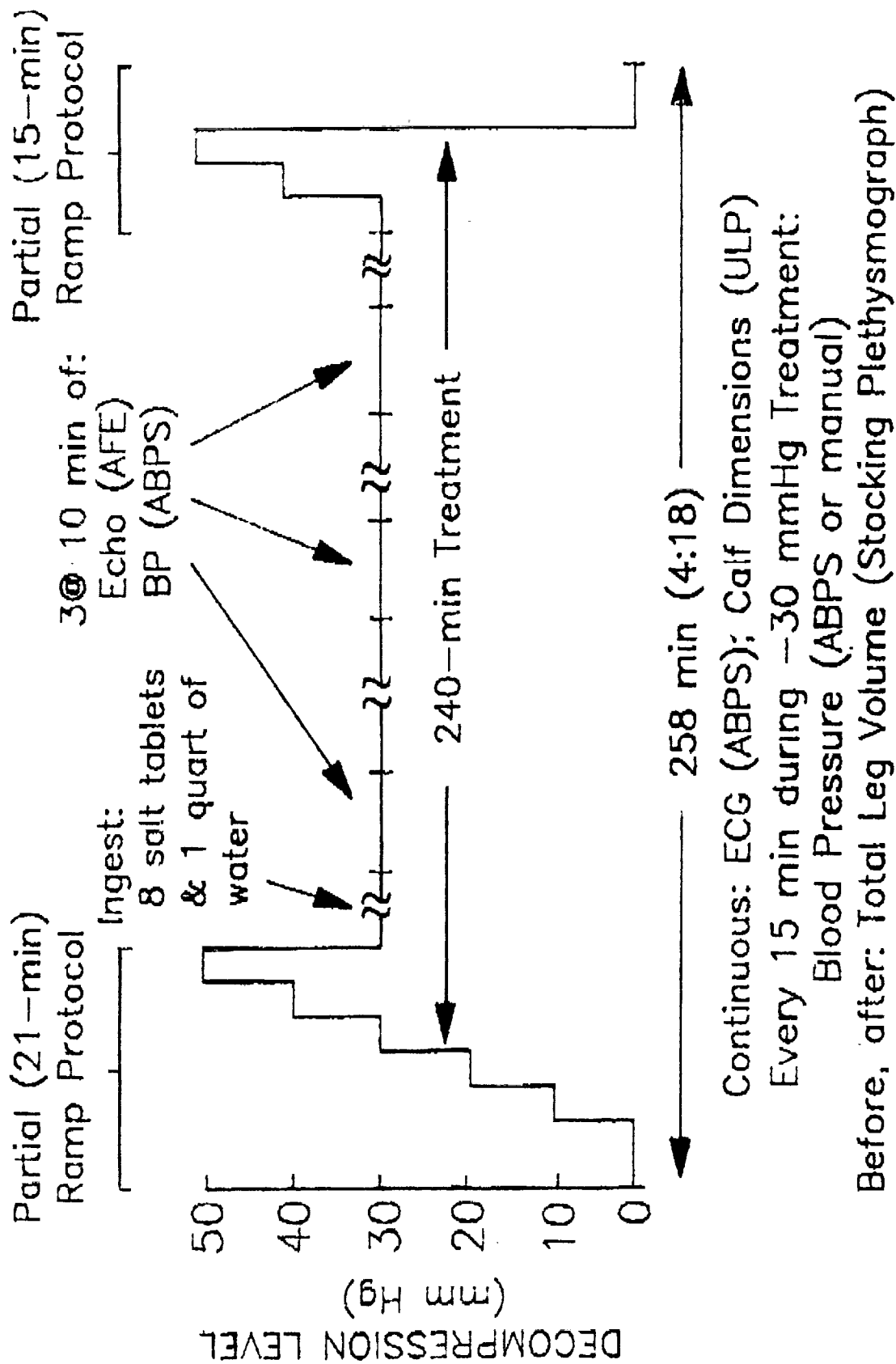


Figure 2. LBNP treatment protocol ("SOAK").

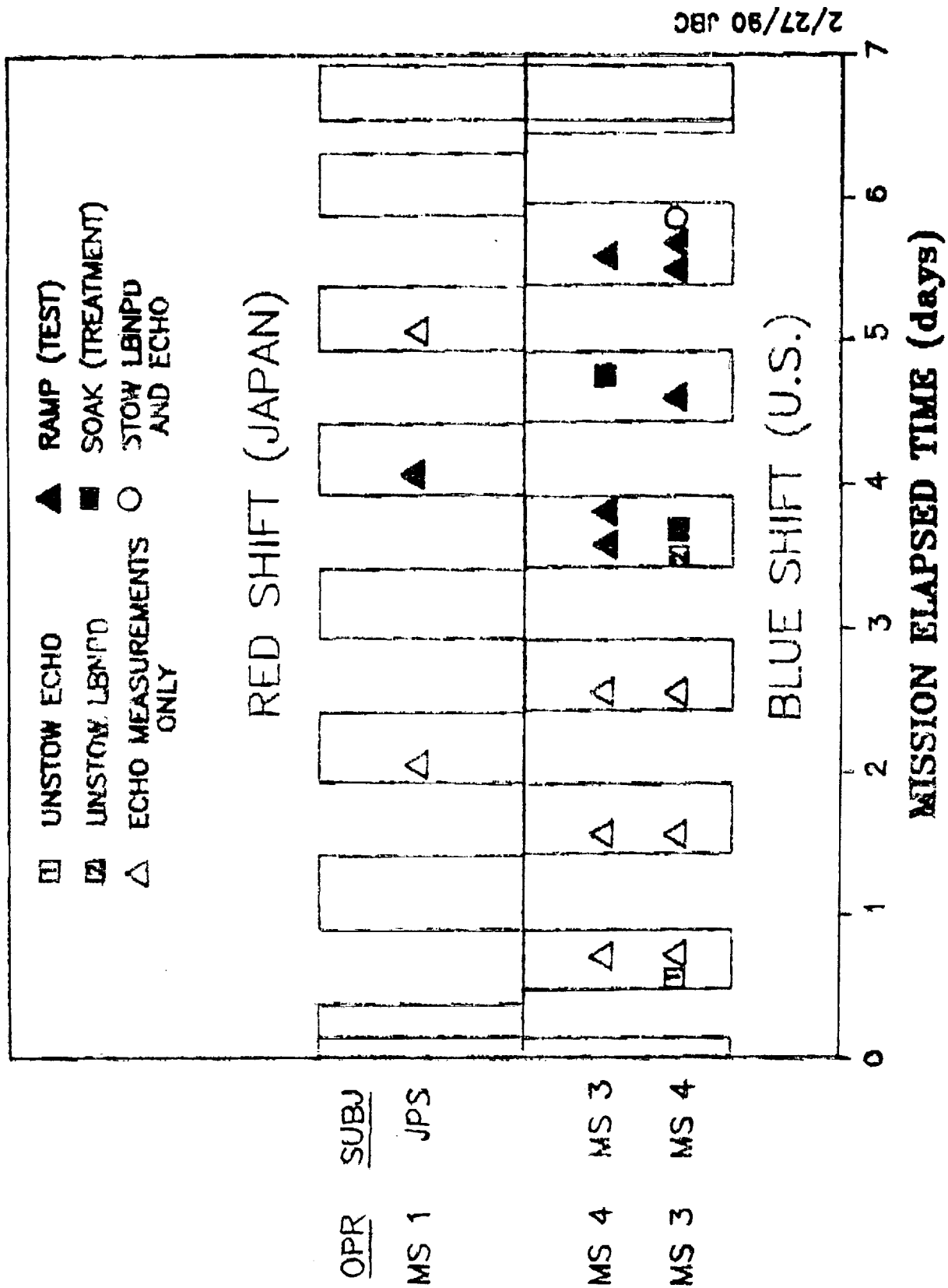


Figure 3. Spacelab-J Experiment E06 ("LBNP").

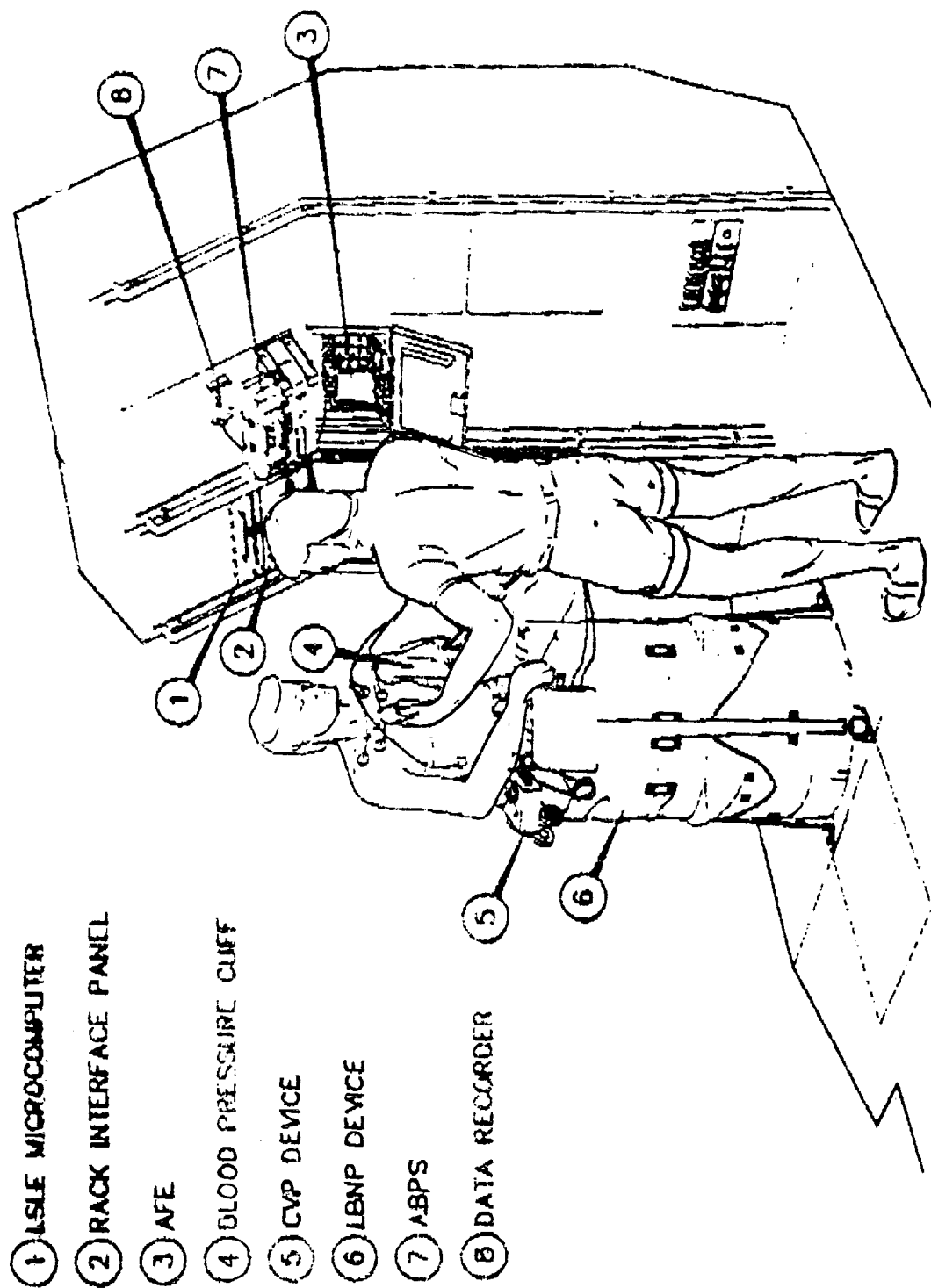


Figure 4. Lower Body Negative Pressure Experiment.



## BONE CULTURE RESEARCH

Nicola C. Partridge  
St. Louis University School of Medicine  
St. Louis, MO

Background and Hypothesis

Among the most overt negative changes experienced by man and experimental animals under conditions of weightlessness are the loss of skeletal mass and attendant hypercalciuria. These clearly result from some disruption in the balance between bone formation and bone resorption (i.e., remodeling), but precisely what this disruption is and how it might occur have not been established. Frost (1987) has suggested that the loss of bone under conditions of weightlessness is due to a decrease not just in weight but also in muscle resistance. He has proposed that bone contains a mechanostat which senses these changes and adjusts the mass accordingly. Work in vitro has suggested that osteoblastic cells respond to mechanical stress but there are presently no published studies documenting the presence and function of mechanoreceptors on such cells. Frost has gone on to suggest that changes in the mechanostat may change responsiveness to circulating agents, such as parathyroid hormone (PTH), resulting in increased numbers of remodelling units without any change in circulating hormone. Since the osteoblast is the target cell for bone-resorbing hormones like PTH, it would suggest that in microgravity, the osteoblast may be more sensitive to such agents.

The experiments described in this paper are aimed at exploring PTH regulation of production of collagenase and protein inhibitors of collagenase (tissue inhibitors of metalloproteases, TIMP-1 and -2) by osteoblast-like osteosarcoma cells under conditions of weightlessness. The

results of this work will contribute to information as to whether a microgravity environment alters the functions and responsiveness of the osteoblast.

### Objectives

The more specific objectives of the BCR experiment are:

- To observe the effects of microgravity on the morphology, rate of proliferation, and behavior of the osteoblastic cells, UMR 106-01.
- To determine whether microgravity affects the hormonal sensitivity of osteoblastic cells.
- To measure the secretion of collagenase and its inhibitors into the medium under conditions of microgravity.

### Methods

The methods employed will consist of the following:

- The osteoblast-like cells, UMR-106-01, will be cultured in four NASDA cell culture chambers.
- Two chambers will be subjected to microgravity on SL-J; two chambers will remain on the ground at KSC as ground controls but subjected to an identical set of culture conditions as on the shuttle.

- Media will be changed four times; twice the cells will receive the hormone parathyroid hormone-related protein (PTHrP) and media collected.
- Cells will be photographed under conditions of microgravity.
- Media and photographs will be analyzed upon return to determine whether functions of the cells changed.

#### Post-Flight Analysis

Post-flight analysis will consist of the following:

- The photomicrographs for the two chambers and the various treatment periods will be analyzed for differences in behavior, morphology, and rates of proliferation of the osteoblastic cells in micro- and unit gravity for the field of observation.
- Measurement of collagenase in the media will be conducted by ELISA assay.
- Measurement of TIMPs in the media will be conducted by ELISA assay.
- Cell protein will also be measured.
- Collagenase and TIMP secretion will be expressed per unit cell protein.

### Expected Results

- UMR cells in microgravity will respond more sensitively to PTHrP.
- Growth will be decreased more than at unit gravity.
- Cells will produce greater amounts of collagenase, perhaps lesser amounts of inhibitors.

From the data, we may obtain knowledge at the cellular level of the behavior and functions of osteoblasts under microgravity and thus gain information as to the mechanisms causing microgravity-induced osteopenia.

### Reference

Frost, H. M. (1987), Anat. Rec. 219, 1-9.

## AUTOGENIC FEEDBACK TRAINING EXPERIMENT: A PREVENTATIVE METHOD FOR SPACE MOTION SICKNESS

Patricia S. Cowings  
NASA Ames Research Center  
Moffett Field, CA USA

### The Problem of Space Motion Sickness

Space motion sickness is a disorder which produces symptoms similar to those of motion sickness on Earth. This syndrome has affected approximately 50% of all astronauts and cosmonauts exposed to microgravity in space, but it differs from what is commonly known as motion sickness in a number of critical ways. There is currently no ground-based method for predicting susceptibility to motion sickness in space. Antimotion sickness drugs have had limited success in preventing or counteracting symptoms in space, and frequently caused debilitating side effects. For example, the Physician's Desk Reference (1988, p. 2300) cautions under Information for Patients that one of the drugs used to counteract motion sickness, "Promethazine may impair the mental and/or physical abilities required for the performance of potentially hazardous tasks such as driving a vehicle or operating machinery." There are no data from space on the effects of this medication on crew performance.

Biomedical data from past space missions indicate that some individuals who have had wide exposure to motion devices and acceleratory forces on Earth or in aircraft, and who have never previously shown any tendency to develop motion sickness symptoms, were severely debilitated in the microgravity environment (Bungo et al., 1987). Conversely, some individuals who had a history of susceptibility to motion sickness were unaffected by symptoms in space.

Symptom episodes vary from mild discomfort to repeated vomiting which sometimes occurs suddenly, with little or no warning. The earliest reported episode began within only 7 minutes of orbit insertion, and malaise has been reported to last from 1 to 5 days. Finding a solution to this biomedical problem has become a high priority goal of NASA because of its potential impact on crew safety, comfort, and operational efficiency during shuttle missions.

Most of the research in this field has been devoted to the study of vestibular physiology, perceptual phenomena, or pharmacological intervention in man and in animals (Reason & Brand, 1975). In contrast, the primary objective of our own research group has been to develop a method of training people to control their own motion sickness symptoms (Cowings, 1990; Blizzard et al., 1975; Cowings et al., 1977; Cowings and Toscano, 1977, 1982; Toscano and Cowings, 1977; Cowings et al., 1986, 1990). Our method of treatment is Autogenic-Feedback Training (AFT), a combination of biofeedback and Autogenic Therapy (Schultz & Luthe, 1969), which involves training physiological self-regulation as an alternative to pharmacological management. The rationale for using AFT to treat motion sickness was based on the observation that there were profound autonomic nervous system (ANS) changes associated with this disorder (Cowings et al., 1986) and, although these responses are highly idiosyncratic, they are repeatable over time (Cowings et al., 1990). By studying physiological and behavioral indicators of human adaptation to the microgravity environment, we hoped to use these training techniques to facilitate adaptation.

## Objectives

1. To evaluate the effectiveness of Autogenic-Feedback Training as a countermeasure for space motion sickness.
2. To compare physiological data and in-flight symptom reports to ground-based motion sickness data.
3. To predict susceptibility to space motion sickness based on pre-flight data of each treatment group crew member.

## Ground Studies

### Physiological Responses to Motion Sickness Stimuli

The relative importance of ANS responses in understanding and treating motion sickness has been a matter of some controversy. Money (1970), in his review of motion sickness research, discussed many possible ANS changes during motion sickness, but correctly noted that there was little consistency in either procedures used or results of the available research.

In a recent paper (Cowings et al., 1986), we examined the data of 127 people, all given the same motion sickness test in order to describe the general trend of ANS responses in all subjects. Our own laboratory work suggested that differences in initial susceptibility may account for at least one major source of variability in ANS responding reported by others. We, therefore, also investigated whether high-, moderate-, and low-susceptible individuals differed in

their ANS responding to motion stimulation. And last, we examined autonomic responses as predictors of motion sickness susceptibility. We used the ANS variables of heart rate, respiration rate, finger pulse volume, and skin resistance because they were easily measured, represent different aspects of the ANS, and have been used in previous studies on motion sickness.

The results clearly showed sympathetic activation of all four ANS responses during motion sickness stimulation. Physiological response levels changed rapidly and dramatically at the onset of stimulation and when the test concluded. We also found differences in ANS responding among motion sickness susceptibility groups, with highly susceptible subjects producing, in general, larger magnitude changes than the moderate or low susceptibles.

In another study, comparisons were made of two separate motion sickness tests on each of 58 subjects (Cowings et al., 1990). Again, the same four physiological responses (heart rate, finger pulse volume, respiration rate, and skin resistance) were measured during both motion tests. The goal of this study was to examine individual differences in physiological responding (i.e., response patterns) to motion stimuli, and determine how these data were related to self-reports of motion sickness malaise experienced. The phenomenon of individual ANS stereotype, that propensity of individuals to respond maximally in the same ANS variable to a variety of different stimuli, is well known in the psychophysiological literature (Cleary, 1974; Engle, 1960; Lacey, 1956; Lacey et al., 1953). In the presence of any stimulus (for example, a loud noise), all subjects might show a rise in heart rate, but some individuals will make a much larger response than others. And for any given individual, the heart rate response may be of greater magnitude than his or her skin resistance level or other measured responses.



The results revealed 11 separate patterns of physiological responding in which all or some combination of the four physiological measures clearly reflected motion sickness malaise levels of each of the 58 subjects. Individual response patterns produced on the first tests were not significantly different than those of the second test. Analyses showed that of the 58 subjects, 27 showed the same response patterns on both tests for all four physiological measures, 14 were stable for three variables, 6 were stable for two, and 11 were stable responders for at least one variable.

### General Procedures of Training

Because certain ANS responses were correlated with, and indeed predictors of motion sickness distress, it was hypothesized that training subjects to control these responses might prevent or reduce symptoms. The observed individual differences in responding suggested that, to be effective, such training would have to be directed at the different responses for different people. In other words, training would have to be "tailored" for each individual. The training procedure we used, AFT, was based on the principals of operant conditioning.

Operant conditioning describes a trial and error process in which the response learned and performed must be followed by either a reward or a punishment (i.e., contingent reinforcement). When a novice is learning better voluntary control over where the basketball goes in shooting foul shots, seeing the ball go through the hoop (success) serves as a reward, and seeing it miss (failure) serves as a punishment. If the novice were blindfolded so that he did not have any knowledge of the results of his shots, he would not learn. It was Miller's contention (Miller,

1969) that visceral and CNS events may be modified by contingent reinforcement in the same way overt behaviors or skeletal responses may be conditioned. Hence, the "same rules" apply for describing the process by which athletic skills are acquired, as in the situation where an individual learns voluntary control of his own heart rate or the vasomotor activity of his hands. To learn control of a physiological response, the subject must be given a means of perceiving that response. The "blindfold" is removed by showing a subject (for example) an amplified display of his own heart rate on a digital panel meter. This process is called biofeedback.

AFT is actually a combined application of several physiological and perceptual training techniques, principal among these are Autogenic Therapy (Schultz and Luthe, 1969) and biofeedback. This combined therapies approach produces a methodology which is appreciably more effective than either of these two techniques when used alone (Blizzard et al., 1975; Cowings and Toscano, 1977). Autogenic exercises provide the subject with a specific set of instructions and method of concentration which are likely to produce the desired response. For example, self-suggestions of warmth in the hands and feet are associated with measurable increases in peripheral vasodilatation (Harano et al., 1973). Consequently, the time normally spent by the subject using a trial and error strategy is shortened and the initial probability of making a correct response is substantially increased. Biofeedback complements Autogenic Therapy by providing immediate sensory information to the subject about the magnitude and direction of a response. Operant conditioning procedures allow for more precise control of a response, as the "reward" (or feedback) can be presented only as the subject makes gradually larger response changes in the desired direction. As a result, the ultimate effectiveness of training is significantly increased.

During a typical training session, subjects are instructed to control a pattern of physiological responses and are given many different feedback displays (visual and auditory), simultaneously. Multiparameter feedback requires additional training in attending to a complex set of feedback signals. Verbal instructions by the experimenter are often required to direct the subject's attention to specific feedback signals and to advise him of alternative strategies when an inappropriate response has occurred. Included in these alternative strategies are elements of systematic desensitization and progressive relaxation of muscle tension monitored at several sites.

The protocol for all of our ground-based studies was essentially the same. First, a rotating chair test was used to induce the initial symptoms of motion sickness. In this way, we could document the pattern of his physiological responses to motion stimulation. The rotating chair tests were conducted by initiating rotation at 6 rpm (0.628 rad/s) and incrementing by 2 rpm (0.209 rad/s) every 5 minutes, with a maximum velocity of 30 rpm (3.142 rad/s). During each 5-minute period of rotation, subjects were instructed to make head movements (front, back, left, and right), in random order, at 2-second intervals. It is these head movements combined with rotation which induce motion sickness symptoms. Every 5 minutes during the test, subjects were asked about the symptoms that they were experiencing using a standardized diagnostic scoring procedure so that we can accurately assess the relationship between his perceived distress and his physiological responses at any given time (Cowings et al., 1986; Graybiel et al., 1968).

Initial exposure to the rotating chair was followed by two (or four) resting baseline sessions and a second rotating chair test. This procedure enabled us to clearly identify which

ANS responses changed from the subject's own resting baseline as a function of motion sickness stimulation. During subsequent AFT sessions, emphasis was placed on training control of those ANS variables that were most responsive in the individual's motion sickness tests. AFT was administered in three sets of four 30-minute sessions (maximum 6 hours) under non-rotating conditions. Each AFT set was followed by a rotating chair test in which the subject attempted to apply AFT to control symptoms. The primary criterion for evaluating treatment success was increased tolerance (i.e., ride for longer durations at higher speeds) to this motion sickness stimulus.

### Results of Ground-Based Research

In preparation for tests of AFT in space, we have conducted investigations on over 200 people. Each study was designed to test the effectiveness of AFT as a countermeasure for motion sickness and the feasibility of using this method to treat space motion sickness in aerospace crews. Another important objective was to determine if the reduction in symptoms observed could be attributed to some experimental factor other than AFT.

In one study, differences in motion sickness tolerance were compared in subjects given AFT, an alternative cognitive task, or no treatment (Toscano and Cowings, 1982). Two hours of AFT were administered to treatment group subjects before the third, fourth, and fifth motion sickness test (6 hours total). Figure 1 shows the performance of all three groups in the motion sickness tests. Results showed that subjects who received AFT had significantly greater motion sickness tolerance than subjects performing an alternative cognitive task ( $p < 0.025$ ) or those

performing no task ( $p < 0.025$ ). Although the cognitive task group had slightly greater tolerance than the no-task control group, it was not significant.

Another experiment was designed to determine if an individual's initial susceptibility to motion sickness was related to his ability to learn control of symptoms (Cowings and Toscano, 1982). Following an initial exposure to a rotating chair test, subjects were assigned to groups based on their motion sickness tolerance. Two AFT treatment groups (highly and moderately susceptible to motion sickness) were compared to two control groups who were matched to the AFT groups for initial susceptibility but were given no treatment. Figure 2 shows the performance of these groups across six motion sickness tests. Results showed that both AFT treatment groups significantly improved their motion sickness tolerance while neither Control group improved significantly. During the last two tests, after 6 hours of AFT, the high and moderate susceptible treatment groups were no longer significantly different in their motion sickness tolerance, while the high and moderate control groups remained significantly different across all tests.

The results of other studies showed: (1) no significant differences between men and women in their ability to apply AFT for symptom control; (2) the ability to control symptoms could be retained for as long as 3 years after training; and (3) the primary component of the treatment effect in each of these studies could be attributed to learned control of physiological responses (Cowings, 1990). The most important studies, however, revealing the likelihood of AFT being a successful treatment in space, were related to the transfer of training effects to a variety of different environments.

## Transfer of Training Effects to Different Motion Environments

Experiments in the literature (Reason and Brand, 1975) and clinical experience show that habituation to a specific nauseogenic situation does not transfer to new situations. Repeated exposure apparently effects primarily the sensory side (or "input" side) of the response system. AFT is aimed at controlling the "output" side, i.e., the various symptoms of motion sickness. To the extent that such control can be learned, we would expect it to be much more likely to transfer to different situations that induce nausea.

An extensive examination of transfer of training was made in another study which involved several different types of motion sickness stimuli. Twenty-four men and women were assigned to two equal groups and matched for sex and initial susceptibility to motion sickness in a rotating chair. The two groups of subjects, an AFT treatment group and a no-treatment control group, were given three types of motion sickness inducing tests at the start of the study: (a) rotating chair test, (b) the combination of optokinetic stimulation with rotation in a chair, and (c) a vertical acceleration test. All subjects received four additional exposures to the rotating chair. Treatment subjects were given 6 hours of AFT over 5 days before tests three, four, and five. The controls received no training. Both groups of subjects were given their second exposure to the battery of different types of motion sickness tests at the end of the experiment. Figure 3 shows the performance of both groups on the transfer tests, vertical acceleration, and optokinetic stimulation. Because these tests had different maximum durations, scores for motion sickness tolerance were based on percentages of the total test completed.

Results showed that subjects given AFT significantly improved their tolerance to the different types of motion sickness tests, whereas the control subjects (habituation only) did not. Furthermore, the Air Force had adopted a similar form of AFT to treat crew members for whom all other methods had proved unsuccessful in combatting persistent air sickness in high performance military planes (Levy et al., 1981; Jones et al., 1985). They have found that such training transfers from the rotating chair on the ground to the variety of maneuvers in military flight well enough to return air crew that otherwise would have been permanently grounded, to active flying duty. These results on transfer of control over response symptoms to different types of stimuli eliciting nausea led us to be hopeful of transfer to the stimuli eliciting symptoms in space. What little preliminary data we have from space flight confirms this hypothesis.

Four crew members (two treatment and two controls) participated in the AFT experiment during a 1985 shuttle mission (Cowings et al., 1986). The treatment subjects were given 6 hours of AFT before the mission (distributed from launch -1 year to launch -3 months), and control subjects received no training. During the mission, one treatment subject was symptom free and the other experienced one symptom episode on the first mission day which did not reach vomiting. The two controls, who had taken anti-motion sickness medication, experienced multiple vomiting episodes on the first day. The physiological data collected in-flight were consistent with reports of malaise, with treatment subjects showing less physiological distress than either of the controls.

## Flight Experiment Design

### Preflight Training

One year prior to the flight the SL-J crew members began their participation in AFTE. One Mission Specialist will receive 6 hours of AFT for the control of motion sickness, and a second Mission Specialist will serve as a control (i.e., will receive no training). In addition, the alternate crew members and the Japanese Payload Specialist will be provided with this training.

1. Baseline data collection. Physiological data are obtained from all subjects during two types of motion sickness tests, a rotating chair and a vertical accelerator. Additionally, data are recorded during two resting baseline (30 minute) sessions, two 12-hour ambulatory sessions during a mission simulation, during zero-g maneuvers in the KC-135 aircraft, and during a 90-minute reclining baseline in the launch position in a shuttle mock-up.

2. Formal AFT sessions. The design of training is much the same as the ground-based studies described above. Twelve 30-minute sessions are administered (at the PI's laboratory) over a 15-day period, with each block (4 consecutive days) of training followed by a motion sickness rotating chair test. The principal criterion for evaluating the success of the AFT treatment is the increased time that crew members tolerate these tests as training progresses.

If the launch should slip more than 4 months, crew members are offered an additional block of training sessions (4 consecutive days).



3. Follow-up AFT sessions. During the launch-6 to 1 month period, AFT training continues in the form of follow-up sessions at any location (e.g., JSC or MSFC). Flight hardware (see Figure 4) will be used to monitor and feedback physiological measures during training for a total of eight (30 minute) sessions.

4. L-10 day session. This 2-hour session is the last time investigators contact crew members prior to the mission. It allows us to document the amount of physiological control retained by the treatment subjects and any differences (from previous sessions) in baseline levels of these subjects or the control subjects.

#### In-Flight Procedures and Flight Hardware

1. Continuous day-time monitoring. During the mission, the physiological responses of both the treatment and control subjects will be monitored and recorded for the first three mission days (waking hours only). The Autogenic-Feedback System-2 (AFS-2) is a portable belt-worn physiological monitoring system (see Figure 4). Developed by NASA in support of space flight experiments, this system can continuously record up to eight physiological responses. This system includes a garment, transducers, biomedical amplifiers, a digital wrist-worn feedback display, and a cassette tape recorder. The entire instrument is powered by a self-contained battery pack. The AFS-2 will record/display: electrocardiogram/heart rate, respiration

waveform/respiration rate, skin conductance level, finger temperature, finger pulse volume, and triaxial accelerations of the head.

2. Timelined and symptom-contingent diagnostic. An eight-item symptom log book will be used by the crew member to note the type and severity of symptoms.

3. Timelined and symptom-contingent AFT sessions. The treatment subject (only) is required to perform daily 15-minute AFT sessions during which control of specific physiological responses are practiced with the aid of the wrist-worn display unit. If that crew member were to experience symptoms in space, he/she is required to apply the AFT methods learned. Symptom-contingent AFT can be performed at the same time that a crew member is conducting other payload activities. It is anticipated that no more than 30 minutes would be required to counteract symptoms.

### Post-Flight Procedures

On the day of landing, AFT investigators are granted a brief (10 minute) interview with the crew members on their experiences with the AFT experiment. Flight hardware, data tapes, and diagnostic log books are returned to the PI's laboratory within 24 hours of touch-down. These data are processed and used within 2 weeks post-flight during a 2-hour private debrief with each of the crew members where the final evaluation of AFT effectiveness during the Spacelab-J mission is determined.

### Summary

Finding an effective treatment of the motion sickness-like symptoms that occur in space has become a high priority for NASA. This experiment utilizes a behavioral medicine approach to solving this problem. This method, Autogenic-Feedback Training (AFT), involves training subjects to voluntarily control several of their own physiological responses to environmental stressors. AFT has been used to reliably increase tolerance to motion sickness during ground-based tests in over 200 men and women under a variety of motion sickness conditions. Such transfer would be expected because the effects of AFT are on the final common response mechanism rather than on initiating stimuli. Thus we might expect it to transfer to space sickness, and our preliminary data suggest that it may. Validation of the effectiveness of AFT as a treatment for space motion sickness will require obtaining data on a total of 16 individuals in space, 8 treatment and 8 control subjects. With the completion of Spacelab-J, this procedure will have been tested on 6 people.

### References

Bungo, M. W., T. M. Bagian, M. A. Bowman, and B. M. Levitan, Eds. (1987), Results of the Life Sciences DSOs Conducted Aboard the Space Shuttle, 1981-1986, Space Biomedical Research Institute, Lyndon B. Johnson Space Center, National Aeronautics and Space Administration, Houston, Texas, p. 121.

Blizzard, D., P. Cowings, and N. E. Miller (1975), "Visceral Responses to Opposite Types of Autogenic Training Imagery," Biological Psychology, 3, 49-55; Also Barber, T. X. et al., Eds. (1976), Biofeedback and Self-Control, Chicago, Aldine Publishing Co.

Cowings, P. S. (1990), "Autogenic-Feedback Training: A Preventive Method for Motion and Space Sickness," in G. Crampton, Ed., Motion and Space Sickness, Boca Raton, Florida, CRC Press, Chapter 17, pp. 354-372.

Cowings, P. S., J. Billingham, and W. B. Toscano (1977), "Learned Control of Multiple Autonomic Responses to Compensate for the Debilitating Effects of Motion Sickness," Therapy in Psychosomatic Medicine, 4, 318-323; Also in W. Luthe and F. Antonelli, Eds. (1977), Autogenic Methods: Application and Perspectives, Rome, Luigi Pozzi S.P.A.; Also in T. X. Barber et al., Eds. (1978), Biofeedback and Self-Control 1977/78, Chicago, Aldine Publishing Co.

Cowings, P. S., and W. B. Toscano (1977), "Psychosomatic Health: Simultaneous Control of Multiple Autonomic Responses by Humans - A Training Method," Therapy in Psychosomatic Medicine, 4, 184-190; Also in W. Luthe and F. Antonelli, Eds. (1977), Autogenic Methods: Application and Perspectives, Rome, Luigi Pozzi S.P.A.

Cowings, P. S., and W. B. Toscano (1982), "The Relationship of Motion Sickness Susceptibility to Learned Autonomic Control for Symptom Suppression," Aviation Space and Environmental Medicine, 53(6), 570-575.

Cowings, P. S., S. Suter, W. B. Toscano, J. Kamiya, and K. Naifeh (1986), "General Autonomic Components of Motion Sickness," Psychophysiology, 23(5), 542-551.

Cowings, P. S., W. B. Toscano, J. Kamiya, N. E. Miller, and J. C. Sharp (1988), Final Report, Spacelab-3 Flight Experiment #3AFT23: Autogenic-Feedback Training as a Preventive Method for Space Adaptation Syndrome, NASA Technical Memorandum No. TM-89412, National Aeronautics and Space Administration, Ames Research Center, Moffett Field, California.

Cowings, P. S., K. Naifeh, and W. B. Toscano (1990), "The Stability of Individual Patterns of Autonomic Responses to Motion Sickness Stimulation," Aviation Space and Environmental Medicine, 61(5), 399-405.

Cleary, P. J. (1974), "Description of Individual Differences in Autonomic Reactions," Psych. Bull., 81, 934-944.

Engle, B. T. (1960), "Stimulus-Response and Individual-Response Specificity," Arch. Gen. Psychiatry, 2, 305-313.

Graybiel, A., C. D. Wood, E. F. Miller, and D. B. Cramer (1968), "Diagnostic Criteria for Grading the Severity of Acute Motion Sickness," Aerospace Medicine, 39, 453-455.

Harano, K., S. Ogawa, and G. A. Naruse (1973), "A Study of Plethysmography and Skin Temperature During Active Concentration and Autogenic Exercises," in W. Luthe, Ed., Autogenic Training: Correlations Psychosomatics, Grune and Stratton, New York, pp. 123-130.

Jones, D. R., R. A. Levy, L. Gardner, R. W. Marsh, and J. C. Patterson (1985), "Self-Control of Psychophysiologic Responses to Motion Stress: Using Biofeedback to Treat Airsickness," Aviation Space and Environmental Medicine, 56, 1152-1157.

Lacey, J. I. (1956), "The Evaluation of Autonomic Response: Toward a General Solution," Ann. N.Y. Acad. Sci., 67, 123-164.

Lacey, J. I., D. E. Bateman, R. VanLehn (1953), "Autonomic Response Specificity: An Experimental Study," Psychosom. Med., 15, 8-21.

Levy, R. A., D. R. Jones, and F. H. Carlson (1981), "Biofeedback Rehabilitation of Airsick Aircrew," Aviation Space and Environmental Medicine, 52, 118-121.

Miller, N. E. (1969), "Learning of Visceral and Glandular Responses," Science, 163, 434-445; Also in T. Barber, L. DiCara, J. Kamiya, N. Miller, D. Shapiro, and J. Stoyva, Eds. (1971), Biofeedback and Self-Control, Chicago, Aldine Atherton, Inc., pp. 3-25.

Money, K. E. (1970), "Motion Sickness," Physiological Reviews, 50, 1-39.

Reason, J. T., and J. J. Brand (1975), Motion Sickness, London, Academic Press.

Schultz, J. H., and W. Luthe (1969), Autogenic Therapy, Vol. I: Autogenic Methods, New York, Grune and Stratton.

Toscano, W. B., and P. S. Cowings (1982), "Reducing Motion Sickness: Autogenic Feedback Training Compared to an Alternative Cognitive Task," Aviation Space and Environmental Medicine, 53(5), 449-453.

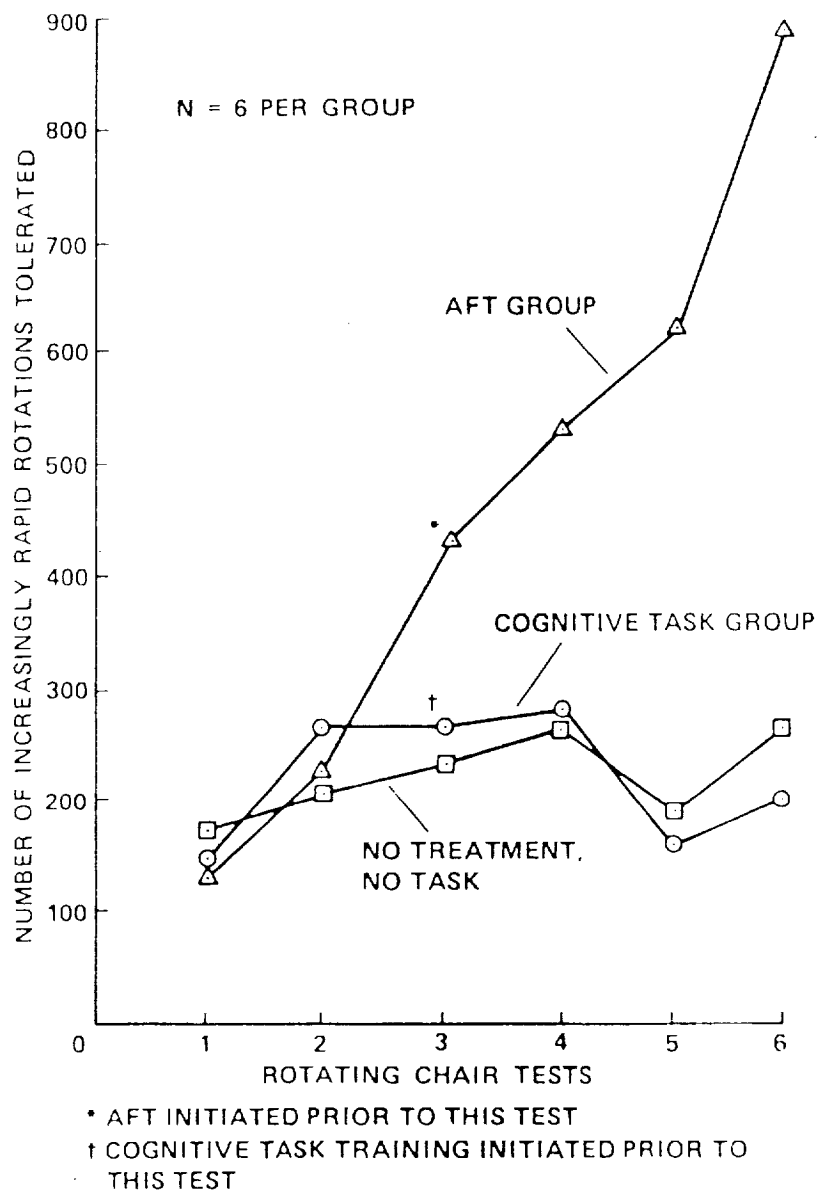


**Figure 1. Effects of AFT treatment compared with those of a distracting cognitive task and no treatment.**

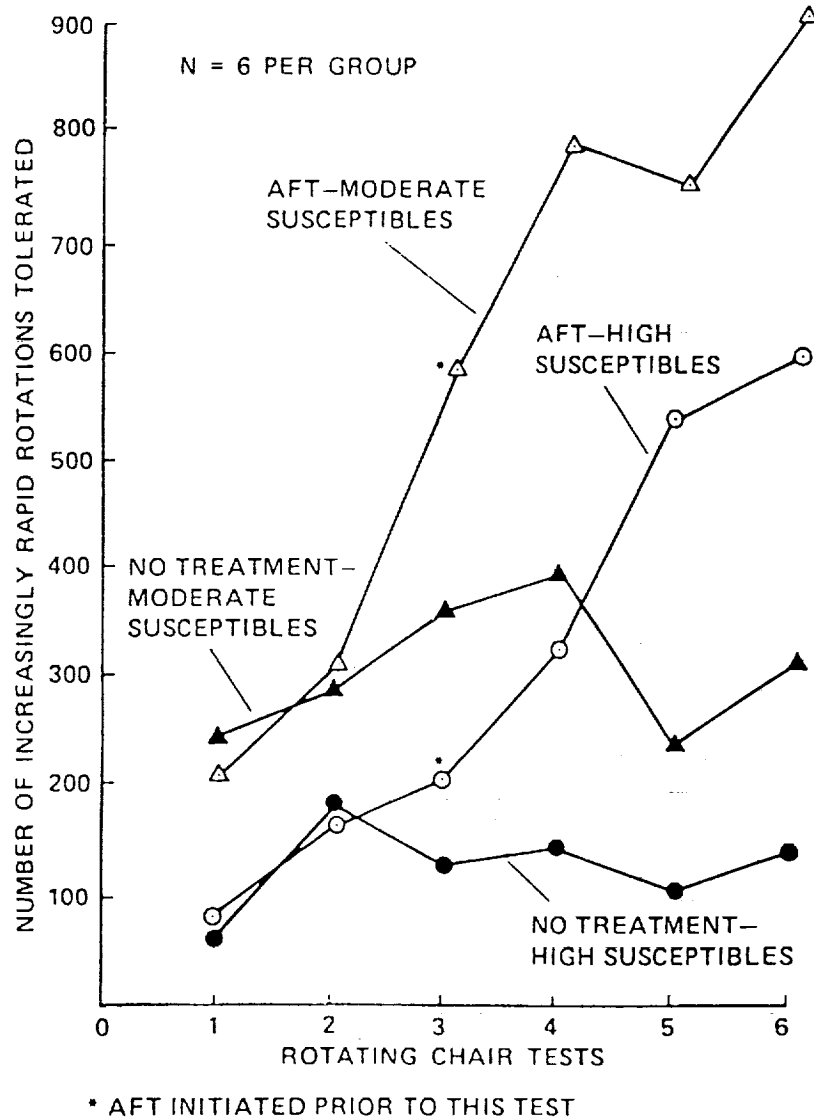


**Figure 2. Effects of AFT treatment for highly and moderate motion sickness susceptible subjects compared to matched controls given no treatment.**



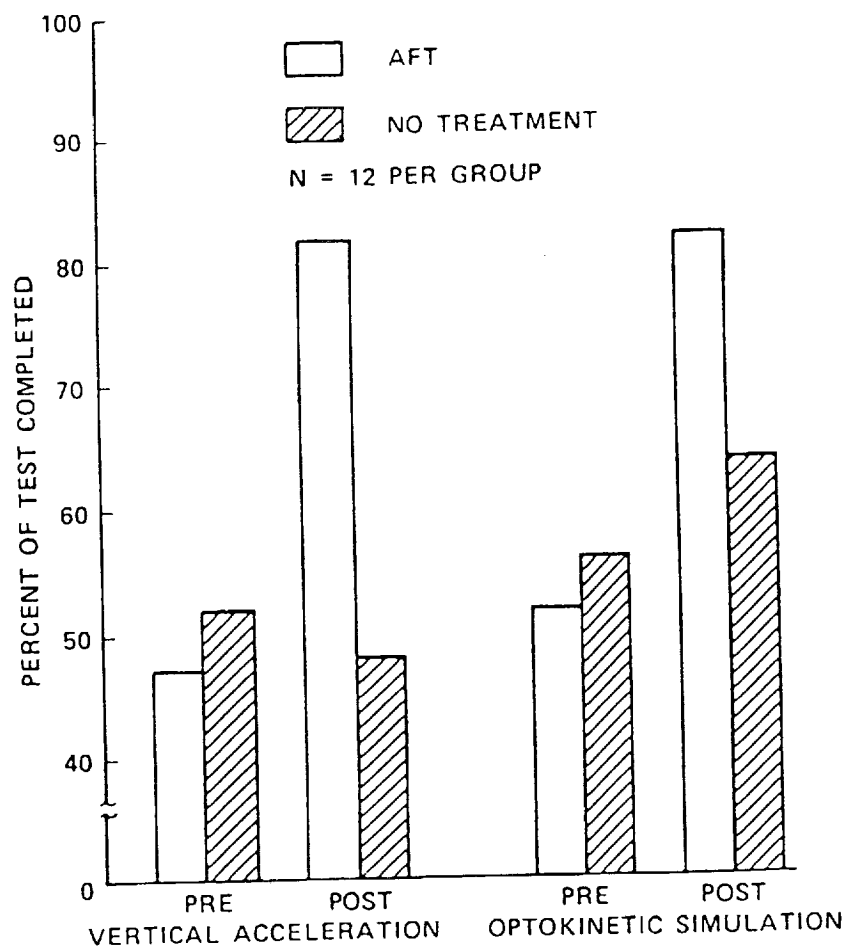
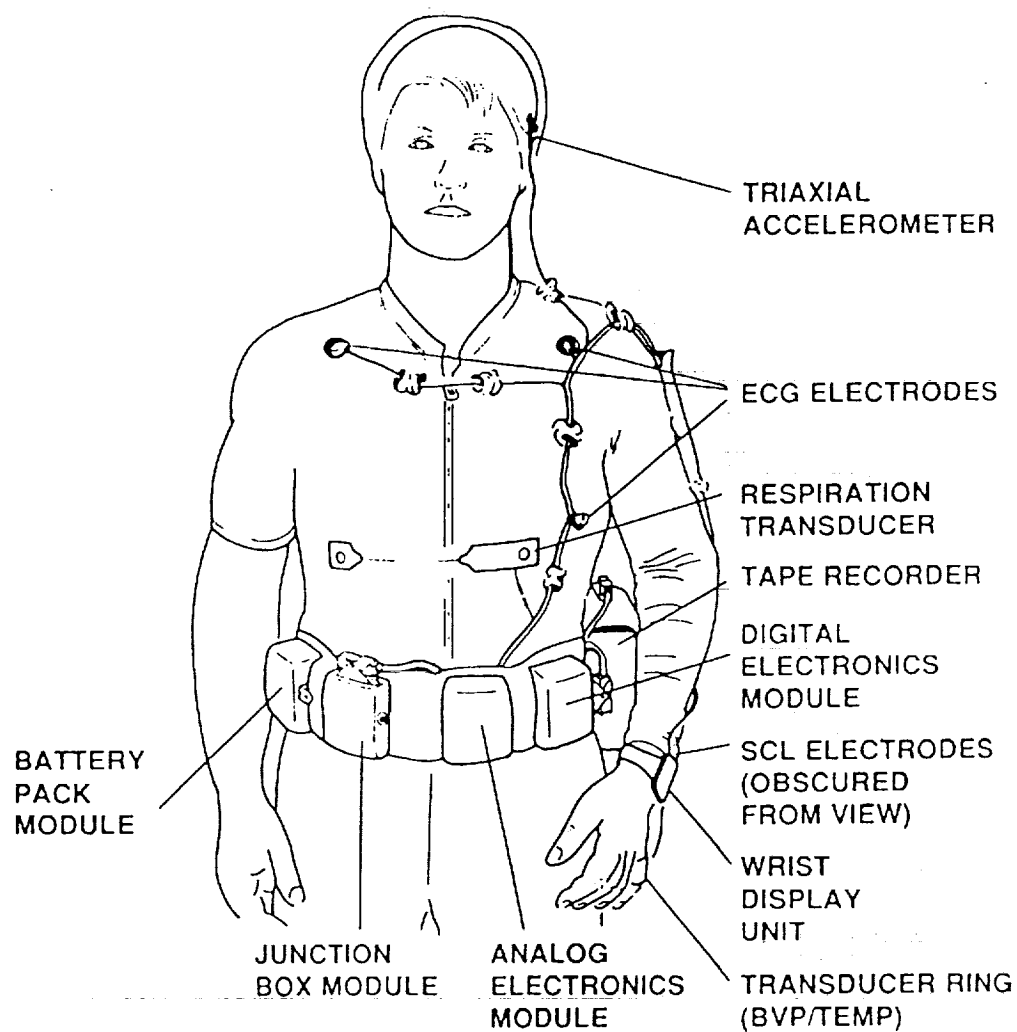


Figure 3. Positive transfer of training for AFT compared to a control group given no treatment.



**Figure 4. The Autogenic-Feedback System-2 (AFS-2). An ambulatory monitoring system as worn by crew members.**

IN-FLIGHT DEMONSTRATION OF THE SPACE STATION FREEDOM  
HEALTH MAINTENANCE FACILITY  
FLUID THERAPY SYSTEM (E300/E05)

Charles W. Lloyd  
NASA Johnson Space Center  
Houston, TX

The Space Station Freedom (SSF) Health Maintenance Facility (HMF) will provide medical care for crew members for up to 10 days. An integral part of the required medical care consists of providing intravenous infusion of fluids, electrolyte solutions, and nutrients to sustain an ill or injured crew member. In terrestrial health care facilities, intravenous solutions are normally stored in large quantities. However, due to the station's weight and volume constraints, an adequate supply of the required solutions cannot be carried onboard SSF. By formulating medical fluids onboard from concentrates and station water as needed, the Fluid Therapy System (FTS) eliminates weight and volume concerns regarding intravenous fluids. The first full-system demonstration of FTS in continuous microgravity will be conducted in Spacelab-Japan (SL-J).

The FTS evaluation consists of two functional objectives and an in-flight demonstration of intravenous administration of fluids. The first is to make and store sterile water and IV solutions onboard the spacecraft. If intravenous fluids are to be produced in SSF, successful sterilization of water and reconstituting of IV solutions must be achieved (Figure 1). The second objective is to repeat the verification of the FTS infusion pump, which had been performed in Spacelab Life Sciences - 1 (SLS-1). During SLS-1, the FTS IV pump was operated in continuous microgravity for the first time. The pump functioned successfully, and valuable knowledge on its performance in continuous microgravity was obtained. Finally, the technique of starting an

IV in microgravity will be demonstrated. The IV technique requires modifications in microgravity, such as use of restraints for equipment and crew members involved.

Hardware for use in the experiment was developed in conjunction with manufacturers in the medical devices field and other fields. Modified available terrestrial hardware was used whenever possible. There are nine major components in the FTS experiment: Source Water Container (SWC), Sterile Water for Injection Assembly (SWI), Intravenous Reconstituting Device (IRD), Large Volume Parenteral Bags (LVP), Intravenous Fluid Infusion Pump (IV Pump), Payload and General Support Computer (PGSC), Fluid Administration Set (FAS), Sample Containment Device (SCD), and Flight Infusion System Test (FIST) equipment. Following is a detailed description of each component and its role in FTS.

The SWC is a steel tank containing pressurized water for use throughout the experiment. Tap water will be used for the experiment. Water from the SWC passes to the SWI (Figure 3), which is a cartridge designed to purify water to USP XXI specifications. Purification of the water will be accomplished by first passing it across a bed of activated carbon, followed by a bed of 50:50 activated carbon and deionizing resin, then several beds of 100% deionizing resin, and finally through an ultrafilter. This process is intended to remove organic and halogenated contaminants and contaminants larger than 10,000 molecular weight. In addition, the fluid will then pass through a sterilizing microfilter to remove particles larger than 0.22 micron in size. A conductivity indicator is used to indicate when the desired purity level has been reached (Figure 3).

After water sterilization has been completed, water is stored in a polyvinyl chloride (PVC) LVP bag. If intravenous fluids are to be formulated, the IRD is used. The IRD is a flow-through pouch containing the constituents (liquid concentrates) of the solution which are to be mixed with the sterile water to reconstitute single units of intravenous fluids. Quick-disconnect fittings and dripless valves allow for easy removal and change of the IRDs and LVPs with fresh supplies.

The pump used in the verification phase is a modified commercially available and widely-used IV pump. It has two pumping channels which allow for the simultaneous infusion of two separate solutions at different rates. This feature also provides redundancy in the event either pump channel fails. The IV pump will deliver fluid solutions via the FAS (made of PVC connecting tubing) to the SCD, which contains a series of ten bags that will be used to hold the samples. The PGSC, a portable personal computer, will control the operation of the IV pump during this part of the experiment. In the FIST phase of the experiment, a crew member will demonstrate the technique of initiating an intravenous infusion on a manikin arm (Figure 2).

Different component configurations will be used for each portion of the experiment. In the sterile water for injection portion, the FTS will be configured only with the following equipment: SWC, SWI, and LVP (Figure 1). Water will be dispensed from the SWC and will pass through the SWI for purification. Sterile water will then pass into a LVP bag until the bag fills. A total of 9 liters of sterile water will be produced throughout the experiment.

Of the 9 liters formed, 5 liters will be used to reconstitute the intravenous solutions. For this part, the IRD will be placed between the SWI and the LVP bag (Figure 4). For the

Spacelab-J mission, solutions of sodium chloride (0.9%) and dextrose (5.0%) will be reconstituted. The volume of fluid in the LVP is controlled by the use of a volumetric assurance enclosure over the LVP bag. Production of sterile water and solutions will be performed concurrently.

The next step in the experiment is the verification of the IV pump (Figure 2). Two bags, one containing sodium chloride solution and one containing dextrose solution, will be attached to the IV pump using the FAS. Since IV pump operation is controlled by the PGSC, the crew member may continue to monitor the filling of the LVP bags in the sterilization and reconstitution part of the experiment, while the computer commands the IV pump to perform the verification tasks. The solutions will be automatically pumped into the SCD. The crew member will interact with the IV pump at 20-minute intervals, but no data will be lost if the crew member is delayed, because the PGSC controls start, stop, and data collection functions.

The final step in the experiment is the demonstration of intravenous infusion in continuous microgravity (Figure 2). A manikin arm designed for practicing the initiation of an IV solution will be used, along with the required supplies. The manikin arm is equipped with venous channels to simulate a patient arm. The IV pump will operate at several infusion rates, and intentional failures will be produced to determine effective methods for coping with the failures.

Only one crew member will be required to perform all of the tasks previously described. The experiment will be performed once during the mission. Shortly before initiating the in-flight

experiment, the crew member will notify the ground team so that a ground control experiment may be performed simultaneously.

Post-flight, the samples will be collected at the landing site and immediately returned to Johnson Space Center for analysis. The Johnson Space Center Biomedical Operations and Research Branch will perform the necessary analyses and tests on the flight and ground control samples to determine if the sterile water and IV solution production parts of the experiment were successful.

In conclusion, this experiment will determine if intravenous solutions can be successfully produced by mixing concentrates and water sterilized onboard a spacecraft. The experiment will also demonstrate the performance of the IV pump in continuous microgravity, and finally, the technique of starting an IV in microgravity will be demonstrated.

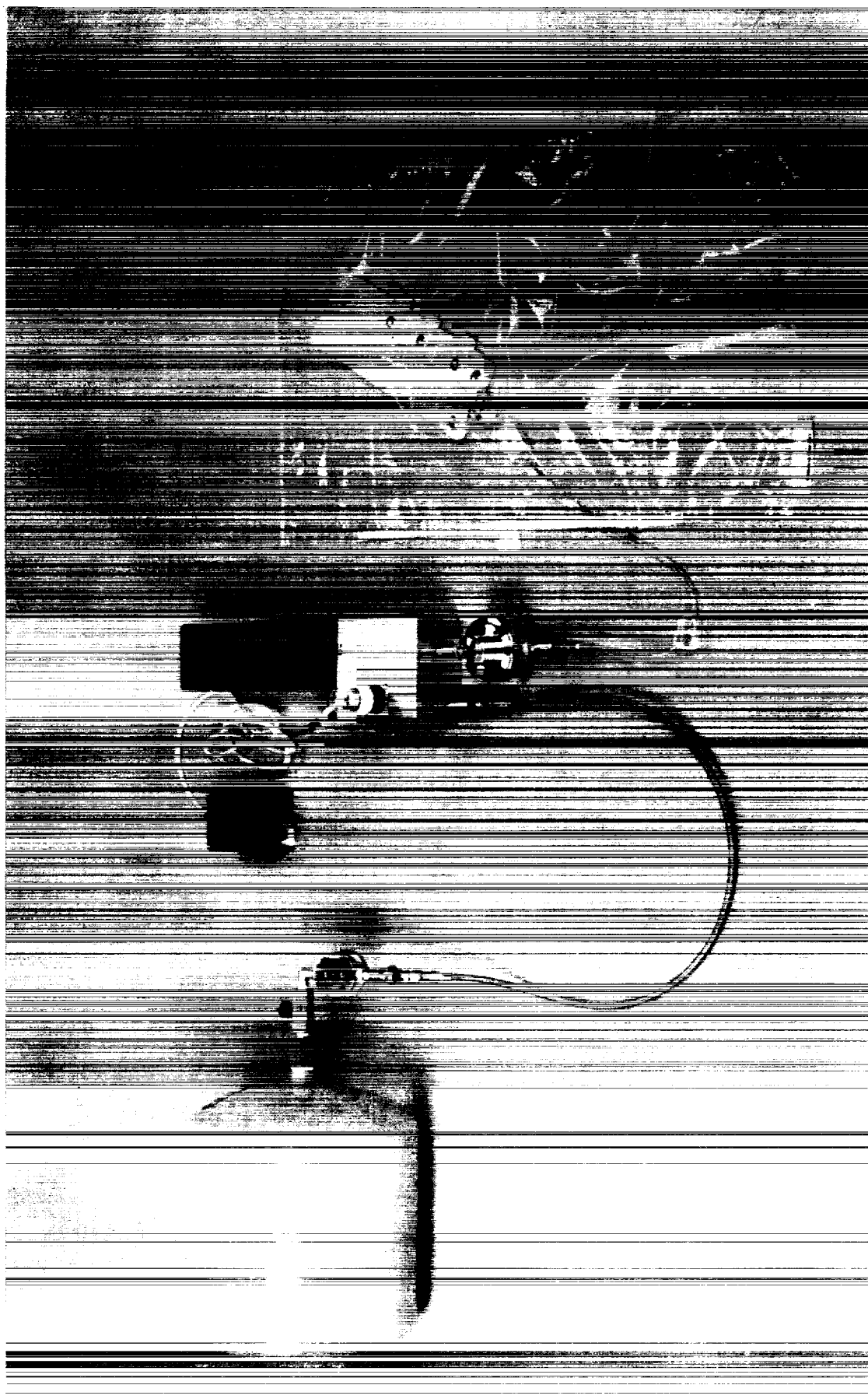


Figure 1. FTS with IV Adaptor to make sterile water for injection.





Figure 2. FTS showing the PGSC and the SCD with the FIST.

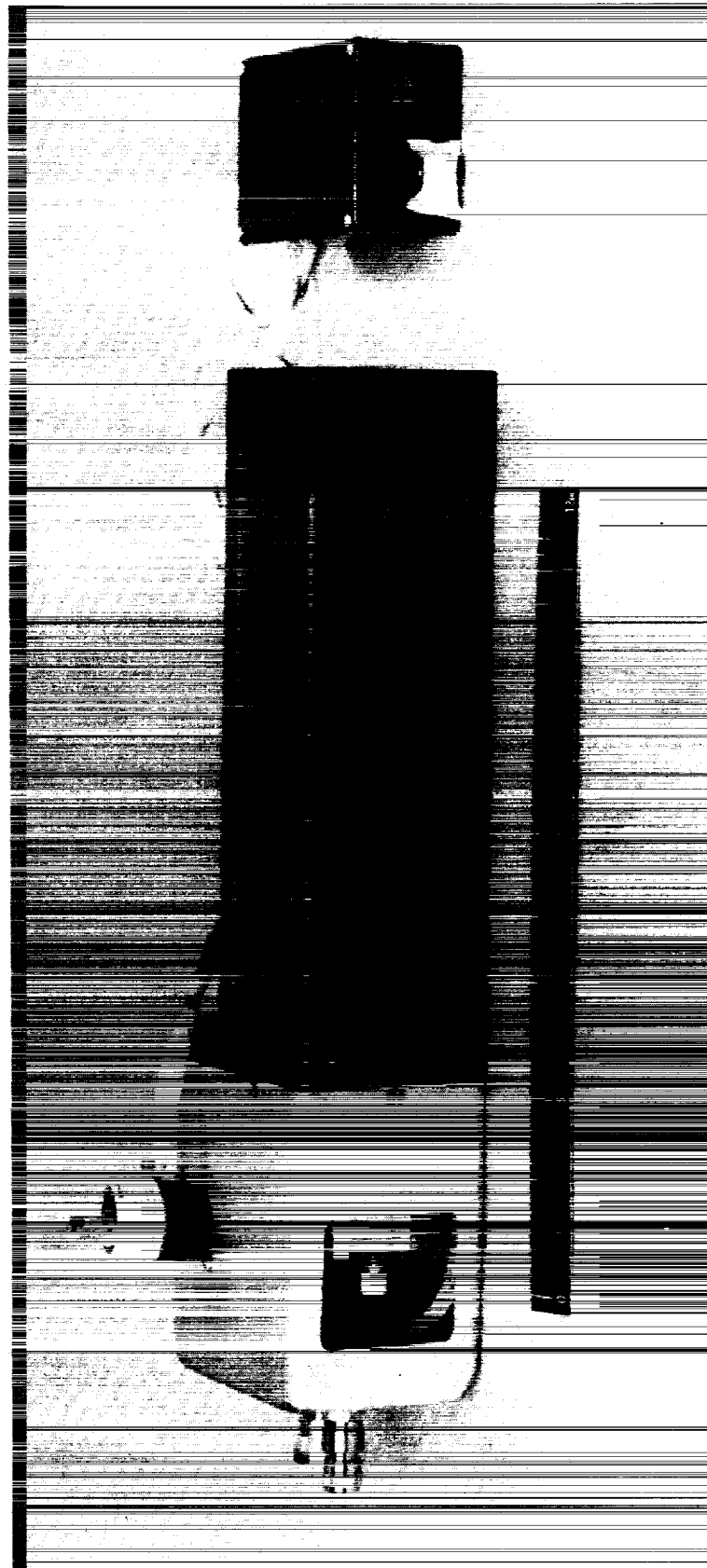


Figure 3. Close-up of the SWI cartridge.

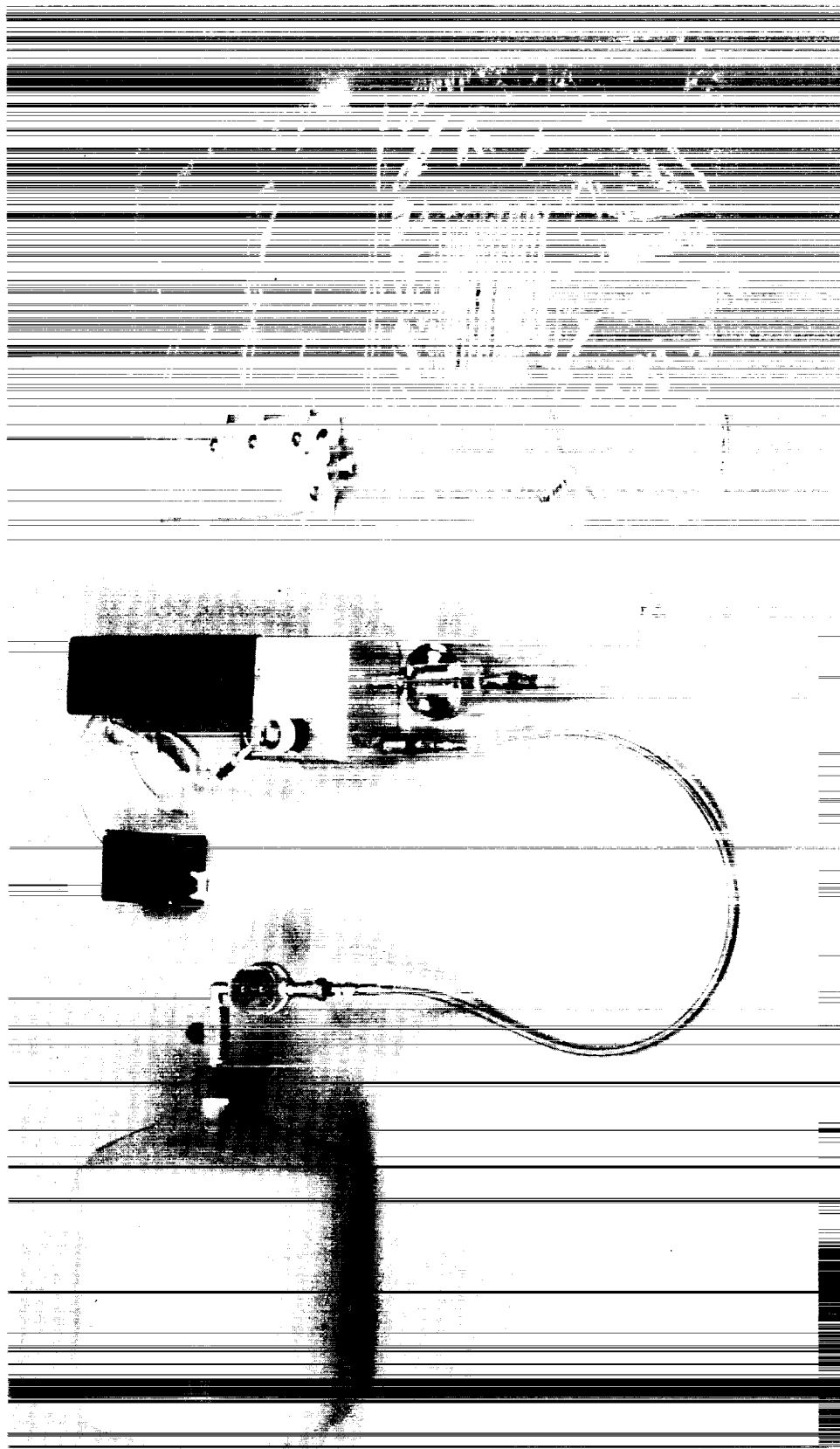


Figure 4. FTS with IV reconstitution bag in place for making either normal saline or dextrose 5%.

# REPORT DOCUMENTATION PAGE

Form Approved  
OMB No. 0704-0188

Public reporting burden for this collection of information is estimated to average 1 hour per response, including the time for reviewing instructions, searching existing data sources, gathering and maintaining the data needed, and completing and reviewing the collection of information. Send comments regarding this burden estimate or any other aspect of this collection of information, including suggestions for reducing this burden, to Washington Headquarters Services, Directorate for Information Operations and Reports, 1215 Jefferson Davis Highway, Suite 1204, Arlington, VA 22202-4302, and to the Office of Management and Budget, Paperwork Reduction Project (0704-0188), Washington, DC 20503.

1. AGENCY USE ONLY (Leave blank)

2. REPORT DATE  
August 1993

3. REPORT TYPE AND DATES COVERED  
**Technical Memorandum**

4. TITLE AND SUBTITLE

**Spacelab J Experiment Descriptions**

6. AUTHOR(S)

**Teresa Y. Miller, Editor**

5. FUNDING NUMBERS

7. PERFORMING ORGANIZATION NAME(S) AND ADDRESS(ES)

**George C. Marshall Space Flight Center  
Marshall Space Flight Center, AL 35812**

8. PERFORMING ORGANIZATION  
REPORT NUMBER

M-725

9. SPONSORING / MONITORING AGENCY NAME(S) AND ADDRESS(ES)

**National Aeronautics and Space Administration  
Washington, D.C. 20546**

10. SPONSORING / MONITORING  
AGENCY REPORT NUMBER

**NASA TM- 4517**

11. SUPPLEMENTARY NOTES

**Prepared by Space Science Laboratory, Science and Engineering Directorate.**

12a. DISTRIBUTION / AVAILABILITY STATEMENT

**Unclassified--Unlimited  
Subject Category: 29**

12b. DISTRIBUTION CODE

13. ABSTRACT (Maximum 200 words)

**This document contains brief descriptions of the experiment investigations for the Spacelab J Mission which was launched from the Kennedy Space Center aboard the Endeavour in September 1992.**

14. SUBJECT TERMS

**Spacelab Missions, Life Sciences, Microgravity Science, Spacelab J**

15. NUMBER OF PAGES

**271**

16. PRICE CODE

**A12**

17. SECURITY CLASSIFICATION  
OF REPORT

**Unclassified**

18. SECURITY CLASSIFICATION  
OF THIS PAGE

**Unclassified**

19. SECURITY CLASSIFICATION  
OF ABSTRACT

**Unclassified**

20. LIMITATION OF ABSTRACT

**Unlimited**